# INVESTIGATING THE PATHOPHYSIOLOGY OF AMYOTROPHIC LATERAL SCLEROSIS USING HUMAN INDUCED PLURIPOTENT STEM CELL TECHNOLOGY

Anna-Claire Devlin

A Thesis Submitted for the Degree of PhD
at the
University of St Andrews

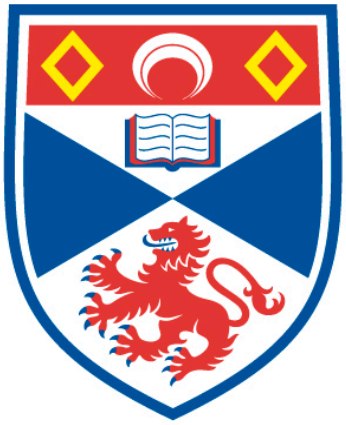

2016

# Investigating the pathophysiology of Amyotrophic Lateral Sclerosis using human induced pluripotent stem cell technology

**Anna-Claire Devlin**

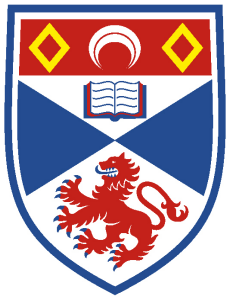

University of
St Andrews

**This thesis is submitted in partial fulfilment for the degree of PhD at the University of St Andrews**

**September 2015**

**1. Candidate's declarations:**

I, Anna-Claire Devlin, hereby certify that this thesis, which is approximately 54,000 words in length, has been written by me, and that it is the record of work carried out by me, or principally by myself in collaboration with others as acknowledged, and that it has not been submitted in any previous application for a higher degree.

I was admitted as a research student in September 2011 and as a candidate for the degree of PhD in September 2012; the higher study for which this is a record was carried out in the University of St Andrews between 2011 and 2015.

Date …… signature of candidate ……

**2. Supervisor's declaration:**

I hereby certify that the candidate has fulfilled the conditions of the Resolution and Regulations appropriate for the degree of PhD in the University of St Andrews and that the candidate is qualified to submit this thesis in application for that degree.

Date …… signature of supervisor ……

**3. Permission for publication:** (*to be signed by both candidate and supervisor*)

In submitting this thesis to the University of St Andrews I understand that I am giving permission for it to be made available for use in accordance with the regulations of the University Library for the time being in force, subject to any copyright vested in the work not being affected thereby. I also understand that the title and the abstract will be published, and that a copy of the work may be made and supplied to any bona fide library or research worker, that my thesis will be electronically accessible for personal or research use unless exempt by award of an embargo as requested below, and that the library has the right to migrate my thesis into new electronic forms as required to ensure continued access to the thesis. I have obtained any third-party copyright permissions that may be required in order to allow such access and migration, or have requested the appropriate embargo below.

The following is an agreed request by candidate and supervisor regarding the publication of this thesis:

PRINTED COPY

**Supporting statement for printed embargo request:**
a) No embargo on print copy

ELECTRONIC COPY

**Supporting statement for electronic embargo request:**
b) Embargo on all or part of print copy for a period of 2 years (maximum five) on the following ground(s):

Publication would preclude future publication

Date …… signature of candidate …… signature of supervisor ……

*Please note initial embargos can be requested for a maximum of five years. An embargo on a thesis submitted to the Faculty of Science or Medicine is rarely granted for more than two years in the first instance, without good justification. The Library will not lift an embargo before confirming with the student and supervisor that they do not intend to request a continuation. In the absence of an agreed response from both student and supervisor, the Head of School will be consulted. Please note that the total period of an embargo, including any continuation, is not expected to exceed ten years.*
*Where part of a thesis is to be embargoed, please specify the part and the reason.*

# Abstract

Amyotrophic Lateral Sclerosis (ALS) is a devastating, adult onset, neurodegenerative disease which remains largely untreatable and incurable, reflecting an incomplete understanding of the key pathogenic mechanisms that underlie motoneuron (MN) loss in the disease. Through the use of induced pluripotent stem cell (iPSCs) technology, cells from the human central nervous system can be studied at a range of time points, including those prior to overt pathology, in order to understand early causative events in ALS. In the present study, human iPSC-derived MNs and astrocytes were used to study the pathophysiology of ALS. Whole-cell patch clamp recording techniques were utilised to investigate whether the functional properties of human iPSC-derived MNs are altered in cells derived from ALS patients compared to those from healthy controls. Patient iPSC-derived MNs harbouring *C9ORF72* or *TARDBP* mutations display an initial period of hyperexcitability followed by a progressive loss of action potential output due to decreases in voltage-activated $Na^+$ and $K^+$ currents. These changes occur in the absence of changes in cell viability. Given evidence in support of non-cell autonomous disease mechanisms in ALS, the potential involvement of interactions between neurons and astrocytes in the pathophysiological phenotype were next investigated. Patient iPSC-derived astrocytes harbouring *C9ORF72* or *TARDBP* G298S mutations cause a loss of functional output in control iPSC-derived MNs, due to a progressive decrease in voltage-activated $Na^+$ and $K^+$ currents. These data show that patient iPSC-derived astrocytes can induce pathophysiological changes in control human iPSC-derived MNs which are similar to those revealed in patient iPSC-derived MNs. This study also utilizes pharmacological agents and genetic editing to demonstrate that the pathophysiological phenotype can be altered. Overall, this study

implicates MN dysfunction, potentially due to non-cell autonomous disease mechanisms, as an early contributor to downstream degenerative pathways that ultimately lead to MN loss in ALS.

# Acknowledgements

Firstly, I would like to express my appreciation and thanks to my primary supervisor Dr. Gareth Miles. Thanks Gareth for all your encouragement, support and guidance; for always being around for a chat; for your advice on both research as well as on my career; for feeding my cells when I went home (and not contaminating them!); and for allowing me to grow as a research scientist/ patching addict!

Thanks to all the past and present members of the Miles Lab, you have been great colleagues and friends over the past 4 years. I'd especially like to thank David, Noboru, Josh, John, Emily, Laurence and Filipe for all their help, for providing lots of laughs and for generally making the place more fun!

I would also like to thank my secondary supervisor Professor Siddharthan Chandran at the University of Edinburgh. Thank you Siddharthan for supplying me with endless resources to complete this PhD as fully as possible; for imparting some of your knowledge and enthusiasm to me; and for all your encouragement and advice. I would also like to thank members of Siddharthan's lab, especially Karen, Bhuvaneish, Chen, Navneet, Dario, Shyamanga and Elaine for supplying me with cells, antibodies and paper figures for the past few years.

I would like to acknowledge the support of the Euan MacDonald Centre for Motor Neurone Disease Research, Edinburgh and the Motor Neurone Disease Association for their funding over the past four years. I really appreciate their strong support, without which I couldn't have completed these studies.

Finally, a massive thanks to my family and friends for supporting me in every possible way! Words cannot express how grateful I am to my Mum and Dad for everything they've done for me and for putting up with me when I got stressed. Thanks to Shauna, Niall, Patrick, Ciaran, Bee-Bee, Monica, Paddy and my grandparents for feigning an interest in "the cells" and to Conan and Sheppy dog for the smiles and cuddles making writing easier. I would also like to thank all of my friends for their support and encouragement; for coming over to visit; for the coffee breaks and movie nights; and for all the laughs along the way!

Le grá,

Anna-Claire

# TABLE OF CONTENTS

**CHAPTER 3**

**IPSC-DERIVED ASTROCYTES HARBOURING *TARDBP* OR *C9ORF72* MUTATIONS CAUSE MN DYSFUNCTION VIA NON-CELL AUTONOMOUS MECHANISMS ..... 136**

# Chapter 1

# Introduction

## Project overview

Amyotrophic lateral sclerosis (ALS) is a fatal, incurable, adult onset neurodegenerative disease characterised by progressive muscle paralysis due to the death of motoneurons (MNs) in the brainstem, spinal cord and motor cortex. Although many mechanisms thought to contribute to the onset and progression of this disease have been described, there remains no known cause, cure or beneficial treatment. To enable the understanding of early causative events in ALS patients, cells from the human central nervous system (CNS) need to be studied. This is now possible through the use of human induced pluripotent stem cell (iPSC) technology, which was first developed in 2006 (Takahashi and Yamanaka, 2006). Using this technology, fibroblasts can be genetically reprogrammed into stem cells, which can then be changed into any cell type in the body. For this project, iPSCs from healthy controls and ALS patients were differentiated into cultures of spinal cord MNs and astrocytes in order to study the properties of MNs and the potential non-cell autonomous disease mechanisms associated with ALS. Early alterations in MN properties have been described in ALS mouse models through the use of electrophysiological analyses with changes in electrical properties also detected in ALS patients. In this project, electrophysiological analyses were used to determine if any such changes were evident in iPSC-derived MNs from ALS patients and if patient iPSC-derived astrocytes act via non-cell autonomous disease mechanisms, causing dysfunction of control iPSC-derived MNs. The following sections will introduce the main topics relevant to this project including the basic principles of motor control, clinical and neuropathological features and genetic mutations associated with ALS, the

mechanisms which are thought to cause and contribute to the onset and progression of ALS and a summary of models of ALS.

## Motor control

Skilled movements comprise a wide range of behaviours, many of which make human life possible. Humans develop and acquire new motor skills throughout their lifetimes, from crawling, walking and running to kicking a ball and playing musical instruments. The development of these skills is required in order for us to adapt to our surroundings, meet our needs and carry out our hobbies and interests. The portion of nervous system that regulates and controls the contractile activity of muscles required for these skills is the motor system. It comprises of the cerebral cortex, basal ganglia, thalamus, cerebellum, brainstem and spinal cord, with skeletal muscle activity entirely dependent on their neural output.

The cerebral cortex, which exerts control over the entire motor system through areas of the motor cortex, represents the highest level of motor control within the nervous system. The motor cortex is comprised of the primary motor cortex, the premotor cortex and the supplementary motor area. Layer V of the primary motor cortex contains the pyramidal neurons that project to the motor nuclei in the brainstem or to interneurons and MNs in the spinal cord through the corticospinal tract. MNs that originate in the primary motor cortex and possess long axons forming the corticobulbar and corticobulbar tracts are often referred to as upper MNs. The primary motor cortex is somatotopically organised with the larger areas devoted to regions of the body where motor control is most finely regulated, such as the lips, face and hands (Sanes and Donoghue, 2000). The premotor cortex connects to other areas of the

motor cortex, as well as to neurons of the spinal cord, brainstem, thalamus and areas of the basal ganglia, playing important roles in the selection of specific movements. Neurons of the supplementary motor area project directly to the spinal cord (He et al., 1995; Nachev et al., 2007) and are shown to be involved in aspects of motor control including task sequencing and movement initiation (Tanji and Shima, 1994). Overall, the motor cortex controls segmental MNs through corticospinal and corticobulbar tracts via supraspinal motor centres, programming movements in response to sensory information, and initiating voluntary movements (di Pellegrino et al., 1992).

The basal ganglia are subcortical nuclei that receive descending input from all parts of the cerebral cortex and send output to the brainstem and the cerebral cortex via the thalamus. Although the basal ganglia don't project directly to the cortex or spinal cord MNs, they influence motor control as neuronal death or dysfunction in this area often results in movement disorders such as Parkinson's or Huntington's disease. Another important component of the motor system is the cerebellum, a highly organized network of cells closely interconnected with the brainstem. Although motor commands are not initiated in the cerebellum, it integrates and modifies motor commands from the descending pathways, smoothing the intended movements and coordinating muscle activity. Without the cerebellum, balance and posture are affected and voluntary movements become erratic (Mauk et al., 2000; Manto et al., 2012). The thalamus is the hub for signal processing of the basal ganglia and cerebellar inputs before they are transmitted to the motor cortex. Damage to the thalamus results in movement disorders similar to those seen after cerebellar or basal ganglia damage (Herrero et al., 2002).

The midbrain, medulla oblongata and pons make up the brainstem, a major and

complex integrating centre adjoining, and structurally continuous with, the brain and spinal cord. The brainstem provides the main motor innervation to the face, head and neck through the brainstem MNs, and communicates with spinal cord MNs via the descending motor tracts including corticospinal, vestibulospinal, reticulospinal, olivospinal, tectospinal and rubrospinal tracts. The brainstem also plays an important role in the regulation of cardiac and respiratory functions, maintaining consciousness and regulating the sleep cycle. Any damage to the brainstem is usually serious and life threatening (Drew et al., 2004; Takakusaki et al., 2004).

Spinal cord MNs, whose cell bodies are located in lamina IX of the ventral horn of the spinal cord, supply skeletal muscles of the limbs and trunk. MNs that originate in the brainstem and spinal cord directly innervate skeletal muscle are termed lower MNs. MN axons exit the CNS through the ventral spinal roots and reach the muscles via peripheral nerve trunks. In the skeletal muscle, the axon of every MN divides repeatedly into many terminal branches, each of which innervates a single muscle fibre. The region of innervation, called the neuromuscular junction (NMJ), is a secure synaptic contact between the MN terminal and the muscle fibre membrane. MNs were first described as "the final common pathway" by Sherrington in 1947 as, regardless of where signals originate, for movements to occur, MNs are always the final neural cell involved. As MNs play such a vital role, spinal cord MNs are often more than two times larger than other spinal cord neurons. However the size of MNs and their dendritic arborisation vary between the locations in which they reside (Kernell and Zwaagstra, 1989; Rekling et al., 2000).

Spinal cord MNs are not just simple relay neurons that communicate motor commands but also play important roles in signal integration to ensure accurate motor

output. Voluntary and rhythmic movements, reflex activation and posture maintenance are mediated by the activation of ionotropic receptors through excitatory signalling via glutamatergic transmission or inhibitory signalling via GABAergic or glycinergic transmission (Cazalets et al., 1996; Butt et al., 2002). Spinal cord MNs are also influenced by modulatory inputs through the release of various chemicals, including peptides and amines, which act via activation of G-protein coupled metabotropic receptors, to alter MN excitability (Miles and Sillar, 2011), for example, during periods of exercise or during the sleep cycle (Rekling et al., 2000).

As MNs provide a direct link between the nervous and musculoskeletal systems, it is vital that they develop and maintain the ability to receive, integrate and generate appropriate signals needed to keep us alive. MN diseases (MNDs), including amyotrophic lateral sclerosis (ALS) and spinal muscular atrophy (SMA), are a group of progressive neurodegenerative diseases that cause MN death and remain incurable. The following sections will discuss ALS in more detail, including the genetic mutations and potential mechanisms involved in the onset and progression of the disease, why MNs are particularly vulnerable in ALS and the models of the disease in which most research has been carried out.

# Amyotrophic lateral sclerosis

## Definition

Amyotrophic Lateral Sclerosis is a devastating, incurable, adult onset neurodegenerative disease primarily affecting MNs in the brainstem, spinal cord and motor cortex. Although MNs are the most vulnerable cell type in this disease, a

number of other cell types are also affected including cortical and spinal cord interneurons and glial cells as well as cells involved in sensory and spinocerebellar pathways (Bruijn et al., 1997; Stephens et al., 2006; Jiang et al., 2009; Vucic et al., 2009; Kang et al., 2013). The vulnerability of MNs in ALS has been attributed to their large cell body, long axonal projections, their large number of cytoskeletal components and to the profile of receptors they express (Cleveland and Rothstein, 2001; Bruijn et al., 2004; Kumar et al., 2011). ALS currently has an incidence in Europe of 2-3 cases per 100,000 individuals and 3-5 cases per 100,000 in the USA (Hardiman et al., 2011). The cause of ALS remains largely unknown, with many cellular mechanisms attributed to its onset and progression. The majority of patients (90-95%) with ALS have no apparent family history of the disease and these are termed sporadic ALS cases (SALS), with the remaining 5-10% having a genetic link which are termed familial ALS cases (FALS). The clinical manifestations of FALS and SALS are very similar; therefore determining the mechanisms underlying the progression of FALS may also provide insights into SALS.

## Clinical presentation

The majority of patients first present with limb onset symptoms including muscle cramps and fasciculations, patients with bulbar onset symptoms have difficulties speaking and swallowing and a small proportion of patients have difficulty breathing (Hardiman et al., 2011). The site of onset begins focally and asymmetrically before spreading. The age of onset of ALS is usually after several decades, following aging of the motor system, when homeostatic defence mechanisms are more vulnerable (Ferraiuolo et al., 2011). To date, there is no definitive test for ALS and formal diagnosis, taking between 9-15 months, is determined when other causes of the

symptoms are ruled out. Most recently, ALS has been linked with frontotemporal dementia (FTD), as a common genetic link was discovered between these diseases, with up to 15% of ALS patients presenting with FTD. Currently there are no beneficial treatments for ALS patients, with the only available disease modifying drug, Riluzole, extending life expectancy by 1-3 months (Bensimon et al., 1994; Bellingham, 2011). The majority of patients die due to denervation of respiratory muscles causing respiratory failure, usually within 3-5 years of symptom onset.

## Neuropathology

As MNs are the main cell type affected in ALS, it is no surprise that MN degeneration is the main pathological feature in ALS patients and animal models. MN degeneration is often accompanied by the degeneration of interneurons in the spinal cord and motor cortex, as well as evidence of reactive gliosis in astrocytes, oligodendrocytes and microglia in these areas (Kawamata et al., 1992; Schiffer et al., 1995; Schiffer and Fiano, 2004; Ince et al., 2011; Blokhuis et al., 2013). Protein aggregates or inclusions are hallmarks of ALS. These aggregates are present in neuronal and glial cells involved in the disease, with mutations in the genes coding for some of the aggregates of accumulated proteins linked to FALS. Ubiquitinated aggregates, the most predominant aggregates found in ALS patients, are classified as either Lewy-body like or skein-like inclusions (Rosen et al., 1993; Tu et al., 1996; Neumann et al., 2006). Ubiquitin- negative inclusions, called Bunina bodies, are accumulations of proteinous material, of which only two proteins have been identified- cystatin C and transferrin (Radunovíc and Leigh, 1996; Sherman and Goldberg, 2001).

Superoxide dismutase 1 (*SOD1*) was the first protein aggregate to be identified in FALS patients. Subsequent studies determined that mutations in the *SOD1* gene were the cause of a proportion of FALS cases (Rosen et al., 1993). *SOD1* mutations were the sole genetic link to ALS up until the discovery of the transactive response-DNA binding protein 43 (TDP-43) in aggregates of ALS patients and animal models in 2006 (Neumann et al., 2006). Since then, the identification of proteins involved in ALS pathophysiology has increased exponentially. The discovery that TDP-43 is a major component of the ubiquitin positive aggregations, which are the predominant aggregates found in ALS, led to the identification of a mutation in the gene responsible for producing TDP-43 protein, *TARDBP* (Neumann et al., 2006; Sreedharan et al., 2008). The *TARDBP* mutation is responsible for approximately 3% of FALS cases and 1.5% of SALS cases (Lattante et al., 2013; Renton et al., 2014). TDP-43 is present in neuronal and glial aggregates in all SALS patients, in most mutant SOD1 negative FALS patients but is absent in mutant *SOD1* related ALS cases (Mackenzie et al., 2007). TDP-43 aggregates are also present in FTD patients, in a subtype called frontotemporal lobar dementia (FTLD- TDP) (Arai et al., 2006; Davidson et al., 2007). These protein aggregates provide an important link between the pathophysiology of FALS and apparent SALS cases. The identification of the proteins present in the ubiquitin positive aggregates has already aided the discovery of genetic mutations, therefore further proteomic and pathological studies may uncover new mutations which will ultimately lead to a better understanding of the processes involved in the pathogenesis of ALS.

# Genetics

## 1.1.1 Overview

Determining genetic origins has facilitated fundamental insights into the mechanisms thought to underlie neuronal degeneration in ALS. So far, the genetic origins of almost 70% of FALS and 11% of SALS cases are known (Renton et al., 2014). Up until 2006, *SOD1* was the only gene known to have a role in the pathogenesis of ALS. Since the discovery of the *TARDBP* mutation in 2006, there has been a rapid advance in the knowledge of genetic involvement in ALS, as well as of the relationships between genetic subtypes and the pathological and clinical phenotypes. The most recently discovered genetic mutations associated with ALS include: Fused in Sarcoma/Translocated in Sarcoma (*FUS/TLS)* (Kwiatkowski et al., 2009; Vance et al., 2009), vesicle-associated-protein B and C *(VAPB)* (Nishimura et al., 2004), angiogenin (*ANG*) (Greenway et al., 2006), valosin- containing protein (*VCP)* (Johnson et al., 2010), ubiquilin 2 *(UBQLN2)* (Deng et al., 2011) and chromosome-9-open reading frame 72 (*C9ORF72)* (DeJesus-Hernandez et al., 2011; Renton et al., 2011). For the remainder of this chapter, I will only go into more detail on the *SOD1*, *TARDBP* and *C9ORF72* mutations. These were chosen as *SOD1* was the first mutation discovered to be associated with ALS and many studies have been carried out on models harbouring this mutation. *TARDBP* and *C9ORF72* mutations are also discussed in more detail as the cells studied in this project harbour these mutations. Mechanisms thought to be involved in the pathogenesis of ALS caused by these mutations will be discussed later in the chapter.

### 1.1.2 SOD1

Superoxide dismutase 1 (SOD1) is a ubiquitously expressed cytosolic and mitochondrial antioxidant enzyme that functions to catalyse superoxide anions to oxygen and hydrogen peroxide. Mutations in the *SOD1* gene, accounting for around 20% of FALS cases, were the first genetic mutations to be linked with ALS (Bowling et al., 1993; Deng et al., 1993; Rosen et al., 1993). This discovery led to the development of the first ALS mouse model, the *SOD1* G93A mouse model (Gurney et al., 1994). To date, more than 110 *SOD1* mutations have been discovered, all of which cause the mutant protein to misfold and accumulate, forming aggregates (Al-Chalabi et al., 2012).

The mechanism of mutant *SOD1* pathogenesis has been widely investigated. Studies have described how both dismutase active forms (Gurney et al., 1994; Wong et al., 1995) and inactive forms (Bruijn et al., 1997; Nagai et al., 2001) of mutant *SOD1* in animal models can lead to the development of the same phenotype which includes MN degeneration, muscle wasting and progressive paralysis. Taken together with the fact that *SOD1* deficient mice show no signs of overt pathology (Reaume et al., 1996), it is thought that a toxic gain of function rather than loss of function of *SOD1* contributes to mechanisms of disease. The majority of findings implicate *SOD1* misfolding, with the misfolded protein causing dysfunction in the cells regulatory processes. Mutant *SOD1* has been found to cause toxic effects on the proteasomal pathway and influence autophagy (Bendotti et al., 2001a; Hadano et al., 2010). The accumulation of mutant *SOD1* aggregates leads to the activation of the unfolded protein response (UPR) with the cell undergoing apoptosis if the UPR is unsuccessful (Bento-Abreu et al., 2010; Robberecht and Philips, 2013; Rotunno and Bosco, 2013).

Interestingly, oxidised wild-type *SOD1* can misfold, aggregate and cause toxicity to MNs in a similar manner to mutant *SOD1* (Bosco et al., 2010). These findings suggest a possible role for wild-type *SOD1* in SALS. Further studies into the mechanisms involved in the pathogenesis of ALS caused by mutant *SOD1* may also reveal mechanisms involved in SALS and other FALS cases.

### 1.1.3 TARDBP

Mutations in *TARDBP* were discovered when exploring the presence of TDP-43 in the characteristic cytosolic protein aggregates in ALS patient post-mortem samples and in animal models of the disease. *TARDBP* was the first mutation to be associated with both ALS and FTLD, leading to the speculation that ALS is a spectrum disorder (Arai et al., 2006; Neumann et al., 2006; Mackenzie et al., 2010). TDP-43 is an RNA-binding protein involved in transcription and RNA transport and splicing, thereby associating RNA metabolism dysfunction with ALS (Polymenidou et al., 2011). TDP-43 is usually located in the nucleus but often shuttles between it and the cytoplasm to carry out its functions. TDP-43 is often located in the cytoplasm when a cell is undergoing stress where it accumulates in temporary stress granules. The stress granules incorporate and inactivate the translation of mRNA until the stress has resolved. This enables the prioritization of protein synthesis and allows for an adequate stress response. Once the stress is resolved, TDP-43 relocates to the nucleus. The proper functioning of TDP-43 is therefore critical during cell stress in order to protect mRNA (Colombrita et al., 2009; Lagier-Tourenne et al., 2010; Parker et al., 2012).

Two mechanisms have been proposed as to how TDP-43 contributes to the pathogenesis of ALS. The first mechanism is through a gain of toxic function of the TDP-43 aggregates. Two scenarios have been associated with this gain of toxic function mechanism. The first is that the mutant gene gains novel toxic activity, independent of the normal function of the gene. The second scenario is where the mutant becomes hyperactive in one of its normal functions by overexpressing either mutant or wild- type *TARDBP*, leading to toxicity. The second scenario is supported by studies in which wild-type TDP-43 has been overexpressed in mouse models (Wils et al., 2010; Xu et al., 2010), a *Drosophila* model (Li et al., 2010) and a *C. elegans* model (Ash et al., 2010) causing the hallmark cytosolic TDP-43 aggregates, as well as other cellular and behavioural phenotypes found in ALS. In most models, overexpression of both mutant and wild type TDP-43 can cause a neurodegenerative phenotype thus supporting a gain-of-function mechanism and a potential overactivation of TDP-43 in the mutants (Da Cruz and Cleveland, 2011). The second proposed mechanism for how TDP-43 contributes to the pathogenesis of ALS is through loss of function. In studies involving TDP-43 knockout mice, TDP-43 is found to play a vital role in embryogenesis as the TDP-43 deficient embryos all die between 3.5 and 8.5 days of embryonic development (Kraemer et al., 2010; Sephton et al., 2010; Wu et al., 2010). However, in mouse models where TDP-43 is inactivated in MNs of the spinal cord alone (Wu et al., 2012; Iguchi et al., 2013) or TDP-43 expression is knocked-down in the CNS and periphery (Yang et al., 2014), an ALS-like phenotype is observed, along with the formation of TDP-43 protein aggregates. Altering the expression levels of TDP-43 in other cell types, including astrocytes, also results in an ALS-like phenotype in some cases (Diaper et al., 2013; Tong et al., 2013; Yang et al., 2014). It should be noted however that models of ALS harbouring the

*TARDBP* mutation have highly variable phenotypes (Polymenidou et al., 2011; Janssens and Van Broeckhoven, 2013).

Findings from current studies suggest that both proposed mechanisms are equally as likely since, through gain of toxic function, cytoplasmic aggregates are increased. This increase in cytoplasmic aggregation of TDP-43 results in nuclear depletion of TDP-43, which in turn causes RNA processing abnormalities through a loss of function. Therefore, the amount and location of TDP-43 expression in cells needs to be tightly regulated as disturbing the normal balance could lead to cellular dysfunction (Kabashi et al., 2009).

### *1.1.4 C9ORF72*

In 2011 a major breakthrough in ALS genetics was made with the discovery of ALS-related mutations in chromosome 9 open reading frame 72 (*C9ORF72*) (DeJesus-Hernandez et al., 2011; Renton et al., 2011). *C9ORF72* mutations are the most common cause of FALS (40%) and account for approximately 7% of SALS cases (DeJesus-Hernandez et al., 2011; Renton et al., 2011), becoming the second genetic mutation to link ALS with FTD. The *C9ORF72* gene consists of a GGGGCC hexanucleotide ($G_4C_2$) repeat expansion that is normally present in numbers of up to 30 repeats. However, ALS patients have between a few hundred to thousands of repeats, with the exact length varying between individuals. Clinically, patients harbouring the *C9ORF72* mutation present more commonly with bulbar onset symptoms, have earlier disease onset with cognitive impairment and the disease progresses faster than non-*C9ORF72* ALS cases (Byrne et al., 2012; Millecamps et al., 2012; Stewart et al., 2012). The function of the normal *C9ORF72* protein remains

unclear, however, it is structurally related to the differentially expressed in normal and neoplastic cells (DENN) domain proteins that function as GDP-GTP exchange factors (GEFs) for the membrane trafficking regulators the Rab GTPases. These findings suggest that the normal function of *C9ORF72* protein may have roles in membrane trafficking and autophagy and alterations to this protein can lead to dysfunction of these processes (Marat et al., 2011; Zhang et al., 2012; Levine et al., 2013).

The mechanisms by which *C9ORF72* mutations lead to ALS pathology have been widely debated. So far, three potential mechanisms have been uncovered. The first potential mechanism is through a loss of function (haploinsufficiency) of the gene containing the repeat expansion. This causes a reduction in *C9ORF72* mRNA levels, as transcript levels have been shown to be decreased in patients with the *C9ORF72* mutation (DeJesus-Hernandez et al., 2011; Renton et al., 2011; Gijselinck et al., 2012). Antisense oligonucleotides (ASOs) have been developed to selectively target and degrade the *C9ORF72* expansion with the aim of being used as therapies in ALS. The use of ASOs have supported the haploinsufficiency mechanism as studies in which ASOs were used, causing a reduction of *C9ORF72* mRNA in a zebrafish model, lead to an ALS-like phenotype including shorter MN axons and locomotor deficits (Ciura et al., 2013). The second proposed mechanism is by gain of RNA toxicity. RNA foci containing the hexanucleotide repeat expansion are found clustered in the nuclei of neurons and glia in ALS patients harbouring the *C9ORF72* mutation, and are thought to act by disrupting protein function (DeJesus-Hernandez et al., 2011). These foci have been found in two forms, with one containing RNA transcribed in the sense direction and the other containing RNA transcribed in the anti-sense direction (Lagier-Tourenne et al., 2013). ASOs selectively target the sense

RNA, which contain the *C9ORF72* repeat, to degrade the expansion. To date ASOs have been shown to suppress formation of RNA foci in studies of human induced pluripotent stem cell (iPSC)- derived neurons and MNs harbouring *C9ORF72* mutations (Donnelly et al., 2013; Fernandes et al., 2013; Sareen et al., 2013). The final proposed mechanism to have a role in the toxicity of the *C9ORF72* mutation is repeat-associated RNA-encoded, non-ATG translation (RAN translation). This mechanism involves the translation of the $G_4C_2$ repeat into polypeptides containing repeating di-amino acids, leading to the formation of inclusions termed dipeptide repeat (DPR) proteins in neurons of *C9ORF72* patients (Ash et al., 2013; Ling et al., 2013; Mori et al., 2013). However, a recent study has challenged the involvement of this mechanism in the pathogenesis of *C9ORF72* ALS as DPR inclusions were rarely found in spinal cord MNs from patients with the *C9ORF72* mutation (Gomez-Deza et al., 2015). As the numbers of repeat expansions in the *C9ORF72* gene vary from patient to patient, it is likely that these mechanisms act in a non-mutually exclusive manner, much in the same way as the gain and loss of function mechanisms in *TARDBP* mutations do. Further understanding of the role of the normal *C9ORF72* protein may help uncover mechanisms by which *C9ORF72* contributes to the pathogenesis of ALS.

The presence of the aforementioned mutations in neuronal and glial cells contributes to the pathogenesis of ALS in a variety of ways. The following sections discuss studies that have demonstrated how these mutations cause MNs to become particularly vulnerable to toxic insult and the potential mechanisms by which they cause ALS pathology.

## Vulnerability of MNs

Although many cell types in the CNS are affected in ALS, MNs display selective vulnerability. However, not all MNs are affected, with oculomotor neurons and sacral MNs controlling sphincter muscles typically spared from degeneration for largely unknown reasons (Radunovíc and Leigh, 1996). Oculomotor MNs have been shown to express lower levels of the motor protein dynein and the intermediate neurofilament peripherin in mouse models and ALS patients, which may be linked to their resistance in ALS (Comley et al., 2015). Within vulnerable MN pools there is also variable vulnerability with large fast fatigable spinal MNs most vulnerable, fast fatigue-resistant MNs less vulnerable and slow tonic MNs the most resistant in ALS (Frey et al., 2000; Hegedus et al., 2007). The large soma size of MNs (50-60 μM) and their long axonal processes are thought to contribute to their vulnerability due to the associated high energy demands, requiring high mitochondrial activity. The high mitochondrial activity can cause increased oxidative stress, which results in accumulation of mutant proteins and oxidative damage. This in turn can lead to impaired energy production, causing normal levels of glutamate to become toxic (Wong et al., 1995; Kong and Xu, 1998). MN axons can be upwards of 1 metre in length in humans, requiring a robust network of neurofilamentous proteins that are crucial for maintaining the cells shape, as well as carrying out axonal transport from the soma to axonal terminals. The hallmark neuropathology of protein aggregates in the cytoskeleton of cells harbouring ALS mutations is especially toxic to MNs whose axonal transport function is critical for motor function (Shaw and Eggett, 2000).

One of the most widely accepted reasons why MNs are particularly susceptible in ALS is due to their high sensitivity to glutamate, which can lead to excitotoxicity

(Rothstein et al., 1995). During normal glutamatergic neurotransmission, glutamate is released from vesicles at the synaptic cleft, activating postsynaptic receptors, with re-uptake carried out by transporter proteins on both neuronal and glial cells, ending excitatory neurotransmission. However, if this process fails or becomes dysfunctional, excitotoxic damage can occur due to the excessive influx of $Ca^{2+}$ from over-stimulation of the glutamate receptors, initiating a cascade of harmful biochemical processes within the cell. The initial evidence implicating dysfunction of glutamate metabolism as a toxic factor in ALS came from studies showing increased levels of glutamate in samples of cerebrospinal fluid (CSF) from ALS patients (Rothstein et al., 1990; Shaw et al., 1995a).

Decreased capacity for glutamate transport and re-uptake in ALS, contributing to excitotoxicity, has been linked to the loss of the astroglial glutamate transporter excitatory amino acid transporter 2 (EAAT2), named GLT-1 in rodents (Bruijn et al., 1997; Bendotti et al., 2001b; Pardo et al., 2006; Kim et al., 2011). Studies have demonstrated the focal loss of EAAT2/GLT1 in the brainstem and spinal cord before any sign of MN degeneration (Howland et al., 2002) and has been accompanied by an increased expression of mutant *SOD1* G93A protein and the oxidative stress marker heme oxygenase-1 (HO-1) in astrocytes of the lumbar spinal cord (Guo et al., 2010). It has also been shown that lowering the expression of EAAT2/GLT-1 in wild type mice, through the administration of ASOs, causes increased glutamate levels, resulting in neurodegeneration and paralysis (Rothstein et al., 1996). Furthermore, disease onset is delayed by increasing expression of the human EAAT2 protein in *SOD1* G93A mice, protecting MNs from cytotoxicity and cell death after exposure to L-glutamate *in vitro*. However their life span remain unaffected (Guo et al., 2003).

Although many of these studies have focused on mouse models harbouring the *SOD1* mutation, human samples from SALS patients have also shown decreased expression of EAAT2, in one case attributed to alterations in RNA processing. Given that aberrant RNA processing is associated with *TARDBP*, *FUS* and *C9ORF72* mutations (Shaw et al., 1995a; Fray et al., 1998; Lin et al., 1998), a similar loss of EAAT2 may occur in cases of ALS involving these mutations.

The postsynaptic glutamate receptors are divided into two broad categories: ionotropic (ligand-gated ion channels) and metabotropic (G-protein coupled). Ionotropic receptors are subclassified as N-methyl-D-aspartate (NMDA) receptors; α-amino-3-hydroxy-5-methyl-4 isoxa-zole propionic acid (AMPA) receptors; and kainate receptors, so called after their pharmacological agonist. Metabotropic receptors are subclassified as mGluR1 to mGluR8 (Shaw and Ince, 1997; Van Den Bosch et al., 2006). AMPA receptors, responsible for the majority of fast excitatory transmission, are composed of four protein subunits named GluR1- 4, with the GluR2 subunit causing AMPA receptors to be impermeable to $Ca^{2+}$ (Shaw and Eggett, 2000; Joshi et al., 2011). Excessive intracellular $Ca^{2+}$ can cause activation of several enzymes including nitric oxide (NO) synthase that, by generating NO in large quantities, can cause toxicity. Mitochondrial dysfunction can also result from excessive intracellular $Ca^{2+}$, leading to the formation of reactive oxygen species (ROS)(Carriedo et al., 2000).

The $Ca^{2+}$ permeability of AMPA receptors vary depending on whether or not the GluR2 subunit is present (Hollmann et al., 1991). The ability of the GluR2 subunit to regulate $Ca^{2+}$ permeability of AMPA receptors in turn depends on RNA editing. RNA editing is a post-transcriptional modification that alters the GluR2 mRNA from a

codon encoding glutamine (Q) to a codon encoding arginine (R) (Sommer et al., 1991). AMPA receptors are $Ca^{2+}$ impermeable if they contain the edited GluR2 (R) subunit. On the other hand, AMPA receptors are $Ca^{2+}$ permeable if they are GluR2-lacking or if they contain the unedited GluR2 (Q) subunit (Hollmann et al., 1991). MNs are thought to be more vulnerable to glutamate toxicity than other cells as some studies have found that MNs express low levels of the GluR2 subunit in their AMPA receptors, implying that they are more permeable to $Ca^{2+}$ than other cells (Williams et al., 1997; Shaw et al., 1999; Van Damme et al., 2002). Other studies have shown that in the presence of ALS mutations, the regulatory capacity of GluR2 is abolished, causing decreased expression of GluR2 resulting in AMPA receptor mediated excitotoxicity (Kruman et al., 1999; Shaw and Eggett, 2000; Avossa et al., 2006; Van Damme et al., 2007; Zhao et al., 2008) However, these findings could not be confirmed by others (Tolle et al., 1993; Morrison et al., 1998; Vandenberghe et al., 2000; Laslo et al., 2001).

Evidence for a possible role of GluR2 in MN viability stems from a study in which transgenic mice, deficient in Q/R editing sites, display increased permeability to $Ca^{2+}$ resulting in neurological dysfunctions, including deficits in dendritic architecture. RNA editing, which includes GluR2 editing, is important for normal brain function and for regulating the electrophysiological properties of ion channels (Feldmeyer et al., 1999). Deficiencies in GluR2 RNA editing have been demonstrated in MNs of ALS patients, although no alterations in GluR2 mRNA expression levels have been detected (Kawahara et al., 2004). No such deficiencies have been detected in the mutant *SOD1* G93A or H46R mouse models (Kawahara et al., 2006). However, one study has demonstrated that crossing mutant *SOD1* mice with mice expressing GluR2

(Q) in their AMPA receptors accelerates disease progression and decreases survival, linking progressive motor decline and late-onset degeneration of spinal MNs with persistently elevated $Ca^{2+}$ influx through AMPA receptors (Kuner et al., 2005).

NMDA receptors, consisting of subunits NR1 and NR2 (A-D), are always $Ca^{2+}$ permeable. The molecular assembly of these receptors is important to prevent glutamate-induced toxicity, with changes in receptor expression levels described in some ALS studies (Shaw et al., 1994; Van Den Bosch et al., 2006). Neurotoxicity mediated by NMDA receptors leading to increased mitochondrial $Ca^{2+}$ and ROS production has been shown to take place in cultured MNs (Carriedo et al., 2000; Urushitani et al., 2001) and in organotypic spinal cord cultures of chick embryos (Brunet et al., 2009).

MNs that innervate voluntary muscles degenerate in ALS whilst, for unknown reasons, oculomotor MNs that regulate eye movements and MNs in Onuf's nucleus controlling external sphincters are resistant to degeneration (Mannen et al., 1977). Inhibitory synaptic transmission, mediated by GABAergic and glycinergic transmission, has been revealed to differ between oculomotor and hypoglossal MNs and may in part underlie their differential vulnerability in ALS (Lorenzo et al., 2006). Marked differences in genes with a function in synaptic transmission are seen between spinal cord MNs and oculomotor MNs in humans, rats and mice, with oculomotor MNs having a higher GABA-mediated chloride current compared to spinal cord MNs. Gene expression differences in the GluR2 subunit of the AMPA receptor have also been identified. GluR2 subunit expression is found at increased levels in oculomotor MNs compared to vulnerable spinal cord MNs in studies of post-mortem samples of control subjects (Dong et al., 1997; Brockington et al., 2013).

Therefore, reduced susceptibility to excitotoxicity, through increased expression of $Ca^{2+}$ impermeable AMPA receptor subunits or enhanced GABAergic transmission, may be an important determinant of the relative resistance of oculomotor MNs to degeneration in ALS (Van Damme et al., 2002; Brockington et al., 2013). Patterns of vulnerability, arranged by the physiological subtypes of axons, exist in two mutant *SOD1* mouse models of ALS where axons of fast-fatigable MNs are affected presymptomatically, followed by fast-fatigue-resistant MN axons at symptom-onset, whilst axons of slow MNs remain resistant (Pun et al., 2006). This study illustrated for the first time the selective vulnerability of MN axons and how affected axons and MNs can be distinguished from non-affected ones, aiding mechanistic investigations. MNs that are most vulnerable to degeneration in ALS have been shown to express higher levels of Ephrin type-A receptor 4 (EPHA4), which plays an important role in development of the nervous system, in particular establishing corticospinal projections (Dottori et al., 1998). EPHA4 levels were higher in the most vulnerable MNs in mutant *SOD1* mice, rat and zebrafish models, as well as in a mutant TDP-43 zebrafish model compared to the resistant MNs (Van Hoecke et al., 2012). EPHA4 has been shown to inhibit neuromuscular re-innervation of axotomized MNs (Goldshmit et al., 2011) preventing MNs from sprouting and recovering their function. Targeting and/or changing EPHA4 levels in animal and cellular models of ALS may reveal other deleterious effects of its overexpression.

Maintenance of intracellular $Ca^{2+}$ homeostasis is fundamental to normal cellular function, however the capacity of MNs to buffer any increases in intracellular $Ca^{2+}$ is limited by the low expression levels of $Ca^{2+}$ binding proteins, including parvalbumin and calbindin D28k, making MNs more vulnerable to increased $Ca^{2+}$ levels.

Expression of $Ca^{2+}$ binding proteins has been found to be higher in MNs which are more resistant in ALS (Ince et al., 1993; Alexianu et al., 1994; Hayashi et al., 2013). The direct consequence of lower expression of $Ca^{2+}$ binding proteins in MNs means that mitochondria have to work harder to buffer $Ca^{2+}$ leading to mitochondrial calcium overload, causing dysfunction. Studies have shown that impaired $Ca^{2+}$ handling and $Ca^{2+}$ dysregulation is linked to the pathogenesis in ALS (Jaiswal et al., 2009; Grosskreutz et al., 2010; Kawamata and Manfredi, 2010; Tradewell et al., 2011; Aggad et al., 2014) and through the use of $Ca^{2+}$ channel agonists, neuromuscular function can be protected (Armstrong and Drapeau, 2013).

Neurodegenerative diseases are characterized by the selective degeneration of specific cellular populations. In ALS, MNs are the most vulnerable cell type due to their large cell size, their sensitivity to glutamate and the glutamate receptor subunits they express as well as their low expression levels of $Ca^{2+}$ binding proteins. As spinal cord MNs are more vulnerable in ALS than oculomotor MNs and those in Onuf's nucleus, identifying mechanisms of vulnerability and resistance in these groups could lead to future therapies.

## Mechanisms of disease in ALS

Many cellular mechanisms have been proposed to contribute to the pathogenesis of ALS. Some reflect activation of neurodegenerative pathways and others are the result of the dysfunction of normal cellular processes. None of these mechanisms appear to act independently but rather they are likely to act together to cause the pathologies found in the disease.

### 1.1.5 Mitochondrial dysfunction

Mitochondria are essential cellular organelles that have central roles in providing energy in the form of adenosine triphosphate (ATP) and regulating intracellular $Ca^{2+}$. They are also sources of reactive oxygen species (ROS) and control apoptosis (Kawamata and Manfredi, 2010; Ferraiuolo et al., 2011). As the function of mitochondria can be linked to most of the proposed causal mechanisms in ALS such as oxidative stress, glutamate excitotoxicity and axonal transport disruption, mitochondria are described as a convergence point in MN degeneration. Altered mitochondrial morphology and accumulation of mutant *SOD1* in vacuolated mitochondria was first described in the *SOD1* G93A and G37R mutant mouse models prior to disease onset (Wong et al., 1995; Bendotti et al., 2001a; Jaarsma et al., 2001; Vehviläinen et al., 2014) and in ALS patient samples (Sasaki and Iwata, 1996a). Abnormal mitochondrial aggregates and mitochondrial dysfunction have also been found in disease models harbouring mutant TDP-43 (Wegorzewska et al., 2009; Shan et al., 2010; Xu et al., 2010, 2011) and in a human induced pluripotent stem cell (iPSC) model harbouring the *C9ORF72* mutation (Kiskinis et al., 2014). The mechanisms by which these alterations in mitochondrial function can contribute to the pathogenesis of ALS include defects in respiratory chain function (Bowling et al., 1993; Menzies et al., 2002), impaired $Ca^{2+}$ buffering capacity (Kruman et al., 1999; Jaiswal et al., 2009; Fuchs et al., 2013), subcellular localisation of *SOD1* (Liu et al., 2004; Deng et al., 2006), mitochondrial dependent oxidative stress (Braun et al., 2011) and disrupted axonal transport of mitochondria in FALS and SALS (Mori et al., 2008; Sasaki et al., 2010). Studies have also shown that mutant *SOD1* has a tendency to accumulate in spinal cord MNs, however, it is the misfolding and localization of

mutant *SOD1* in the mitochondria, rather than the formation of mutant *SOD1* aggregates, that contribute to the disease (Wong et al., 1995; Jaarsma et al., 2001; Dupuis et al., 2004; Vehviläinen et al., 2014).

Most if not all studies recognise that mitochondrial dysfunction is a key element in the pathogenesis of ALS, however the extent to which its dysfunction contributes to the disease onset and progression remains to be determined. Some studies have disputed how crucial mitochondrial dysfunction is in the pathogenesis of ALS, with findings varying in degrees of involvement, These include studies which demonstrate that mitochondrial dysfunction in neuronal and glial cells trigger the onset of MN degeneration (Kong and Xu, 1998), that restoring mitochondrial function after MN degeneration onset does not extend the life span of ALS mouse models (Zhu and Sheng, 2011; Pehar et al., 2014) and that restoring function can extend ALS model life span (Miquel et al., 2012). The identification of whether mitochondrial dysfunction is the primary cause or rather a consequence of ALS pathology may be fundamental in the search for new therapeutic strategies.

### 1.1.6 Endoplasmic reticulum stress

The accumulation of misfolded or unfolded protein in intracellular inclusions is a pathological hallmark of ALS. The endoplasmic reticulum (ER) is the first compartment where secreted and membrane proteins are synthesized and folded. As the ER has roles in cellular homeostasis, protein folding and lipid biosynthesis, alterations in any of these processes can lead to increased protein synthesis, changes in $Ca^{2+}$ levels or the accumulation of misfolded protein. The ER requires an efficient network of chaperones to promote folding and prevent abnormal aggregation of

proteins. However, if levels of misfolded protein become uncontrollable, ER stress can occur (Atkin et al., 2006; Ferraiuolo et al., 2011; Ozcan et al., 2012). ER stress induces the unfolded protein response (UPR) to re-establish homeostasis by increasing the protein folding capacity and quality control mechanisms of the ER (Walter and Ron, 2011). Although UPR activation is required in times of cellular stress, its prolonged activation triggers apoptotic signalling, causing irreversible damage to cells through diverse mechanisms (Ferraiuolo et al., 2011; Matus et al., 2013).

The involvement of ER stress in ALS is supported by the finding of increased levels of ER stress markers in patient spinal cords (Atkin et al., 2008) and co-localisation of ER stress markers with *SOD1* inclusions in mutant *SOD1* mouse models at early stages of the disease (Atkin et al., 2006). Furthermore, vulnerable MNs appear to be selectively prone to ER stress in mutant *SOD1* mouse models since they display upregulation of ER stress markers preceding MN degeneration (Saxena et al., 2009; Bernard-Marissal et al., 2012). TDP-43 pathology has also been linked to ER stress which can be mediated via either mitogen-activated protein kinase/ extracellular signal-regulated kinases (ERK1/2) (Ayala et al., 2011), ER $Ca^{2+}$ signalling dysregulation (Aggad et al., 2014; Mutihac et al., 2015) or stress granule formation (Walker et al., 2013). ER stress has also been shown in post-mortem tissue from patients with the *C9ORF72* repeat expansion where aggregation prone proteins cause neurotoxicity by inducing ER stress (Zhang et al., 2014).

Biomarkers of ALS are needed to assess disease prognosis and the efficacy of clinical trials. One possible biomarker option has been uncovered when ER chaperones, under conditions of cell stress, have been secreted into the extracellular space. ER

chaperones are up-regulated in the CSF of ALS patients (Atkin et al., 2008), suggesting that measuring stress factors in CSF may prove a useful tool to monitor ALS disease progression. Recently, screens for biomarkers in blood samples from SALS patients and mutant *SOD1* mice have demonstrated an up-regulation in the ER stress-responsive chaperones compared to controls (Nardo et al., 2011), again suggesting their possible use in diagnosis and therapeutics (Matus et al., 2013). ER stress stimuli determine how the UPR integrates information regarding the control of cell fate and is therefore a promising target for the manipulation and modulation of cell death and survival mechanisms. As studies of SALS and FALS samples have provided evidence for ER stress in ALS, regardless of the specific genetic alteration, ER dysfunction may act as a promising general target.

### 1.1.7 Oxidative stress

The process of oxidative stress is a major contributor to ALS pathology. It occurs when oxygen-derived species, by-products of metabolic processes that utilise molecular oxygen, are generated at levels beyond those that antioxidant defences are able to cope with, causing damage to the cell and their proteins, lipids and nucleic acids (Bergeron, 1995). Oxidative damage has been identified in post-mortem studies of SALS tissue (Shaw et al., 1995b; Ilieva et al., 2007; D'Amico et al., 2013) and has been linked to *SOD1* mutations which alter the normal role of *SOD1* in catalysing the conversion of superoxide radicals to hydrogen peroxide and oxygen (Cluskey and Ramsden, 2001; Barber et al., 2006; Kiskinis et al., 2014). However, as not all studies have found that inactive *SOD1* causes MN degeneration, mutant *SOD1* may cause oxidative stress via another mechanism, likely by toxic gain of function (Barber and Shaw, 2010).

A role for oxidative stress in other FALS cases has been demonstrated using yeast models harbouring mutant TDP-43 (Duan et al., 2010; Braun et al., 2011) and a *Drosophila* model expressing TDP-43 in MNs (Zhan et al., 2014). In both models, markers for oxidative stress are increased. In response to cell stress, including oxidative stress, TDP-43 is also recruited to stress granules, and once endogenous TDP-43 accumulates, either in mutant or non-mutant form, it can form protein aggregates leading to cell dysfunction (Colombrita et al., 2009; Ayala et al., 2011; Dewey et al., 2011; Parker et al., 2012). Mutant *C9ORF72* has also been linked to oxidative stress in human tissue. The use of a methylation promoter reduces the vulnerability of the cells to oxidative stress (Liu et al., 2014), with increases in the oxidative stress response detected in human iPSC derived MNs (Kiskinis et al., 2014). It has also been shown that oxidative stress may play a role in SALS. Oxidation resistance 1 (OXR1) has been shown to be up-regulated in the spinal cord of end-stage ALS patients as well as in the presymptomatic mutant *SOD1* mouse model (Oliver et al., 2011). Mice deficient in OXR1 display neurodegeneration suggesting that OXR1 could serve as a neuroprotective factor in neurodegenerative diseases (Oliver et al., 2011).

Oxidative stress can cause considerable damage to MN and glial populations, and is capable of influencing other mechanisms implicated in ALS. However, the ultimate toxic insults that cause increased levels of reactive oxygen species (ROS) are still largely unknown, leading to speculation as to whether oxidative stress is a primary cause of disease or a downstream consequence. The definitive cause in the majority of ALS cases remains unknown; therefore attempts to target possible causes and consequences, including oxidative stress for therapeutic intervention, may prove

beneficial. As treatment can be started only after symptom onset and clinical diagnosis, the underlying cause of oxidative stress may be less relevant than the downstream effects it has. Recently, studies have shown that by treating ALS affected cells with antioxidants, disease progression is delayed and survival extended. These studies were conducted in: a mutant *SOD1* mouse model (Benatar, 2007), in a mutant *SOD1* mouse crossed with a neuron specific antioxidant (OXR1) expressing mouse (Liu et al., 2015) and in cultures of mutant *SOD1* astrocytes before co-culturing with MNs (Cassina et al., 2008; Marchetto et al., 2008). Antioxidants have also been used in studies involving ALS mutations other than mutant *SOD1* (Rojas et al., 2014). Alterations in electrophysiological properties found in a neuroblastoma cell line transfected with mutant TDP-43 have been ameliorated after treatment with an antioxidant (Dong et al., 2014). Furthermore, in HeLA cells transfected with mutant TDP-43 and overexpressing OXR1, OXR1 binds to mutant TDP-43 and reduces cytoplasmic mislocalisation (Finelli et al., 2015). These findings suggest that targeting oxidative stress pathways may uncover beneficial treatments that could be used for all ALS patients, regardless of the underlying cause.

### 1.1.8 Protein misfolding

In addition to MN loss from the brainstem, spinal cord and motor cortex, a universal pathological hallmark of ALS is the presence of abnormal intracellular deposits of aggregated proteins in MNs (Strong et al., 2005). Protein misfolding is the likely initiator of the formation of protein aggregates. The ubiquitin proteasome system (UPS), one of the main mechanisms controlling the degradation of misfolded proteins, has, in some studies, impaired proteasomal activity that correlates with the formation of protein aggregates in ALS (Urushitani et al., 2002; Tashiro et al., 2012). Misfolded

mutant proteins can accelerate the formation of protein aggregates by impairing the degradation pathways. Hyaline conglomerates rich in neurofilamentous protein which are found in spinal cord MNs from ALS patients, especially those with *SOD1* mutations (Ince et al., 1998), can lead to perturbations in axonal function. Increased neurofilament phosphorylation is seen in the perikarya of MNs harbouring *TARDBP* mutations, which may also contribute to axonal neurofilament transport dysfunction (Ackerley et al., 2000).

Many studies investigating *SOD1* misfolding and aggregation use wild-type *SOD1* as, although mutant *SOD1* is more prone to misfolding, wild-type *SOD1* can also be induced to misfold and form aggregates in a similar way (Rakhit et al., 2002; Atkin et al., 2006; Bosco et al., 2010). It has been demonstrated that overexpression of wild-type *SOD1* can induce an ALS -like pathology causing mild motor abnormalities even in the absence of mutant *SOD1*(Jaarsma et al., 2000), suggesting that misfolding of wild-type *SOD1* could be involved SALS. *SOD1* aggregates have been identified in SALS cases in studies conducted by one group (Shibata et al., 1994). However, these results have not been reproduced by other groups (Watanabe et al., 2001; Liu et al., 2009). Studies of protein aggregation in three mutant *SOD1* mouse models demonstrated that mutant *SOD1* aggregates appear late in the disease in parallel with progressive motor phenotypes, suggesting that aggregates are involved in later stages and are unlikely to be a main toxic feature (Karch and Borchelt, 2008).

Ubiquitin-positive TDP-43 inclusions are a key pathological feature of SALS and many non-*SOD1* FALS cases, including those harbouring *TARDBP* and *C9ORF72* mutations (Arai et al., 2006; Neumann et al., 2006; Mackenzie et al., 2007). As described earlier, TDP-43 is redistributed to the cytosol from the nucleus in ALS and

FTLD tissue before the formation of visible inclusions (Giordana et al., 2010; Sasaki et al., 2010). These findings suggest that these TDP-43 inclusions, in a similar way to *SOD1* inclusions, are not likely to be the key toxic species (Barmada et al., 2014). Whilst it remains unclear as to how the process of protein misfolding and aggregate formation contributes to the pathogenesis of ALS and if the aggregates are themselves toxic, it is likely that the protein constituents and their conformation in these aggregates will provide important insights into the mechanisms behind the formation of these pathological hallmarks.

### 1.1.9 Apoptosis

Apoptosis, or programmed cell death, is a mechanism by which cells die after the activation of processes within a cell, without damaging neighbouring cells. The process of apoptotic cell death is rapid in relation to the time course of ALS, making it difficult to provide conclusive evidence for its involvement in the disease. The potential involvement of apoptosis in the pathogenesis of ALS has been supported by studies showing that in ALS patient tissue samples, degenerating spinal cord MNs morphologically resemble apoptotic cells due to the presence of cytoplasmic and nuclear clusters and apoptotic body formation (Troost et al., 1995; Martin, 1999). However, these cytoplasmic and nuclear clusters were not evident in all studies (Migheli et al., 1994). The redistribution of cell death proteins and activation of caspase-3 in ALS patient samples and in mutant *SOD1* mice provides further evidence in support of the involvement of apoptosis in the pathogenesis of ALS (Martin, 1999; Li et al., 2000; Pasinelli et al., 2000; Kang et al., 2003). The activation of mitochondrial apoptotic pathways has been identified in mutant *SOD1* mouse spinal cords (Guégan et al., 2001) and it has been shown that blockade of this mitochondrial

apoptotic pathway can halt the degeneration of MNs and extend their survival in mutant *SOD1* G93A animals (Sathasivam and Shaw, 2005; Reyes et al., 2010) .

Apoptosis has also been identified as a potential pathological disease mechanism in some models harbouring *TARDBP* mutations. Cell lines and primary mouse MNs harbouring the TDP-43 M337V mutation display increased caspase-3 staining compared to MNs with wild-type TDP-43 (Mutihac et al., 2015). Studies of SALS patient tissue samples indicate that the intracellular accumulation of TDP-43 fragments leads to activation of apoptotic pathways (Rutherford et al., 2008). In addition, inhibition of apoptosis in a mutant *TARDBP Drosophila* model prevented MN toxicity (Zhan et al., 2013). Apoptosis may also occur in models harbouring the *C9ORF72* mutation as studies have indicated that the accumulation of di-peptide repeats (DPRs) trigger apoptotic pathway activation and lead to MN degeneration (Stepto et al., 2014).

Although studies have demonstrated the involvement of apoptosis in the pathogenesis of ALS and that targeting and blocking apoptosis increases the lifespan of ALS animal models (Li et al., 2000; Reyes et al., 2010; Zhan et al., 2013), it is unlikely that this is the primary cause of the degenerative processes in ALS. As apoptosis is required during normal development, blocking it entirely would lead to other problems. Regulating apoptosis through the UPR may act as an alternative to blocking apoptosis completely in order to uncover the true role of apoptosis in ALS.

### 1.1.10 Axonal transport dysfunction

Axonal transport is a vital cellular function for MNs and defects in this process have been implicated as a mechanism of disease in ALS (LaMonte et al., 2002). The

components required for axonal transport are specialised motor proteins such as dynein, dynactin-1 and kinesin, and cytoskeletal actin filaments and microtubules. Decreased expression levels of some of these proteins are found in spinal cord MNs from post-mortem SALS patient samples (Jiang et al., 2005; Ikenaka et al., 2012). Due to these alterations in the expression of motor proteins, the cargos which motor proteins transport can accumulate within the degenerating MNs, causing dysfunction (Soo et al., 2011). Transport dysfunction can also occur when neurofilaments, responsible for maintaining correct morphology and size of MNs, accumulate in the pathological protein aggregates seen in ALS (Collard et al., 1995; Rao and Nixon, 2003). Studies implicating axonal transport in the pathogenesis of ALS include those carried out in mutant *SOD1* G93A mouse models where defects in fast retrograde and anterograde axonal transport of MNs have been identified, with these defects often occurring presymptomatically (Williamson and Cleveland, 1999; Bilsland et al., 2010; Ikenaka et al., 2012; Millecamps and Julien, 2013). The accumulation of mitochondria in the soma due to defects in axonal transport has been demonstrated in studies of SALS patients (Sasaki and Iwata, 1996b) and ALS mouse models harbouring *SOD1* or *TARDBP* mutations (Magrané and Manfredi, 2009; Bilsland et al., 2010; Wang et al., 2013; Magrané et al., 2014), causing downstream mitochondrial dysfunction and contributing to MN degeneration. mRNA transport deficits also occur due to the presence of *TARDBP* mutations that impair axonal transport abilities (Alami et al., 2014). Alterations in axonal transport can also cause the accumulation of autophagosomes, whose pathway is responsible for regulating intracellular content recycling, leading to cellular dysfunction (Sasaki, 2011).

Axonal degeneration can also occur in mutant *SOD1* mouse models independently of deficits in axonal transport (Marinkovic et al., 2012). One study has shown that even by enhancing mitochondrial mobility in mutant *SOD1* mice, the onset of ALS-like symptoms were unaffected (Zhu and Sheng, 2011). Alterations in axonal transport organelles and their proteins in ALS patients most likely indicate that they become more vulnerable due to the various disease processes on-going in their environment. Overall, it remains unclear whether defects in axonal transport are a cause or a consequence of ALS. As MNs have particularly long axons, they are uniquely vulnerable to defects in axonal transport, therefore, even if other processes are involved in disease initiation, inhibition and dysfunction of axonal transport may play a critical part in the resulting disease mechanisms.

### 1.1.11 Non-cell autonomy

Whether MN degeneration in ALS is mediated via processes within MNs (cell autonomous) or is caused by populations of other cells (non-cell autonomous) has been widely investigated over a number of years. Glial cells are the most numerous cells of the CNS, of which there are four types: astrocytes, oligodendrocytes, microglia and ependymal cells. The initial evidence implicating non-cell autonomy in ALS came from studies in which increased levels of glutamate were found in CSF samples from ALS patients (Rothstein et al., 1990; Shaw et al., 1995a). The increased glutamate levels in patient CSF has been linked to the decreased expression of the astroglial transporter, EAAT2 (GLT-1 in rodents), which removes glutamate from the extracellular space, terminating neuronal excitation (Bruijn et al., 1997; Bendotti et al., 2001b; Pardo et al., 2006; Kim et al., 2011). Decreased GLT-1 expression has also been found in ALS mutant *SOD1* mouse models before any signs of MN degeneration

(Howland et al., 2002). Non-cell-autonomous processes in glial cells are believed to be implicated not only in disease progression, but also to be related with the onset and early stages of the disease, thus underlying MN dysfunction and loss.

Microglia are the primary immune cells of the CNS responsible for protection against various pathogens. Their involvement in ALS has been demonstrated in a chimeric mouse model where disease progression is delayed when MNs expressing mutant h*SOD1* are surrounded by wild-type microglia whereas control MNs surrounded by mutant h*SOD1* expressing microglia degenerate (Clement et al., 2003). The involvement of microglia in ALS has also been supported by further studies in which the deletion of mutant *SOD1* from microglia slowed disease progression and led to the release of less toxic factors from microglia (Beers et al., 2006; Boillée et al., 2006; Lee et al., 2012; Frakes et al., 2014). These findings suggest a possible neuroprotective role for wild-type microglia in ALS (Boillée et al., 2006; Ilieva et al., 2009; Lasiene and Yamanaka, 2011).

Oligodendrocytes, responsible for the production of myelin sheaths surrounding neurons, provide electrical insulation essential for rapid signal conduction. NG2 cells (polydendrocytes) differentiate into oligodendrocytes *in vitro.* NG2 cells are also one of the first cells that respond to any alteration in CNS environment (Nishiyama et al., 2009). In ALS mouse models and ALS patients, the capacity of NG2 cells to differentiate into oligodendrocytes is unaffected by the presence of ALS mutations (Kang et al., 2010). However, new oligodendrocytes fail to mature and express reduced myelin basic protein, resulting in grey matter demyelination (Kang et al., 2013). Extensive degeneration of oligodendrocytes in the spinal cord is also seen in ALS patient samples and in mutant *SOD1* mice prior to disease onset (Stieber et al.,

2000; Jaarsma et al., 2008; Kim et al., 2013). These findings suggest that oligodendrocytes may contribute to MN degeneration in ALS (Philips et al., 2013; Cui et al., 2014; Satoh et al., 2015).

Astrocytes, which are divided into either protoplasmic (located in grey matter) or fibrous (located in white matter) types, account for the majority of glial cells in the brain and spinal cord and have long been associated with roles as support cells, aiding the organization of neuronal networks and supplying neuronal nutrients through their connection and maintenance of the blood brain barrier (Montgomery, 1994). Astrocytes play vital roles in glutamate reuptake through their transporters, including EAAT2, in order to prevent excitotoxicity. They are also an important component of the astrocyte-neuron lactate shuttle (ANLS) model. This model begins with neuronal activity, which causes an increase in extracellular glutamate. The extracellular glutamate is taken up by EAAT2, followed by the increase in intracellular $Na^+$ that activates the $Na^+/K^+$ ATPase, increasing ATP consumption, glucose uptake and glycolysis in astrocytes. This causes a large increase in lactate production which, when released into the extracellular space, is used as an energy source for neurons for the production of ATP (Pellerin and Magistretti, 1994; Pellerin et al., 2007).

Astroglial activation, or astrogliosis, is characterized by hypertrophy of cell bodies and cytoplasmic processes as well as the up-regulation of intermediate filament protein expression, namely GFAP and vimentin. Reactive astrogliosis in ALS was first revealed by increased GFAP staining in the subcortical white matter in SALS patient samples (Kushner et al., 1991) and in the ventral and dorsal horns of the spinal cords of SALS patients (Schiffer et al., 1996; Schiffer and Fiano, 2004). Astrocytes derived from mutant *SOD1* mice are also found to be dysfunctional. They are less

efficient at glutamate uptake compared to controls, and have reduced trophic response to activation, resulting in failure to protect MNs effectively (Benkler et al., 2013). Early studies of the astroglial glutamate transporters have revealed lower expression of EAAT2 (GLT-1) in SALS samples and in mutant *SOD1* mouse models (Rothstein et al., 1995; Bruijn et al., 1997), linking dysfunctional astrocytes to glutamate excitotoxicity. The failure of glutamate re-uptake by EAAT2 causes sustained elevation of neuronal intracellular $Ca^{2+}$ initiating a cell death cascade. The permeability of AMPA receptors to $Ca^{2+}$ also plays a role in excitotoxicity, as MNs express low levels of the GluR2 subunit making them more permeable to $Ca^{2+}$, leaving MNs to rely on astrocytes to induce GluR2 subunit up-regulation. Astrocytes expressing mutant h*SOD1* lose their ability to regulate GluR2 expression, increasing MN vulnerability to AMPA receptor-mediated excitotoxicity (Van Damme et al., 2007). Wild-type astrocytes have been found to have neuroprotective roles in some studies in a similar manner as wild-type microglia. The transplantation of wild-type astrocyte precursors into transgenic *SOD1* G93A rats causes an increase in survival time and slows physical decline in motor deficits compared to the mutant *SOD1* rats with mutant *SOD1* astrocytes (Lepore et al., 2008). However, transplants of human astrocyte precursors into *SOD1* G93A mice has failed to slow the disease progression (Lepore et al., 2011).

Damage to MNs by neighbouring cells expressing mutant *SOD1* appears to be required for MN degeneration, since no pathology has been seen in mice in which only MNs express mutant *SOD1* (Pramatarova et al., 2001; Lino et al., 2002). Conversely, several studies have shown that wild-type MNs degenerate in the presence of mutant *SOD1* astrocytes (Yamanaka et al., 2008; Diaz-Amarilla et al.,

2011; Papadeas et al., 2011). The development of stem cell technology has aided the study of ALS in cell culture-based assays, enabling the co-culture of different cell types. Using this technology, mouse embryonic stem cell (ESC)- derived MNs expressing wild type or mutant *SOD1* have been co-cultured with primary *SOD1* G93A astrocytes. The mutant *SOD1* astrocytes cause primary mouse MNs and ESC derived MNs, harbouring either wild type or mutant *SOD1*, to degenerate (Di Giorgio et al., 2007; Nagai et al., 2007). These studies have also shown that spinal MNs are specifically targeted by the toxic factors released by mutant astrocytes, as these were the sole cell type affected. Interestingly direct co-culture of astrocytes with MNs is not required in order to cause toxicity as MNs cultured with mutant *SOD1* astrocyte conditioned medium (ACM) also degenerate (Nagai et al., 2007). In a humanised *in vitro* ALS model, non-cell autonomous disease mechanisms have been linked to *SOD1* FALS and SALS, as primary astrocytes from SALS and *SOD1* FALS patients, co-cultured with human ESC-derived MNs, cause MN death (Haidet-Phillips et al., 2011). Silencing mutant *SOD1* in *SOD1* FALS patient astrocytes prevents MN death, but mutant *SOD1* does not cause SALS astrocyte toxicity. However, SALS and FALS astrocytes have both been shown to trigger MN death through a similar mechanism, necroptosis, a programmed form of cell death/ necrosis (Re et al., 2014).

Whilst it is largely accepted that mutant *SOD1* harbouring astrocytes act via non-cell autonomous mechanisms to cause MN death in ALS, the same can't be said for mutant TDP-43. Studies that suggest that mutant TDP-43 does not act via non-cell autonomous disease mechanisms include one utilising human iPSC-derived astrocytes generated from fibroblasts of a patient harbouring a *TARDBP* M337V mutation. Even though these astrocytes display TDP-43 mislocalisation, increases in levels of TDP-43

and decreases in cell survival, they did not effect the survival of MNs derived from healthy control iPSCs (Serio et al., 2013). Similarly, astrocytes from mouse models either lacking TDP-43 or overexpressing mutant TDP-43 fail to cause the death of wild-type spinal MNs in culture (Haidet-Phillips et al., 2013). Glial-restricted precursors transplanted into the wild-type rat spinal cord differentiate into astrocytes. Similar to *in vitro* findings, astrocytes with TDP-43 mutations fail to affect wild-type MNs *in vivo* (Haidet-Phillips et al., 2013). However, not all studies support these findings. Rats in which the expression of mutant TDP-43 (M337V mutation) is restricted to astrocytes exhibit a progressive loss of MNs and skeletal muscles denervation, resulting in progressive paralysis. They also have decreases in astroglial glutamate transporter levels and display high levels of reactive gliosis (Tong et al., 2013). The potential non-cell autonomous effect of mutant TDP-43 astrocytes on wild-type MNs has also been studied in primary cultures of wild-type spinal cord MNs after exposure to ACM from primary mutant *SOD1* and mutant TDP-43 astrocytes. Application of the ACM causes MN degeneration through nitroxidative stress, with both mutations triggering cell death through this common pathogenic pathway (Rojas et al., 2014). Therefore, further studies are required in order to decipher if non-cell autonomy is a common disease mechanism among all ALS cases or if it acts only in specific genetic cases.

Many studies have been carried out to determine how and why glial cells selectively target MNs to initiate or cause the onset and progression of ALS pathology. The most studied pathways involve oxidative stress and mitochondrial dysfunction, however the roles they play still remain poorly understood. It has been suggested that the initial release of toxic factors, initiated by the processes of oxidative stress and

mitochondrial dysfunction, lead to MN death (Catania et al., 2001; Ferri et al., 2004; Cassina et al., 2005, 2008; Marchetto et al., 2008; Chen et al., 2010; Re et al., 2014). The possible influence of oxidative stress and mitochondrial dysfunction in non-cell autonomy is supported by the finding that mutant astrocytes exposed to antioxidants and mitochondrial inhibitors, *in vitro* and *in vivo*, delay the onset of ALS and extend life expectancy (Cassina et al., 2008; Marchetto et al., 2008). Activation of the nuclear factor erythroid-2-related transcription factor 2 (Nrf2) in astrocytes has been shown to have a role in regulating antioxidant defences. Nrf2 over-expression in mutant h*SOD1* G93A mouse astrocytes has been found to prevent toxicity to MNs, again delaying disease onset and extending survival (Vargas et al., 2008; Johnson et al., 2009; Petri et al., 2012). More recently, primary cultures of mouse spinal cord MNs exposed to ACM from cultures of mutant *SOD1* or mutant TDP-43 astrocytes, results in MN toxicity and cell death through $Na^+$ channel activation and nitroxidative stress. These MNs survive when they are co-cultured with antioxidants and $Na^+$ channel blockers (Rojas et al., 2014).

ALS is a fatal neurodegenerative disorder with limited identified targets, biomarkers, and therapeutic options. A better understanding of the molecular mechanisms underlying this disease is necessary in order to develop novel therapeutic strategies. Evidence from many studies, including those mentioned above, suggests that a complex pathological interplay between MNs and glial cells exists. The mechanisms involved and pathways in which these occur needs to be explored further. Non-cell autonomy has been strongly linked with glial cells harbouring mutant *SOD1* with some studies showing similar features in glial cells harbouring *TARDBP* mutations. Connecting non-cell autonomy with other genetic causes of ALS, including *C9ORF72*

and SALS cases, could lead to the discovery of a common disease mechanism, enabling the generation of beneficial therapeutic treatments for all. In Chapter 2, I will describe non-cell autonomous effects of iPSC-derived astrocytes harbouring *C9ORF72* or *TARDBP* mutations on control iPSC-derived MNs.

### 1.1.12 Excitotoxicity

Glutamate, the main excitatory neurotransmitter in the CNS, exerts its effects through various ionotropic and metabotropic postsynaptic receptors. Glutamate reuptake transporters, of which EAAT2 is the most abundant, remove glutamate from the synaptic cleft and terminate the excitatory signal. Under normal conditions, glutamate is released from the presynaptic neuron and activates NMDA and AMPA receptors, causing an influx of both $Na^+$ and $Ca^{2+}$ ions, leading to an action potential if threshold is reached (Shaw and Ince, 1997). Excitotoxicity is divided into two types: classical and slow. Classical excitotoxicity refers to neuronal degeneration that occurs after an increase in the extracellular glutamate concentration that results from increased glutamate release or the deficient re-uptake of glutamate by EAAT2 (GLT-1). Slow excitotoxicity is the death of a weakened postsynaptic neuron in the presence of normal synaptic glutamate levels (Heath and Shaw, 2002; Van Damme et al., 2005b; Van Den Bosch et al., 2006). In both these forms of excitotoxicity, glutamatergic neurotransmission plays a pivotal role. When glutamate is released from the presynaptic neuron, either ionotropic or metabotropic glutamate receptors may be activated. Ionotropic glutamate receptors are ligand-gated cation channels, while metabotropic glutamate receptors are G- protein coupled receptors that influence second messenger systems. Ionotropic receptors can be further subdivided into three classes (Seeburg, 1993): AMPA, NMDA and KA (kainate) receptors.

Functionally, AMPA receptors are the most important glutamate receptors to mediate fast excitatory transmission whilst NMDA receptors mediate the late component of excitatory transmission (Watkins and Evans, 1981; Collingridge and Singer, 1990) and play a key role in the induction of synaptic plasticity (Nicoll and Malenka, 1999).

The involvement of excitotoxicity in the pathogenesis of ALS was first proposed when increased levels of glutamate were found in samples of cerebrospinal fluid (CSF) from ALS patients (Rothstein et al., 1990; Shaw et al., 1995a), with similar increases later identified in mutant *SOD1* mice (Alexander et al., 2000). It has been suggested that plasma and CSF from ALS patients contain toxic components as application of either plasma or CSF from ALS patients to cultured neurons leads to excitotoxicity (Couratier et al., 1993; Sen et al., 2005). Cell death was prevented in cortical neurons upon application of the AMPA receptor blocker CNQX, which prevented further excitotoxic insult (Couratier et al., 1993).

Excitotoxicity has also been implicated in studies which found that glutamate transport function in the brain and spinal cord of SALS patients is decreased (Rothstein et al., 1992). Further studies have revealed this was caused by the selective loss of the astroglial glutamate transporter, EAAT2 (GLT1), in the motor cortex and spinal cord (Rothstein et al., 1995). Alterations in expression of EAAT2 (GLT-1) have been identified in SALS patients (Rothstein et al., 1995; Fray et al., 1998; Lin et al., 1998) and mutant *SOD1* rodent models (Bruijn et al., 1997; Bendotti et al., 2001b; Pardo et al., 2006; Kim et al., 2011), however not all studies are in agreement (Deitch et al., 2002). Further studies have demonstrated the focal loss of EAAT2 (GLT1) in the brainstem and spinal cord before any MN degeneration (Howland et al., 2002), accompanied by an increased expression of mutant *SOD1* protein and the oxidative

stress marker heme oxygenase-1 (HO-1) in astrocytes in the lumbar spinal cord (Guo et al., 2010). A study in which expression of EAAT2 (GLT-1) was lowered in control mice through the administration of antisense oligonucleotide (ASO), demonstrated an increase in glutamate levels, leading to neurodegeneration and paralysis providing further evidence for the involvement of loss of EAAT2 in ALS (Rothstein et al., 1996). Disease onset is delayed by increased expression of the human EAAT2 protein in *SOD1* G93A mice, with MNs protected from cytotoxicity and cell death after exposure to L-glutamate *in vitro*. However, life span is unaffected by increased EAAT2 expression (Guo et al., 2003).

Mitochondrial dysfunction has also been linked to excitotoxicity, as studies have shown that mutant *SOD1* interferes with mitochondrial function, which becomes more pronounced during disease progression and often affects the spinal cord more than other tissues (Jaarsma et al., 2000, 2001; Higgins et al., 2003). Mitochondrial dysfunction likely contributes to excitotoxicity through defects in the $Ca^{2+}$ buffering capacity of the mitochondria (Urushitani et al., 2001; Bilsland et al., 2008; Jaiswal and Keller, 2009; Jaiswal et al., 2009). This defect will have more pronounced consequences in MNs as these organelles play a crucial role in $Ca^{2+}$ buffering in MNs. This defect can further lead to an increase in the cytoplasmic $Ca^{2+}$ concentration, causing over-activation of $Ca^{2+}$ dependent enzymes, resulting in neuronal death through excitotoxic mechanisms. Mitochondrial dysfunction has recently been linked to excitotoxicity in ALS cases other than those caused by mutant *SOD1*. Miro1, a key regulator of mitochondrial movement, is reduced in SALS patient spinal cord samples, as well as in mutant *SOD1* mice and mutant TDP-43 mice. Excessive glutamate challenge *in vitro* and *in vivo* causes further reduction in Miro1 expression,

linking excitotoxicity to Miro1 deficiency and mitochondrial dysfunction (Zhang et al., 2015). Therefore, excitotoxicity caused by mitochondrial dysfunction could occur in all cases of ALS, regardless of their genetic mutation or lack thereof.

AMPA receptor-mediated excitotoxicity has been implicated in the selective degeneration of MNs in ALS (as discussed above). MNs are particularly vulnerable to excessive AMPA receptor stimulation due to the presence of a large proportion of GluR2 lacking ($Ca^{2+}$ permeable) AMPA receptors. Under normal conditions, AMPA receptors contain the unedited GluR2 subunit and are $Ca^{2+}$ impermeable (Wright and Vissel, 2012). The regulation of intracellular $Ca^{2+}$ concentration is important in maintaining cellular function and preventing excitotoxic insults. In SALS patients, the editing efficiency of GluR2 mRNA is found to be reduced in spinal cord MNs compared to controls (Takuma et al., 1999; Kawahara et al., 2004, 2006; Kwak et al., 2010) resulting in $Ca^{2+}$ permeable subunits. It has also been demonstrated that crossing mutant *SOD1* mice with mice expressing the $Ca^{2+}$ permeable AMPA receptor subunit, GluR2 (Q), accelerates disease progression and decreases survival (Kuner et al., 2005).

Many studies have provided convincing evidence that MN death in mutant *SOD1*-MNs involves non- cell-autonomous processes (Bruijn et al., 1997; Di Giorgio et al., 2007, 2008; Nagai et al., 2007; Marchetto et al., 2008; Wang et al., 2008). It is generally accepted that astrocytes are crucial to keep the synaptic glutamate concentration low, a vital role of EAAT2 (GLT-1). Astrocytes have been shown to influence the subunit composition of the AMPA receptor as they determine the GluR2 expression in MNs (Van Den Bosch et al., 2006; Van Damme et al., 2007). These studies suggest that factors released from astrocytes can influence MN sensitivity to

excitotoxicity by affecting the expression levels of GluR2 and the amount of $Ca^{2+}$ permeable AMPA receptors. The presence of mutant *SOD1* in the astrocytes can effect the secretion of these factors, leading to a lower expression of GluR2, an increase in $Ca^{2+}$ permeable AMPA receptors and cause MNs to be more vulnerable to excitotoxicity (Van Damme et al., 2005a, 2007; Foran and Trotti, 2009).

#### 1.1.12.1 Excitability alterations revealed using electrophysiological recordings

The mutant *SOD1* G93A mouse model has been widely studied since its generation in 1994 (Gurney et al., 1994). The generation of a detailed time-course of the stages of neurodegeneration and the cellular and molecular mechanisms involved in ALS has revealed that electrophysiological abnormalities are one of the first alterations observed in this ALS mouse model (Kanning et al., 2010). The first study to demonstrate alterations in MN excitability in the mutant *SOD1* mouse model of ALS was published in 2003 (Pieri et al., 2003). In this study whole-cell patch-clamp recordings were obtained from cultures of embryonic day 15 (E15) mouse MNs (incubated for 2-3 weeks). An increased firing frequency of mutant *SOD1* MNs compared to wild-type MNs was revealed and mutant *SOD1* MNs were classified as hyperexcitable (Pieri et al., 2003). Hyperexcitability has also been revealed in studies of cultured spinal cord MNs obtained from mutant *SOD1* G93A mice at embryonic and neonatal stages (Kuo et al., 2004). Increases in the persistent $Na^+$ current were found to underlie this hyperexcitability, but only in high input conductance MNs (Kuo et al., 2005). Further evidence of perturbations in $Na^+$ currents has come from recordings of MNs dissociated from E15 *SOD1* G93A mice (recorded within 2 weeks of culturing). In these MNs, voltage-dependent $Na^+$ channels display a more rapid

recovery from fast inactivation compared to wild-type MNs (Zona et al., 2006). However, hyperexcitability has not been observed in all mutant *SOD1* mouse models. Spinal cord MNs isolated from neonatal *SOD1* G85R mice and recorded from between P6-P10 (Bories et al., 2007), and MNs from mice which were low expressors of the h*SOD1* mutation (*SOD1* G93A-Low and *SOD1* G85R) and recorded from between P6-P10 display hypoexcitability (Pambo-Pambo et al., 2009). Spinal cord MNs are not the only neurons to display electrophysiological alterations in the *SOD1* G93A mouse model. Hypoglossal MNs in *SOD1* G93A mice, from postnatal day 4 (P4)-P10, display hyperexcitability, increased persistent $Na^+$ currents and an enhanced frequency of spontaneous transmission compared to wild-type mice. *SOD1* G93A interneurons from the superior colliculus also display hyperexcitability and synaptic changes from P10-12, all occurring months before MN degeneration and symptom onset (van Zundert et al., 2008). E17.5 spinal cord MNs from mutant *SOD1* G93A mice also display hyperexcitability, with these changes linked to morphological changes of the MNs, which may act as a compensatory mechanism (Martin et al., 2013). Whether or not hyperexcitability is a key contributor to MN degeneration remains to be determined.

The persistent $Na^+$ current ($I_{NaP}$) constitutes a small proportion of the voltage-gated $Na^+$ current that mediates the upstroke of an action potential (Hodgkin and Huxley, 1952). $I_{NaP}$ has been shown to dramatically affect the excitability of neurons as it is activated in the subthreshold range and can amplify the response of a neuron to synaptic input and enhance its repetitive firing capabilities. Therefore, any increases in $I_{NaP}$ can dramatically alter cell firing and facilitate hyperexcitability, which can lead to excitotoxicity (Crill, 1996; Kuo et al., 2006; Stafstrom, 2007). In the *SOD1* G93A

mouse model, hyperexcitability of spinal cord MNs and hypoglossal MNs has been attributed to increases in $I_{NaP}$ (Kuo et al., 2005; Zona et al., 2006; van Zundert et al., 2008). However, as these changes begin at P4, these properties and many others are likely to undergo developmental changes. A detailed study of more than 100 wild-type and mutant *SOD1* G93A MNs carried out by Quinlan et al. 2011, from P0- P12, found that although the $I_{NaP}$ increases during development in both mouse models, mutant *SOD1* MNs have an $I_{NaP}$ twice the size of wild-type MNs. Additional changes in mutant *SOD1* MNs, occurring in advance of normal effects of maturation, included decreases in spike width of the action potentials and a shorter time course of the after-spike after-hyperpolarization. They also found that by comparing all measured properties in wild type and mutant *SOD1* G93A MNs, approximately 55% of changes associated with the *SOD1* G93A mutation could be attributed to an increased rate of maturation. Overall, their results suggest that although the development of wild-type and mutant *SOD1* MNs follow a similar developmental pattern, the rate of development is accelerated in the mutant *SOD1* MNs (Quinlan et al., 2011).

Hyperexcitability, detected in mutant *SOD1* G93A MNs at neonatal and postnatal time-points, long before symptom onset, has been shown not to extend into the later stages of the mouse model. A study by Delestrée et al. 2014, revealed that adult mutant *SOD1* MNs are not hyperexcitable at a time-point preceding muscle denervation. In fact, they revealed that a substantial fraction of spinal cord MNs became hypoexcitable, as they were unable to produce sustained firing in response to current ramps (Delestrée et al., 2014). Different types of MNs exist, some which innervate fast contracting muscle fibres (F-type MNs) that are vulnerable in ALS and those which innervate slow-contracting fibres (S-type MNs), which are more resistant

in ALS. Recordings from both types of MNs in neonatal mice found that although S-type MNs from mutant *SOD1* mice did display hyperexcitability, the F-type MNs did not. The authors concluded that hyperexcitability is not required for MNs to undergo degeneration (Leroy et al., 2014).

As discussed, the above studies have revealed changes in MN excitability in mutant *SOD1* MNs. Many of these have utilised mutant *SOD1* mice spinal cord slices, some of which cultured these as organotypic slices or dissociated the spinal cord MNs, culturing them for 1-2 weeks. Excitability alterations have also been revealed using non- traditional cell-based models of ALS, including the exposure of wild type MNs to ALS affected astrocyte conditioned medium (ACM) or through the use of stem cell models. One such study by Fritz et al. 2013, shows that culturing primary wild type spinal cord cultures with ACM from mutant h*SOD1* G93A astrocytes, increases $I_{NaP}$ and repetitive firing of MNs leading to cell death. Exposure of the cultures to voltage-gated $Na^+$ (Nav) channel blockers prevents MN death caused by the h*SOD1* G93A ACM. This study demonstrates that excitability alterations occur in MNs before they undergo cell death and further implicates non-cell autonomy as a disease mechanism in ALS (Fritz et al., 2013). Changes in excitability have also been revealed in MNs harbouring ALS mutations other than *SOD1*, including *TARDBP*, *C9ORF72* and *FUS*. MN-like cell lines transfected with mutant TDP-43 were hyperexcitable compared to those transfected with wild-type TDP-43, with amelioration of hyperexcitability after treatment with an antioxidant for 24 hours (Dong et al., 2014). Human iPSC-derived MNs from ALS patients have also demonstrated alterations in excitability. Hyperexcitability was uncovered in iPSC-derived MNs harbouring *SOD1*, *C9ORF72* and *FUS* mutations at time-points of up to two weeks in culture (Wainger et al.,

2014). In an earlier study using iPSC-derived MNs harbouring a *C9ORF72* mutation, MNs were found to be hypoexcitable. However, this was shown after seven weeks in culture (Sareen et al., 2013). Due to the different time-points at which recordings were obtained, it is possible that both cases hold true for iPSC-derived MNs harbouring *C9ORF72* mutations. My findings relating to these studies will be described in Chapter 2.

Spinal cord MNs are not the only cell type to exhibit excitability alterations in ALS. Spinal interneurons have also been implicated in ALS as *SOD1* G93A mice display enhanced activity from early and presymptomatic time-points. This enhanced activity could also contribute to excitotoxicity as a result of the degeneration of inhibitory interneurons or is a result of their dysfunction (Jiang et al., 2009). Cortical hyperexcitability has been shown in many studies of ALS patients and in animal models of the disease. Both SALS and *SOD1* ALS patients are found to exhibit cortical hyperexcitability (Zanette et al., 2002; Turner et al., 2005; Vucic and Kiernan, 2007; Vucic et al., 2009). Cortical hyperexcitability is shown to be present in ALS patients even before the onset of clinical symptoms as presymptomatic carriers of mutant *SOD1* display cortical hyperexcitability before going on to develop symptoms of ALS (Vucic et al., 2008). It has been proposed that cortical hyperexcitability occurs before alterations in lower MNs, as no evidence of their dysfunction has been found within their target muscles (Menon et al., 2014), however changes to the function of lower MNs could be undetectable using compound muscle action potential (CMAP) responses of the abductor pollicis brevis (APB) muscle of the hand as indicators. Studies of cerebral post-mortem samples from ALS patients reveal a loss of inhibitory interneurons compared to controls, with these changes linked to the hyperexcitability

seen in patients using transcranial magnetic stimulation (TMS) (Ziemann et al., 1997; Maekawa et al., 2004). Using the Wobbler mouse model of ALS, cortical hyperexcitability has also been demonstrated. These studies have revealed an increase in excitatory synaptic transmission and reduction in inhibition due to a decreased number of inhibitory interneurons (Thielsen et al., 2013) and a decrease in GABAergic inhibition (Nieto-Gonzalez et al., 2011), both of which may lead to cortical hyperexcitability in this mouse model. Taken together, temporal changes in cell excitability from *in vivo* studies currently supports the findings that MNs are initially hyperexcitable at embryonic and post-natal time-points, followed by a loss of action potential output in adulthood, preceding muscle denervation.

In a similar manner to mutant *SOD1* mouse models, persistent $Na^+$ conductances have been implicated in changes in axonal excitability observed in ALS patients (Kiernan, 2009; Vucic and Kiernan, 2010; Kanai et al., 2012). Fasciculations are a prominent clinical symptom in ALS and can occur due to alterations in the motor terminal environment. Studies of ALS patients in which multiple axonal excitability parameters were measured, revealed increased intracellular $Ca^{2+}$ concentration, higher $Na^+$ conductances and decreased $K^+$ conductances, all of which can lead to fasciculations (Bostock et al., 1995; Kanai et al., 2006, 2012; Vucic and Kiernan, 2006, 2007). There is a potential for axonal excitability properties to predict patient prognosis since larger $K^+$ currents have been associated with decreased survival times (Kanai et al., 2012). The findings that properties of ion channels in the axonal membrane are altered has been demonstrated in patients with SALS and with *SOD1*-FALS (Vucic et al., 2008; Shibuya et al., 2011) and more recently in *C9ORF72* FALS and SALS patients (Geevasinga et al., 2015). Therefore, a similar mechanistic link

may exist between the various causes of ALS, regardless of whether or not patients harbour a known genetic mutation.

In the studies mentioned above, hyperexcitability has been linked to MN degeneration and is largely seen as an excitotoxic disease mechanism that needs to be ameliorated. However, a recent study has suggested that a link exists between hyperexcitability and neuroprotection. This study by Saxena et al., demonstrated that mutant *SOD1* causes vulnerable α-MNs to become dependent on endogenous neuroprotection signalling involving excitability and mammalian target of rapamycin (mTOR). mTOR is a signalling pathway that integrates intra and extracellular signals and regulates cell metabolism, proliferation, growth and survival (Laplante and Sabatini, 2012). Enhancing MN excitability in *SOD1* G93A mice through activation of cholinergic C-bouton inputs to MNs reversed the accumulation of misfolded *SOD1*. MN excitability is controlled by these C-boutons, a specific class of synaptic input that originates from a small cluster of spinal interneurons (Miles et al., 2007; Zagoraiou et al., 2009; Saxena et al., 2013). Reducing MN excitability by inhibiting the metabotropic cholinergic signalling lowered ER stress, but enhanced misfolded mutant *SOD1* accumulation and prevented mTOR activation in α-MNs. These results suggest that excitability and mTOR are key endogenous neuroprotective mechanisms in MNs to counteract disease progression in ALS (Saxena et al., 2013). Interestingly, alterations in C-boutons had previously been identified in presymptomatic mutant *SOD1* mouse models. In these studies, C-boutons were enlarged, even at presymptomatic stages, and remained larger throughout the symptomatic stages (Pullen and Athanasiou, 2009; Herron and Miles, 2012). Recently, neuregulin-1 (NRG1), a protein vital for balancing excitatory and inhibitory connections was shown to be closely associated

with the cholinergic C- boutons that innervate spinal cord MNs (Issa et al., 2010; Gallart-Palau et al., 2014). Transient increases in NRG1 expression in C- boutons were found in the mutant *SOD1* G93A mouse model and continued to occur during disease progression (Gallart-Palau et al., 2014). These studies suggest that alterations in C-bouton size and protein expression may act as compensatory mechanisms in ALS.

Many pathogenic mechanisms have been proposed for the selective MN degeneration in ALS including oxidative stress, aggregate formation, non-cell autonomy, axonal transport defects, mitochondrial dysfunction and excitotoxicity. This multitude of contributing factors indicates that ALS is a complex disease but it is becoming more and more evident that at least some of the pathogenic mechanisms are interconnected. The only approved treatment for ALS, Riluzole, acts to diminish the effects of excitotoxicity by inhibiting pre-synaptic glutamate release. It has also been shown to block $I_{NaP}$ (Urbani and Belluzzi, 2000) and to reduce the increase in $I_{NaP}$ found in mutant *SOD1* MNs, which are thought to underlie hyperexcitability (Kuo et al., 2005). However, Riluzole can only extend survival by a few months (Bellingham, 2011). In order for beneficial therapeutics to be developed, it may be important to target many of the processes by which excitotoxicity is thought to damage MNs in ALS.

## Models of ALS

The development of suitable models is vital in order to study diseases. Many models have been generated to study neurodegenerative diseases, including ALS, in mice, rats, dogs, *Drosophila*, *C. elegans*, yeast, embryonic and induced pluripotent stem cells (McGoldrick et al., 2013). Whilst none of these models are without fault, they all

have their place in ALS research due to the specific research opportunities they each provide. Some of these models along with their advantages and disadvantages will be discussed below.

## Animal models

The generation of ALS animal model systems has made it possible to deepen our understanding of the disease and to identify a number of mechanisms involved in ALS pathogenesis. *SOD1* mutations were first associated with ALS in 1993 (Rosen et al., 1993) and a mouse line in which the human *SOD1* gene was expressed was generated the following year (Gurney et al., 1994). This mouse model recapitulated many of the ALS patient phenotypes including MN degeneration, muscle denervation and progressive paralysis (Gurney et al., 1994). Many more mutant *SOD1* mouse models have since been generated, with their ALS-like phenotypes varying according to mutation and transgene expression level. High expressers of *SOD1* G93A develop an ALS phenotype earlier than low expressers (Turner and Talbot, 2008). *SOD1* is ubiquitously expressed and converts superoxide to hydrogen peroxide in order to protect cells from oxidative stress (Reaume et al., 1996). So far, models generated to identify the way in which mutant *SOD1* causes ALS via toxic gain of function include mice, rats, zebrafish, *Drosophila*, and *C. elegans*. These animals have a lethal phenotype, many of which recapitulate ALS patient phenotypes, characterized by muscle denervation, reactive gliosis, and loss of MNs. This phenotype is most often induced by overexpression of the mutant *SOD1* protein; therefore, animals overexpressing the wild-type protein should serve as a control in these experiments.

*SOD1* mutations, H46R and G93A, have also been modelled in rats with the G93A mutation causing a more aggressive disease. Both these mutations lead to progressive MN degeneration and an ALS-like phenotype (Nagai et al., 2001; Howland et al., 2002). The nematode worm *Caenorhabditis elegans* (*C. elegans*) despite its apparent simplicity has developed into an important biomedical research model. The simplicity and cost-effectiveness of their generation makes it an effective *in vivo* model. Locomotor deficits have been found in *C. elegans* expressing various *SOD1* mutations, along with defects in ventral nerve cord processes and reduced NMJ synapses, with phenotypes varying between mutations (Gidalevitz et al., 2009; Lim et al., 2012). Another animal model widely used in ALS research is the zebrafish. Their use as a model of disease has become very popular due to their simple and transparent embryo and the ease by which mutations can be induced and replicated. ALS-like phenotypes seen in zebrafish with *SOD1* mutations include MN loss, axonal retraction and motor abnormalities (Sakowski et al., 2012; McGown et al., 2013). *Drosophila melanogaster* are one of the most studied organisms in biomedical research as they are simple to care for, relatively inexpensive to use, they have a short generation time and their full genome has been sequenced. To date, *Drosophila* expressing human wild-type *SOD1*, *SOD1* A4V and *SOD1* G85R mutations in MNs have been generated. Overexpression of either wild- type or mutant *SOD1* causes progressive motor deficits in the climbing ability of transgenic flies as well as electrophysiological defects, indicating that human *SOD1* is toxic to flies, even in its wild-type form. MN loss was not detected due to the short life span of this model (Watson et al., 2008).

Since the discovery of the involvement *TARDBP* mutations in ALS, various TDP-43 mouse models have been created (Sreedharan et al., 2008; Wegorzewska et al., 2009;

Swarup et al., 2011; Xu et al., 2011). As with the *SOD1* models, phenotypes vary between models according to the promoter used to drive TDP-43 expression and expression levels achieved. Overexpression of the wild-type TDP-43 gene is toxic in almost all mouse models created (Xu et al., 2010; Wegorzewska and Baloh, 2011). Human and mouse wild-type TDP-43 overexpression results in varied and dose-dependent progressive gait abnormalities (Shan et al., 2010; Wils et al., 2010; Xu et al., 2010). *TARDBP* knockout mice have revealed that TDP-43 is vital for early embryonic development (Kraemer et al., 2010; Wu et al., 2010) and that altering TDP-43 protein levels effects neuronal function and survival. Rats expressing mutant TDP-43 display features of TDP-43 proteinopathies including TDP-43 inclusions and cytoplasmic mislocalisation of phosphorylated TDP-43. Overexpression of mutant TDP-43, but not wild-type TDP-43, causes paralysis and MN death (Zhou et al., 2010). Zebrafish embryos expressing either human wild- type or mutant TDP-43 mRNA both exhibit decreased axon length and increased irregular branching. However, no evidence of cytoplasmic mislocalisation has been found, which is a key feature of TDP-43 proteinopathies (Kabashi et al., 2009; Laird et al., 2010). Knockout of *TARDBP* in *Drosophila* or *C. elegans* is deleterious to their development. Animals that reach adulthood display dramatic motor defects (Feiguin et al., 2009) and have reduced life span. Some of these defects can be rescued in part by human TDP-43 neuronal expression, with TDP-43 overexpression causing MN toxicity (Ash et al., 2010; Li et al., 2010; Diaper et al., 2013; Estes et al., 2013).

Animals in which *C9ORF72* orthologues have been identified are mice, zebrafish and *C. elegans*, making them ideal models for studying *C9ORF72* mutations. The three main mechanisms by which *C9ORF72* mutations are thought to cause ALS pathology

are: haploinsufficiency (loss of function), repeat RNA mediated toxicity (RNA foci formation) and dipeptide protein toxicity. As none of these mechanisms have been demonstrated as the sole cause, various models that recapitulate disease pathology need to be generated. The first *C9ORF72* model generated was the zebrafish, where knockdown of *C9ORF72* caused abnormal axonal branching and altered swimming behaviour (Ciura et al., 2013). However, reduction of *C9ORF72* (up to 75%) in a mouse model did not cause any ALS-like phenotype but did reveal minor alterations in RNA expression profiles (Lagier-Tourenne et al., 2013). Transgenic *Drosophila* overexpressing $G_4C_2$ in MNs caused motor deficits, with expression in all neurons resulting in lethality (Hirth, 2010). Similarly, overexpression of $G_4C_2$ in zebrafish embryos cause locomotor deficits, with RNA foci present in apoptotic nuclei (Lee et al., 2013).

These animal models have provided initial and substantial insights into the pathogenic mechanisms linked to ALS mutations, however many questions remain due to the complexity of possible mechanisms leading to MN death. Whilst it is likely that mitochondrial dysfunction, protein aggregation, oxidative damage, excitotoxicity, non-cell autonomous effects, axonal transport defects and aberrant RNA processing contribute to the pathogenesis of ALS to varying degrees, in order to understand the cause, develop a treatment and find a cure for this disease, even more research into potential disease mechanisms need to be carried out. *SOD1* rodent models have provided much of what we understand about ALS, but as *SOD1* mutations account for approximately only 2% of all ALS cases (Rosen et al., 1993), findings in these models may be limited to a subset ALS disease mechanisms. Many of these animal models have been used to study the effectiveness of potential therapeutics in preclinical

studies. However, as treatment is initiated at a presymptomatic stage in these models, results uncovered in preclinical studies may not be translatable to patients whose symptoms will have presented long before administration of potential therapeutics (Benatar, 2007). Some models lack key pathological and phenotypical traits such as progressive paralysis, which is hallmark in ALS patients (Lagier-Tourenne et al., 2013). Many of these animal models carry multiple copies of mutant genes, especially the *SOD1* G93A mouse model that is not comparable to expression levels found in patients.

Animal models have long been used in clinical trials to determine if a therapeutic candidate has the potential to benefit patients. As millions of pounds have been spent, with almost no drug treatments proving beneficial, guidelines have been introduced to reduce the number of unwarranted clinical trials by identifying and preventing false positives in preclinical studies. These guidelines include: model validation ideally with at least two species in the pre-clinical phase before clinical testing begins; replication of results in multiple labs; the careful design of preclinical experimental therapeutic approaches; ensuring any methodological techniques are without error; stating when the experimental drug has been administered i.e. at presymptomatic of symptomatic stages; and stating any possible conflict, including the sources of funding and if a pharmaceutical company provided the drugs (Ludolph et al., 2010). Therefore, using whole animal models as well as stem cell models, potential therapeutics can be more rigorously tested, using a variety of assays, with only the most promising candidates progressing to further stages, decreasing the amount of money wasted on unsuccessful trials.

## Stem cell models of ALS

To date, numerous cell culture models of FALS and SALS have been generated including models involving *SOD1*, *TARDBP*, *FUS* and *C9ORF72* mutations. The generation of these models has enabled the study of specific cell types harbouring specific mutations which can be manipulated in a less complex manner than in whole animal models. An important example of such a study is the co-culture of primary mutant *SOD1* astrocytes with primary, embryonic stem cell (ESC) derived or induced pluripotent stem cell (iPSC) derived control MNs (Di Giorgio et al., 2007, 2008; Nagai et al., 2007; Serio et al., 2013). Although non-cell autonomy had been previously suggested and demonstrated in animal models, identifying the toxic factors released by these astrocytes in culture is likely to be simpler as there are not as many external factors and other cell types involved.

### 1.1.13 Embryonic stem cells

Embryonic stem cells (ESCs) are pluripotent stem cells derived from blastocysts, an early-stage preimplantation embryo, which have the ability to differentiate into any cell type, including cells from the CNS, when exposed to appropriate signals (Jessell, 2000). The first ESCs were derived from mouse embryos (mESCs) (Evans and Kaufman, 1981). ESCs have since been derived from many other species including humans (hESCs) (Thomson, 1998). Neural progenitor cells (NPCs) derived from ESCs are an attractive treatment strategy for cell replacement and as a model to study neurodegenerative diseases, including ALS. hESC lines are an attractive model due to their continuous self-renewal capacity and their ability to differentiate into almost all cell types. In order for these cells to have the potential to be used in personalized cell

therapies or for transplantation, methods to maintain pluripotency in xeno-free conditions need to be established (Ying et al., 2008).

Mouse ESCs were first differentiated into MNs in 2002 and were shown to have the ability to extend axonal projections and form synapses with target muscles (Wichterle et al., 2002). Further studies of their functional properties revealed their ability to develop appropriate neurotransmitter receptors, intrinsic properties required for appropriate action potential firing as well as functional synapses with muscle fibers (Miles et al., 2004). Following this, hESC derived MNs were generated, with the process taking longer and requiring additional trophic factors compared to mESC derived MN generation (Li et al., 2005; Shin et al., 2005; Singh et al., 2005). hESC derived MNs also developed appropriate functional properties and receptors, with postsynaptic acetylcholine receptor clustering occurring when co-cultured with muscle cells (Li et al., 2005; Lee et al., 2007; Wada et al., 2009).

The generation of MNs from NPCs can be carried out through either formation of embryoid bodies (EBs)(Di Giorgio et al., 2007; Hu and Zhang, 2009; Karumbayaram et al., 2009b), direct differentiation into neural rosettes (Li et al., 2005; Lee et al., 2007) or progressive differentiation of EBs into neural rosettes (Marchetto et al., 2008; Karumbayaram et al., 2009a). Neural cells can then be directed toward a spinal MN identity via the caudalising and ventralising actions of retinoic acid and sonic hedgehog (Jessell, 2000). These methods result in different MN purity levels, with variability common between batches, cell lines and lab groups generating them. Post-differentiation, ESC-derived MNs can express Islet-1 and Hb9, early markers of MN differentiation, SMI-32, a MN neurofilament marker and choline acetyltransferase (ChAT), a mature MN marker (Peljto et al., 2010). They are also positive for general

neuronal synaptic markers including vesicular glutamate transporters (VGLUTs) and vesicular acetylcholine transporter (VAChT) (Shneider et al., 2009) and can form functional NMJs, indicated by the incorporation of α- bungarotoxin when co-cultured with myotubes and from sharp electrode recordings revealing endplate potentials which respond to glutamate (Miles et al., 2004; Li et al., 2005; Marchetto et al., 2008) (Li et al., 2005; Marchetto et al., 2008). Along with anatomical makers, such analysis of MN function is crucial to validate the MN generation protocol (Miles et al., 2004; Lee et al., 2007; Wada et al., 2009).

Embryonic stem cells are a very beneficial tool, enabling the study of disease specific mutations at disease relevant levels in many cell types and serve as a potential drug-screening tool. mESCs with mutations in *SOD1* have been used as a drug screening tool in recent years and have successfully revealed a number of potential drugs, including a kinase inhibitor, which increased the survival of mutant *SOD1* mouse MNs (Linseman et al., 2004; Koh et al., 2011; Yang et al., 2013) and the survival of human iPSC-derived MNs from patients harbouring either a *SOD1* or *TARDBP* mutation (Yang et al., 2013). hESCs have been widely used in cell replacement treatments of Parkinson's disease and have shown promising results through the partial restoration of motor behaviour. However, the ethical issues associated with the use of ESCs are currently a major drawback to their use as large numbers of aborted foetuses are required to carry out such treatments. Other problems associated with this model include their development into tumours in some animal models and they have also been shown to cause immune rejection. Furthermore, as hESCs, unlike mESCs, do not contain disease mutations, including those associated with ALS, they may not be the most beneficial and informative model to use in ALS research.

### 1.1.14 Induced pluripotent stem cells

In 2006, a landmark study defined the factors required to turn differentiated somatic cells into pluripotent cells, capable of producing any cell type from the three germ layers. This study showed that mouse embryonic and adult fibroblasts become pluripotent when they express transcription factors octamer 3/4 (Oct4), SRY box–containing gene 2 (Sox2), Kruppel-like factor 4 (Klf4), and c-Myc (Takahashi and Yamanaka, 2006). These cells were termed induced pluripotent stem cells (iPSCs). Shortly afterwards, iPSCs were generated from human fibroblasts, enabling the study of patient specific and disease relevant cells, with mutations present at physiological levels unlike many of the animal models (Takahashi et al., 2007; Yu et al., 2007; Park et al., 2008).

iPSCs were first generated from a FALS patient harbouring a *SOD1* mutation in 2008 and differentiated into MNs using the same protocol as used for the generation of hESC-derived MNs (Dimos et al., 2008). iPSC-derived MNs were subsequently generated from ALS patients harbouring TDP-43 mutations (Sreedharan et al., 2008; Bilican et al., 2012; Zhang et al., 2013), *SOD1* mutations (Amoroso et al., 2013; Chen et al., 2014; Kiskinis et al., 2014), *C9ORF72* mutation (Almeida et al., 2013; Donnelly et al., 2013; Sareen et al., 2013; Wainger et al., 2014) and from a patient with SALS (Burkhardt et al., 2013). Patient iPSC-derived MNs have been used in many studies to unravel the disease mechanisms underlying ALS. Astrocytes have also been generated from iPSCs to investigate potential non-cell autonomous disease mechanisms associated with ALS (Roybon et al., 2013; Serio et al., 2013).

Human iPSC-derived neurons and astrocytes harbouring ALS mutations have recapitulated many of the pathologies and dysfunctions previously demonstrated in animal models of the disease as well as from patient samples. These include studies of iPSC-derived MNs harbouring *SOD1* mutations where signs of neurofilament aggregation that lead to the degeneration of neurites (Chen et al., 2014), defects in the mitochondrial transport system, changes in the mitochondrial morphology, ER stress (Kiskinis et al., 2014) and hyperexcitable membranes (Wainger et al., 2014) are described. iPSC-derived MNs from patients with an M337V TDP-43 mutation have increased levels of the soluble and detergent-resistant TDP-43 protein (Bilican et al., 2012). iPSC-derived astrocytes harbouring the same mutation show similar increases in the level of the TDP-43 protein, with protein aggregates mislocalised to cytoplasm of the cells (Bilican et al., 2012). Despite reduced survival of mutant TDP-43 expressing astrocytes, when co-cultured with control or mutant MNs, MN viability is unaffected (Serio et al., 2013). iPSC-derived MNs harbouring three different TDP-43 mutations (M337V, G298S and Q343R) exhibit an increased amount of the insoluble TDP-43 protein, increased transcriptional level of the genes involved in RNA metabolism and a reduced transcriptional level of genes encoding cytoskeleton proteins (Egawa et al., 2012). iPSCs from patients with the *C9ORF72* ALS mutation have also been generated, with characteristic RNA foci identified in MNs, as well as excitability alterations (Sareen et al., 2013). Upon treatment of MNs harbouring *C9ORF72* mutations with antisense oligonucleotides (ASOs), RNA foci lost and normal levels of gene transcription returned in MNs (Sareen et al., 2013). In iPSC lines generated from patients with SALS, hyperphosphorylated aggregates of TDP-43 have been observed in the nuclei of MNs. However, the ubiquitin-positive granules that are normally always present in SALS patient post-mortem samples are not

present in these cells. It is possible that ubiquitination may occur at a later time period than hyperphosphorylation and that the cells were not cultured long enough to see this process occur (Burkhardt et al., 2013).

iPSCs can be used not only to search for new compounds as potential drug treatments for ALS or identification of disease mechanisms, especially in SALS, but also to explore alternative modes of therapy including their use in cell based therapies (Di Giorgio et al., 2007; Ling et al., 2013; Serio et al., 2013; Yang et al., 2013). It is important to differentiate iPSCs derived from patients into cell types other than MNs to investigate the causes and mechanisms involved in all ALS cases, including those involving non-cell autonomy. iPSCs from ALS patients, unlike many animal models and mESCs, express mutations at a disease relevant and a disease causative level, making the findings potentially more translatable to therapeutics. As the majority of ALS cases are sporadic, the ability to generate iPSCs from SALS patients is a major benefit to this model, making it perhaps one of the most promising models currently available in which potential therapeutics can be tested prior to translation to whole-organism models or human trials.

In the following chapters, I will describe pathophysiological changes in ALS revealed using human iPSC-derived MNs and astrocytes from patients harbouring *TARDBP* or *C9ORF72* mutations. In Chapter 2, the physiological properties of control and patient iPSC-derived MNs, cultured for up to 10 weeks, will be described. Data from iPSC-derived MN cultures treated with potential therapeutic agents and data from a *C9ORF72* patient line that was gene-edited using CRISPR/Cas9 technology will also be presented. In Chapter 3, I will describe the results from a study on the potential involvement of non-cell autonomous disease mechanisms in ALS. For these studies,

iPSC-derived MNs from healthy individuals were co-cultured with astrocytes generated from healthy controls and patients harbouring *TARDBP* or *C9ORF72* mutations, as well as a gene-edited line from a *C9ORF72* patient. The results of these studies provide further evidence of the importance of early physiological changes in in ALS pathogenesis and support a role for non-cell autonomous disease mechanisms in ALS-related MN dysfunction.

# Chapter 2

# Human iPSC-derived motoneurons harbouring *TARDBP* or *C9ORF72* ALS mutations are dysfunctional despite maintaining viability

**This chapter is adapted from published work in:**

**Devlin A.-C, Burr K, Borooah S, Foster JD, Niven E, Shaw CE, Chandran S, Miles GB, Cleary EM, Geti I, Vallier L, Shaw CE, Chandran S, Miles GB, Niven E, Shaw CE, Chandran S, Miles GB (2015)**

**Human iPSC-derived motoneurons harbouring *TARDBP* or *C9ORF7*2 ALS mutations are dysfunctional despite maintaining viability.**

**Nat Commun 6:1–33 (Devlin et al., 2015)**

# 1. Introduction

Amyotrophic lateral sclerosis (ALS) is a rapidly progressing, fatal neurodegenerative disease for which no effective treatment exists. Although the mechanisms underlying motoneuron (MN) loss in ALS remain unclear, recent pathological and genetic discoveries have provided important insights that implicate common mechanisms across both ALS and fronto-temporal dementia (FTD) as well as a link between familial and sporadic ALS (Al-Chalabi et al., 2012; Renton et al., 2014). The discovery of a common pathological signature characterised by cytoplasmic accumulation of TDP-43 in sporadic forms of FTD and ALS along with the discovery of mutations in *TARDBP* and *C9ORF72* in familial and sporadic forms of these diseases has become increasingly influential in shaping our understanding of ALS and related disorders (Neumann et al., 2006; Sreedharan et al., 2008; DeJesus-Hernandez et al., 2011; Renton et al., 2011). Nonetheless, despite the many advances driven by accumulating genetic discoveries there has been a striking failure to translate experimental observations into therapies (Benatar, 2007). This reflects, in part, the absence of appropriate human cell-based models in which to validate disease mechanisms and test candidate therapeutics prior to lengthy and costly clinical trials. Human induced pluripotent stem cell (iPSC) systems have the potential to bridge this gap. Specifically, they allow us to study the consequences of mutation(s) expressed at disease-relevant levels in functional disease-relevant cell types. It has previously been reported that iPSC-derived human neurons and astroglia recapitulate key aspects of the adult human pathology and biochemistry that are hallmarks of ALS (Dimos et al., 2008; Bilican et al., 2012; Egawa et al., 2012; Donnelly et al., 2013; Sareen et al., 2013; Zhang et al., 2013; Kiskinis et al., 2014; Wainger et al., 2014). In addition to

revealing aspects of the molecular pathology of MNs derived from ALS patients, iPSC-derived neurons may reveal early and subtle pathophysiological changes, which may highlight new targets for therapeutic interventions that ultimately aim to maintain MN function in ALS.

Interestingly, physiological analyses have already revealed changes in the functional properties of MNs at very early stages (embryonic and early postnatal) in transgenic rodent models of ALS. Several studies have demonstrated presymptomatic hyperexcitability of MNs due to perturbations in their intrinsic properties, particularly $Na^+$ currents (Pieri et al., 2003; Kuo et al., 2005; Zona et al., 2006; Bories et al., 2007; van Zundert et al., 2008; Quinlan et al., 2011; Fuchs et al., 2013). Neuronal hyperexcitability, again thought to relate to changes in $Na^+$ currents, has also been shown in studies of ALS patients (Kanai et al., 2006; Vucic et al., 2008), while recent studies of human iPSC-derived MNs have reported conflicting results of hyperexcitability (Wainger et al., 2014) versus hypoexcitability (Sareen et al., 2013). Taken together these findings suggest that perturbations in the intrinsic biophysical properties of MNs lead to aberrant activity that may reflect and contribute to the earliest events that ultimately lead to irreversible neurodegeneration in ALS. Furthermore, they demonstrate the sensitive nature of electrophysiological studies of MN function and highlight their potential to reveal important early pathogenic mechanisms occurring prior to molecular or anatomical signs of neurodegeneration.

In the present study detailed, temporal electrophysiological analyses of human iPSC-derived MNs is undertaken to investigate whether MN dysfunction represents an early feature of ALS pathogenesis common to neurons carrying mutations in *TARDBP* and *C9ORF72*. Findings demonstrate the development of appropriate functional properties

in both control and patient iPSC-derived MNs but reveal a progressive loss of action potential output, spontaneous synaptic activity and ionic conductances in patient derived MNs regardless of their genotype, which occurs prior to any overt changes in cell viability. Loss of ionic conductances is partially recovered in iPSC-derived MNs harbouring the *C9ORF72* mutation following the application of the acid-sensing ion channel blocker, amiloride. Meanwhile, genetic-editing of the repeat expansion of *C9ORF72* using the CRISPR/Cas9 system restores functionality of MNs.

# 2. Methods

## 2.1. iPSC lines

For this study, 8 iPSC lines from 6 individuals were utilised: 1 male M337V TDP-43 ALS patient (2 clones; D1 and D3); 1 female *C9ORF72* ALS patient (2 clones, S6 and 2H9 Carrier-1Δ); 1 male *C9ORF72* ALS patient (1 clone, R2); 2 female healthy controls (2 clones, R6 and M2; 1 clone, D6) and 1 male healthy control (1 clone, D9). iPSCs were generated from fibroblasts as previously described (Yusa et al., 2011; Bilican et al., 2012). At least 4 iPSC differentiations were performed for each line (Control: D6 = 8, D9, = 6, M2 = 7, R6 = 4; *TARDBP*: D1 = 6, D3 = 8; *C9ORF72:* S6 =4, R2 = 4) with control and patient iPSC differentiations always run in parallel. iPSCs were established by virally transducing $10^5$ fibroblasts with the Yamanaka reprogramming factors *OCT4, SOX2, KLF4* and *c-MYC* using either lentiviral (Vectalys) or Sendai (Life technologies) reprogramming kits. Cells were maintained in MEF media at 37°C and 5% $CO_2$. MEF media consisted of KO-DMEM (Invitrogen), 2 mM L-glutamine (Invitrogen), 10 % FBS (Invitrogen) and 1% penicillin/streptomycin (Invitrogen). After 5 days the cells were split and re-plated as single cells on to a MEF feeder plate. On day 7 media was changed to KSR and FGF2 consisting of advanced DMEM (Invitrogen), 20% serum replacer (Invitrogen), 1 µl/ml FGF2 (PeproTech), 1% penicillin/streptomycin (Invitrogen), 1% L-glutamine (Invitrogen) and 0.007 µl/ml 2-mercaptoethanol (Invitrogen). After approximately 21 days, colonies with compact human embryonic cell-like morphology were expanded and clonal lines were established. Human iPSC lines were maintained long term on

CF-1 irradiated mouse embryonic fibroblasts, with KO-DMEM (Invitrogen) supplemented with 20% knockout serum replacement (Invitrogen), 10 ng/mL basic FGF2 (PeproTech), 1% L-glutamine (Invitrogen), 0.007 µl/ml 2-mercaptoethanol (Invitrogen) and 1% penicillin/streptomycin (Invitrogen) at 37°C and 5% $CO_2$. For the neural conversion, the cells were transitioned to feeder-free culture conditions in MTESR1 media (Stem Cell Technologies) and passaged three times before use. Members of Siddharthan Chandran's lab at the University of Edinburgh, Chris Shaw's lab at King's College London and Ludovic Vallier's lab at the University of Cambridge carried out the generation and differentiation of iPSCs into neuronal lineages.

## 2.2.iPSC differentiation to a MN lineage

Differentiation of iPSCs into a neuronal and MN lineage was performed using modifications of previously established and validated protocols (Bilican et al., 2012; Amoroso et al., 2013). The iPSCs were neuralised to neuroectoderm using dual SMAD inhibition in CDM [(50% Iscove's Modified Dulbecco's Medium (IMDM) (Invitrogen), 50% F12, 5 mg/ml bovine serum albumin (BSA, Europa), 1% chemically defined Lipid 100x (Invitrogen), 450 mM Monothioglycerol (Sigma), 7 mg/ml Insulin (Roche), 15 mg/ml Transferrin (Roche), 1% penicillin/streptomycin], supplemented with 1 mM N- acetyl cysteine (Sigma), 10 µM Activin Inhibitor (R&D Systems) and 2 µM Dorsomorphin (Merck Millipore). This medium was changed every 2-3 days for 4-10 days. Neurospheres were patterned to a caudal, spinal cord identity in CDM, 1 mM N-acetyl cysteine, 5 ng/ml fibroblast growth factor (FGF; PeproTech)/heparin (Sigma; 20 µg/ml) and 0.1 µM retinoic acid (Sigma) for 4-10

days, changing medium every 2-3 days. Caudalised neural stem cells (NSCs) were ventralised in the presence of Advanced Dulbecco's Modified Eagle Medium (DMEM) Nutrient Mixture F12 (Invitrogen), 1% penicillin/streptomycin, 0.5% GlutaMAX, 1% B-27, 0.5% N-2 supplement, 5 ng/ml FGF+Heparin, 1 μM retinoic acid and 1 μM purmorphamine (Merck Millipore) for 4-10 days, changing the medium every 2-3 days. The FGF/Heparin was removed from the medium and replaced with 0.5 μM purmorphamine, with the cells cultured for another 4-14 days, changing the medium every 2-3 days. Caudalised and ventralised NSCs were transitioned to MN maturation medium containing advanced DMEM/F12, 1% penicillin/streptomycin, 0.5% B-27, 0.5% N-2 supplement, 2 ng/ml Heparin, 10 ng/ml brain- derived neurotrophic factor (BDNF; R&D systems), 10 ng/ml glial cell line-derived neurotrophic factor (GDNF; R&D systems), 10 μM forskolin (R&D systems), 0.1 μM retinoic acid and 0.1 μM purmorphamine for 2-6 weeks, changing the medium every 2-3 days. Technical staff in Siddharthan Chandran's lab at the University of Edinburgh performed these MN differentiation steps.

MN progenitors were next dissociated with the Papain Dissociation System (Worthington Biochemical), plated at 50 x $10^3$ cells per well in 24-well plates with 13 mm glass coverslips coated with poly-ornithine (Sigma), laminin (Sigma), fibronectin (Sigma) and Matrigel (BD Biosciences). Plate down medium consisted of Neurobasal medium (Invitrogen), 1% penicillin/streptomycin, 0.5% GlutaMAX, 0.5% B-27, 0.5% N-2 Supplement, 20 ng/ml basic FGF, 1 μM retinoic acid, 1 μM purmorphamine, 1 μM mouse Smo agonist SAG (Merck Millipore)(Amoroso et al., 2013). 24 hours post-plating, 20 ng/ml ciliary neurotrophic factor (CNTF; R&D systems), 10 ng/ml GDNF and 10 μM forskolin were added, with this medium used until day 14, feeding

every 3 days. From day 14, RA, SAG, purmorphamine and forskolin was removed from the medium, with cells then maintained for up to 10 weeks. As an indication that neuronal differentiation was successful, with few mitotic cells present, immunostaining for the mitotic marker Ki67 was performed (3-4 weeks post-plating). Less than 7% of cells expressed Ki67 in control and patient iPSC-derived cultures.

## 2.3. Immunofluorescence

Cells were fixed in 4% (wt/vol) paraformaldehyde for 10 minutes, permeabilized in 0.1% Triton X-100 at room temperature for 10 minutes and blocked in 3% (vol/vol) goat or donkey serum for 45 minutes. They were then incubated in primary antibodies for 45 minutes (Table 2.1) followed by secondary antibodies for 20 minutes (Alexa Fluor dyes, Invitrogen). The nuclei were counterstained with DAPI (Sigma) for 5 minutes and coverslips were mounted on slides with FluorSave (Merck). Fluorescent imaging was performed on fields of view containing uniform DAPI staining using an Axioscope (Zeiss) microscope. Images were processed with Axiovision V 4.8.1 (Zeiss) and immunolabelled cells counted manually by a blinded observer within ImageJ64 (v 1.47) software. Karen Burr in Siddharthan Chandran's lab at the University of Edinburgh carried out the immunofluorescence staining and imaging for Fig. 2.1A, C and Fig. 2.2B.

| Antibody | Host | Company | Concentration |
|---|---|---|---|
| **B3-Tubulin** | Mouse monoclonal | Sigma | 1:1000 |
| **HB9** | Mouse monoclonal | Developmental Studies Hybridoma Bank | 1:250 |
| **GFAP** | Rabbit polyclonal | Dako | 1:500 |
| **SMI-32** | Mouse monoclonal | Covance | 1:250 |
| **Ki67** | Mouse monoclonal | Dako | 1:200 |
| **SOX1** | Goat polyclonal | R&D systems | 1:100 |
| **Nestin** | Mouse monoclonal | Milipore | 1:100 |
| **Brachyury** | Goat polyclonal | R&D systems | 1:100 |
| **Eomes** | Rabbit polyclonal | Abcam | 1:600 |
| **Fox A2** | Goat polyclonal | R&D systems | 1:100 |
| **GATA-4** | Mouse monoclonal | Santa Cruz | 1:100 |

**Table 2.1: List and concentration of antibodies used**

## 2.4. Repeat primed (RP-) PCR

RP-PCR was used to confirm the presence or absence of the *C9ORF72* hexanucleotide repeat expansion in control or carrier neurons. PCR amplification was carried out using Multiplex Mastermix (Qiagen); 7% DMSO, 0.6 M Betaine, 7.6 µM Primer F (CTGTAGCAAGCTCTGGAACTCAGGAGTCG), 3.6 µm Primer Repeat R (TACGCATCCCAGTTTGAGACGCCCCGGCCCCGGCCCCGGCCCC), 11.6 µM Tail R (TACGCATCCCAGTTTGAGACG), 8 µM 7-deaza-2'-dGTP and 200 ng DNA. Cycling conditions were performed as per manufacturer's recommendations except for the annealing temperature which was 68°C for 15 cycles, then 60°C for a further 20 cycles. PCR products were separated on an ABI 3130xL analyser (Life Technologies) and data were analysed using GeneMarker software (Soft Genetics). Elaine Cleary in Siddharthan Chandran's lab at the University of Edinburgh performed RP-PCR and the following RNA-FISH protocols, and provided the figure panels in Fig. 2.1D, E.

## 2.5. RNA- fluorescence in situ hybridization (FISH)

FISH was performed using an Alexa 546- conjugated $(GGCCCC)_4$ oligoneucleotide probe (IDT). Briefly, cells on glass coverslips were fixed in 4% PFA for 30 mins, permeabilized in 70% ethanol at 4°C, incubated with 50% formamide/2X SSC for 10 min at room temperature, and hybridized for 2 hours at 37°C with the oligoneucleotide probe (0.16 ng/µl) in hybridization buffer consisting of 50% formamide, 2X SSC, 10% dextran sulphate, yeast tRNA (1 mg/ml), salmon sperm DNA (1 mg/ml) and 0.2% Tween-20. The cells were washed twice with 50% formamide/1X SSC for 30 min at 37°C and once with 2X SSC at room temperature for 30 mins. Immunostaining was performed as described above.

## 2.6. CRISPR/Cas9

The isogenic *C9ORF72* Δ $G_4C_2$ iPSC line was generated from a *C9ORF72* ALS patient iPSC line using CRISPR/Cas9 mediated genome editing. The Clustered Regularly Interspaced Short Palindromic Repeats (CRISPR) system, based on a bacterial protein from the *Streptococcus pyogenes,* targets and modifies the genomic sequence. The patient iPSC line used to generate the isogenic iPSC (Carrier-1) has 2X $G_4C_2$ repeats in the wild-type allele (analysed by Sanger sequencing) and approximately 750 repeats in the mutant allele (analysed by southern blot). In brief, two guide RNA's gRNA-1: 5'GACTCAGGAGTCGCGCGCTA-3' and gRNA-2: GGCCCGCCCCGACCACGCCC flanking $G_4C_2$ expansion repeats were cloned into the pSpCas9 (BB)-2A-GFP vector. *C9ORF72* patient iPSCs were transfected with these vectors to induce double strand break in the DNA sequence at precise locus

resulting in deletion of $G_4C_2$ repeats. Repeat primed PCR was used to screen individual iPSC clones for deletion $G_4C_2$. Sanger sequencing *C9ORF72* $G_4C_2$ locus of positive clone suggested that complete deletion of $G_4C_2$ repeats in the mutant allele and 1X $G_4C_2$ from the wild-type allele.

## 2.7. Cell viability assays

Cell counts were performed, with the observer blinded to cell type, on 20 IR-DIC images for each cell type (control, *TARDBP* and *C9ORF72*) at each 2-week time-point throughout the 10 weeks cells were maintained. IR-DIC images were chosen at random from a database of images (40 x magnification) that were obtained whenever whole-cell patch-clamp recordings were attempted. Cell counts were fitted with a negative binomial generalised linear model and the effect of time assessed with a likelihood ratio test.

For LDH assays, cell culture medium was collected from control and patient derived lines, which were differentiated in parallel to enable direct comparisons. Medium was collected twice per week across weeks 3-10 post-plating from *TARDBP* (D1 and D3), *C9ORF72* (S6 - 2 experiments and R2) and control lines (D6 - 2 experiments, M2 and R6). LDH activity (mU/ml) was calculated for each cell type using LDH assay kits (Abcam). LDH activity was plotted versus post-plating date, and compared between cell types using linear models. Nuclear morphology was assessed, with the observer blinded to cell type, by counting the number of pyknotic nuclei in 40 images taken from control and patient-derived lines at 9-10 weeks post-plating. Statistical analysis was performed using a one-way ANOVA followed by Tukey's post-hoc test.

## 2.8. Pharmacological treatment in culture

Amiloride hydrochloride hydrate (Sigma) was dissolved in DMSO to 100 mM and used at final concentrations between 25 μM and 100 μM in cell culture medium (Friese et al., 2007). Amiloride was applied to MN cultures from 24 hours post-plating and then throughout their time in culture.

## 2.9. Electrophysiology

Whole-cell patch-clamp recordings were used to assess the functionality of iPSC-derived MNs. Voltage-clamp mode was used to investigate intrinsic membrane properties. Current-clamp mode was used to investigate the firing properties of MNs. Experiments were carried out in a recording chamber which was perfused continuously with oxygenated artificial cerebral spinal fluid (aCSF) at room temperature (22-24°C). Whole-cell patch-clamp recordings were made from cells visualised by IR-DIC microscopy using an Olympus upright BX51WI microscope with a 40X submersion lens. Patch electrodes (4.0-5.0 MΩ resistance) were pulled on a Sutter P-97 horizontal puller (Sutter Instrument Company, Novato, CA) from borosilicate glass capillaries (World Precision Instruments, Sarasota, FL). Recorded signals were amplified and filtered (4kHz low-pass Bessel filter) using a MultiClamp 700B amplifier (Axon Instruments, Union City, CA) and acquired at ≥ 10kHZ using a Digidata 1440A analog-to-digital board and pClamp10 software (Axon Instruments). Whole-cell capacitance ($C_m$), input resistance ($R_N$), series resistance ($R_S$) and resting membrane potential (RMP) values were calculated using pClamp10 software. Only cells with an $R_s < 20M\Omega$, a RMP more hyperpolarised than -20mV and $R_N > 100$ MΩ were included in data analysis. $R_s$ values were not significantly different between

control, *C9ORF72* and *TARDBP* lines. Cells were defined as neurons if they had clear fast-inactivating inward currents (≥ 50pA). In a subset of experiments such currents were found to be TTX-sensitive (data not shown). Recordings from glial cells, which were clearly distinguishable based on their hyperpolarised RMP and absence of inward currents, were excluded from all analyses. An on-line P4 leak subtraction protocol was used for all recordings of voltage-activated currents. Descriptions of voltage and current-clamp protocols are provided in the results section.

The aCSF used for all electrophysiological recordings contained the following in mM: 127 NaCl, 3 KCl, 2 $CaCl_2$, 1 $MgSO_4$, 26 $NaHCO_3$, 1.25 $NaH_2PO_4$, 10 D- glucose (equilibrated with 95% $O_2$ and 5% $CO_2$ at room temperature, pH 7.45; osmolarity, ~ 310mOsm). The pipette solution contained (in mM): 140 potassium methane-sulfonate, 10 NaCl, 1 $CaCl_2$, 10 HEPES, 0.2 EGTA, 3 ATP-Mg, 0.4 GTP, (pH 7.2-7.3, adjusted with KOH; osmolarity adjusted to ~ 300mOsm with sucrose). All drugs were made up as concentrated stock solutions in single use vials and stored at -20°C. The final concentrations were achieved by diluting stock solutions in aCSF. Stock solutions of GABA and glycine were made up in distilled water. Stock solutions of glutamate were made up in 0.1M NaOH. Drug application was via addition to the perfusate.

Electrophysiological data were analysed using Clampfit10 software (Axon Instruments) or Dataview (courtesy of Dr. W.J. Heitler, University of St. Andrews). Data from each type of iPSC line (control, *TARDBP* and *C9ORF72*) were pooled for all analyses. Peak $Na^+$ currents and peak $K^+$ currents ($log_{10}$ transformed), $C_m$, $R_N$, and RMP were compared across the three different types of cell lines using factorial ANOVAs with post-plating date (in 2 week bins; 3-4, 5-6, 7-8, 9-10) and cell line

type (control, *TARDBP* or *C9ORF72*) as factors. Two-tailed t-tests were used for comparing MNs, which were either amiloride treated or untreated, and for comparisons of the C9 Carrier-1 mutant line and its isogenic control. Frequency-Current *(f-I)* relationships were compared across cell lines using linear models fitted to the initial, most linear portion of the *f*-I relationship (≤40pA above rheobase). Pair-wise comparisons were made using Tukey's honest significant difference test, where necessary.

For the purposes of statistical comparisons, spontaneous synaptic activity and action potential generation were classified as either present or absent. These binary data were fitted with a logistic regression using post-plating date, transformed with a second order polynomial, and cell line type as factors. Contrasts were made using Wald's tests and P values adjusted using a Bonferroni correction.

Firing properties were further analysed by assigning cells into four categories (No-Spike/Single/Adaptive/Repetitive). These data were then fitted with a multinomial logistic regression using type of iPSC line and either peak $K^+$ or peak $Na^+$ currents ($log_{10}$ transformed) as factors. Using these models, predicted probabilities for each firing mode were calculated over a range of $K^+$ and $Na^+$ current magnitudes for all types of iPSC lines. Factors within the multinomial logistic regression were assessed with likelihood ratio tests. Statistical analyses were performed using SPSS, R and the software packages MASS, multcomp and nnet. Joshua Foster from Gareth Miles' lab at the University of St Andrews carried out statistical analyses on the *f*-I relationships, synaptic activity data, action potential data and generated Fig. 2.8. All data are presented as mean ± SE.

# 3. Results

## 3.1. Differentiation of MNs from human iPSC lines

iPSCs were generated from fibroblasts of ALS patients and healthy individuals as previously described (Yusa et al., 2011; Bilican et al., 2012). 8 iPSC lines were utilised: 2 clones from 1 *TARDBP* patient (lines D1 and D3); clones from 2 different *C9ORF72* patients (lines S6, 2H9 Carrier-1Δ and R2); 2 clones from 1 healthy control (lines R6 and M2); and single clones from 2 additional healthy controls (lines D6 and D9; see methods for further details), with each line differentiated a minimum of 4 times. All iPSCs used in the study exhibited silencing of the four transgenes used to induce pluripotency with subsequent activation of endogenous OCT4, SOX2, and KLF4 (Fig. 2.1A). Pluripotency was confirmed by expression of pluripotency markers OCT4, SOX2, TRA-1-60 and NANOG and through the use of RT-PCR. Three germ layer differentiation was confirmed by SOX1, Nestin, Brachyury, Eomes, FOXA2 and GATA-4 expression (Fig. 2.1C). All clones used had a normal karyotype, with genotyping confirming mutations in *TARDBP* lines and hexanucleotide GGGGCC repeat expansions in *C9ORF72* lines shown by repeat prime PCR (Fig. 2.1B, D). RNA foci containing GGGGCC hexanucleotide repeat expansions were also revealed in *C9ORF72* lines using fluorescence in situ hybridization (FISH; Fig. 2.1E).

Differentiation into a neuronal and MN lineage was performed using a modified version of established protocols which enabled the maintenance of cells for up to 10 weeks (Bilican et al., 2012; Amoroso et al., 2013)(Fig. 2.2A). At weeks 5-6 post-plating, immunohistochemistry was performed on iPSC-derived MNs to assess the relative expression of glial, neuronal and MN markers. Quantitative immunolabelling

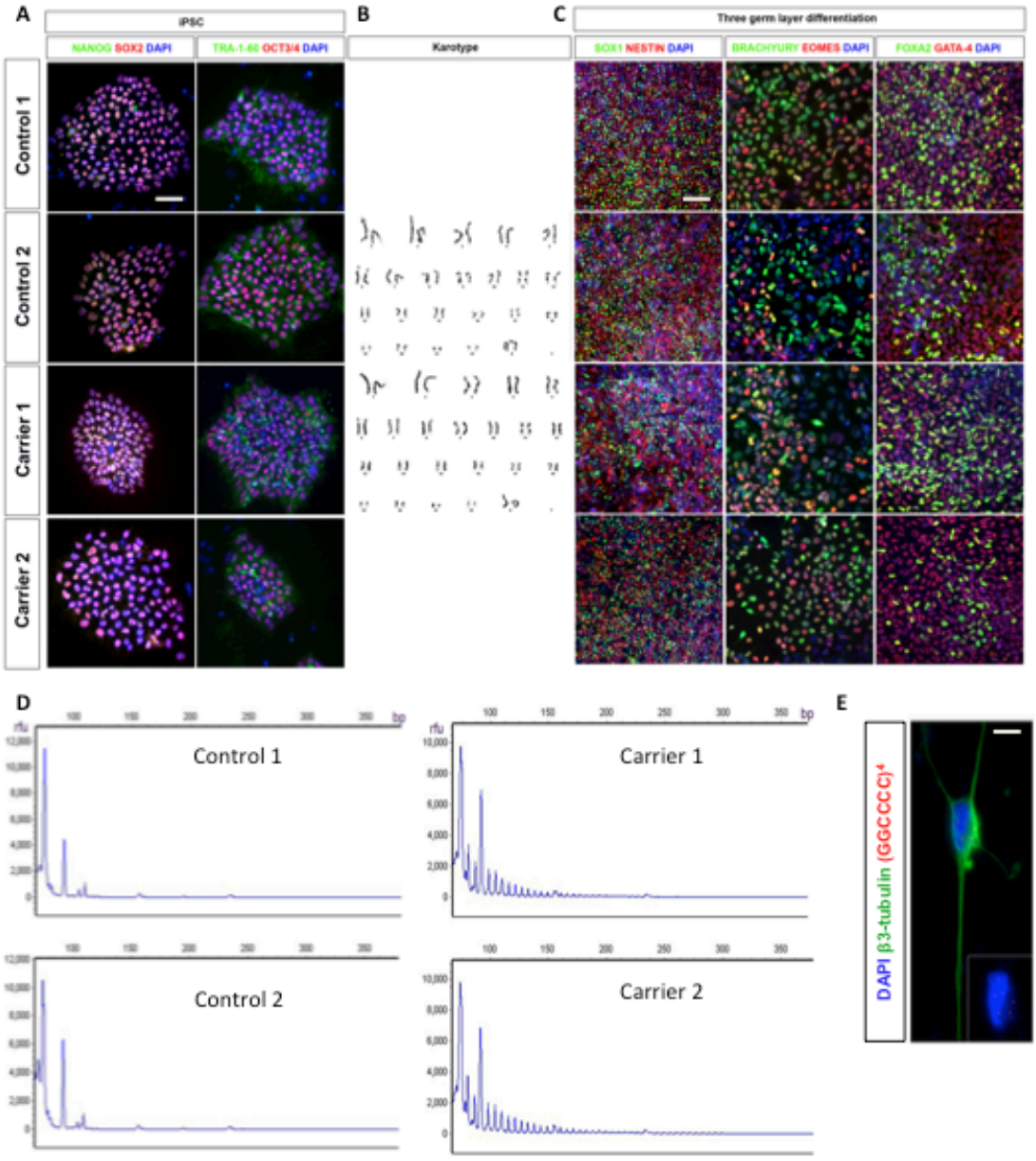


**Figure 2.1: Confirmation of pluripotency and three germ layer differentiation.**

Figure caption on following page

**Figure 2.1: Confirmation of pluripotency and three germ layer differentiation.**

(A) Immunohistochemical labelling of the pluripotency markers NANOG, SOX2, OCT3/4 and TRA- 1-60 in feeder free iPSCs from controls and patients harbouring the *C9ORF72* mutation [for *TARDBP*, see (Bilican et al., 2012) scale bar =50 μm]. (B) Karyotypes of control and patient-derived iPSCs. (C) Immunohistochemical staining of the three germ layers differentiated from control and patient iPSC lines: neuroectoderm (SOX1 and nestin); mesoderm (brachyury and Eomes); and endoderm (FOXA2 and GATA-4; see antibodies Table 2.1, scale bar =50 μm; Parts A, B and C were generated by Karen Burr in Siddharthan Chandran's lab at the University of Edinburgh) (D) RT- PCR analysis demonstrating the presence or absence of the *C9ORF72* hexanucleotide repeat expansion. (E) Representative image of GGGGCC RNA foci of the *C9ORF72* hexanucleotide repeat expansion in an iPSC-derived neurons from a patient harbouring the *C9ORF72* mutation. RNA fluorescence in-situ hybridisation (FISH) was carried out using an Alexa 546 conjugated $(GGCCCC)_4$ probe (Scale bar =10 μm; Parts D and E were generated by Elaine Cleary in Siddharthan Chandran's lab at the University of Edinburgh) .

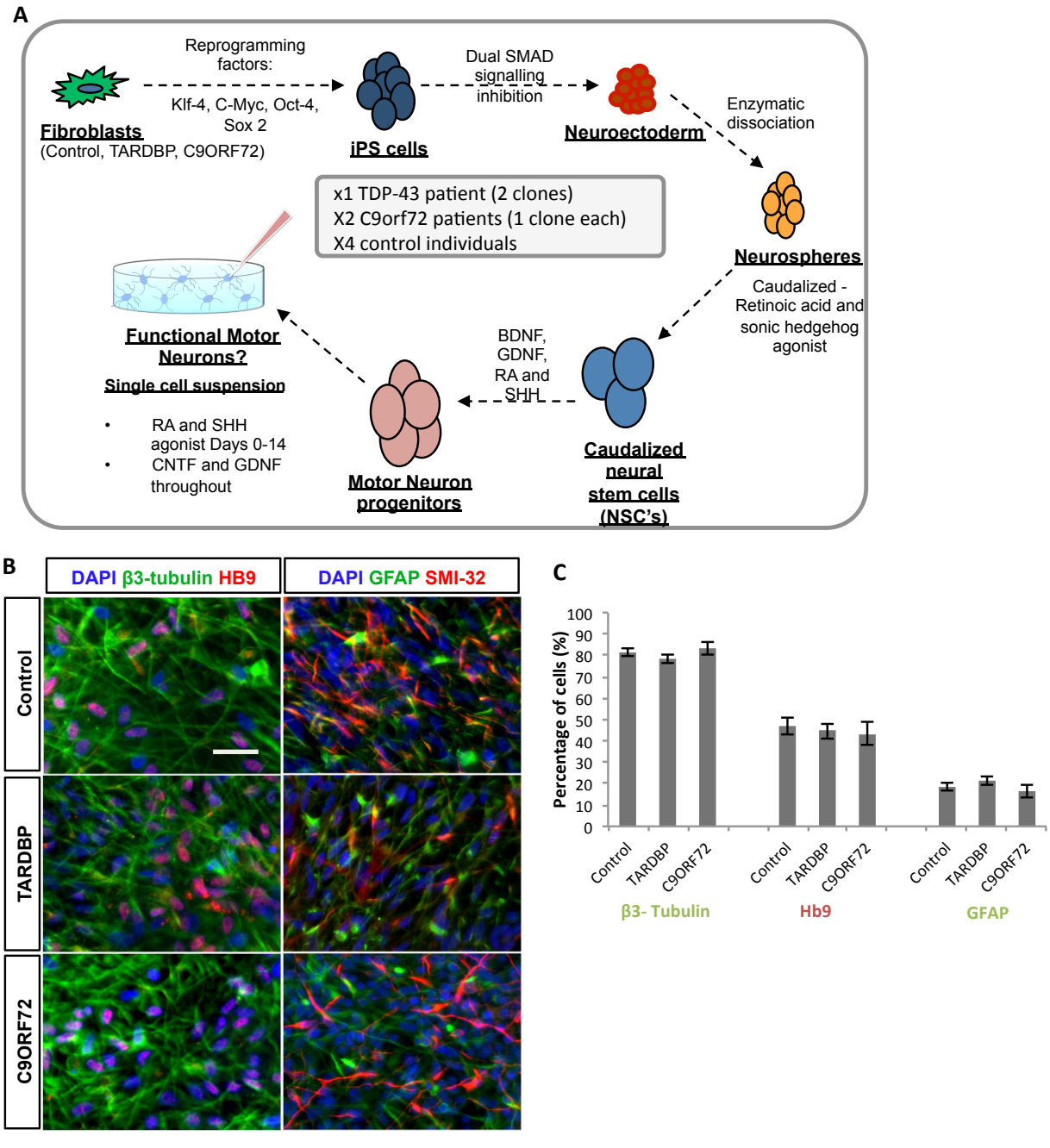


**Figure 2.2: Differentiation of MNs from control and patient iPSC lines.**

Figure caption on following page

**Figure 2.2: Differentiation of MNs from control and patient iPSC lines.**

(A) Schematic diagram of method of iPSC differentiation into MNs (B) Immunohistochemical staining of differentiated iPSCs (control, *TARDBP* and *C9ORF72* lines) using antibodies raised against β3-tubulin, Hb9, SMI-32 and glial fibrillary acidic protein (GFAP) (scale bar = 50 μm; Karen Burr in Siddharthan Chandran's lab at the University of Edinburgh provided images for Part B). (C) Proportion of differentiated iPSCs expressing β3-tubulin, Hb9 and GFAP (total cells counted: control, 1,126 cells; *TARDBP*, 1,224 cells; *C9ORF72*, 1,534 cells).

for β3-tubulin and GFAP revealed comparable neuronal and astroglial differentiation from 1 control (D6) and 2 patient (*TARDBP* D1 and *C9ORF72* S6) iPSC lines (β3-tubulin: Control $\overline{x}$ 81.5 ± s.e.m 1.7%, *TARDBP* 78.4 ± 2.2%, *C9ORF72* 83.4 ± 3.1%; GFAP: Control 18.5 ± 1.7%, *TARDBP* 21.6 ± 2.2%, *C9ORF72* 16.6 ± 3.1%; Fig. 2.2B, C) as well as a similar proportion of Hb9-positive MNs (Control $\overline{x}$ 46.8 ± s.e.m 3.8% *TARDBP* 44.6 ± 3.7%, *C9ORF72* 43.4 ± 5.2%; Fig. 2.2B, C). Positive and negative controls were used to demonstrate that the antibody was specific to the correct cell types (data not shown). These findings are consistent with previous reports of MN-enriched cultures derived from *TARDBP* iPSC lines (Bilican et al., 2012).

## 3.2. Comparable viability of neurons derived from control and ALS patient iPSCs

Having established equivalent MN enriched cultures from both control and patient iPSC lines, investigations were carried out to determine if there were any differences in cell viability between neurons derived from control and ALS patient iPSCs. The initial observations suggested that control and patient iPSC-derived neurons with either *TARDBP* or *C9ORF72* ALS mutations were indistinguishable, based on cell morphology (Fig. 2.3A), up to the latest time point investigated (10 weeks post-plating). To confirm this, quantitative analyses of cell viability using cell counts, lactate dehydrogenase (LDH) assays and assessment of nuclear morphology were performed. Cell counts revealed no difference between patient derived lines compared to controls throughout the 10 weeks in culture (80 images analysed per cell type; Fig.

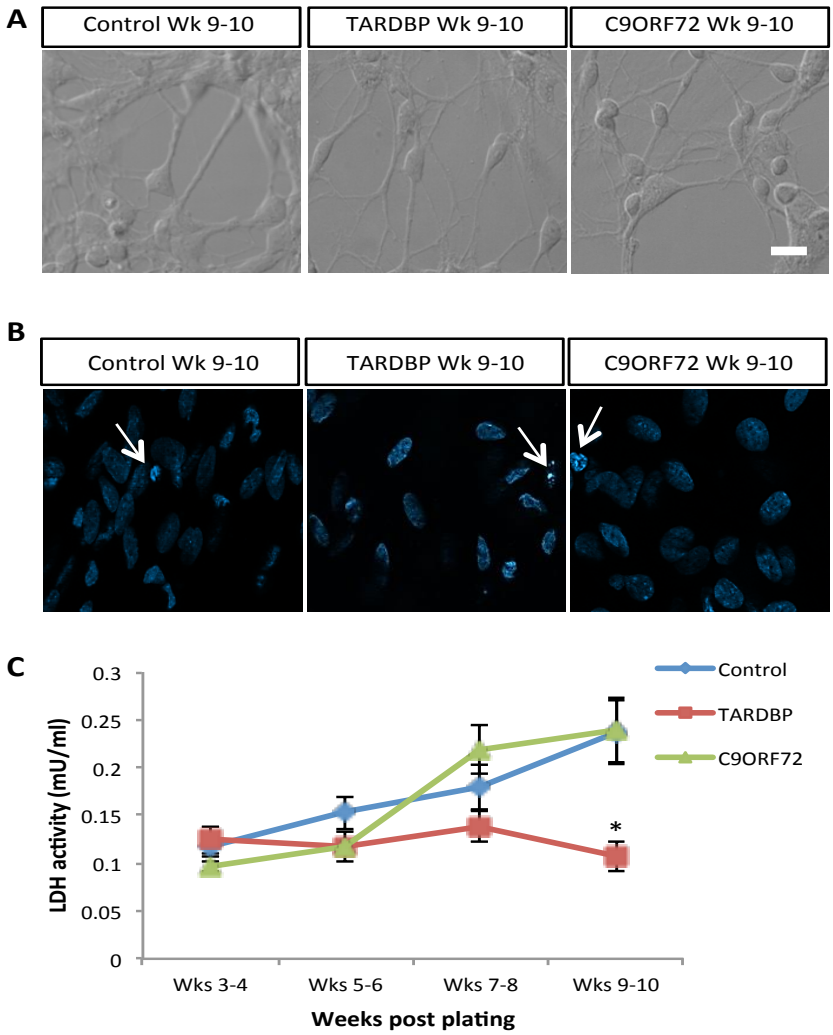


**Figure 2.3: Equivalent viability of control and patient iPSC-derived MNs**.

(A) IR-DIC images of iPSC-derived MNs from control, *TARDBP* and *C9ORF72* lines at weeks 9–10 post plating (scale bar, 20 μm). (B) Representative images of nuclear stained cells for cell density and pyknotic nuclei counts (arrows indicate pyknotic nuclei). (C) LDH activity plotted for control and patient iPSC-derived cultures from weeks 3–10 post plating (Control lines (D6: two experiments, M2 and R6), *TARDBP* lines (D1 and D3), *C9ORF72* (S6: two experiments and R2); data are plotted as $\bar{x} \pm$ s.e.m; *, patient line significantly different to control lines, $P<0.05$; factorial ANOVA).

2.3B). Nuclear morphology was assessed, using counts of pyknotic nuclei, at 9-10 weeks post-plating in 1 control (D6), 1 *TARDBP* (D1) and 1 *C9ORF72* (S6) line. No differences were found in the percentage of cells with pyknotic nuclei in patient lines compared to controls (Control $\overline{x}$ 8.2% ± s.e.m 0.58, n = 3386 cells; *TARDBP* 8.4% ± 0.25, n = 1558; *C9ORF72* 5.4% ± 0.36, n = 2336; Fig. 2.3B). Analysis of LDH activity in 2 *TARDBP* lines (D1, D3), 2 *C9ORF72* lines (S6, R2) and 3 control lines (D6, M2, R6) revealed no greater LDH activity in patient compared to control lines at any time point during the 10 weeks in culture (Fig. 2.3C). There was in fact less LDH activity in *TARDBP* lines at 9-10 weeks post-plating (Fig. 2.3C). In summary, cell counts, counts of pyknotic nuclei and LDH assays failed to reveal any differences in viability between neurons derived from iPSC lines harbouring *TARDBP* or *C9ORF72* mutations compared to controls.

## 3.3. Hyperexcitability followed by progressive loss of functional output in patient iPSC-derived MNs

Given that standard cell viability assays failed to reveal overt effects of *TARDBP* or *C9ORF72* mutations on iPSC-derived cell viability, sensitive electrophysiological analyses were carried out to uncover any signs of neuronal dysfunction. Such analyses have previously revealed some of the earliest changes in transgenic mouse models of ALS, supporting a pathogenic role for early functional changes in ALS-affected MNs (Pieri et al., 2003; Kuo et al., 2005; Zona et al., 2006; Bories et al., 2007; van Zundert et al., 2008; Quinlan et al., 2011; Fuchs et al., 2013).

Whole-cell patch-clamp recordings were obtained from the largest neurons visualised via infrared-differential interference contrast (IR-DIC) microscopy in cultures from 2

to 10 weeks post-plating. The selection of the largest neurons for recordings along with the high degree of MN enrichment ensured studied cells were predominantly MNs. In a subset of experiments this was supported by *post-hoc* SMI-32 labelling of neurons filled with an alexa fluor dye during recordings (Fig. 2.4A). A high proportion of recovered neurons (78%; 18 of 23 cells) were found to be SMI-32 positive. Therefore, the possibility that some recordings were from spinal interneurons could not be excluded. However, data from mixed neuronal populations are also valuable given that ALS affects a wide range of neuronal cells types including cortical neurons and spinal interneurons (Ilieva et al., 2009). The passive membrane properties of MNs derived from control and patient iPSCs were first compared. For these and all other electrophysiological analyses, data were pooled for control (D9, D6, R6 and M2), *TARDBP* (D1, D3) and *C9ORF72* (R2, S6) iPSC lines (see Table 2.3 and Fig. 2.9 for data and sample sizes separated by iPSC line). Whole-cell capacitance ($C_m$) values were similar across control and patient iPSC-derived MNs (Table 2.2), although MNs harbouring *C9ORF72* mutations had lower $C_m$ compared to MNs harbouring *TARDBP* mutations at weeks 3-4, weeks 7-8 and weeks 9-10 ($P<0.001$), and control MNs had lower $C_m$ compared to MNs harbouring *TARDBP* mutations at weeks 7-8 and weeks 9-10 ($P<0.0001$). No significant differences were found between the input resistance ($R_N$) of MNs derived from control, *TARDBP* or *C9ORF72* iPSCs from weeks 3 to 10 post-plating (Table 2.2). MNs harbouring a *TARDBP* mutation had more depolarised resting membrane potentials (RMP) compared to controls at weeks 3-4 ($P< 0.001$) and weeks 9-10 ($P< 0.0001$), while the RMPs of MNs with a *C9ORF72* mutation were more depolarised than controls at weeks 7-8 ($P< 0.0001$) (Table 2.2). The largest differences in RMP between control

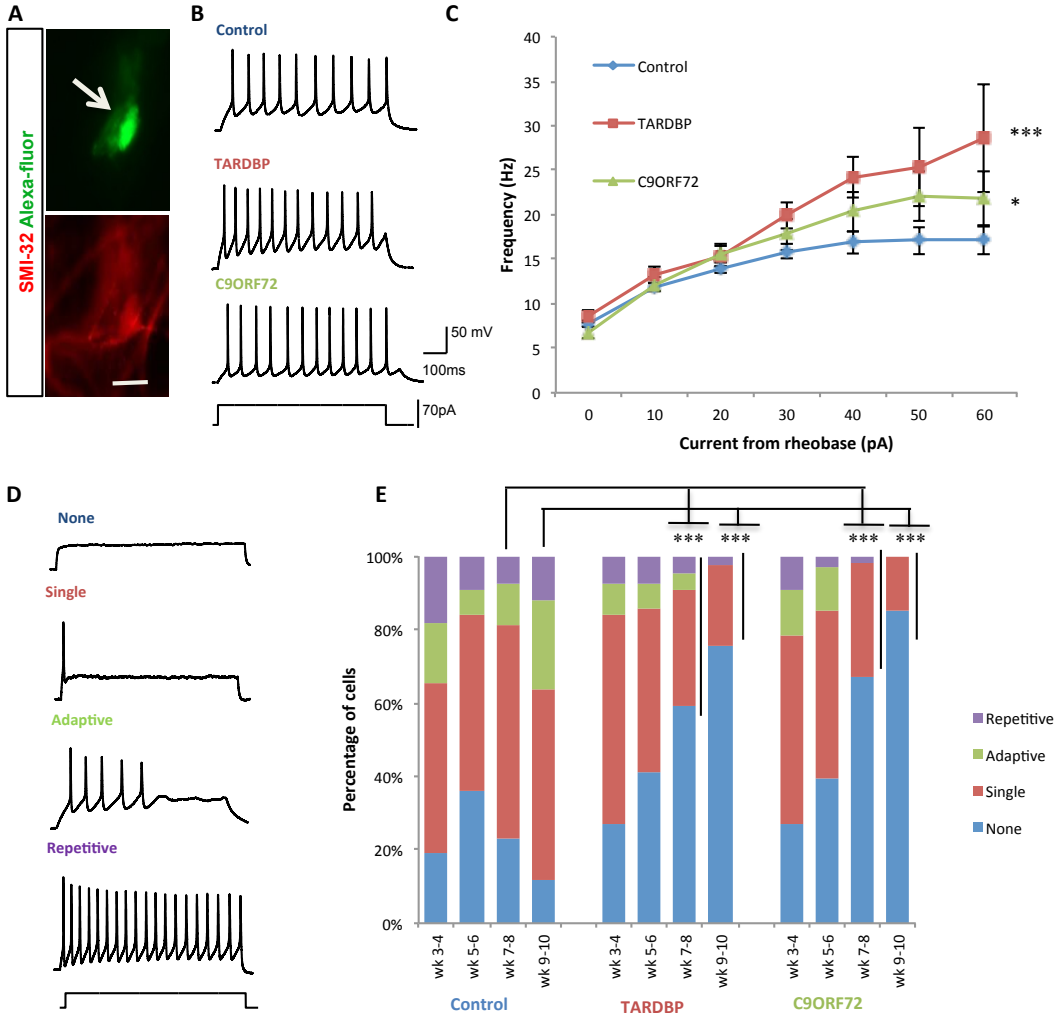


**Figure 2.4: Hyperexcitability followed by loss of action potential output in patient iPSC-derived MNs.**

Figure caption on following page

**Figure 2.4: Hyperexcitability followed by loss of action potential output in patient iPSC-derived MNs.**

(A) Fluorescent image of a cell filled with Alexa Fluor 488 dye during whole-cell patch-clamp recordings and immunolabelling with an antibody raised against SMI-32 (arrow heads point to cell soma; scale bar =10 μm). (B) Repetitive firing in response to square current injection in iPSC-derived MNs from control, *TARDBP* and *C9ORF72* lines. (C) Frequency-current (*f–I*) relationships generated for repetitively firing iPSC-derived MNs from control (n= 62), *TARDBP* (n =19) and *C9ORF72* (n =19) lines recorded from weeks 2–6 post plating (data are plotted as $\overline{x}$ ± s.e.m. with lines of best fit; *, patient line significantly different to control, P<0.05; ***, P<0.0001; linear model with multiple contrast for the gradient values, and adjusted with Bonferroni correction). (D) Examples of the four categories of firing observed in iPSC-derived MNs (repetitive, adaptive, single or no firing). (E) Proportion of cells exhibiting each firing category in iPSC-derived MNs from control (n=702), *TARDBP* (n=380) and *C9ORF72* (n=239) lines across weeks 3–10 post plating (***, patient lines significantly different to control lines at same time-point, P<0.0001; logistic regression with multiple Wald's test and Bonferroni correction).

| Passive membrane properties | Control | TARDBP | C9ORF72 |
|---|---|---|---|
| **$C_m$(pF)** | | | |
| Weeks 3-4 | 10.4 ± 0.4(196) | 12.0 ± 0.5(103) | 8.7 ± 0.3(102)$^{\#\#}$ |
| Weeks 5-6 | 11.6 ± 0.3(322) | 11.2 ± 0.4(171) | 10.1 ± 0.5(69) |
| Weeks 7-8 | 10.7 ± 0.3(216) | 16.1 ± 1.1(96)$^{***}$ | 11.9 ± 0.9(52)$^{\#\#}$ |
| Weeks 9-10 | 14.0 ± 0.6(111) | 19.7 ± 1.2(82)$^{***}$ | 14.5 ± 0.7(42)$^{\#\#}$ |
| **$R_N$(MΩ)** | | | |
| Weeks 3-4 | 727 ± 22 | 660 ± 33 | 723 ± 33 |
| Weeks 5-6 | 774 ± 21 | 788 ± 27 | 768 ± 42 |
| Weeks 7-8 | 774 ± 23 | 762 ± 38 | 772 ± 45 |
| Weeks 9-10 | 709 ± 30 | 688 ± 39 | 643 ± 58 |
| **RMP(mV)** | | | |
| Weeks 3-4 | -45.6 ± 0.8 | -39.9 ± 1.0$^{**}$ | -44.8 ± 1.2 |
| Weeks 5-6 | -42.8 ± 0.7 | -40.4 ± 1.0 | -44.2 ± 1.5 |
| Weeks 7-8 | -45.6 ± 0.8 | -43.2 ± 1.4 | -37.9 ± 1.5$^{***}$ |
| Weeks 9-10 | -49.8 ± 1.1 | -40.1 ± 1.9$^{***}$ | -45.2 ± 1.9 |

Values are mean ± SEM; number of cells noted in parentheses.
*Significantly different to controls (**,p<0.001; ***,p<0.0001)
$^{\#}$ Significant difference between patient lines($^{\#\#}$,p<0.001; $^{\#\#\#}$,p<0.0001)

**Table 2.2: Passive membrane properties of MNs derived from iPSC lines**

and patient iPSC-derived MNs were apparent toward the end of the time course studied. It should be noted that these numbers may represent an underestimation of the extent of membrane potential depolarisation in patient iPSC-derived MNs because cells that were more depolarised than -20 mV were excluded from all analyses to avoid the inclusion of cells that were depolarised due to damage associated with the establishment of recordings.

Current-clamp mode recordings of iPSC-derived MNs demonstrated that by 2 weeks post-plating all lines developed the ability to repetitively fire trains of action potentials in response to current injections. To compare the excitability of repetitively firing patient and control iPSC-derived MNs, frequency-current (*f-I*) relationships were generated from responses to a series of injected current steps (0 to 145 pA, in 10 pA increments, 1s duration). Comparisons were performed on data pooled from recordings of repetitively firing cells at weeks 2-6 post-plating (Fig. 2.4B, C). No differences were observed in rheobase current between control and patient iPSC-derived MNs (Control $\overline{x}$ 22.7 ± s.e.m. 2.6 pA, n = 62; *TARDBP* 23.4 ± 4.1 pA, n = 19; *C9ORF72* 17.1 ± 3.2 pA, n = 19). However, data demonstrated hyperexcitability in both the *TARDBP* and *C9ORF72* lines compared to controls, as indicated by the greater slopes of their *f-I* relationships (Control $\overline{x}$ 0.18 ± s.e.m 0.01 Hz/pA, *TARDBP* 0.34 ± 0.02 Hz/pA, *C9ORF72* 0.27 ± 0.01 Hz/pA; $P<0.05$). No significant difference was detected between the excitability of MNs derived from the *TARDBP* and *C9ORF72* lines. Thus, in parallel with findings in animal models of ALS, human MNs harbouring two different ALS-related mutations are initially more excitable than controls. Not all iPSC-derived MNs produced repetitive trains of action potentials demonstrating an incomplete functional maturation in some neurons. Several different

output patterns were observed in response to current injections that included repetitive, adaptive, single and no firing (Fig. 2.4D). Repetitive firing was defined as a train of action potentials that lasted for the duration of the square current injection (1s), while adaptive firing was defined as multiple action potentials that ceased before the end of the current stimuli. When data were compared across MNs derived from control, *TARDBP* and *C9ORF72* iPSC lines, no difference in the relative proportion of firing versus non-firing cells were found from weeks 3 to 6 post-plating (Control firing 70.4%, n=419, *TARDBP* firing 64.0%, n =214; *C9ORF72* firing 67.7%, n =149; Fig. 2.4E). However, at weeks 7-8 and 9-10 post-plating the number of cells able to fire action potentials decreased significantly in *TARDBP* and *C9ORF72* lines compared to controls ($P<0.0001$), while the ratio of firing versus non-firing cells remaining unchanged throughout the 10 weeks in control lines (Weeks 7-8: control firing 77.0%, n=183; *TARDBP* firing 40.9%, n=88; *C9ORF72* firing 32.6%, n=49; Weeks 9-10: control firing 88.1%, n=110; *TARDBP* firing 24.3%, n=78; *C9ORF72* firing 14.6%, n=41; Fig. 2.4E). These data demonstrate a loss of action potential output from iPSC-derived MNs harbouring ALS-related mutations rendering them non-functional despite their continued viability in culture.

## 3.4. Loss of synaptic activity in patient iPSC-derived MNs

Following investigation of the output produced by iPSC-derived MNs, their ability to receive synaptic input was examined, which is reported to be attenuated in ALS patients (Matsumoto et al., 1994; Sasaki and Maruyama, 1994; Ince et al., 1995) and animal models of the disease (Schutz, 2005; Chang and Martin, 2009; Jiang et al., 2009). First, it was assessed whether iPSC-derived MNs could respond to the major

excitatory neurotransmitter (NT) glutamate (100 μM) or the inhibitory NTs GABA (100 μM) and glycine (100 μM). This was assessed by bath applying these NTs during voltage-clamp recordings from iPSC-derived MNs held at -60 mV (Fig. 2.5A). Depolarising currents were recorded from MNs derived from both control and patient iPSC lines in response to glutamate applications (Fig. 2.5A). Control and patient iPSC- derived MNs also responded to GABA and glycine (Fig. 2.5A) with depolarising currents as expected based on the theoretical reversal potential for chloride in our recording solutions. Thus, both control and patient iPSC-derived MNs developed receptors required to respond to major NTs. Next, assessments were carried out to determine if iPSC-derived MNs receive functional synaptic inputs in culture. Spontaneous synaptic activity was observed in our recordings of both control and patient iPSC-derived MNs throughout the time-period studied (Fig. 2.5B). Consistent with previous reports (Bilican et al., 2012; Wainger et al., 2014), these inputs were predominantly excitatory as evidenced by a lack of outward currents, even when cells were held at -40 mV, which is well above the reversal potential for chloride (Fig. 2.5B). The proportion of cells that received any synaptic input (defined as at least 1 event per minute) was similar in control and patient iPSC-derived MNs from weeks 3-6 post-plating (3-6 weeks: 33.2% of controls, n=518; 33.5% of *TARDBP*, n=274; 22.2% of *C9ORF72*, n=171; Fig. 2.5C). The occurrence of synaptic activity then decreased in both patient derived lines from weeks 7-10 compared to controls (7-8 weeks: 34.2% of controls, n=216; 4.1% of *TARDBP*, n=96; 11.5% of *C9ORF72*; n=52; 9-10 weeks: 37.8% of controls, n=111; 6.1% of *TARDBP*, n=82; and 9.5% of *C9ORF72*; n=42; $P<0.05$; Fig. 2.5C). In cells cultured from 2-6 weeks

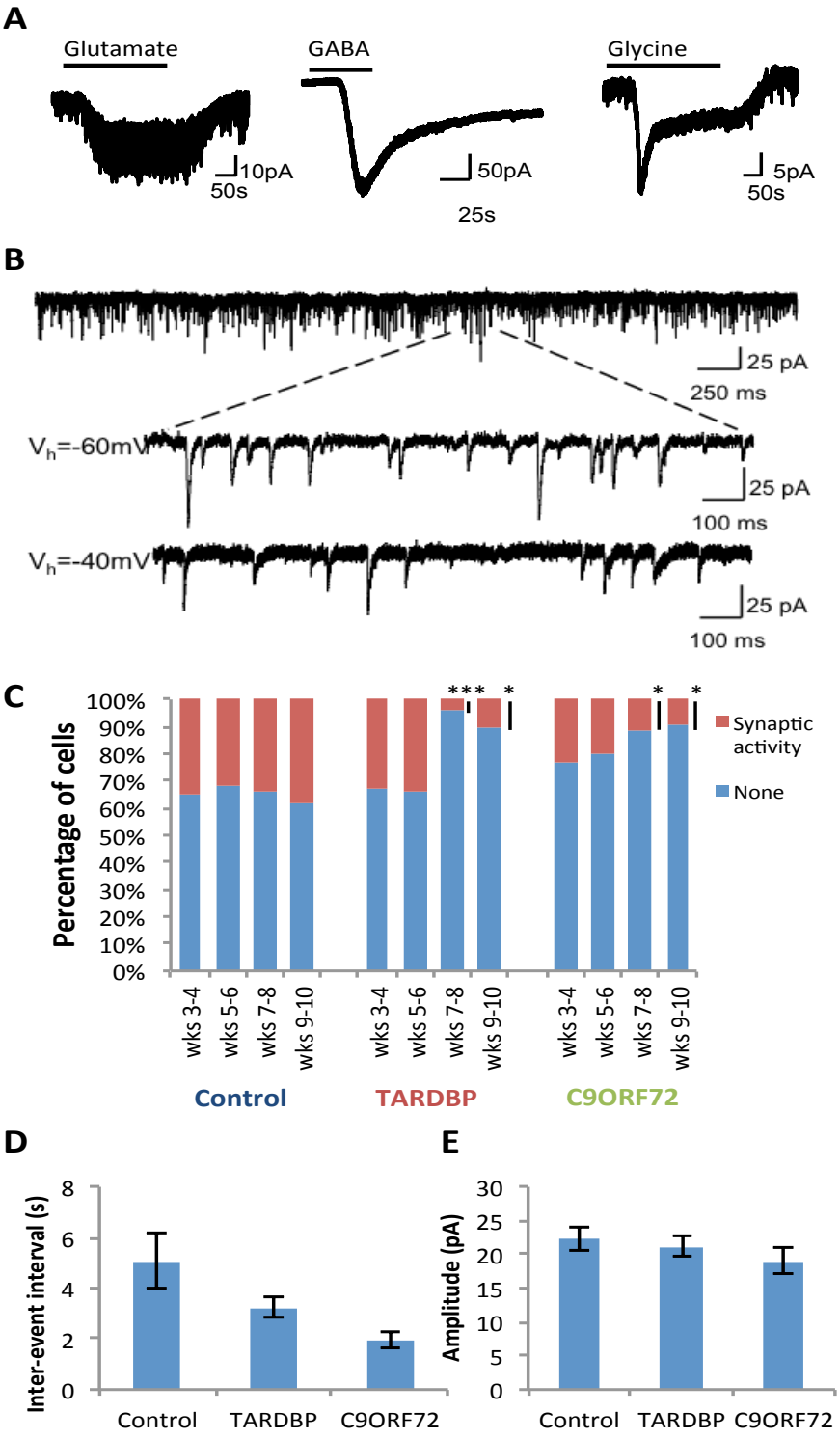


**Figure 2.5: Loss of synaptic input to patient iPSC-derived MNs.**

Figure caption on following page

**Figure 2.5: Loss of synaptic input to patient iPSC-derived MNs.**

(A) Current responses in iPSC-derived MNs during bath application of glutamate (100 μM), GABA (100 μM) and glycine (100 μM). (B) Voltage-clamp recordings of spontaneous synaptic activity in iPSC-derived MNs at different holding potentials. (B) Proportion of cells displaying synaptic activity from weeks 3–10 post plating in iPSC-derived MNs from control (n=845), *TARDBP* (n=417) and *C9ORF72* (n=265) lines. (*, patient lines significantly different to control, $P<0.05$; ***, $P<0.0001$; logistic regression with multiple Wald's tests and Bonferroni correction). (D) Graphs of inter-event interval and (E) amplitude of synaptic events recorded from control and patient iPSC-derived MNs.

we analysed the inter-event-interval and amplitude of synaptic events. Neither parameter differed between controls and patient iPSC-derived MNs (Fig. 2.5D). In summary, these data demonstrate a loss of synaptic input to *TARDBP* and *C9ORF72* iPSC-derived MNs, which may reflect the parallel loss of action potential output in these cultures or perturbations in synaptic transmission between cultured cells.

## 3.5. Loss of voltage-activated currents in patient iPSC-derived MNs

To investigate mechanisms underlying the progressive loss of action potential output from patient iPSC-derived MNs, voltage-clamp recordings of voltage-activated currents involved in action potential generation were performed. Fast, inactivating $Na^+$ currents (Fig. 2.6A), which underlie the upstroke of the action potential, were investigated by using a series of depolarising voltage steps (-70 to 20 mV, 2.5 mV increments, 10 ms duration) from a holding potential of -60 mV (Fig. 2.6B, C). No differences in the current-voltage (I-V) relationships or peak $Na^+$ currents were found between MNs derived from patient and control iPSCs at weeks 3-4 post-plating (Peak current: $\bar{x}$ control 1375 ± s.e.m 93 pA, n=196; *TARDBP* 1132 ± 101 pA, n=103; *C9ORF72* 1075 ± 103 pA, n=102; Fig. 2.6B, D). However, from week 5 post-plating a progressive loss of $Na^+$ currents in MNs derived from patient iPSCs was observed. Peak $Na^+$ currents were reduced compared to controls from weeks 5-10 post-plating in *C9ORF72* iPSC-derived MNs ($P<0.0001$) and from weeks 7-10 post-plating in *TARDBP* iPSC-derived MNs ($P<0.01$), while peak currents were also smaller in neurons derived from *C9ORF72* iPSCs compared to those derived from *TARDBP* iPSCs ($P<0.05$) from week 7 onwards (weeks 5-6: $\bar{x}$ control 875 ± s.e.m 53 pA,

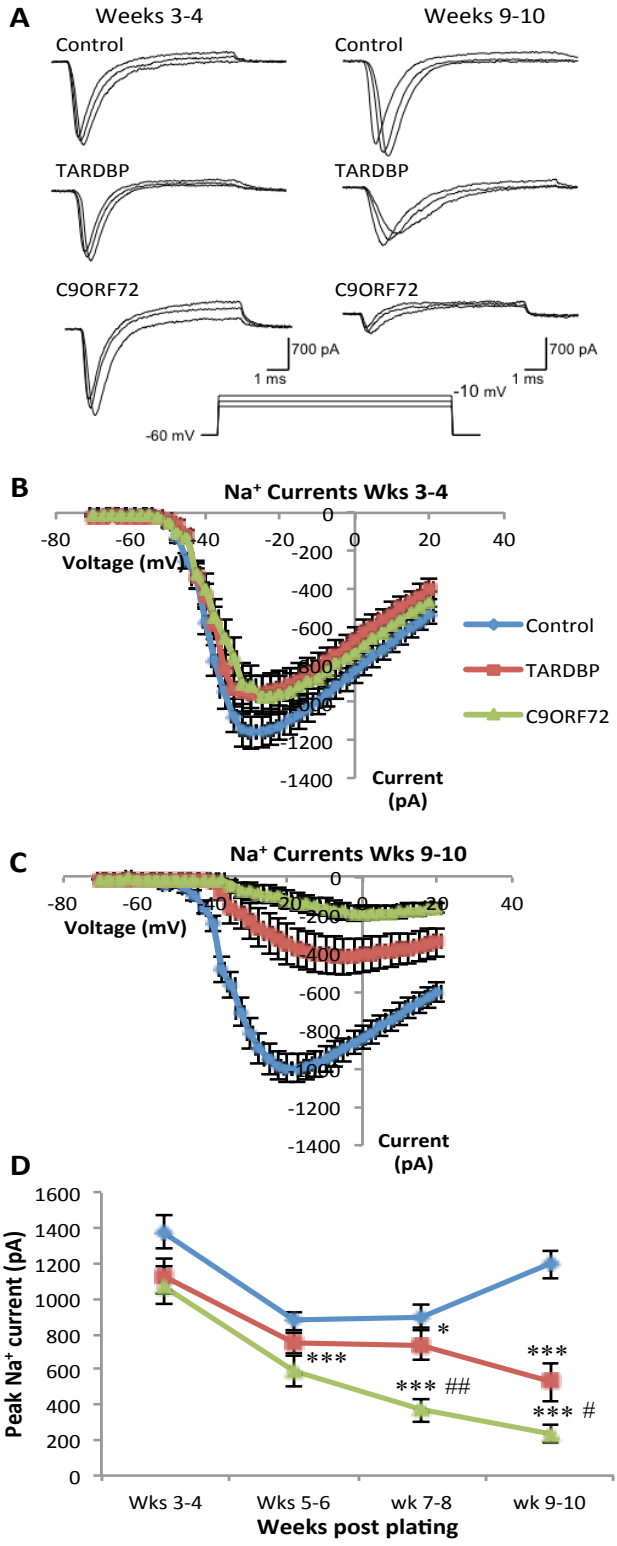


**Figure 2.6: Loss of fast-inactivating $Na^+$ currents in patient iPSC-derived MNs.**

Figure caption on following page

**Figure 2.6: Loss of fast-inactivating $Na^+$ currents in patient iPSC-derived MNs.**

(A) Raw data showing fast, inactivating $Na^+$ currents in control, *TARDBP* and *C9ORF72* iPSC-derived MNs at week 3–4 and weeks 9–10. (B) Current–voltage relationships of peak $Na^+$ currents recorded from control and patient iPSC-derived MNs at weeks 3–4. (C) Current–voltage relationships of peak $Na^+$ currents recorded from control and patient iPSC-derived MNs at weeks 9–10. (D) Peak fast, inactivating $Na^+$ currents plotted from weeks 3–10 for control (n=847), *TARDBP* (n=452) and *C9ORF72* (n=264) iPSC-derived MNs. (data are plotted as $\overline{x}$ ± s.e.m, *, patient line significantly different to controls, P<0.05; ***, P<0.0001; #, significant difference between patient lines, P<0.05; ##, P<0.001; linear model with multiple Wald's tests and Bonferroni correction).

n=322; *TARDBP* 751 ± 64 pA, n= 171; *C9ORF72* 587 ± 84 pA, n=69; weeks 7-8: control 902 ± 64 pA, n=216; *TARDBP* 741 ± 85 pA, n=96; *C9ORF72* 371 ± 66 pA, n=52; weeks 9-10: control 1196 ± 78 pA, n=111; *TARDBP* 529 ± 108 pA, n=82; *C9ORF72* 236 ± 49 pA, n=42; Fig. 2.6A, C, D). Having revealed a progressive loss of $Na^+$ currents, it was next assessed whether this reflected a more general decrease in voltage-activated currents in patient iPSC- derived MNs.

This was achieved by measuring persistent $K^+$ currents (Fig. 2.7A) elicited by a series of depolarising voltage steps (-70 to 40 mV, 10 mV increments, 500 ms duration) from a holding potential of -60 mV (Fig. 2.7B, C). At weeks 3-4 post-plating peak $K^+$ currents were comparable in *TARDBP* and control iPSC-derived MNs but were smaller in MNs derived from *C9ORF72* iPSCs when compared to controls (Peak current: $\bar{x}$ control 853 ± s.e.m 57 pA, n=196; *TARDBP* 799 ± 86 pA, n=103; *C9ORF72* 565 ± 57 pA, n=102; Fig. 2.7A, B, D). A progressive decline in peak $K^+$ currents in patient iPSC- derived MNs was next observed, with MNs harbouring a *C9ORF72* mutation having significantly smaller $K^+$ currents than controls at all time-points ($P<0.0001$) and MNs derived from *TARDBP* iPSCs having smaller $K^+$ currents compared to controls from weeks 7-8 post-plating onwards (weeks 5-6: $\bar{x}$ control 769 ± s.e.m 44 pA, n= 322; *TARDBP* 661 ± 54 pA, n= 171; *C9ORF72* 490 ± 61 pA, n=69; weeks 7-8: control 804 ± 57 pA, n=216; *TARDBP* 626 ± 84 pA, n=96; *C9ORF72* 276 ± 41 pA, n=52; weeks 9-10: control 897 ± 64 pA, n=111; *TARDBP* 505 ± 95 pA, n=82; *C9ORF72* 158 ±29 pA, n=42; $P<0.05$; Fig. 2.7B, C, D). $K^+$ currents were also smaller in MNs derived from *C9ORF72* compared to *TARDBP* iPSCs from weeks 5-6 post-plating onwards ($P<0.05$).

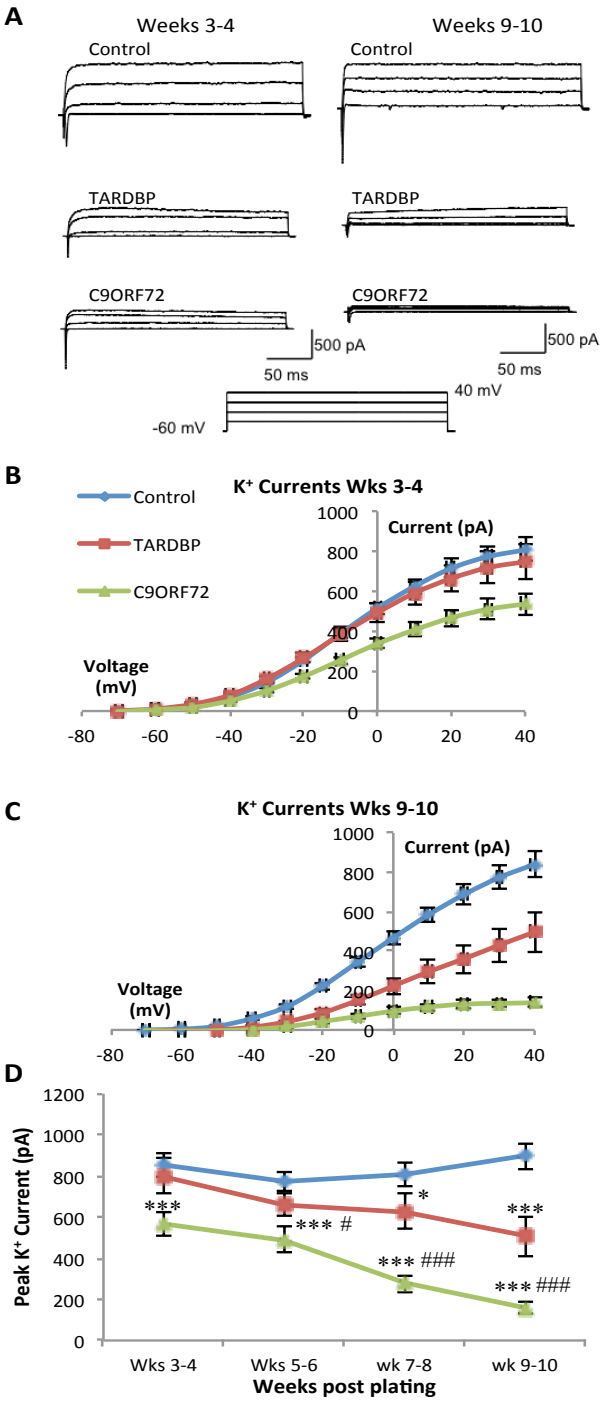


**Figure 2.7: Loss of persistent voltage-activated $K^+$ currents in patient iPSC-derived MNs.**

Figure caption on following page

**Figure 2.7: Loss of persistent voltage-activated $K^+$ currents in patient iPSC-derived MNs.**

(A) Raw data showing persistent $K^+$ currents in control, *TARDBP* and *C9ORF72* iPSC-derived MNs at week 3–4 and weeks 9–10. (B) Current–voltage relationships of peak $K^+$ currents recorded from control and patient iPSC-derived MNs at weeks 3–4. (C) Current–voltage relationships of peak $K^+$ currents recorded from control and patient iPSC-derived MNs at weeks 9–10. (D) Peak $K^+$ currents plotted from weeks 3–10 for control (n=847), *TARDBP* (n=452) and *C9ORF72* (n=264) iPSC-derived MNs (data are plotted as $\overline{x}$ ± s.e.m; *, patient line significantly different to control, P<0.05; ***, P<0.0001; #, significant difference between patient lines, P<0.05; ###, P<0.0001; linear model with multiple Wald's tests and Bonferroni correction).

Taken together these data demonstrate a progressive reduction in both fast, inactivating $Na^+$ currents and persistent, voltage -activated $K^+$ currents in patient iPSC-derived MNs. Given the similar time courses of current loss and action potential loss, and the observation that current loss precedes changes in the probability of firing, it is likely that reductions in voltage-activated currents underlie the progressive loss of functional output in MNs harbouring ALS-related mutations. To examine this further, the relationship between the magnitude of voltage-activated $Na^+$ and $K^+$ currents and the type of output produced by iPSC-derived MNs was investigated for cells in which both voltage- and current-clamp data were available (control n = 448; *TARDBP* n = 230; *C9ORF72* n =176). Plots of raw data indicated similar relationships between peak currents and firing categories in all iPSC lines 3-6 weeks post-plating; larger currents were associated with greater output (Fig. 2.8A). To assess this relationship further multinomial logistic regressions were fitted to the data using the firing categories (No Spike/ Single/ Adaptive/ Repetitive) as the outcome variables with the type of iPSC line (control, *TARDBP* or *C9ORF72*) and peak current ($Na^+$ or $K^+$) as the predictor variables. Using these models the predicted probabilities for each firing category based on the measured currents were assessed. Models showed that both $Na^+$ and $K^+$ currents were strong predictors of firing category ($Na^+$ model, $P< 0.001$; $K^+$ model, $P< 0.001$). In addition, the type of iPSC line contributed to the predicted firing outcome ($Na^+$ model, $P< 0.01$; $K^+$ model, $P< 0.05$). As expected, the probability of a cell failing to spike in response to current injection decreases with increasing peak $Na^+$ or $K^+$ currents (No- Spike category; Fig. 2.8B, C).

In comparison, the probability of a cell exhibiting adaptive or repetitive firing in response to current injection increases with increasing peak $Na^+$ or $K^+$ currents (Adaptive and Repetitive categories; Fig. 2.8B, C). Whereas, the probability of a cell exhibiting only single spikes is highest at an intermediary value of peak $Na^+$ or $K^+$ currents (Single category; Fig. 2.8B, C). Overall, the modelled probabilities suggest an ordered response of firing outcome when $Na^+$ or $K^+$ currents are increased (No-Spike < Single < Adaptive < Repetitive; Fig. 2.8B, C). In summary, these findings suggest that the mode of iPSC-derived MN firing (Single/Adaptive/Repetitive) is governed by the size of $Na^+$ and $K^+$ currents. Therefore the reduced probability of spiking observed in patient iPSC-derived MNs (Fig. 2.8C) is likely to reflect perturbations in $Na^+$ and $K^+$ currents as a consequence of the *TARDBP* and *C9ORF72* mutations they harbour.

## 3.6.iPSC-derived MNs harbouring *C9ORF72* mutation display promising functional recovery after amiloride treatment

Having revealed a progressive loss of action potential output, $Na^+$ currents and $K^+$ currents, in patient iPSC-derived MNs we next wanted to determine if the observed phenotype could be modified by pharmacological agents which target ion channels. The effects of the acid-sensing ion channel blocker amiloride was first assessed because it has been shown to have neuroprotective roles in studies involving multiple sclerosis and also blocks $Na^+$ and $Ca^{2+}$ channels (Friese et al., 2007). iPSC-derived MNs harbouring *C9ORF72* mutations were cultured in amiloride at concentrations between 25 μM and 100 μM from 24 hours post-plating until recordings were obtained. At weeks 7-8 and 9-10 post-plating, recordings were obtained from patient

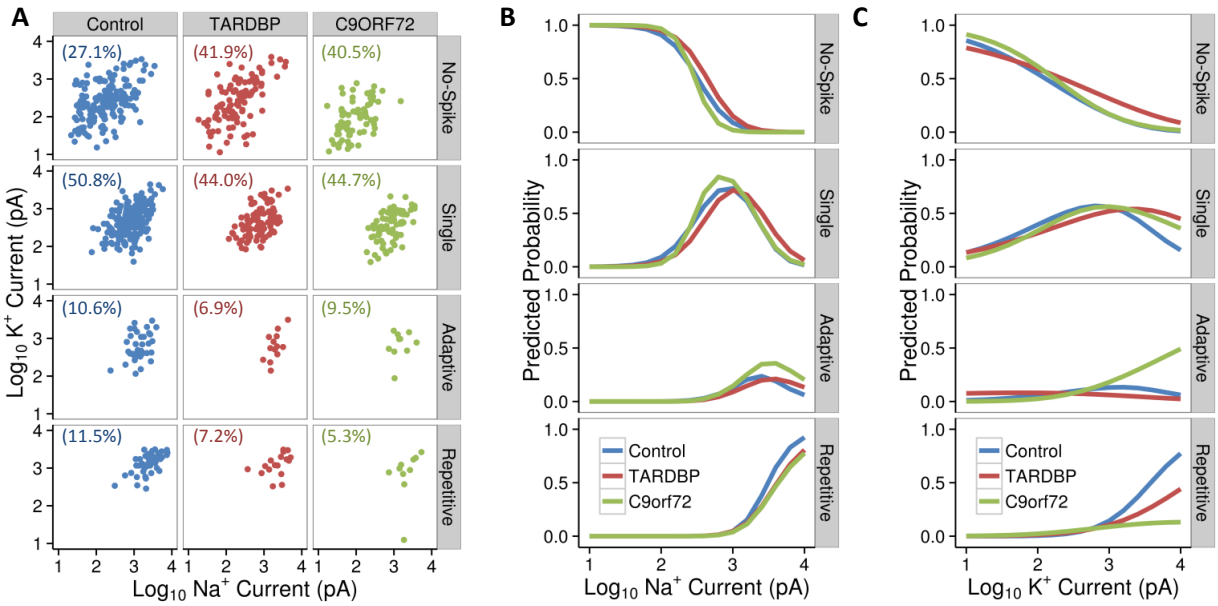


**Figure 2.8: Peak $Na^+$ and $K^+$ currents predict firing categories of iPSC-derived MNs**

(A) Relationship between peak $Na^+$ and $K^+$ currents and action potential firing category were determined using multinomial logistic regressions in control (n=448), *TARDBP* (n=230) and *C9ORF72* (n=176) iPSC-derived MNs at 3–6 weeks post plating. Values in parentheses denote the proportion, as a percentage, of iPSC-derived MNs exhibiting each firing category. (B) Predicted probability of each firing category calculated over a range of peak $Na^+$ currents. (C) Predicted probability of each firing category calculated over a range of peak $K^+$ currents. (Joshua Foster from Gareth Miles' lab at the University of St Andrews generated this figure).

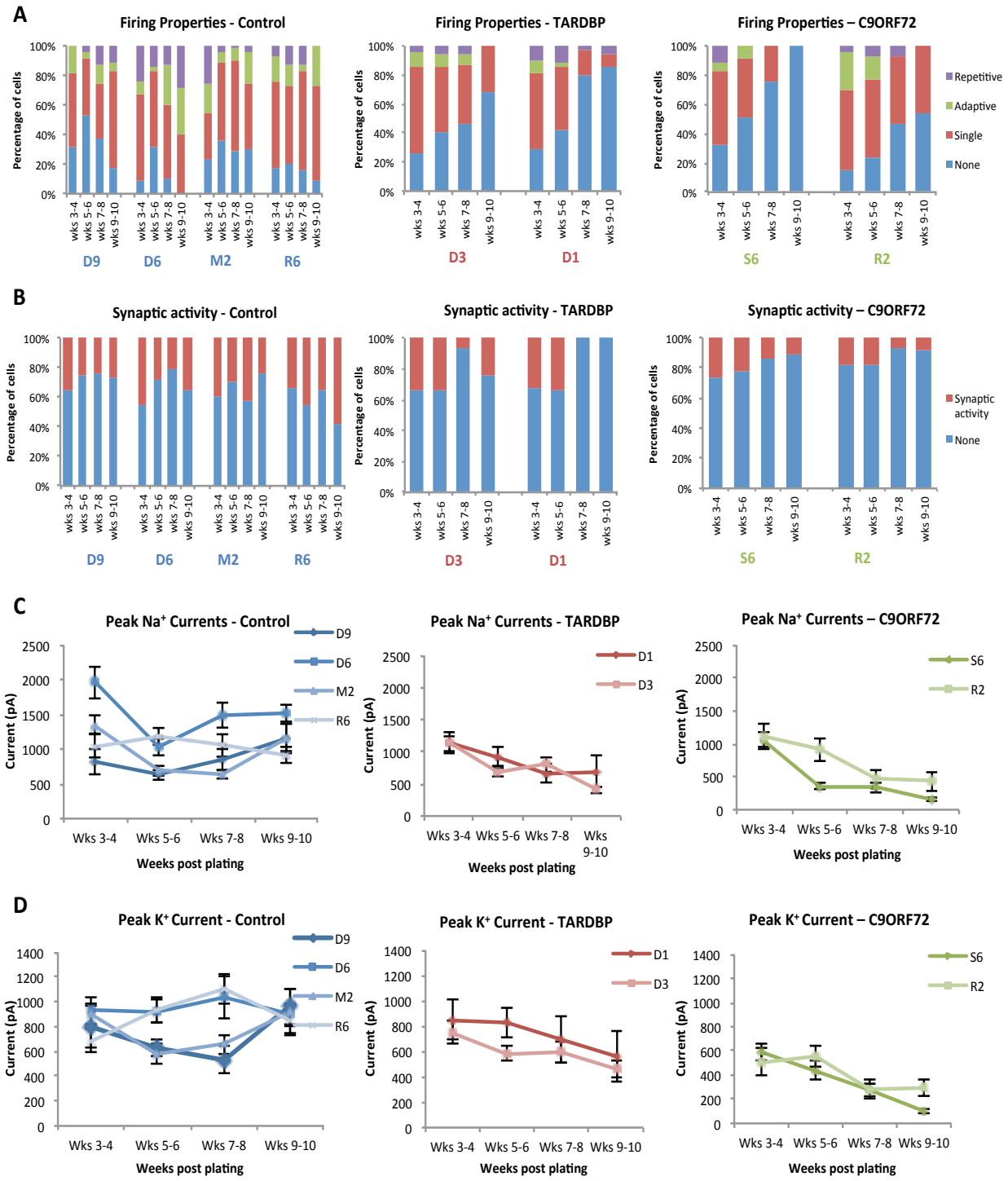


**Figure 2.9: Physiological properties of MNs derived from individual iPSC lines.**

Figure caption on following page

**Figure 2.9: Physiological properties of MNs derived from individual iPSC lines.**

(A) Firing properties for each of the 8 iPSC lines utilised: (controls lines: D9, D6, M2 and R6; *TARDBP* lines: D1 and D3; *C9ORF72* lines: S6 and R2). (B) Percentage of cells in which synaptic activity was present for each iPSC line. (C) Peak $Na^+$ currents and (D) peak $K^+$ currents in each iPSC line from 3- 10 weeks post-plating (see Table 2.3 for sample sizes).

**A**

| | | $C_m$ (pF) | $R_N$ (MΩ) | RMP (mV) |
|---|---|---|---|---|
| D6 Control | | | | |
| | Wks 3-4 | 12.7 ± 0.8 | 519.7 ± 40.1 | -45.7 ± 1.6 |
| | Wks 5-6 | 13.8 ± 0.7 | 756.9 ± 49.7 | -41.6 ± 1.4 |
| | Wks 7-8 | 12.9 ± 1.2 | 672.7 ± 60.0 | -47.4 ± 2.3 |
| | Wks 9-10 | 14.6 ± 0.9 | 619.3 ± 52.7 | -50.4 ± 1.7 |
| D9 Control | | | | |
| | Wks 3-4 | 9.4 ± 1.1 | 784.1 ± 62.1 | -40.7 ± 2.2 |
| | Wks 5-6 | 10.5 ± 0.4 | 793.5 ± 38.0 | -41.2 ± 1.1 |
| | Wks 7-8 | 12.3 ± 0.7 | 685.4 ± 63.5 | -44.5 ± 2.1 |
| | Wks 9-10 | 10.7 ± 0.8 | 784.2 ± 84.1 | -48.6 ± 2.1 |
| R6 Control | | | | |
| | Wks 3-4 | 9.3 ± 0.4 | 831.2 ± 27.3 | -46.5 ± 1.3 |
| | Wks 5-6 | 10.9 ± 0.6 | 721.7 ± 40.5 | -48.1 ± 1.4 |
| | Wks 7-8 | 9.8 ± 0.6 | 749.5 ± 48.7 | -49.1 ± 1.6 |
| | Wks 9-10 | 12.3 ± 0.9 | 801.9 ± 47.1 | -49.5 ± 1.8 |
| M2 Control | | | | |
| | Wks 3-4 | 9.8 ± 0.5 | 758.9 ± 35.7 | -46.9 ± 1.4 |
| | Wks 5-6 | 10.9 ± 0.5 | 827.7 ± 38.1 | -40.8 ± 1.6 |
| | Wks 7-8 | 9.7 ± 0.4 | 859.4 ± 33.2 | -45.5 ± 1.3 |
| | Wks 9-10 | 18.0 ± 1.7 | 652.7 ± 68.1 | -50.45 ± 3.2 |
| D1 TARDBP | | | | |
| | Wks 3-4 | 13.6 ± 0.9 | 652.1 ± 52.3 | -39.0 ± 1.7 |
| | Wks 5-6 | 12.9 ± 0.8 | 773.3 ± 51.3 | -40.4 ± 1.7 |
| | Wks 7-8 | 24.3 ± 2.4 | 602.7 ±72.7 | -43.6 ± 2.5 |
| | Wks 9-10 | 28.4 ± 1.6 | 503.6 ± 51.9 | -43.9 ± 3.9 |
| D3 TARDBP | | | | |
| | Wks 3-4 | 10.5 ± 0.5 | 668.8 ± 43.4 | -40.9 ± 1.3 |
| | Wks 5-6 | 10.4 ± 0.4 | 795.9 ± 32.3 | -40.4 ± 1.3 |
| | Wks 7-8 | 11.5 ± 0.6 | 850.7 ± 41.3 | -43.1± 1.6 |
| | Wks 9-10 | 12.8 ± 1.1 | 834.0 ± 48.3 | -37.2 ± 1.6 |
| S6 C9ORF72 | | | | |
| | Wks 3-4 | 9.4 ± 0.4 | 734.7 ± 41.8 | -45.3 ± 1.3 |
| | Wks 5-6 | 11.5 ± 0.6 | 761.9 ± 61.0 | -43.7 ± 1.7 |
| | Wks 7-8 | 11.8 ± 0.9 | 769.5 ± 52.3 | -39.0 ± 1.9 |
| | Wks 9-10 | 15.9 ± 0.9 | 520.8 ± 69.7 | -47.1 ± 2.2 |
| R2 C9ORF72 | | | | |
| | Wks 3-4 | 7.5 ± 0.4 | 694.5 ± 54.1 | -43.6 ± 2.4 |
| | Wks 5-6 | 8.1 ± 0.6 | 777.9 ± 55.7 | -44.9 ± 2.7 |
| | Wks 7-8 | 12.2 ± 2.6 | 781.51 ± 93.0 | -35.1 ± 2.3 |
| | Wks 9-10 | 11.6 ± 1.1 | 887.7 ± 75.0 | -41.4 ± 3.5 |

**B**

| | | V-clamp No. Cells | I-clamp No. Cells |
|---|---|---|---|
| D6 Control | | | |
| | Wks 3-4 | 53 | 46 |
| | Wks 5-6 | 85 | 64 |
| | Wks 7-8 | 33 | 30 |
| | Wks 9-10 | 34 | 32 |
| D9 Control | | | |
| | Wks 3-4 | 33 | 22 |
| | Wks 5-6 | 97 | 82 |
| | Wks 7-8 | 38 | 24 |
| | Wks 9-10 | 19 | 18 |
| R6 Control | | | |
| | Wks 3-4 | 35 | 29 |
| | Wks 5-6 | 74 | 55 |
| | Wks 7-8 | 51 | 45 |
| | Wks 9-10 | 33 | 33 |
| M2 Control | | | |
| | Wks 3-4 | 77 | 68 |
| | Wks 5-6 | 66 | 50 |
| | Wks 7-8 | 94 | 81 |
| | Wks 9-10 | 25 | 23 |
| D1 TARDBP | | | |
| | Wks 3-4 | 50 | 38 |
| | Wks 5-6 | 54 | 43 |
| | Wks 7-8 | 34 | 34 |
| | Wks 9-10 | 35 | 34 |
| D3 TARDBP | | | |
| | Wks 3-4 | 53 | 43 |
| | Wks 5-6 | 118 | 90 |
| | Wks 7-8 | 61 | 54 |
| | Wks 9-10 | 47 | 44 |
| S6 C9ORF72 | | | |
| | Wks 3-4 | 73 | 61 |
| | Wks 5-6 | 40 | 35 |
| | Wks 7-8 | 38 | 36 |
| | Wks 9-10 | 28 | 28 |
| R2 C9ORF72 | | | |
| | Wks 3-4 | 29 | 27 |
| | Wks 5-6 | 29 | 26 |
| | Wks 7-8 | 14 | 13 |
| | Wks 9-10 | 13 | 13 |

**C**

| | Synaptic events No. cells | *f*-I relationship No. cells |
|---|---|---|
| D6 Control | 11 | 10 |
| D9 Control | 13 | 3 |
| R6 Control | 5 | 24 |
| M2 Control | 9 | 25 |
| D1 TARDBP | 11 | 7 |
| D3 TARDBP | 16 | 12 |
| S6 C9ORF72 | 8 | 15 |
| R2 C9ORF72 | 1 | 4 |

**Table 2.3: Properties of each line separated.**

**Table 2.3: Properties of each line separated**

(A) Passive membrane properties, (B) number of cells used for analysis from voltage and current clamp recordings, (C) number of cells used for synaptic activity and *f-I* relationships broken down by line.

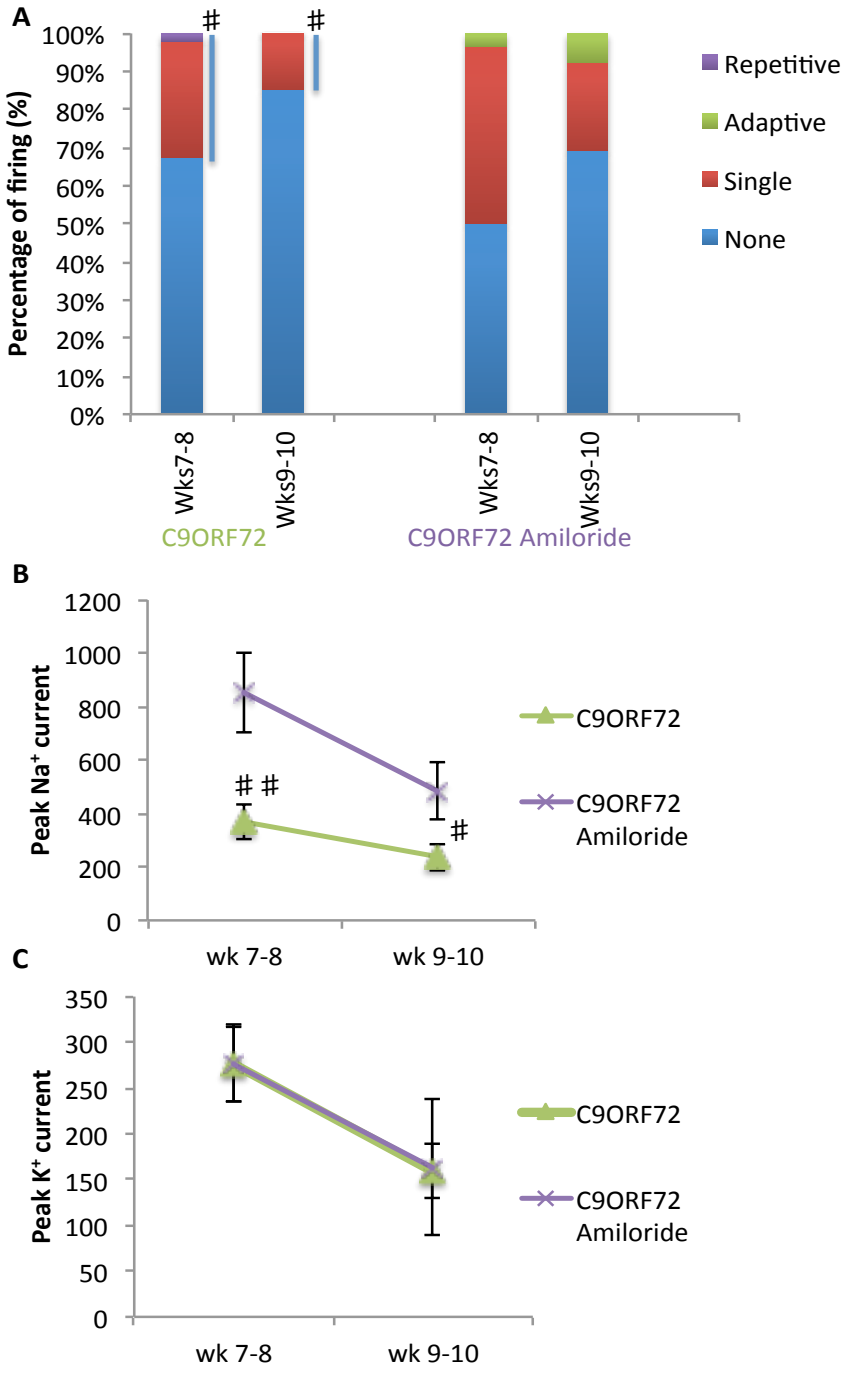


**Figure 2.10: iPSC-derived MNs harbouring *C9ORF72* mutation display promising functional recovery after amiloride treatment.**

Figure caption on following page

**Figure 2.10*:* iPSC-derived MNs harbouring *C9ORF72* mutation display promising functional recovery after amiloride treatment.**

(A) Proportion of cells exhibiting each firing category observed in iPSC-derived MNs harbouring *C9ORF72* mutation untreated (n=90) and treated (n=43) with 25 μM-100 μM amiloride (repetitive, adaptive, single or no firing) across weeks 7–10 post plating (#, significant difference between treated and untreated lines, P<0.05). (B) Peak $Na^+$ currents plotted from weeks 7–10 for *C9ORF72* (n=79) and *C9ORF72* amiloride treated (n=60) iPSC-derived MNs (data are plotted as $\overline{x} \pm$ s.e.m; #, significant difference between treated and untreated lines, P<0.05; # #, significant difference between treated and untreated lines, P<0.01; two-tailed t-tests). (C) Peak $K^+$ currents plotted from weeks 7–10 for *C9ORF72* (n=79) and *C9ORF72* amiloride treated (n=60) iPSC-derived MNs (data are plotted as $\overline{x} \pm$ s.e.m; two-tailed t-tests).

iPSC-derived MNs to determine if their dysfunctional phenotype could be reversed after drug exposure. The number of cells able to fire action potentials increased significantly ($P<0.05$) in the *C9ORF72* iPSC-derived MNs treated with amiloride compared to the non-treated cells at weeks 7-10 (Weeks 7-8: *C9ORF72* firing 32.6%, n=49; *C9ORF72* amiloride treated firing 50%, n=30; Weeks 9-10: *C9ORF72* firing 14.6%, n=41; *C9ORF72* amiloride treated firing 30.7%, n=13; Fig. 2.10A). These data demonstrate a partial functional recovery of the *C9ORF72* iPSC-derived MNs treated with amiloride compared to those that were untreated. Amiloride treatment on control MNs did not affect their output properties (data not shown).

We next investigated whether amiloride affected the loss of fast, inactivating $Na^+$ currents in iPSC-derived MNs harbouring *C9ORF72* mutations by using a series of depolarising voltage steps (-70 to 20 mV, 2.5 mV increments, 10 ms duration) from a holding potential of -60 mV (Fig. 2.10B). Peak $Na^+$ currents were significantly larger in *C9ORF72* MNs treated with amiloride at weeks 7-8 ($P<0.01$) and 9-10 ($P<0.05$) compared to those untreated (Peak current: weeks 7-8 $\overline{x}$ *C9ORF72* 371 ± s.e.m 67 pA, n=52; *C9ORF72* amiloride treated 853 ± 151 pA, n=40; weeks 9-10 *C9ORF72* 236 ± 49 pA, n=42; C9ORF72 amiloride treated 484 ± 109 pA, n=20; Fig. 2.10B). However, when we assessed whether this reflected a more general effect on voltage-activated currents, we found no changes in the persistent $K^+$ currents in amiloride treated *C9ORF72* iPSC-derived MNs compared to those untreated (Peak current: weeks 7-8 $\overline{x}$ *C9ORF72* 276 ± s.e.m 41 pA, n=52; *C9ORF72* amiloride treated 277 ± 41 pA, n=36; weeks 9-10 *C9ORF72* 158 ± 29 pA, n=42; *C9ORF72* amiloride treated 163 ± 73 pA, n=11; Fig. 2.10C). These data demonstrate that using pharmacological agents

that target ion channels, the pathophysiological phenotype can be modified. These data also support the use of human iPSC based model to study ALS as their culture conditions can be manipulated easily and, when accompanied by electrophysiological analyses, can be utilised as a model for drug screening.

## 3.7. Genetic editing of iPSC-derived MNs harbouring *C9ORF72* mutations reverses the dysfunctional phenotype

It was next investigated whether mutant genes could be removed from patient iPSC-derived MNs to reverse their dysfunctional phenotype. Through the use of the CRISPR/Cas9 genome editing, an isogenic control line was generated from the iPSCs of a *C9ORF72* patient (S6, Carrier-1). The Clustered Regularly Interspaced Short Palindromic Repeats (CRISPR) system, based on a bacterial protein from the *Streptococcus pyogenes,* targeted and modified the genomic sequence of the *C9ORF72* patient iPSC line by removing the $G_4C_2$ hexanucleotide repeat expansion. Upon removal of the $G_4C_2$ repeat expansion, an isogenic control line was generated. From this line, MNs were generated, plated and recorded from at weeks 3-10 and compared to the non-edited *C9ORF72* MN line. The number of cells able to fire action potentials increased significantly ($P<0.0001$) in the gene-edited *C9ORF72* iPSC-derived MNs (2H9 Carrier-1Δ) compared to the non-edited lines (C9 Carrier-1) at weeks 3-6 and 7-10 post-plating (Weeks 3-6: C9 Carrier-1 firing 60.4%, n=96; 2H9 Carrier- 1Δ firing 100%, n=20; Weeks 7-10: C9 Carrier-1 firing 14.1%, n=64; 2H9 Carrier-1Δ firing 93.3%, n=45; Fig. 2.11A).

We next investigated the currents underlying the functional output of the iPSC-derived MNs (Fig. 2.11B, C). The magnitude of peak $Na^+$ currents were significantly

greater in the 2H9 Carrier-1Δ MNs at weeks 3-6 and 7-10 ($P<0.0001$) compared to the unedited C9 Carrier-1 iPSC-derived MN line (Peak current: weeks 3-6 $\overline{x}$ C9 Carrier-1 889 ± s.e.m 107 pA, n=89; 2H9 Carrier-1Δ 2129 ± 246 pA, n=20; weeks 7-10 C9 Carrier-1 237 ± 55 pA, n=52; 2H9 Carrier-1Δ 3429 ± 268 pA, n=46; Fig. 2.11B). Persistent $K^+$ currents were also larger in *C9ORF72* gene edited iPSC-derived MNs compared to the unedited lines (Peak current: weeks 3-6 $\overline{x}$ C9 Carrier-1 453 ± s.e.m 45 pA, n=137; 2H9 Carrier-1Δ 1824 ± 166 pA, n=20; weeks 7-10 C9 Carrier-1 137 ± 20 pA, n=112; 2H9 Carrier-1Δ 2422 ± 169 pA, n=44; Fig. 2.11C). These data demonstrate a functional recovery of patient iPSC-derived MNs upon editing of the *C9ORF72* gene and that by using an isogenic control line, further implicates the presence of the $G_4C_2$ hexanucleotide repeat expansion as the cause of the pathophysiological phenotype observed.

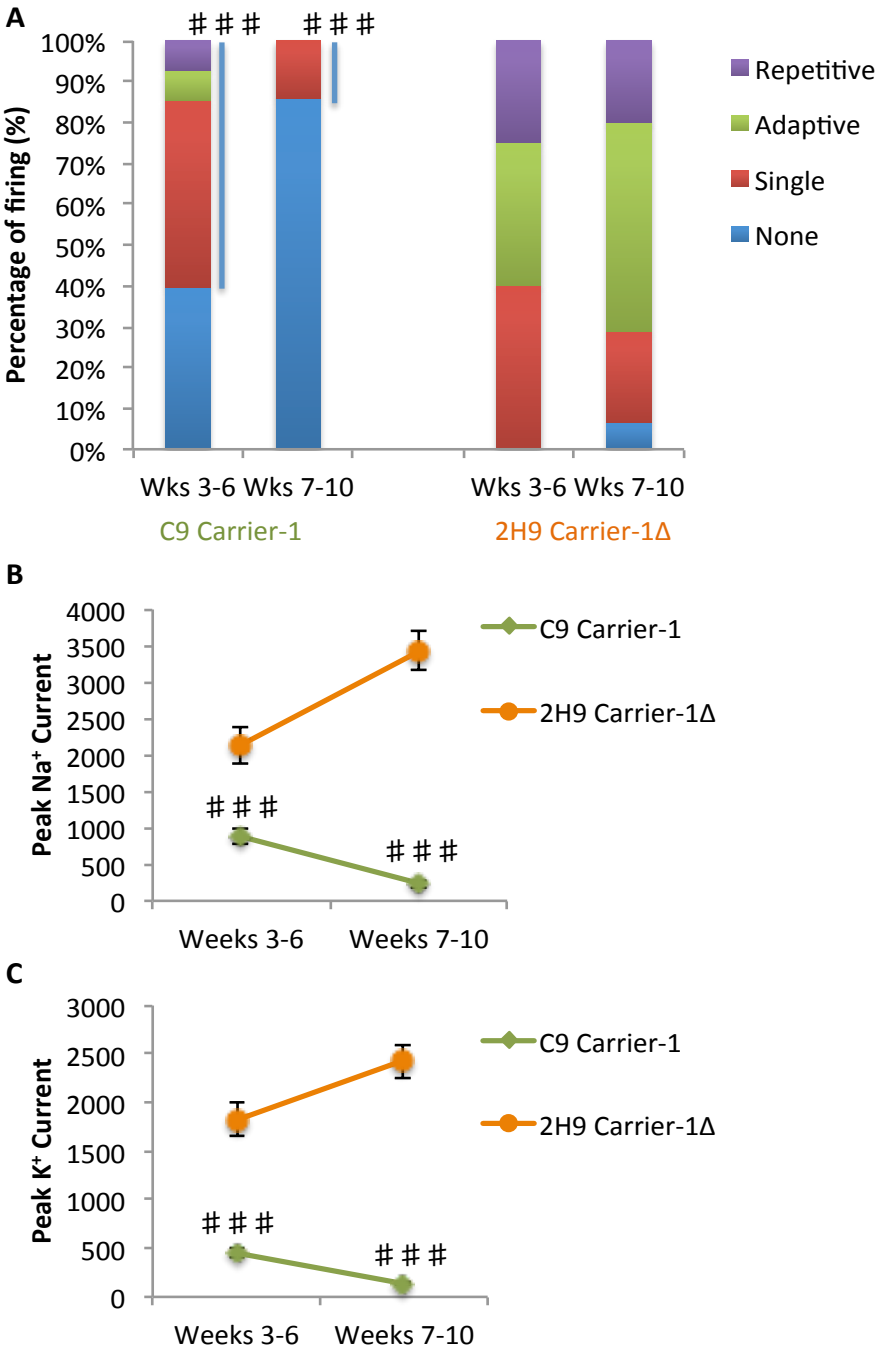


**Figure 2.11: Gene-edited *C9ORF72* iPSC-derived MNs display a reversed phenotype compared to the non-edited line.**

Figure caption on following page

**Figure 2.11: Gene-edited *C9ORF72* iPSC-derived MNs display a reversed phenotype compared to the non-edited line.**

(A) Proportion of cells exhibiting each firing category (repetitive, adaptive, single or no firing) observed in iPSC-derived MNs harbouring *C9ORF72* mutation (S6 line, C9 Carrier-1; n=160) and in its isogenic control line (2H9 Carrier-1Δ; n=65) across weeks 3–10 post plating (###, significant difference between C9 mutant and isogenic control lines, P<0.0001; binomial logistic regression). (B) Peak $Na^+$ currents plotted from weeks 3–10 for S6 line, C9 Carrier-1 (n=141) and 2H9 Carrier-1Δ (n=66) iPSC-derived MNs (data are plotted as $\overline{x}$ ± s.e.m; ###, significant difference between C9 mutant and isogenic control lines, P<0.0001; two-tailed t-tests). (C) Peak $K^+$ currents plotted from weeks 7–10 for *C9ORF72* (n=141) and 2H9 Carrier-1Δ (n=66) iPSC-derived MNs (data are plotted as $\overline{x}$ ± s.e.m; ###, significant difference between C9 mutant and isogenic control lines, P<0.0001; two-tailed t-tests).

# 4. Discussion

This study demonstrated that MNs derived from human iPSCs obtained from healthy individuals or patients harbouring *TARDBP* or *C9ORF72* ALS mutations develop appropriate physiological properties. However, temporal analysis revealed that patient iPSC-derived MNs display an initial period of hyperexcitability, followed by a progressive loss in action potential output and synaptic activity. This loss of functional output appears to result from a progressive decrease in voltage-activated $Na^+$ and $K^+$ currents that occurs in the absence of overt changes in cell viability. It has also shown that treatment of iPSC-derived MNs harbouring *C9ORF72* mutations with amiloride improves their functional output, likely due to increasing their peak $Na^+$ currents, while removal of the mutant *C9ORF72* gene from one of the *C9ORF72* ALS patient iPSC lines led to them retaining their functional output capability, behaving in a similar manner as MNs derived from healthy individuals. These novel data from ALS-affected human MNs indicate that early dysfunction or loss of ion channels may contribute to the initiation of downstream degenerative pathways that ultimately lead to MN loss in ALS and highlights the potential usefulness of human iPSC-derived neurons as a model for therapeutic drug screening.

Given that all neurons must be by definition excitable, it is critical that protocols established for the derivation of MNs from iPSCs are validated via the electrophysiological demonstration of appropriate functional properties. Previous studies have demonstrated the ability of human iPSC-derived MNs to fire action potentials in response to current injection and to receive spontaneous synaptic inputs (Bilican et al., 2012; Almeida et al., 2013; Amoroso et al., 2013; Sareen et al., 2013;

Zhang et al., 2013; Wainger et al., 2014). In this study, both current- and voltage-clamp recordings were utilised to not only demonstrate that iPSC-derived MNs can develop appropriate output and receive synaptic input, but to also investigate the temporal profile of voltage-activated currents underlying these functional properties. Comparable rates of morphological and physiological maturation were observed in control and patient iPSC-derived MNs, with all lines reaching equivalent maturity approximately 3 weeks post-plating. These analyses provide a detailed validation of the phenotype of iPSC-derived MNs as well as enabling more sensitive functional comparisons between control and patient iPSC-derived MNs. The protocol utilised in this study preferentially generated MNs expressing markers of limb-innervating lateral motor column MNs, the most susceptible MNs in ALS. Furthermore, this protocol also preferentially generates lateral motor column interneurons and astrocytes, enabling the study of the most vulnerable and toxic cells involved in ALS (Amoroso et al., 2013). Given that the ultimate goal of ALS therapeutics is to preserve vulnerable MN function, it is critical that detailed functional analyses of iPSC-derived MNs are performed alongside more common analyses of cellular pathology such as, protein aggregation, RNA accumulation and changes in gene expression (Mitne-Neto et al., 2011; Bilican et al., 2012; Almeida et al., 2013; Donnelly et al., 2013; Sareen et al., 2013; Zhang et al., 2013; Kiskinis et al., 2014; Wainger et al., 2014).

Previous studies of ALS patients (Kanai et al., 2006; Vucic and Kiernan, 2006; Vucic et al., 2008), human iPSCs (Wainger et al., 2014) and animal models of the disease (Pieri et al., 2003; Kuo et al., 2005; Zona et al., 2006; Bories et al., 2007; van Zundert et al., 2008; Quinlan et al., 2011; Fuchs et al., 2013) have reported early

hyperexcitability of spinal MNs and corticospinal neurons of the motor cortex. In this study, it was shown that the most functionally mature (repetitive firing) MNs derived from patient iPSCs harbouring *TARDBP* or *C9ORF72* mutations also exhibit hyperexcitability at early stages in culture. Although hyperexcitability was transient in this study and does not persist into symptomatic stages in animal models of ALS (Fuchs et al., 2013; Delestrée et al., 2014) an initial phase of increased activity might contribute to and/or trigger a cascade of excitotoxic disease mechanisms involving pathological changes in $Ca^{2+}$ handling, (von Lewinski et al., 2008; Jaiswal and Keller, 2009) accumulation of intracellular $Ca^{2+}$ and the eventual activation of cell death pathways. In opposition to this, however, recent work supports a link between hyperexcitability and neuroprotection (Saxena et al., 2013), particularly when hyperexcitability is induced via activation of cholinergic C-bouton inputs to MNs (Miles et al., 2007; Zagoraiou et al., 2009) which are known to be enlarged presymptomatically in ALS model mice (Pullen and Athanasiou, 2009; Herron and Miles, 2012). These data suggest that MN hyperexcitability might represent an early compensatory mechanism in ALS-affected MNs. To determine the true role of hyperexcitability in ALS, it will be important for future studies to examine the effects of finely controlled manipulations of excitability on human MNs.

Following an early stage of hyperexcitability, patient iPSC-derived MNs were found to progressively lose their ability to generate action potentials. This was evidenced by a reduction in the proportion of patient iPSC-derived MNs which were able to fire repetitive or even single spikes. In comparison, the proportion of control iPSC-derived MNs in each of the firing categories remained unchanged throughout the 10

weeks studied. Thus, despite remaining viable in culture, ALS-affected MNs were gradually rendered non-functional. These findings of a progressive loss of MN output are consistent with recent reports of hypoexcitability of iPSC-derived MNs harbouring a *C9ORF72* mutation (Sareen et al., 2013) and reduced output of spinal MNs in mSOD1 mice (Delestrée et al., 2014). The latter study, which involved *in vivo* recordings from presymptomatic mSOD1 mice, showed that a significant proportion of MNs could not discharge repetitively in response to current ramps although their NMJs remained functional. Thus, dysfunction at the MN cell body appears to precede that at the NMJ. Taken together, these findings highlight the importance of addressing early perturbations in mechanisms underlying spike generation at the MN soma when considering disease pathogenesis and potential treatment strategies for ALS.

Importantly, this work has addressed an apparent contradiction arising from recent studies performing similar electrophysiological analysis of ALS patient iPSC-derived MNs. Wainger et al (Wainger et al., 2014) recently reported hyperexcitability of iPSC-derived MNs harbouring a *SOD-1* mutation at approximately 4 weeks post-plating, a time point equivalent to when this study also observed hyperexcitability in iPSC-derived MNs harbouring *TARDBP* or *C9ORF72* mutations. In contrast, Sareen et al (Sareen et al., 2013) reported hypoexcitability in iPSC-derived MNs harbouring *C9ORF72* mutations at a time point comparable to week 7-8 post-plating in this study, when loss of MN output was first observed. Thus, these recent studies support this study's observation of a progression from hyperexcitability to hypoexcitability. Although this progression is consistent with work in animal models (Delestrée et al., 2014), it should be noted that iPSCs represent a developmental model that may be difficult to directly compare to aging *in vivo*. It also remains unclear whether

mechanistic links exist between hyperexcitability and hypoexcitability, which will be important to address in future studies. The fibroblasts utilised for the generation of iPSCs for present study were obtained from patients between the ages of 39-67 within one year post-diagnosis. These differences are also an important caveat to consider when comparing disease time-courses *in vivo*, which could widely differ depending on disease progression.

Although the focus was on the intrinsic properties of MNs, a concomitant reduction in the proportion of patient iPSC-derived MNs that received synaptic inputs was observed. Loss of synaptic activity may simply reflect a general loss of action potential generation in culture. However, given evidence of loss and dysfunction of synapses in ALS (Matsumoto et al., 1994; Sasaki and Maruyama, 1994; Ince et al., 1995; Schutz, 2005; Chang and Martin, 2009; Jiang et al., 2009), specific deficits in synaptic transmission might also contribute to reductions in synaptic activity recorded from patient iPSC-derived MNs. Although it was demonstrated that iPSC-derived MNs expressed post-synaptic receptors required to receive input, comparisons could not be made between the magnitude of responses to NTs across control and patient iPSC-derived MNs due to difficulties in obtaining long-term recordings, as required for drug applications, from sufficient numbers of cells. It will be interesting in future studies, focussed on synaptic function, to investigate the possibility that either pre-or post-synaptic machinery is altered in cultures from patient iPSCs.

Following the demonstration of reduced output from patient iPSC-derived MNs, voltage-clamp recordings were utilised to investigate the mechanisms likely to underlie this loss of function. Previous studies have demonstrated changes in both the density and function of $Na^+$ and $K^+$ channels in animal models of ALS

(Kuo et al., 2005; Zona et al., 2006; Pieri et al., 2009; Quinlan et al., 2011), ALS patients (Bostock et al., 1995; Tamura et al., 2006; Vucic and Kiernan, 2006) and patient iPSC-derived MNs (Sareen et al., 2013; Wainger et al., 2014). These analyses revealed a progressive loss of voltage-activated $Na^+$ (fast, inactivating) and $K^+$ (persistent) currents in patient iPSC-derived MNs. Given that current loss began before and continued in parallel with changes in firing probability, and that $Na^+$ and $K^+$ current magnitudes are excellent predictors of firing patterns, reductions in voltage-activated currents most likely underlie the loss of functional output observed in patient iPSC-derived MNs. It has also been shown that treatment of the *C9ORF72* patient line with amiloride, an acid-sensing ion channel blocker found to be neuroprotective in studies of multiple sclerosis (Friese et al., 2007), led to the partial recovery of firing capabilities and a mild preservation of $Na^+$ currents in MNs. However, peak $K^+$ currents were unaffected by the treatment. These data show that by manipulating ion channels using pharmacological agents, the pathophysiological phenotype can be modified. Mechanisms underlying the initial hyperexcitability of MNs are less clear. Waigner et al (Wainger et al., 2014) proposed that reductions in delayed rectifier $K^+$ currents underlie hyperexcitability in iPSC-derived MNs harbouring *SOD-1* mutations. Although a lower $K^+$ current magnitude in MNs harbouring *C9ORF72* mutations was observed at hyperexcitable stages, the same was not true for MNs harbouring *TARDBP* mutations. Thus, reductions in $K^+$ currents are unlikely to be the sole mechanism underlying hyperexcitability in patient iPSC-derived MNs. Either loss or dysfunction of channels may underlie the loss of current observed in patient iPSC-derived MNs. Regardless of the exact effect on ion channels, these data are consistent with the recent proposal that ALS involves channelopathy-like mechanisms, a view which stemmed from the demonstration that mutant SOD1

inhibits the conductance of a mitochondrial ion channel (Israelson et al., 2010). Interestingly, although ALS-related mutations may cause a general loss of voltage-activated currents, the lack of change in input resistance in patient iPSC-derived MNs indicates that leak channels are unaffected. Furthermore, depolarisation of the resting membrane potential, again with no changes in input resistance, suggests additional membrane proteins are affected, one possibility being the $Na^+/K^+$ pump for which reduced expression has been shown in mSOD1 mice (Ellis et al., 2003).

In this study, iPSC-derived MNs harbouring mutations in two different genes associated with ALS, *TARDBP* and *C9ORF72*, were utilised. *TARDBP* encodes the RNA-binding protein TDP-43 which can act as a transcription repressor, and splicing regulator, and can also contribute to RNA stability and transport (Tollervey et al., 2011; Arnold et al., 2013; Alami et al., 2014). Mutations in *TARDBP* are associated with deficits in RNA processing (Xu et al., 2011; Lagier-Tourenne et al., 2012). Although the exact function of *C9ORF72* remains unknown, its mutant form also appears to cause aberrant RNA processing (DeJesus-Hernandez et al., 2011; Renton et al., 2011; Donnelly et al., 2013). Thus, defects in RNA processing provide a mechanistic link between *TARDBP* and *C9ORF72*-mediated ALS and may contribute to loss of voltage-activated currents in patient iPSC-derived MNs. This study also demonstrates that by genetically editing a *C9ORF72* patient iPSC line by removing the $G_4C_2$ repeat expansion, the pathophysiological phenotype is reversed, linking the presence of the hexanucleotide repeat expansion with the observed dysfunction. In support of this, recent work has shown that the expression of genes involved in neuronal excitability, including those encoding ion channels, is altered in iPSC-derived MNs with *C9ORF72* mutations (Sareen et al., 2013). Common effects on

RNA processing might also in part explain why MNs derived from *TARDBP* and *C9ORF72* iPSC lines exhibited similar pathophysiology; hyperexcitability followed by a loss of functional output due to a reduction in the magnitude of voltage-activated currents. Alternative interpretations include the possibility that perturbations in ion channels and MN output represent core disease mechanisms common to many forms of ALS, including both familial and sporadic ALS given the demonstration of *TARDBP* and *C9ORF72* mutations in both of these forms of the disease. The successful removal of the ALS phenotype, which was caused by the presence of the $G_4C_2$ repeat expansion, using the CRISPR/Cas9 technique, has demonstrated the importance and benefits of using an isogenic control line. As there are many unresolved technical challenges to overcome before this tool has the potential to be used in gene therapies, taking advantage of this technology in a variety of patient iPSC lines to confirm that the presence of certain mutations are the cause of the phenotypes observed is important. Further experiments utilising a variety of patient iPSC lines will be needed to confirm the relevance of the findings described in this study to a wide spectrum of ALS cases.

In summary, this study has provided important new insight into early ALS disease mechanisms by investigating pathophysiological changes in iPSC-derived MNs from ALS patients with two different genetic mutations. It was also shown that MN output is severely compromised, due to the loss of voltage-activated currents, prior to any other overt signs of neurodegeneration. These data suggest that 'functional loss' of MNs may render the motor system inactive prior to neurodegeneration of MNs, which would likely occur at a time-point extended beyond that used in this study, highlighting the importance of addressing MN function, perhaps by targeting ion

channels, when designing new treatment strategies for ALS. Furthermore, these findings demonstrate the usefulness of sensitive physiological studies of human iPSC-derived MNs for future work aiming to develop much needed therapeutics for this devastating disease.

# Chapter 3

# iPSC-derived astrocytes harbouring *TARDBP* or *C9ORF72* mutations cause MN dysfunction via non-cell autonomous mechanisms

# 1. Introduction

Selective degeneration and death of one or more neuronal type is the defining feature of human neurodegenerative diseases. One such fatal, incurable neurodegenerative disease is ALS which is characterized by the selective, premature degeneration and death of MNs (Robberecht and Philips, 2013). Mice expressing various ALS-related mutations, including *SOD1* (Rosen et al., 1993) and *TARDBP* (Wegorzewska et al., 2009) mutations, have recapitulated the fatal paralysis seen in ALS patients, and their use has been an important contributor to defining FALS disease mechanisms. These mechanisms include mitochondrial dysfunction, protein aggregation and misfolding, glutamate excitotoxicity, hyperexcitability, oxidative stress, and dysregulation of transcription and RNA processing (Beckman et al., 2001; Bruijn et al., 2004; Kuo et al., 2004; Ferraiuolo et al., 2011). Most recently, the development of human stem cell-based models have aided the study of this disease, enabling the investigation of disease processes in cells derived from SALS and FALS patients. Unlike many of the currently available animal models, patient derived cells express disease relevant levels of ALS-related mutations.

The fundamental pathological basis for ALS remains to be determined along with the insults that specifically target and cause degeneration of MNs. Although traditionally viewed as a disease mainly affecting MNs due to dysfunctional processes occurring within them, evidence suggests that degeneration also involves toxic signals from multiple other cell types including astrocytes, microglia and oligodendrocytes (Ilieva et al., 2009). Non-cell autonomous disease mechanisms were first implicated in ALS when increased levels of glutamate were found in CSF samples from ALS patients (Rothstein et al., 1990; Shaw et al., 1995a). These increased levels were associated

with a decrease in the expression of the astroglial transporter, EAAT2 (GLT-1 in rodents), which removes glutamate from the extracellular space, terminating neuronal excitation (Bruijn et al., 1997; Bendotti et al., 2001b; Pardo et al., 2006; Kim et al., 2011). The failure of glutamate re-uptake by EAAT2 results in sustained elevation of neuronal intracellular $Ca^{2+}$, initiating a cell death cascade. The permeability of AMPA receptors to $Ca^{2+}$ also plays a role in excitotoxicity, as MNs express low levels of the GluR2 subunit making them more permeable to $Ca^{2+}$, leaving MNs to rely on astrocytes to induce GluR2 subunit up-regulation. Astrocytes expressing mutant h*SOD1* lose their ability to regulate GluR2 expression thereby increasing MN vulnerability to AMPA receptor-mediated excitotoxicity (Van Damme et al., 2007). Additional research has firmly established the contribution of neighbouring glial cells to the degeneration of MNs (Boillée et al., 2006; Lobsiger and Cleveland, 2007; Yamanaka et al., 2008). These studies, which utilise primary mutant *SOD1* astrocytes from rodent models (Di Giorgio et al., 2007; Nagai et al., 2007; Cassina et al., 2008; Fritz et al., 2013; Phatnani et al., 2013; Rojas et al., 2014) and patient samples (Marchetto et al., 2008; Haidet-Phillips et al., 2011; Re et al., 2014), illustrate how wild-type MNs from rodent models or derived from human embryonic stem cells are selectively targeted, leaving other cell types unaffected. Non-cell-autonomous processes involving glial cells harbouring mutant *SOD1* are implicated not only in disease progression, but also the onset and early stages of the disease.

Mutant *SOD1* genes are expressed ubiquitously in humans and mice and expression exclusively in mouse MNs is not sufficient to cause disease (Pramatarova et al., 2001; Lino et al., 2002; Boillée et al., 2006). However, mutant *SOD1* expression in non-neuronal cells contributes to MN toxicity and thereby, disease onset and progression (Ilieva et al., 2009). The involvement of microglia in ALS has also been supported by

studies in which, upon deletion of mutant *SOD1* from microglia, disease progression slowed and fewer toxic factors were released, compared to when the microglia expressed mutant *SOD1* (Clement et al., 2003; Beers et al., 2006; Boillée et al., 2006; Lee et al., 2012; Frakes et al., 2014). Evidence that astrocytes also play a negative role in human ALS was provided by a recent study showing that astrocytes generated from post mortem spinal cords from *SOD1* or sporadic ALS patients adversely affect the viability of cultured ESC-derived mouse MNs (Haidet-Phillips et al., 2011). There is therefore increasing evidence that the presence of the mutant *SOD1* protein in these glial cells contributes significantly to the progression of ALS in animal models.

Relatively little is known regarding the non-cell-autonomous toxicity mediated by ALS mutations other than *SOD1*, or in SALS cases. Unlike studies of astrocytes harbouring mutant *SOD1*, which are in agreement that they are toxic to MNs, studies investigating the toxic effects of astrocytes harbouring *TARDBP* mutations have reported conflicting results. Human iPSC-derived astrocytes from a patient harbouring an M337V *TARDBP* mutation did not effect the survival of control iPSC-derived MNs (Serio et al., 2013). Similarly, astrocytes lacking TDP-43 or overexpressing mutant *TARDBP* failed to cause the death of control MNs in co-culture or when implanted into wild-type rat spinal cords (Haidet-Phillips et al., 2013). Conversely, wild-type MNs in transgenic rats, where the *TARDBP* M337V mutation was restricted to astrocytes, progressively degenerated indicating that *TARDBP* mutations can cause non- cell autonomous death of MNs (Tong et al., 2013). Primary wild-type MNs exposed to astrocyte- conditioned medium (ACM) from primary astrocyte cultures of mutant TDP-43 mice also provides evidence for the non-cell autonomous effect of *TARDBP* mutations by causing MN death (Rojas et al., 2014). Astrocytes taken from SALS patient post-mortem samples have also been shown to cause control MNs to die

(Haidet-Phillips et al., 2011), as have induced astrocytes (i-astrocytes), generated from SALS patients and patients with *C9ORF72* mutations (Meyer et al., 2013).

MN excitability alterations have been described in mutant *SOD1* mouse models (Pieri et al., 2003; Kuo et al., 2004; van Zundert et al., 2008; Quinlan et al., 2011; Delestrée et al., 2014), in ALS patients (Vucic and Kiernan, 2006; Kanai et al., 2012) and in iPSC-derived MNs harbouring *SOD1*, *C9ORF72*, *TARDBP* or *FUS* mutations (Sareen et al., 2013; Wainger et al., 2014; Devlin et al., 2015). These studies focused on the possible cell autonomous mechanisms that could lead to the onset and progression of ALS. However, a recent study showed that these changes can be mediated by non-cell autonomous disease mechanisms (Fritz et al., 2013). Acute exposure of mouse primary wild-type spinal cord MN cultures to conditioned medium derived from mouse astrocytes (ACM) expressing mutant *SOD1* caused MN hyperexcitability, a similar phenotype to those described in early embryonic and postnatal mutant *SOD1* MNs (Pieri et al., 2003; Kuo et al., 2004; Quinlan et al., 2011) and iPSC-derived MN studies (Wainger et al., 2014; Devlin et al., 2015). In the present study, detailed electrophysiological analyses of a humanised *in vitro* model has been carried out where healthy control iPSC-derived MNs are co-cultured with iPSC-derived astrocytes from control, *TARDBP*, *C9ORF72* and C9 gene edited patient lines. These data reveal the ability of control iPSC-derived MNs to develop appropriate functional properties when co-cultured with all iPSC-derived astrocyte lines. However, iPSC-derived MNs co-cultured with *TARDBP* or *C9ORF72* iPSC-derived astrocytes undergo a progressive loss of action potential output and a decrease in ionic conductances compared to MNs co-cultured with the control iPSC-derived astrocyte line. These pathophysiological alterations occurred in the absence of any overt changes in MN viability. Recordings obtained from control MNs co-cultured with

astrocytes derived from an iPSC line in which the *C9ORF72* mutation was removed revealed a reversal of the pathophysiological phenotype.

# 2. Methods

## 2.1.iPSC Lines

For this study we used 6 iPSC lines from 6 individuals: 1 male M337V TDP-43 ALS patient (1 clone, M337V[1]); 1 male G298S TDP-43 ALS patient (1 clone, G298S); 1 female *C9ORF72* ALS patient (1 clone, Carrier 1 gene edited clones); 2 male *C9ORF72* ALS patients (1 clone, Carrier 2; 1 Clone, Carrier 3) and 1 female healthy control (1 clone, CTRL). iPSCs were generated from fibroblasts as previously described (Yusa et al., 2011; Bilican et al., 2012; Devlin et al., 2015). In addition, an isogenic/gene edited control line was generated from the Carrier 1 *C9ORF72* patient line using the CRISPR-Cas9 system to remove the $G_4C_2$ repeat expansion on *C9ORF72* (Carrier1-$\Delta G_4C_2$). At least 4 iPSC differentiations were performed for each line with control and patient iPSC differentiations always run in parallel. iPSCs were established by virally transducing $10^5$ fibroblasts with the Yamanaka reprogramming factors *OCT4, SOX2, KLF4* and *c-MYC* using either lentiviral (Vectalys) or Sendai (Life technologies) reprogramming kits. See Chapter 2 methods for full details. Members of Siddharthan Chandran's lab at the University of Edinburgh, Chris Shaw's lab at King's College London and Ludovic Vallier's lab at the University of Cambridge carried out the generation and differentiation of iPSCs into neuronal lineages.

[1] Subsequent data available post-submission revealed that the most recent iPSC-derived astrocytes generated from the M337V TDP-43 patient had irregular karyotyping which likely impacted the results from co-cultures with this line.

## 2.2. Generation of Astrocytes from iPSC Lines

Generation of neurospheres from iPSC lines and their patterning to acquire MN progenitor identity were carried out as previously described (Bilican et al., 2012; Serio et al., 2013). Neurospheres were mechanically chopped at the beginning of the enrichment phase and cultured in NSCR EF20 medium containing Advanced DMEM/F12 (Invitrogen), 1% N2 supplement (Invitrogen), 0.1% B-27 supplement (Invitrogen), 1% nonessential amino acids (NEAA; Invitrogen), 1% penicillin/streptomycin (Invitrogen), 1% GlutaMAX solution (Invitrogen), 20 ng/mL fibroblast-growth factor 2 (FGF-2; PeproTech), and 20 ng/mL epidermal growth factor (EGF; R&D Systems) for 2–4 weeks (depending on the size of the chopped spheres). After enrichment, the spheres were propagated in NSCR medium and passaged mechanically by chopping them every 2 weeks. Monolayer cultures were generated by dissociating the spheres with the Papain Dissociation System (Worthington Biochemical) and plated on plates coated with Matrigel (BD Biosciences; 1:80 dilution). The monolayer astrocyte progenitor cells (APCs) cultures were propagated in NSCR EF20 medium and passaged when confluent by using Accutase (Sigma) (split ratio 1:2–1:3). Astrocyte populations were obtained by differentiating the APCs for 14 days with AstroMED CNTF containing Neurobasal medium (Invitrogen), 0.2% B-27 supplement, 1% NEAA, 1% penicillin/streptomycin, 1% GlutaMAX and 10 ng/mL ciliary neurotrophic factor (CNTF; R&D Systems), on Matrigel-coated plates or tissue culture flasks. Differentiated astrocytes were plated on Matrigel coated 96-well plates at a density of $3 \times 10^4$ cells per well. Chen Zhao in Siddharthan Chandran's lab carried out astrocyte generation from neurospheres.

## 2.3. MN generation from iPSC lines

Differentiation of iPSCs into a neuronal and MN lineage was performed using modifications of previously established and validated protocols (Bilican et al., 2012; Amoroso et al., 2013; Devlin et al., 2015). Only control iPSC-derived MNs were used for these studies. See methods Chapter 2 for full details. Technical staff in Siddharthan Chandran's lab at the University of Edinburgh performed these steps.

## 2.4. Astrocyte and MN co-cultures

Astrocytes were plated at a density of 150 x $10^3$ cells per well in 24-well plates on plastic coverslips (Thermo Scientific) coated with laminin (Sigma), fibronectin (Sigma) and Matrigel (BD Biosciences) in EF20 medium for between 5-7 days. Astrocytes were then differentiated for a further two weeks in AstroMED CNTF. Control iPSC-derived MN progenitors were dissociated with the Papain Dissociation System (Worthington Biochemical) and plated at a density of 50 x $10^3$ cells per well on top of the astrocytes once the astrocyte medium had been removed. MN plate down medium consisted of Neurobasal medium, 1% penicillin/streptomycin, 0.5% GlutaMAX, 0.5% B-27, 0.5% N-2 Supplement, 20 ng/ml basic FGF, 1 μM retinoic acid, 1 μM purmorphamine, 1 μM mouse Smo agonist SAG (Merck Millipore)(Amoroso et al., 2013). 24 hours post MN plating, 20 ng/ml CNTF; R&D, 10 ng/ml GDNF and 10 μM forskolin) were added, with this medium used until day 14, feeding every 3 days. From day 14, RA, SAG, purmorphamine and forskolin was removed from the medium, with cells then maintained for up to 10 weeks.

## 2.5. Immunofluorescence

Cells were fixed in 4% (wt/vol) paraformaldehyde for 10 minutes, permeabilized in 0.1% Triton X-100 at room temperature for 10 minutes and blocked in 3% (vol/vol) goat or donkey serum for 45 minutes. They were then incubated in primary antibodies for 45 minutes (Table 3.1) followed by secondary antibodies for 20 minutes (Alexa Fluor dyes, Invitrogen). The nuclei were counterstained with DAPI (Sigma) for 5 minutes and coverslips were mounted on slides with FluorSave (Merck). Fluorescent imaging was performed on fields of view containing uniform DAPI staining using an Axioscope (Zeiss) microscope. Images were processed with Axiovision V 4.8.1 (Zeiss) and immunolabelled cells counted manually by a blinded observer within ImageJ64 (v 1.47) software. Chen Zhao in Siddharthan Chandran's lab at the University of Edinburgh carried out the immunofluorescence staining and imaging presented in Fig. 1A.

| Antibody | Host | Company | Concentration |
|---|---|---|---|
| **Vimentin** | Goat polyclonal | Millipore | 1:50 |
| **B3-Tubulin** | Mouse monoclonal | Sigma | 1:1000 |
| **GFAP** | Rabbit polyclonal | Dako | 1:500 |
| **NFIA** | Rabbit polyclonal | Abcam | 1:100 |
| **S100β** | Rabbit polyclonal | Dako | 1:400 |

**Table 3.1:** List of primary antibodies used

## 2.6. RNA- FISH

FISH was performed using an Alexa 546- conjugated $(GGCCCC)_4$ oligoneucleotide probe (IDT). See methods Chapter 2 for full details. Immunostaining was performed as described above. Elaine Cleary in Siddharthan Chandran's lab at the University of Edinburgh carried out these steps and provided the images for Fig. 3.1C.

## 2.7. CRISPR/Cas9

The isogenic *C9ORF72* Δ $G_4C_2$ iPSC line was generated from a *C9ORF72* ALS patient iPSC line using CRISPR/Cas9 mediated genome editing. See methods Chapter 2 for full details. Bhuvaneish Thangaraj Selvaraj in Siddharthan Chandran's lab at the University of Edinburgh performed these steps.

## 2.8. Cell viability assays

For LDH assays, cell culture medium was collected from control iPSC-derived MNs co-cultured with control, patient derived and gene-edited iPSC-derived astrocytes, which were differentiated in parallel to enable direct comparisons. Medium was collected twice per week across weeks 3-10 post-plating from MN co-cultures with control, *C9ORF72* (Carrier 1) and gene-edited (Carrier-1 Δ) astrocytes. LDH activity (mU/ml) was calculated for each cell type using LDH assay kits (Abcam). LDH activity was plotted versus post-plating date, and compared between cell types using one-way ANOVAs.

Survival analysis of control iPSC-derived MNs was performed, with the observer blinded to the cell lines, by counting the number of MNs on the Carrier (C9) or Carrier-1 Δ astrocytes stained with the MN marker SMI-32. 20 images were taken

from each line at weeks 5-6 and 7-10 post-plating. Statistical analysis was performed using a one-way ANOVA followed by Tukey's post-hoc test.

## 2.9. Electrophysiology

Whole-cell patch-clamp recordings were used to assess the functionality of control iPSC-derived MNs. Voltage-clamp mode was used to investigate intrinsic membrane properties. Current-clamp mode was used to investigate the firing properties of MNs. Experiments were carried out in a recording chamber which was perfused continuously with oxygenated artificial cerebral spinal fluid (aCSF) at room temperature (22-24°C). Whole-cell patch-clamp recordings were made from cells visualised by infrared-differential interference contrast (IR-DIC) microscopy using an Olympus upright BX51WI microscope with a 40X submersion lens. Patch electrodes (4.0-5.0 MΩ resistance) were pulled on a Sutter P-97 horizontal puller (Sutter Instrument Company, Novato, CA) from borosilicate glass capillaries (World Precision Instruments, Sarasota, FL). Recorded signals were amplified and filtered (4kHz low-pass Bessel filter) using a MultiClamp 700B amplifier (Axon Instruments, Union City, CA) and acquired at ≥ 10kHZ using a Digidata 1440A analog-to-digital board and pClamp10 software (Axon Instruments). Whole-cell capacitance ($C_m$), input resistance ($R_N$), series resistance ($R_S$) and resting membrane potential (RMP) values were calculated using pClamp10 software. Only cells with an $R_s < 20M\Omega$, a RMP more hyperpolarised than -20mV and $R_N > 100$ MΩ were included in data analysis. $R_s$ values were not significantly different between control iPSC-derived MNs co-cultured with control, *C9ORF72*, *TARDBP* or gene edited iPSC-derived astrocytes. Cells were defined as neurons if they had clear fast-inactivating inward currents (≥ 50pA). Recordings from glial cells were excluded from all analyses. An on-line P4

leak subtraction protocol was used for all recordings of voltage-activated currents. Descriptions of voltage and current-clamp protocols are provided in the results section.

The aCSF used for all electrophysiological recordings contained the following in mM; 127 NaCl, 3 KCl, 2 $CaCl_2$, 1 $MgSO_4$, 26 $NaHCO_3$, 1.25 $NaH_2PO_4$, 10 D- glucose (equilibrated with 95% $O_2$ and 5% $CO_2$ at room temperature, pH 7.45; osmolarity, ~ 310mOsm). The pipette solution contained (in mM): 140 potassium methane-sulfonate, 10 NaCl, 1 $CaCl_2$, 10 HEPES, 1 EGTA, 3 ATP-Mg, 0.4 GTP, (pH 7.2-7.3, adjusted with KOH; osmolarity adjusted to ~ 300mOsm with sucrose).

Electrophysiological data were analysed using Clampfit10 software (Axon Instruments). Data from control iPSC-derived MNs co-cultured with the *C9ORF72* iPSC-derived astrocytes lines (3 lines) and the gene- edited iPSC-derived astrocytes (3 lines) were pooled for all analyses. Peak $Na^+$ currents and peak $K^+$ currents ($log_{10}$ transformed), $C_m$, $R_N$, and RMP were compared across the five different co-culture groups using one-way ANOVAs. Frequency-Current *(f-I)* relationships were compared across cell lines using general linear models. Pair-wise comparisons were made using Tukey's honest significant difference test, where necessary.

For the purposes of statistical comparisons, spontaneous synaptic activity and action potential generation were classified as either present or absent. These binary data were fitted with a general linear model and contrasts were made using Wald's tests and P values adjusted using a Bonferroni correction.

# 3. Results

## 3.1. Generation of iPSCs and differentiation into astrocytes

Using a previously described method (Bilican et al., 2012), six iPSC lines were generated from fibroblasts, including one line from one healthy individual (CTRL), three lines from three ALS patients carrying the *C9ORF72* mutation (Carrier 1, Carrier 2 and Carrier 3) and two lines from two ALS patients harbouring *TARDBP* mutations, one with an M337V mutation and one with an G298S mutation. Additionally, a gene-edited line was generated from Carrier 1 using CRISPR-Cas9 technology to remove the $G_4C_2$ repeat expansion on *C9ORF72* (Carrier1-$\Delta G_4C_2$). Immunocytochemistry showed high expression levels of APC markers, vimentin and nuclear factor I-A (NFIA), and astrocyte markers, S100 calcium binding protein β (S100β) and glial fibrillary acidic protein (GFAP) in our cultures (Fig. 3.1A). Quantification of immunolabelling for S100β, GFAP and a neuronal marker βIII-tubulin revealed that highly pure astrocyte populations were generated from iPSC lines with comparable differentiation (Fig. 3.1B). This suggests that the presence of the ALS mutations do not interfere with the differentiation of astrocytes from iPSCs. Next, we asked whether RNA foci could be detected in astrocytes harbouring *C9ORF72* mutations derived from patient iPSCs. To determine this, RNA FISH was performed using a probe against the GGGGCC repeat. Nuclear RNA foci were detected in all *C9ORF72* mutant astrocyte lines but not in control or the isogenic gene-edited (Carrier-1Δ) lines demonstrating that the presence of the $G_4C_2$ repeat expansion causes formation of RNA foci in astrocytes (Fig. 3.1C).

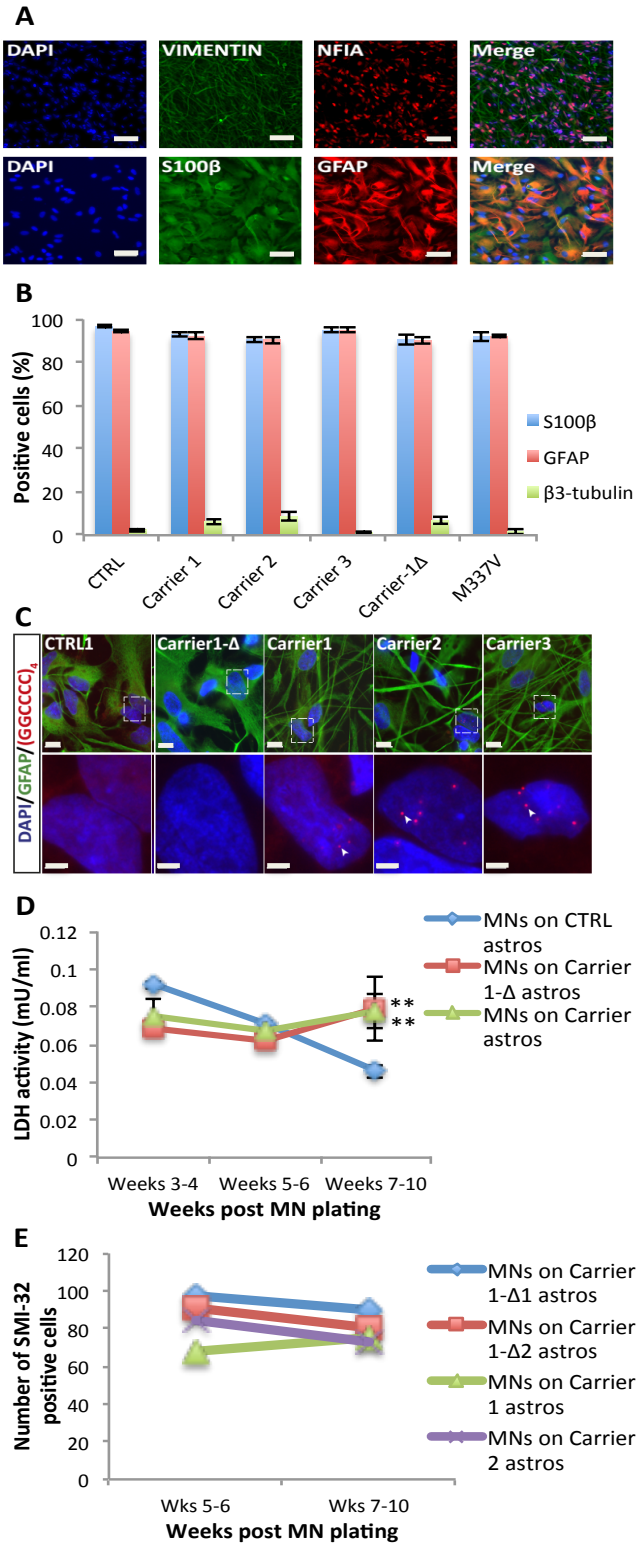


**Figure 3.1: Generation of astrocytes from ALS patient and healthy control iPSCs do not affect MN viability in co-culture.**

Figure caption on following page

**Figure 3.1: Generation of astrocytes from ALS patient and healthy control iPSCs do not affect MN viability in co-culture**

(A) Representative immunohistochemical images of astrocyte progenitor cells (APCs), labelled with vimentin and NFIA, and of astrocytes, labelled with GFAP and S100β, derived from iPSCs (scale bar, 50 μm; Images generated by Chen Zhao at the University of Edinburgh). (B) Quantification of the percentage of differentiated astrocytes in control, *C9ORF72*, *TARDBP* and gene edited iPSC lines. (C) Representative images of cells containing RNA foci, revealed using an antisense probe against the $G_4C_2$ repeat expansion, co-labelled with the astrocytic marker GFAP (Scale bars, 10 μm top panel, 2.5 μm bottom panel; Images generated by Chen Zhao at the University of Edinburgh). (D) LDH activity plotted for control MNs co-cultured with control, C9 patient and gene-edited iPSC-derived astrocytes cultures from weeks 3–10 post plating (data are plotted as $\overline{x} \pm$ s.e.m. $P<0.01$; one way ANOVA). (E) Quantification of the percentage of MNs when co-cultured with C9 patient and gene-edited iPSC-derived astrocytes.

## 3.2. Patient iPSC-derived astrocytes do not alter the viability of control iPSC-derived MNs

Having established equivalent astrocyte enriched cultures from both control and patient iPSC lines, we first investigated whether there were any differences in cell viability between MNs co-cultured with control, patient or gene edited iPSC-derived astrocytes. Our initial observations suggested that control iPSC-derived MNs plated on control, patient or gene edited iPSC-derived astrocytes were morphologically indistinguishable. To confirm this we performed quantitative analyses of cell viability using lactate dehydrogenase (LDH) assays and MN cell counts. Analysis of LDH activity in control iPSC-derived MNs co-cultured with 1 control line (CTRL), 3 *C9ORF72* lines (Carrier 1, 2 and 3) and 2 gene edited lines (Carrier-1Δ1 and Carrier-1Δ2) revealed greater LDH activity in *C9ORF72* astrocyte co-cultures and in the gene edited astrocyte co-cultures compared to co-cultures with control astrocytes at weeks 7-10 ($P<0.01$; one way ANOVA with Tukey's honest significant difference; Fig. 3.1D). However, as there was an indication from general observations using IR-DIC microscopy of higher astrocytic death in the *C9ORF72* astrocytes, we performed immunocytochemistry on the iPSC-derived MN and astrocyte co-cultures at weeks 5-6 and 7-10. We found that there was a similar proportion of SMI-32 positive control iPSC-derived MNS co-cultured with either *C9ORF72* mutant astrocytes or the gene edited astrocytes (Fig. 3.1E). In summary, although an LDH assay suggested higher cell death in co-cultures with *C9ORF72* and gene edited astrocytes compared to controls, MN counts failed to reveal any differences in MN viability when co-cultured with *C9ORF72* astrocytes or gene edited astrocytes.

## 3.3. Patient iPSC derived astrocytes cause control iPSC-derived MNs to lose functional output

As the standard cell viability assays failed to uncover overt pathologies in control iPSC-derived MNs caused by the patient iPSC-derived astrocytes, we next used electrophysiological analyses to investigate whether patient iPSC-derived astrocytes had any affect on the function of control MNs. Whole-cell patch-clamp recordings were obtained from the largest neurons visualized via IR-DIC microscopy in the co-cultures from 3 to 10 weeks post MN plating. Selecting the largest neurons ensured recordings were predominantly obtained from MNs (Devlin et al., 2015).

We first compared the passive membrane properties of control iPSC-derived MNs co-cultured with control, patient or gene edited iPSC-derived astrocytes. For these and all other electrophysiological analyses, data were pooled for control iPSC-derived MNs co-cultured with the *C9ORF72* (Carrier 1,2 and 3) iPSC-derived astrocyte lines and for the gene edited (Carrier 1- Δ1, 2 and 3) iPSC-derived astrocyte lines. At weeks 3-4, whole-cell capacitance ($C_m$) values were similar across MNs plated on CTRL, *C9ORF72*, gene edited and *TARDBP* G298S astrocytes but were significantly smaller in MNs plated on *TARDBP* M337V astrocytes (see Table 3.2 for $\overline{x} \pm$ s.e.m. and sample sizes; one-way ANOVA with Tukey's honest significant difference). From weeks 5-10, MNs plated on *C9ORF72* astrocytes had significantly smaller $C_m$ values compared to those on gene-edited astrocytes and from weeks 7-10 compared to MNs on CTRL astrocytes. MNs co-cultured with both *TARDBP* astrocyte lines had significantly smaller $C_m$ values compared to those on CTRL and gene edited astrocytes at weeks 7-10. Input resistance ($R_N$) values were significantly higher in

| Passive membrane properties | MNs on CTRL astros | MNs on C9 astros | MNs on Carrier-1Δ astros | MNs on M337V astros | MNs on G298S astros |
|---|---|---|---|---|---|
| **$C_m$ (pF)** | | | | | |
| **Weeks 3-4** | 23.8 ± 0.9 (n=50) | 26.2 ± 0.8 (n=153) | 27.3 ± 1.1 (n=74) | 16.9 ± 0.7 (n=52)** ♯♯ ††† | 24.4 ± 1.2 (n=39) |
| **Weeks 5-6** | | 25.6 ± 1.4 (n=53) ††† | 33.4 ± 1.6 (n=49) | | |
| **Weeks 7-10** | 27.2 ± 1.6 (n=43) | 20.2 ± 1.1 (n=61) ** ††† | 31.2 ± 2.6 (n=33) | 17.5 ± 0.8 (n=67) ***††† | 19.9 ± 1.2 (n=23)*††† |
| **$R_N$ (MΩ)** | | | | | |
| **Weeks 3-4** | 540 ± 45 | 579 ± 38 | 564 ± 46 | 789 ± 64* ♯† | 560 ± 73 |
| **Weeks 5-6** | | 377 ± 38 | 391 ± 44 | | |
| **Weeks 7-10** | 457 ± 48 | 514 ± 55 | 470 ± 62 | 721 ± 56*† | 524 ± 90 |
| **RMP (mV)** | | | | | |
| **Weeks 3-4** | -48.3 ± 1.9 | -49.5 ± 1.2 | -42.0 ± 1.7 | -45.3 ± 1.9 | -53.5 ± 1.9 |
| **Weeks 5-6** | | -44.0 ± 1.8 † | -50.2 ± 2.2 | | |
| **Weeks 7-10** | -49.8 ± 2.1 | -43.1 ± 1.5 | -43.4 ± 2.4 | -40.3 ± 1.4** | -47.7 ± 2.8 |

Values are mean ± SEM; number of cells noted in parentheses.
*Significantly different to controls (*, P<0.05;**,P<0.001; ***,P<0.0001)
# Significant difference between patient lines(#, P<0.05; ##,p<0.001)
† Significantly different from gene-edited patient lines(†, P<0.05; †††,p<0.0001)

**Table 3.2:** Passive membrane properties

MNs co-cultured with M337V astrocytes at weeks 3-4 and 7-10 compared to those on CTRL, *C9ORF72*, gene edited and G298S *TARDBP* astrocytes. MNs co-cultured with *C9ORF72* astrocytes had a more depolarised resting membrane potential (RMP) at weeks 3-4 compared to MNs co-cultured with gene edited astrocytes while MNs co-cultured with M337V *TARDBP* astrocytes had a more depolarised RMP compared to CTRL astrocytes at weeks 7-10 (Table 3.2; $P<0.05$). These findings indicate that ALS patient iPSC-derived astrocytes cause changes to the passive membrane properties of control iPSC-derived MNs. Most changes are associated with measurements of cell size therefore it is likely that the patient iPSC-derived astrocytes impair or reduce the ability of axons and dendrites to grow, as seen in studies of ALS mouse models and patient samples (Nagai et al., 2007; Gallardo et al., 2014).

Current-clamp mode recordings of control iPSC-derived MNs, co-cultured with control, *C9ORF72*, gene edited or *TARDBP* iPSC-derived astrocytes, demonstrated their ability to repetitively fire trains of action potentials in response to current injection. In order to compare the excitability of repetitively firing MNs co-cultured with control, patient or gene edited iPSC-derived astrocytes, frequency-current (*f-I*) relationships were generated from responses to a series of injected current steps (0 to 145pA, in 10pA increments, 1s duration). Comparisons were performed on data pooled from recordings of repetitively firing cells at weeks 3-6 post MN plating (Fig. 3.2A). Analyses of the slope of the combined *f-I* relationship found no differences between MNs co-cultured with control, *C9ORF72*, gene edited or *TARDBP* astrocytes (Fig. 3.2B). However, rheobase current differed between MNs plated on *C9ORF72* astrocytes compared to MNs plated on control astrocytes and on *TARDBP* M337V astrocytes (Control $\overline{x}$ 15.6 ± s.e.m. 1.4pA, n=16, *C9ORF72* 26.1 ± 3.2, n=26, gene

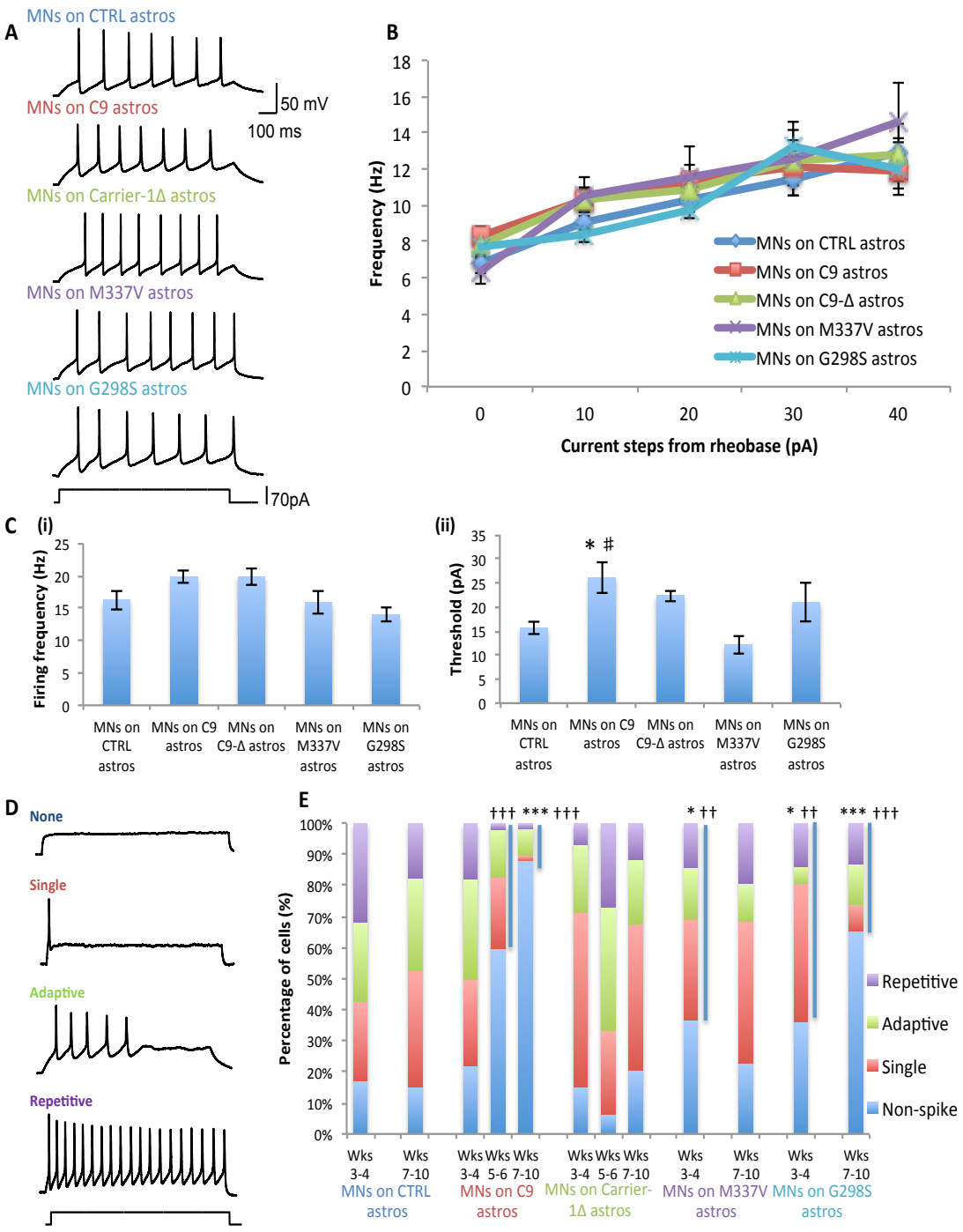


**Figure 3.2: Loss of action potential output in control iPSC-derived MNs co-cultured with C9ORF72 and TARDBP G298S iPSC-derived astrocytes.**

Figure caption on following page

**Figure 3.2: Loss of action potential output in control iPSC-derived MNs co-cultured with *C9ORF72* and *TARDBP* G298S iPSC-derived astrocytes.**

(A) Repetitive firing in response to square current injection in control iPSC-derived MNs co-cultured with CTRL, *C9ORF72*, gene-edited, *TARDBP* M337V and G298S iPSC-derived astrocytes. (B) Frequency-current (*f–I*) relationships generated for repetitively firing control iPSC-derived MNs co-cultured with CTRL (n=15), *C9ORF72* (n=26), gene-edited (n=15), *TARDBP* M337V (n=7) and G298S (n=5) astrocyte lines recorded from weeks 2–6 post plating (data are plotted as $\overline{x}\pm$ s.e.m.) (C) Properties of repetitively firing MNs including (i) firing frequency and (ii) threshold (*, significantly different to MNs on control astrocytes, P<0.05; ♯, significantly different to MNs on patient astrocytes, P<0.05.) (D) Examples of the four categories of firing observed in iPSC-derived MNs (repetitive, adaptive, single or no firing). (E) Proportion of cells exhibiting each firing category in MNs co-cultured with CTRL (n=87), *C9ORF72* (n=247), gene-edited (n=155), T*ARDBP* M337V (n=106) and G298S (n=59) iPSC-derived astrocyte lines across weeks 3–10 post plating (*significantly different to MNs on control astrocytes, P<0.05; ***, P<0.0001; ††significantly different to MNs on gene edited astrocytes, P<0.01; †††, P<0.0001; general linear model with multiple Wald's test and Bonferroni correction).

edited 22.3 ± 1.2, n=15; M337V 12.1 ± 1.8, n=7; G298S 21 ± 4, n=5; P<0.05; one-way ANOVA; Fig. 3.2C(ii)), suggesting some degree of hypoexcitability in MNs on *C9ORF72* iPSC-derived astrocytes.

Four output patterns including repetitive, adaptive, single and no firing were observed in MNs cultured on astrocytes in response to current injections (Fig. 3.2D). Repetitive firing was defined as a train of action potentials that lasted for the duration of the square current injection (1s), while adaptive firing was defined as multiple action potentials that stopped before the end of the current stimuli. Cells defined as having an adaptive output pattern were unable to repetitively fire in response to any of the series of current steps applied. When firing output data of control iPSC-derived MNs co-cultured with control, *C9ORF72*, gene edited or *TARDBP* iPSC-derived astrocytes were compared, the relative proportion of firing versus non-firing cells from weeks 3-4 post MN plating was smaller in MNs co-cultured with *TARDBP* astrocytes compared to those on control or gene edited astrocytes (Control firing 82.9%, n=47; *C9ORF72* firing 78.1%, n=151; gene edited firing 84.9%, n=73; *TARDBP* M337V 63.2%, n=49; *TARDBP* G298S 63.8%, n=36 Fig. 3.2E; *significantly different to MNs on CTRL astrocytes, P<0.05; †† significantly different to MNs on gene edited astrocytes, P<0.01; general linear model with multiple Wald's tests and Bonferroni correction). At weeks 5-6 and 7-10 post MN plating, the number of cells able to fire action potentials decreased significantly in MNs co-cultured with *C9ORF72* or *TARDBP* G298S astrocytes compared to MNs co-cultured with gene edited and control astrocytes. The ratio of firing versus non-firing remained unchanged in MNs co-cultured with control or gene edited astrocytes throughout these time-points (Weeks 5-6: *C9ORF72* firing 40.3%, n=38; gene edited firing 93.7%, n=48; Weeks 7-10: control firing 85%, n=40; *C9ORF72* firing 12.0%, n=58; gene edited firing

79.4%, n=34; *TARDBP* M337V firing 77.1%, n=57; *TARDBP* G298S firing 34.7%, n=23; Fig. 3.2E; ***significantly different to MNs plated on CTRL astrocytes, P<0.0001; ††† significantly different to MNs on gene edited astrocytes, P<0.0001) (See Fig. 3.3 for firing separated by line). These data demonstrate a loss of functional output in control iPSC-derived MNs co-cultured with *C9ORF72* or *TARDBP* G298S iPSC-derived astrocytes compared to those on control or gene edited astrocytes, with the number of firing cells on *TARDBP* M337V astrocytes returning to a similar proportion as control and gene edited co-cultures at weeks 7-10.

## 3.4. Synaptic inputs to control iPSC-derived MNs are not affected by ALS patient iPSC-derived astrocytes

Following investigation of the output produced by iPSC-derived MNs, we next examined their ability to receive synaptic input. The proportion of cells that received any synaptic input (defined as at least 1 event per minute) was similar in MNs co-cultured with CTRL, ALS patient and gene edited iPSC-derived astrocytes from weeks 3-10 post-plating (3-4 weeks: 14.3% on CTRLs, n=49; 35.9% on *C9ORF72*, n=114; 8.1% on gene edited, n=74; 13.4% on *TARDBP* M337V, n=52; 17.9% on *TARDBP* G298S, n=39; 5-6 weeks: 15.1% on *C9ORF72*, n=33; 30.7% on gene edited, n=39; weeks 7-10: 16.2% on CTRL, n= 43; 9.5% on *C9ORF72*, n=42; 13.6% on gene edited, n=22; 17.9% on *TARDBP* M337V, n=67; 8.6% on *TARDBP* G298S, n=23; Fig. 3.4A). In cells cultured from 2-6 weeks we analysed the inter-event-interval and amplitude of synaptic events. The inter-event interval differed between MNs co-cultured with *TARDBP* G298S astrocytes compared to those on gene-edited astrocytes (P<0.05; one-way ANOVA; Fig. 3.4B), whilst the amplitude remained the

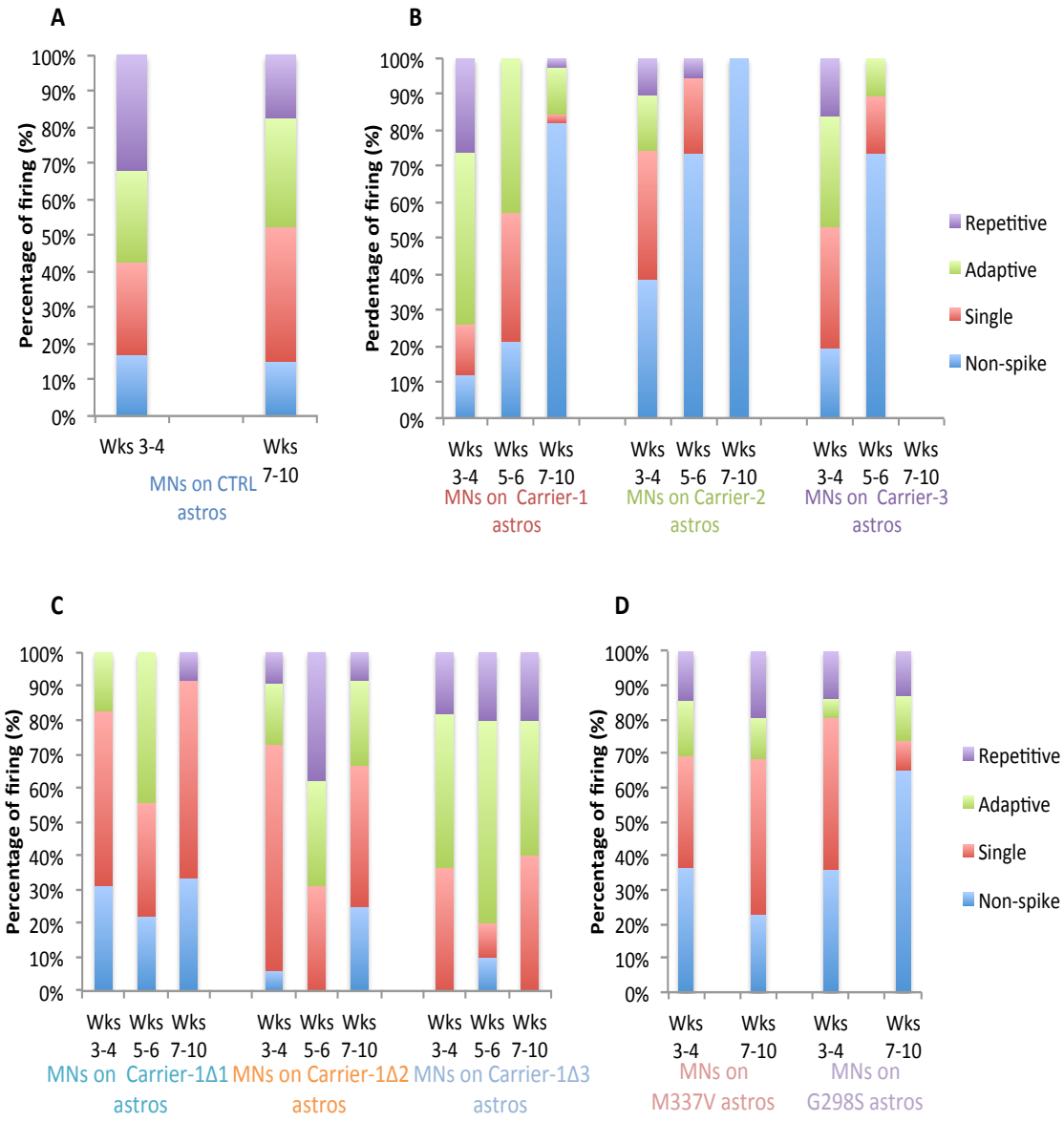


**Figure 3.3: Action potential output in control iPSC-derived MNs co-cultured with control, *C9ORF72*, gene edited, *TARDBP* M337V or G298S iPSC-derived astrocytes.**

Figure caption on following page

**Figure 3.3: Action potential output in control iPSC-derived MNs co-cultured with control, *C9ORF72*, gene edited, *TARDBP* M337V or G298S iPSC-derived astrocytes.**

Proportion of control iPSC-derived MNs exhibiting each firing category when co-cultured with (A) CTRL iPSC-derived astrocytes (n=87), (B) *C9ORF72* iPSC-derived astrocytes (Carrier 1, n=103; Carrier 2, n=77; Carrier 3, n=81), (C) gene-edited iPSC-derived astrocytes (Carrier-1Δ1, n=50; Carrier-1Δ2, n=74; Carrier-1Δ3, n=31), (D) *TARDBP* M337V (n=106) and G298S (n=59) iPSC-derived astrocyte lines across weeks 3–10 post plating. Firing data for MN co-cultured with *TARDBP* M337V astrocytes at weeks 3-4 were significantly different from those at weeks 7-10.

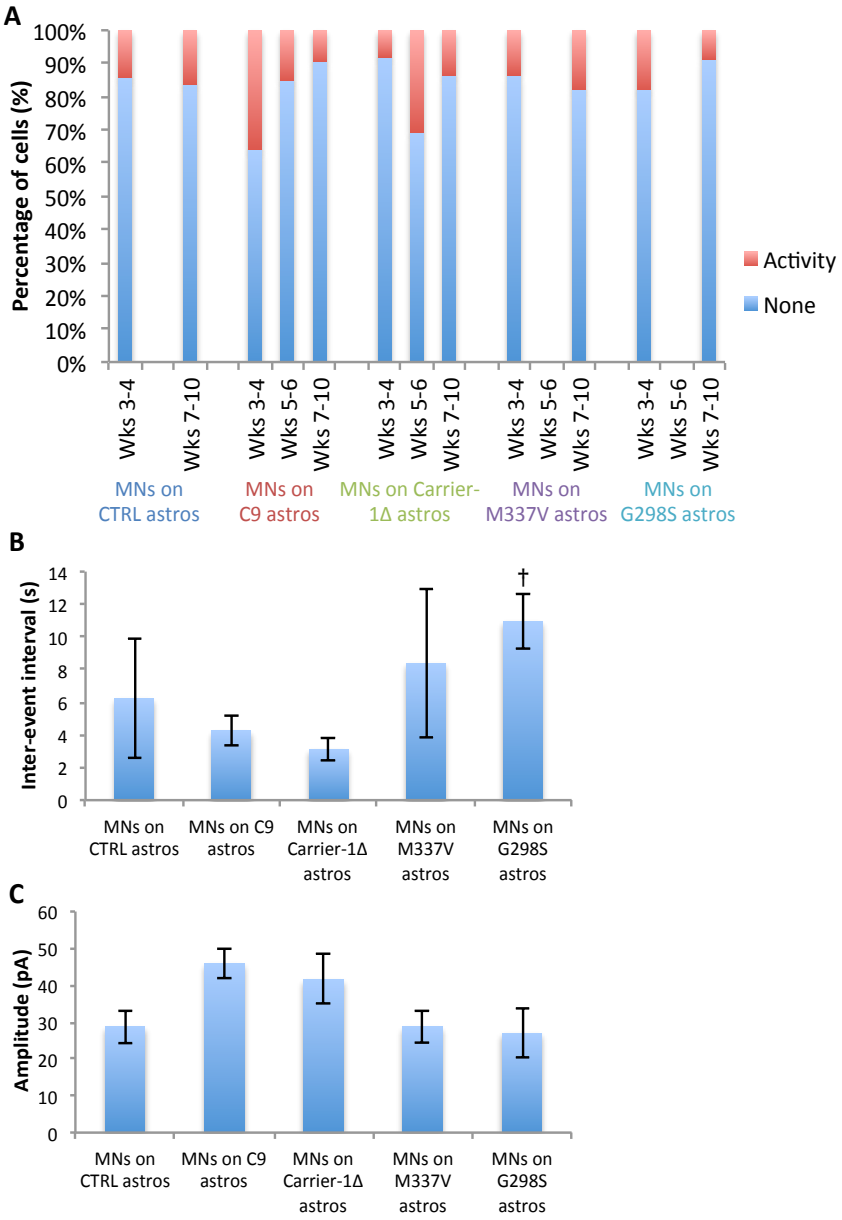


**Figure 3.4: MN synaptic inputs are unaffected by the presence of patient iPSC-derived astrocytes.**

Figure caption on following page

**Figure 3.4: MN synaptic inputs are unaffected by the presence of patient iPSC-derived astrocytes.**

(A) Proportion of cells displaying synaptic activity from weeks 3–10 post plating in control iPSC-derived MNs co-cultured with CTRL (n=92), *C9ORF72* (n=189), gene edited (n=135), *TARDBP* M337V (n=119) or G298S (n=62) iPSC-derived astrocytes. (B) Graphs of inter-event interval and (C) amplitude of synaptic events recorded from control iPSC-derived MNs co-cultured with control, patient and gene edited iPSC-derived astrocytes (†significantly different to MNs on gene edited astrocytes, $P<0.05$; one way ANOVA with Tukey's post-hoc tests and Bonferroni correction).

same in all lines (Fig. 3.4C) (See Fig. 3.5 for data separated by line). In summary, these data demonstrate that synaptic input to control iPSC-derived MNs remains largely unaffected by ALS patient iPSC-derived astrocytes despite the loss of action potential output in these cultures.

## 3.5. Patient iPSC derived astrocytes cause loss of voltage-activated currents in control iPSC-derived MNs

To investigate the mechanisms underlying the progressive loss of action potential output in control MNs co-cultured with *C9ORF72* and *TARDBP* G298S iPSC-derived astrocytes, voltage-clamp recordings were performed to assess voltage-activated currents involved in action potential generation.

Fast inactivating $Na^+$ currents were first investigated by using a series of voltage steps (-70 to 20 mV, 2.5 mV increments, 10 ms duration) from a holding potential of -60 mV (Fig. 3.6A). We found no differences in the current (I-V) relationships or peak $Na^+$ currents between MNs co-cultured with control, *C9ORF72* or gene edited iPSC-derived astrocytes at 3-4 weeks post MN plating. However MNs co-cultured with both *TARDBP* astrocyte lines had significantly lower peak $Na^+$ currents than those on control, *C9ORF72* or gene edited astrocyte lines (Peak current: control $\bar{x}$ 2,232 ± s.e.m. 211 pA, n= 49; *C9ORF72* 2,067 ± 120 pA, n= 153; gene edited 2,110 ± 209 pA, n= 74; *TARDBP* M337V 1,446 ± 180 pA; *TARDBP* G298S 1,272 ± 167 pA; Fig. 3.6C; $P<0.05$; one-way ANOVA after log transformation with Tukey's post-hoc test). From weeks 5-10 post MN plating, there was a progressive decrease in peak $Na^+$ currents in MNs co-cultured with *C9ORF72* or *TARDBP* G298S iPSC-derived astrocytes compared to co-cultures with control or gene edited iPSC-derived

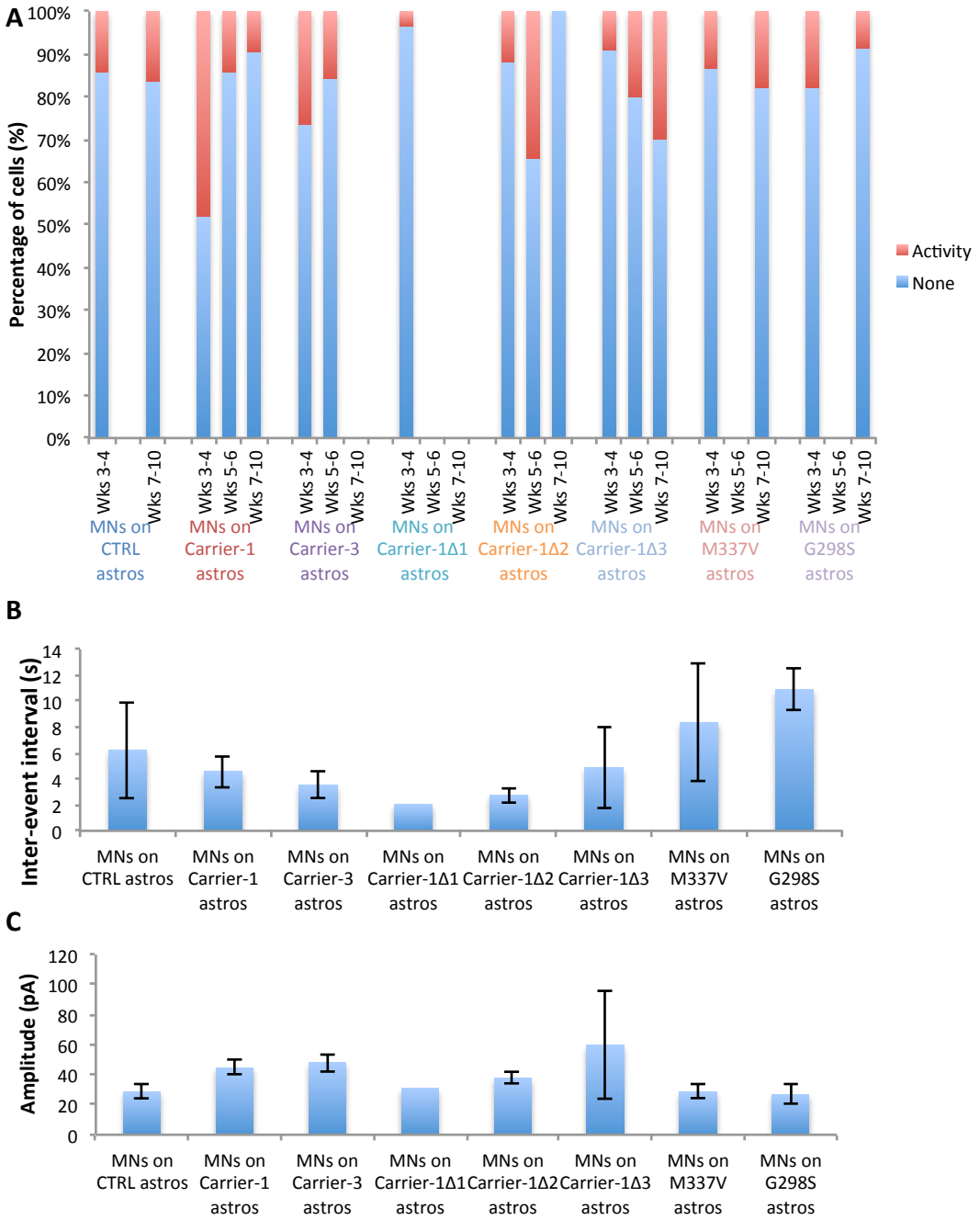


**Figure 3.5: MN synaptic inputs in co-cultures with CTRL, patient and gene edited iPSC-derived astrocyte lines.**

Figure caption on following page

**Figure 3.5: MN synaptic inputs in co-cultures with CTRL, patient and gene edited iPSC-derived astrocyte lines.**

(A) Proportion of cells displaying synaptic activity from weeks 3–10 post plating in control iPSC-derived MNs co-cultured with CTRL (n=92), *C9ORF72* (Carrier-1, n=104; Carrier-3, n=83), gene edited (Carrier-1Δ1, n=29; Carrier-1Δ2, n=75; Carrier-1Δ3, n=31), *TARDBP* M337V (n=119) or G298S (n=62) iPSC-derived astrocytes. (B) Graphs of inter-event interval and (C) amplitude of synaptic events recorded from control iPSC-derived MNs co-cultured with control, patient and gene edited iPSC-derived astrocytes.

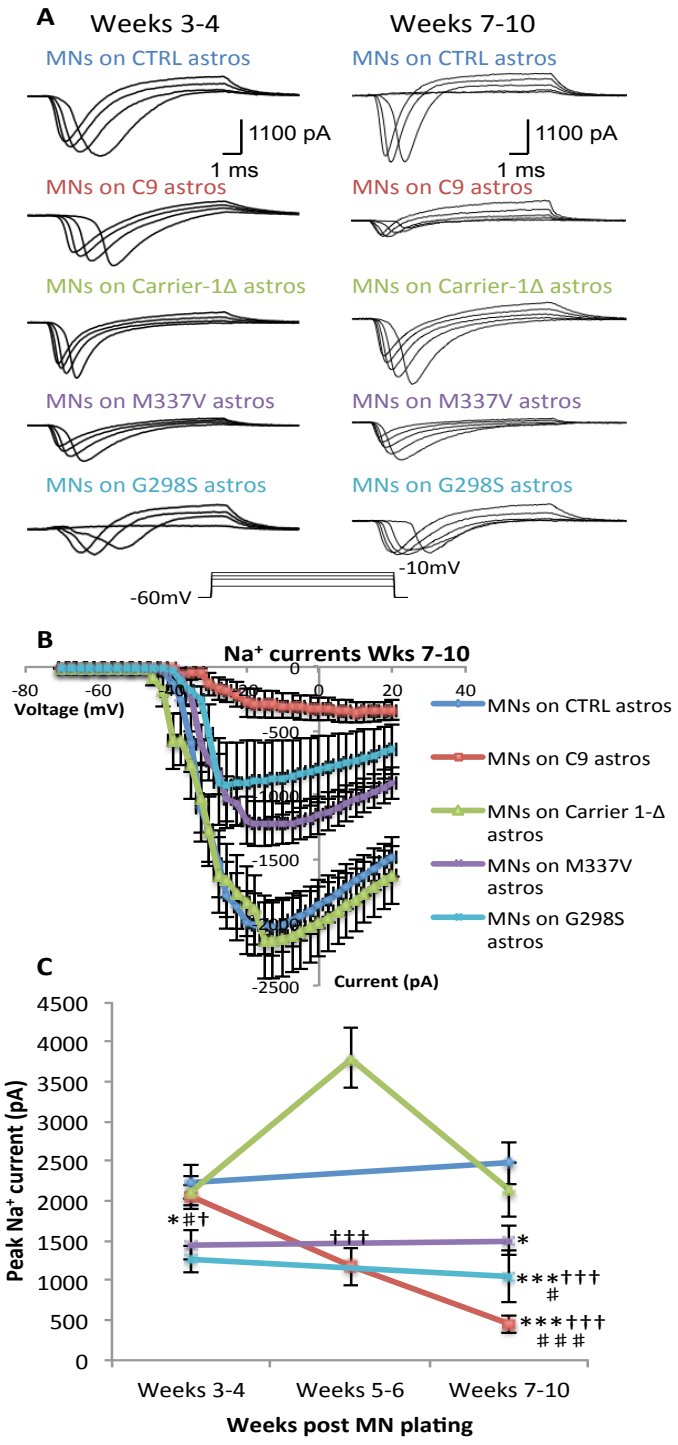


**Figure 3.6: Loss of fast, inactivating $Na^+$ currents in control iPSC-derived MNs co-cultured with ALS patient iPSC-derived astrocytes.**

Figure caption on following page

**Figure 3.6: Loss of fast, inactivating $Na^+$ currents in control iPSC-derived MNs co-cultured with ALS patient iPSC-derived astrocytes.**

(A) Raw data showing fast, inactivating $Na^+$ currents in control iPSC-derived MNs co-cultured with CTRL, *C9ORF72*, gene-edited and *TARDBP* iPSC-derived astrocytes at week 3–4 and weeks 7–10. (B) Current–voltage relationships of peak $Na^+$ currents recorded from control iPSC-derived MNs on CTRL, patient and gene-edited iPSC-derived astrocytes at weeks 7–10. (C) Peak fast, inactivating $Na^+$ currents plotted from weeks 3–10 for MNs co-cultured with CTRL (n=93), *C9ORF72* (n=266), gene-edited (n=156), *TARDBP* M337V (n= 118) or *TARDBP* G298S (n=62) iPSC-derived astrocytes (data are plotted as $\overline{x}$ ± s.e.m; *significantly different to MNs on controls astrocytes, P<0.05; ***, P<0.0001; #significant difference between MNs co-cultured with patient astrocyte lines, P<0.05; ###, P<0.0001; †significantly different to MNs on gene edited astrocytes, P<0.05; †††, P<0.0001; one way ANOVA with Tukey's post-hoc tests and Bonferroni correction).

astrocytes, with peak $Na^+$ currents in MNs co-cultured with *TARDBP* M337V astrocytes remaining smaller than those on control astrocytes (Weeks 5-6: *C9ORF72* $\bar{x}$ 1,174 ± s.e.m. 233 pA, n= 53; gene edited 3,795 ± 371, n= 49; Weeks 7-10: control 2,480 ± 268 pA, n=44; *C9ORF72* 458 ± 113 pA, n=60; gene edited 2,147 ± 345 pA, n=33; *TARDBP* M337V 1,501 ± 189; *TARDBP* G298S 1052 ± 335; Fig. 3.6B,C; $P<0.05$) (See Fig. 3.7 for data separated by line).

We next investigated whether the progressive loss of $Na^+$ currents reflected a more general decrease in voltage -activated currents in control MNs co-cultured with *C9ORF72* iPSC-derived astrocytes. Persistent $K^+$ currents were measured by eliciting a series of voltage steps (-70 to 40 mV, 10 mV increments, 500 ms duration) from a holding potential of -60 mV (Fig. 3.8A). At weeks 3-4 post MN plating, peak $K^+$ currents were comparable in MNs co-cultured with control, *C9ORF72*, gene edited and *TARDBP* G298S iPSC-derived astrocytes but were lower in MNs co-cultured with *TARDBP* M337V iPSC-derived astrocytes (Peak current: Control $\bar{x}$ 1,788 ± s.e.m. 148 pA, n=46; *C9ORF72* 1,913 ± 98 pA, n=147; gene edited 1,634 ± 127 pA, n=74; *TARDBP* M337V 1,125 ± 130 pA, n=52; *TARDBP* G298S 1,564 ± 128 pA, n=38; Fig. 3.8C, one-way ANOVA after log transformation with Tukey's post-hoc test). Similar to $Na^+$ currents, peak $K^+$ currents progressively declined in control MNs co-cultured with *C9ORF72* and *TARDBP* iPSC-derived astrocytes from weeks 5-10 compared to MNs co-cultured with control or gene edited iPSC-derived astrocytes (Weeks 5-6: *C9ORF72* $\bar{x}$ 1,070 ± s.e.m. 165 pA, n=53; gene edited 2,673 ± 233 pA, n=43; Weeks 7-10: Control 2,069 ± 160 pA, n=41; *C9ORF72* 438 ± 99 pA, n=60; gene edited 1,816 ± 248 pA, n=33; *TARDBP* M337V 997 ± 118 pA, n= 66; *TARDBP* G298S 988 ± 217 pA, n=21; Fig. 3.8B,C; $P<0.05$) (See Fig. 3.9 for data separated by line).

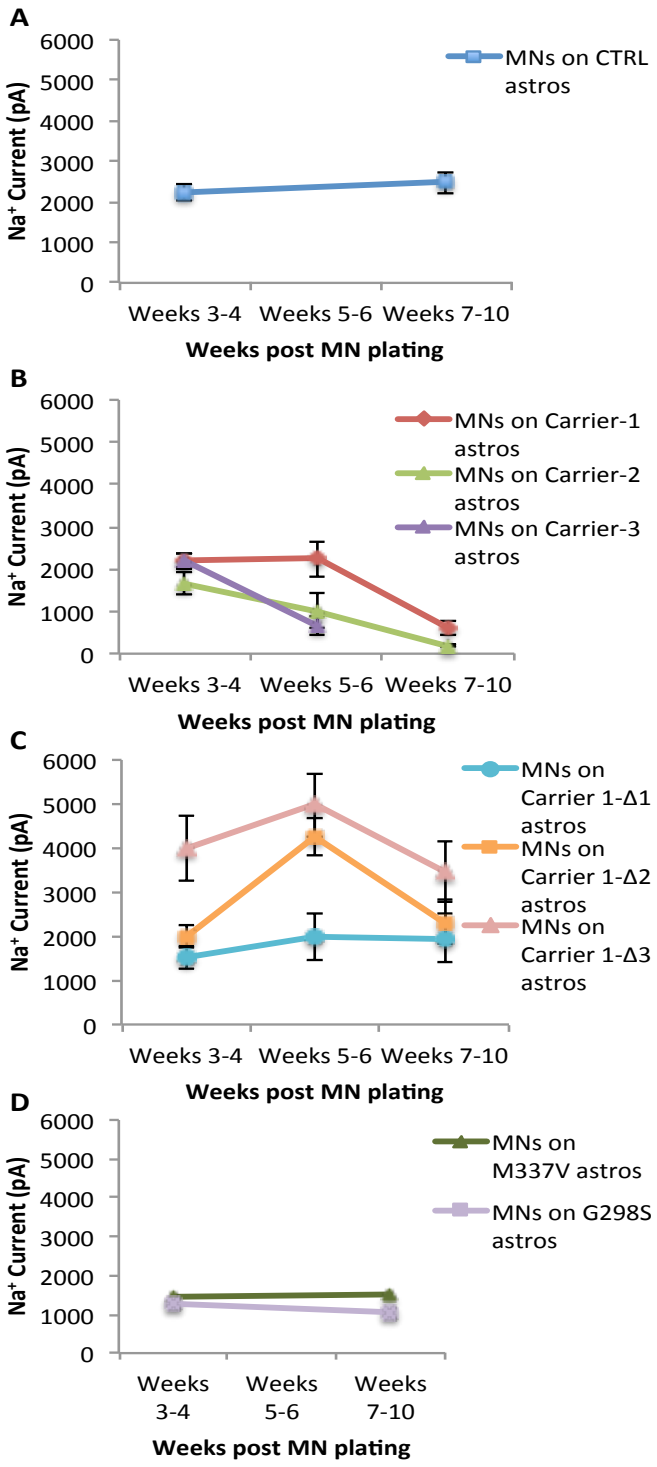


**Figure 3.7: Fast, inactivating $Na^+$ currents in control iPSC-derived MNs co-cultured with control, ALS patient and gene edited iPSC-derived astrocytes.**

Figure caption on following page

**Figure 3.7: Fast, inactivating $Na^+$ currents in control iPSC-derived MNs co-cultured with control, ALS patient and gene edited iPSC-derived astrocytes.**

Peak fast, inactivating $Na^+$ currents plotted from weeks 3–10 for MNs co-cultured with (A) CTRL (n=93), (B) *C9ORF72* (Carrier1, n=106; Carrier 2, n=79; Carrier 3, n=82), (C) gene-edited (Carrier-1Δ1, n=50; Carrier-1Δ2, n=75; Carrier-1Δ3, n=31), (D) *TARDBP* M337V (n= 118) or *TARDBP* G298S (n=62) iPSC-derived astrocytes (data are plotted as $\overline{x}$ ± s.e.m.).

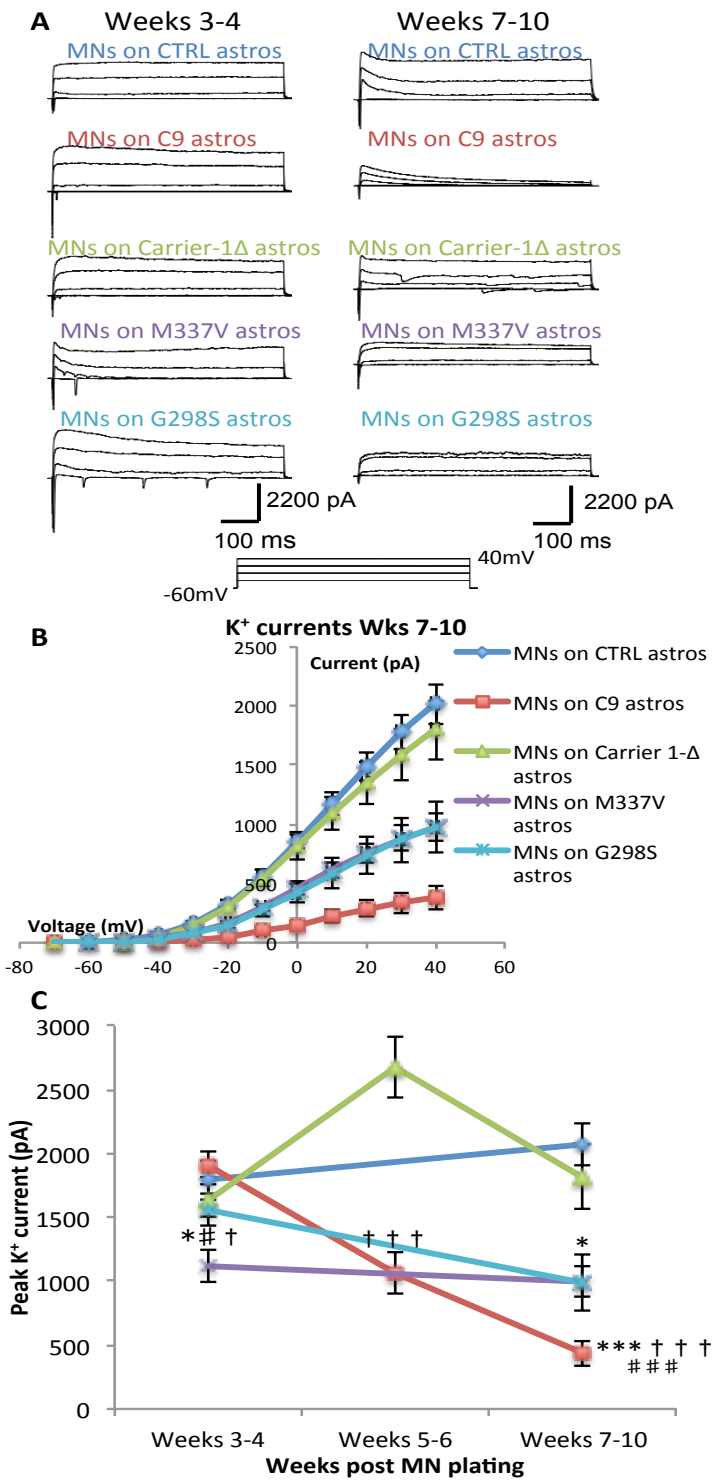


**Figure 3.8: Loss of persistent voltage-activated $K^+$ currents in control iPSC-derived MNs co-cultured with ALS patient iPSC-derived astrocytes.**

Figure caption on following page

**Figure 3.8: Loss of persistent voltage-activated $K^+$ currents in control iPSC-derived MNs co-cultured with ALS patient iPSC-derived astrocytes.**

(A) Raw data showing persistent $K^+$ currents in control iPSC-derived MNs co-cultured with CTRL, *C9ORF72*, gene-edited and *TARDBP* iPSC-derived astrocytes at week 3–4 and weeks 7–10. (B) Current–voltage relationships of peak $K^+$ currents recorded from control iPSC-derived MNs on CTRL, patient and gene-edited iPSC-derived astrocytes at weeks 7–10. (C) Peak $K^+$ currents plotted from weeks 3–10 for MNs co-cultured with CTRL (n=93), *C9ORF72* (n=266), gene-edited (n=156), *TARDBP* M337V (n= 118) or *TARDBP* G298S (n=62) iPSC-derived astrocytes (data are plotted as $\overline{x}$ ± s.e.m; * significantly different to MNs on controls astrocytes, P<0.05; ***, P<0.0001; #significant difference between MNs co-cultured with patient astrocyte lines, P<0.05; ###, P<0.0001; †significantly different to MNs on gene edited astrocytes, P<0.05; †††, P<0.0001; one way ANOVA with Tukey's post-hoc tests and Bonferroni correction).

These data demonstrate a progressive reduction in both fast, inactivating $Na^+$ currents and persistent, voltage-activated $K^+$ currents in control iPSC-derived MNs co-cultured with *C9ORF72* iPSC-derived astrocytes, which likely underlies their loss of functional output. Therefore, non-cell autonomous disease mechanisms involving interactions between astrocytes harbouring *C9ORF72* or *TARDBP* G298S mutations and healthy control MNs cause dysfunction in healthy MNs, despite unaltered viability of MNs.

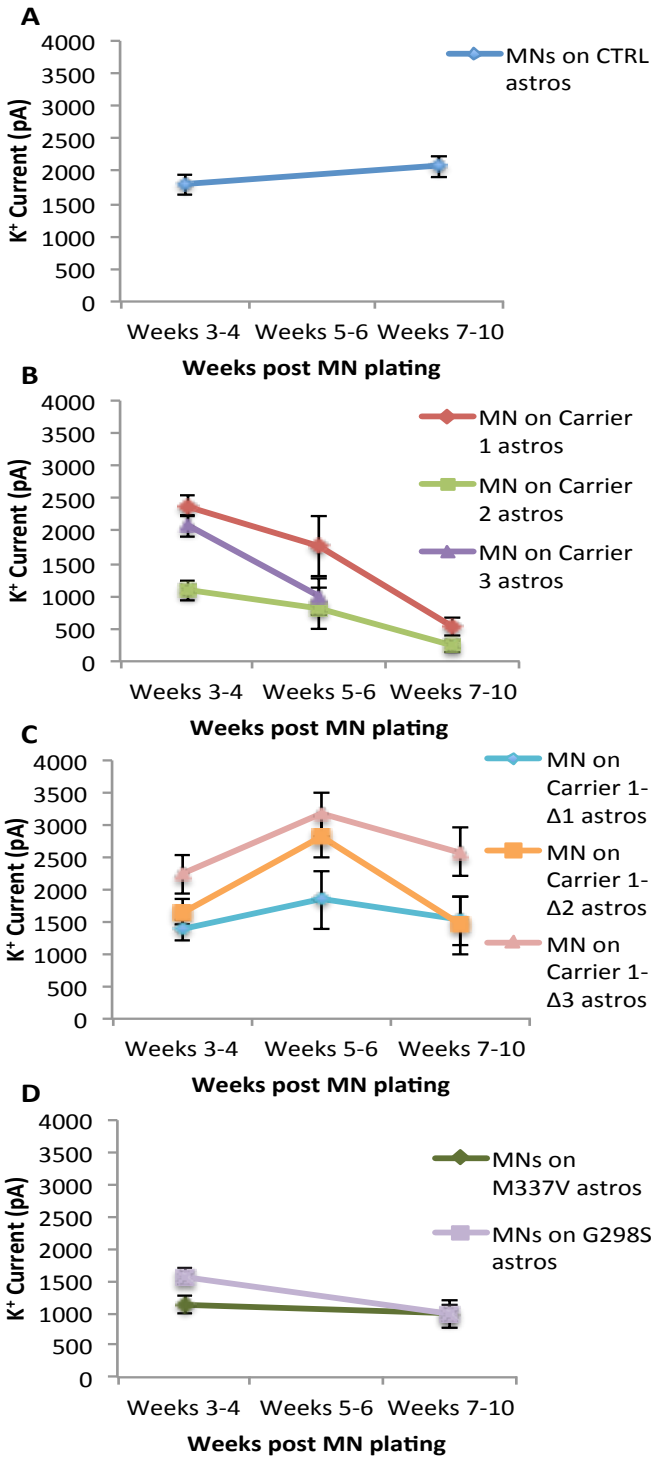


**Figure 3.9: Persistent voltage-activated $K^+$ currents in control iPSC-derived MNs co-cultured with control, ALS patient and gene edited iPSC-derived astrocytes.**

Figure caption on following page

**Figure 3.9: Persistent voltage-activated $K^+$ currents in control iPSC-derived MNs co-cultured with control, ALS patient and gene edited iPSC-derived astrocytes**

Peak persistent $K^+$ currents plotted from weeks 3–10 for MNs co-cultured with (A) CTRL (n=93), (B) *C9ORF72* (Carrier1, n=106; Carrier 2, n=79; Carrier 3, n=82), (C) gene-edited (Carrier-1Δ1, n=50; Carrier-1Δ2, n=75; Carrier-1Δ3, n=31), (D) *TARDBP* M337V (n= 118) or *TARDBP* G298S (n=62) iPSC-derived astrocytes (data are plotted as $\overline{x} \pm$ s.e.m.).

# 4. Discussion

Although the pathophysiology of ALS involves the selective dysfunction and ultimate death of MNs, processes within neighbouring non-neuronal cells significantly contribute to the development of MN-specific degeneration. To study in more detail how non-neuronal cells adversely affect MNs, whole-cell patch-clamp recordings were obtained from control iPSC-derived MNs co-cultured with control, *C9ORF72*, gene edited or *TARDBP* (M337V and G298S) iPSC-derived astrocytes. These results demonstrated that control iPSC-derived MNs develop appropriate physiological properties when co-cultured with control, ALS patient and C9 gene edited iPSC-derived astrocytes at weeks 3-4. However, temporal analysis revealed that *C9ORF72* and *TARDBP* G298S patient iPSC-derived astrocytes cause control iPSC-derived MNs to undergo a progressive loss of action potential output resulting from a progressive decrease in voltage-activated $Na^+$ and $K^+$ currents that occurs in the absence of changes in synaptic activity or overt changes in MN viability. It is also revealed that control iPSC-derived MNs co-cultured with gene edited astrocytes retain their functional properties providing further evidence that the presence of the $G_4C_2$ repeat expansion is deleterious to cells in which it is present as well as neighbouring cells. These novel data come from the first reported study in which human iPSC-derived MNs have been co-cultured with human iPSC-derived astrocytes harbouring the *C9ORF72* mutation and the first demonstrating non-cell autonomous disease mechanisms through the use of electrophysiological recordings in a humanised *in vitro* model. It has also been demonstrated that by removing the $G_4C_2$ repeat expansion from astrocytes, control MNs remain functional. These data strongly suggest that *C9ORF72* and *TARDBP* G298S mutations act via non-cell autonomous

disease mechanisms in ALS and that mechanistic variations exist between *TARDBP* mutations.

It has previously been shown, utilising both current- and voltage-clamp recordings, that the current protocol for MN generation from iPSCs yields MNs that develop appropriate output due to the expression of voltage-activated currents and receive synaptic input, (Bilican et al., 2012; Devlin et al., 2015). Comparable rates of morphological and physiological maturation were observed in control and patient iPSC-derived MNs, followed by a loss of functional output in iPSC-derived MNs from patients harbouring *TARDBP* and *C9ORF72* mutations. These findings were initially associated with cell autonomous disease mechanisms as 80% of the cultures were neurons, 50% of which were MNs (Devlin et al., 2015). However, the present study implicates astrocytes as mediators of MN dysfunction. Many studies report that ALS involves, at least in part, non-cell- autonomous disease mechanisms and that astrocytes participate these processes which lead to the death of MNs (Rothstein et al., 1995; Bruijn et al., 1997; Di Giorgio et al., 2007; Nagai et al., 2007; Cassina et al., 2008). Astrocytes, broadly subclassified as protoplasmic or fibrous, are diverse and have many heterogeneous functions. The proposed mechanisms through which astrocytes have been shown to cause MN death so far are by triggering nitroxidative stress, necroptosis and MN hyperexcitability (Fritz et al., 2013; Re et al., 2014; Rojas et al., 2014). A population of astrocytes have been isolated in the grey matter of the spinal cord in mutant *SOD1* rats and have been termed “aberrant astrocytes”. These astrocytes are highly proliferative, do not express detectable levels of GLT-1 and appear to drive MN death in a cell-type specific manner (Diaz-Amarilla et al., 2011). Therefore by studying astrocytes from regions in which vulnerable MNs in ALS are located, specific secretion factors may be identified which cause or influence MN

degeneration, aiding in the search for treatment targets for ALS patients. It has also been shown that the enrichment of the protein complex of α2-Na/K ATPase and α-adducin in mutant *SOD1* mice astrocytes cause MN degeneration as, after knockdown of the protein complex in mutant *SOD1* astrocytes or treatment with digoxin, MNs were spared and the lifespan of mutant SOD1 mice was increased (Gallardo et al., 2014). Direct astrocytic contact does not appear to be required to cause MN death as studies in which medium was collected from primary astrocytes harbouring ALS mutations *in vitro*, caused wild-type MNs to degenerate (Nagai et al., 2007; Rojas et al., 2014). Astrocyte conditioned medium (ACM) taken from primary cultures of mutant *SOD1* astrocytes also cause wild-type MNs to undergo electrophysiological changes, namely hyperexcitability (Fritz et al., 2013). Therefore it is possible that previous evidence of hyperexcitability demonstrated in mutant *SOD1* mouse models (Pieri et al., 2003; Kuo et al., 2004; van Zundert et al., 2008; Quinlan et al., 2011) and iPSC-derived MNs harbouring *SOD1*, *C9ORF72* or *TARDBP* mutations (Wainger et al., 2014; Devlin et al., 2015) could result from influences of mutation harbouring astrocytes.

There is ample evidence that astrocytes expressing mutant *SOD1* contribute to the pathogenesis of ALS, with studies indicating that such astrocytes release neurotoxic factors that kill healthy control MNs in culture (Nagai et al., 2007; Cassina et al., 2008; Marchetto et al., 2008; Fritz et al., 2013; Re et al., 2014). Understanding whether the *TARDBP* or *C9ORF72* mutation carrying astrocytes have a comparable neurotoxic effect is therefore of great interest. Previously reported studies on non- cell autonomous disease mechanisms associated with *TARDBP* mutations are conflicting whilst there is only one reported study of the potential non-cell autonomous effect of astrocytes harbouring the *C9ORF72* mutation. Human iPSC-derived astrocytes from a

patient harbouring an M337V *TARDBP* mutation were found to display the characteristic TDP-43 pathologies, a pathological hallmark in non *SOD1* ALS cases, and were more vulnerable to cell death under basal culture conditions. Although the astrocytes themselves were more vulnerable, they did not affect the survival of control iPSC-derived MNs (Serio et al., 2013). In the present study, although the *TARDBP* M337V astrocytes caused control MNs to have smaller $Na^+$ and $K^+$ currents throughout the period they were studied, MNs only showed a transient deficit in firing output and a weeks 3-4 but were functional at weeks 7-10, having the same ability to produce functional output as control MNs on control and gene edited astrocytes. Similarly, astrocytes derived from mice lacking TDP-43 or overexpressing mutant *TARDBP* failed to cause the death of control MNs in co-culture or when implanted into wild-type rat spinal cords (Haidet-Phillips et al., 2013). In opposition to these findings it has been demonstrated that wild-type MNs undergo degeneration in transgenic rats in which the expression of the *TARDBP* M337V mutation is restricted to astrocytes (Tong et al., 2013) and that control MNs degenerate as a result of nitroxidative stress after exposure to astrocyte- conditioned medium (ACM) from primary astrocyte cultures of mutant TDP-43 mice, (Rojas et al., 2014). In the present study, astrocytes harbouring the *TARDBP* G298S mutation caused control MNs to lose their ability to produce functional output and led to a decrease in their peak $Na^+$ and $K^+$ currents throughout the time period that they were studied. Within this study alone, it is therefore evident that variations occur in the potential non-cell autonomous involvement of mutations within and between various genes associated with ALS. A key question in understanding how *TARDBP* mutations cause cellular toxicity in ALS is how the various mutations alter the normal function of TDP-43. One study, using stable isogenic cell lines expressing a single copy of either wild type TDP-43,

*TARDBP* G298S, *TARDBP* Q331K or *TARDBP* M337V, showed that all three *TARDBP* mutations exhibit longer protein half-lives compared with wild-type TDP-32, suggesting that abnormal stability may be a common feature for *TARDBP* mutations in ALS. However, it was also shown that the *TARDBP* G298S mutation generates higher TDP-43 stability suggesting that an intrinsically increased half-life may contribute to the underlying mechanism for the accumulation of TDP-43 aggregations found in ALS patients (Ling et al., 2010). This study alone supports the idea that inherent variability exists between *TARDBP* mutations therefore TDP-43 protein stability should be taken into account in these studies in order to directly compare the apparent conflicting results, which may be due to abnormal TDP-43 stability.

Potential non-cell-autonomous disease mechanisms in SALS have been explored using SALS patient post-mortem astrocytes which, when co-cultured with control MNs, cause MN degeneration (Haidet-Phillips et al., 2011). Induced astrocytes (i-astrocytes) have also been generated from SALS patients and patients with *C9ORF72* mutations and co-cultured with mouse embryonic stem cell (ESC) derived MNs. The i-astrocytes are generated directly from patient fibroblasts, bypassing the formation of iPSCs (Meyer et al., 2013; Caiazzo et al., 2015). The i-astrocytes from *C9ORF72* ALS patients, SALS patients and *SOD1* ALS patients caused the mESC-derived MNs to degenerate. In the present study, using both human iPSC-derived MNs and astrocytes harbouring the *C9ORF72* mutation cause control iPSC-derived MNs to become dysfunctional, without altering their viability. The phenotype caused by one of the *C9ORF72* astrocyte lines (Carrier 3) was so severe at weeks 7-10 that no recordings obtained from MNs co-cultured with these astrocytes were included in the results as their electrophysiological properties did not fit required criteria (had

currents < 50pA and had a membrane potential more depolarised than -20mV).

Previous studies of ALS patients (Kanai et al., 2006; Vucic et al., 2008), human iPSCs (Sareen et al., 2013; Wainger et al., 2014; Devlin et al., 2015) and animal models of the disease (Pieri et al., 2003; Kuo et al., 2005; Zona et al., 2006; Bories et al., 2007; van Zundert et al., 2008; Fritz et al., 2013; Fuchs et al., 2013; Delestrée et al., 2014) have reported excitability alterations in spinal cord MNs and in corticospinal neurons of the motor cortex. These alterations in excitability include hyperexcitability (Pieri et al., 2003; Vucic and Kiernan, 2007; Quinlan et al., 2011; Kanai et al., 2012; Wainger et al., 2014; Devlin et al., 2015) and hypoexcitability/ loss of function (Fuchs et al., 2013; Sareen et al., 2013; Delestrée et al., 2014; Devlin et al., 2015). Whilst it has been suggested that preventing hyperexcitability in MNs increases MN survival (Fritz et al., 2013; Wainger et al., 2014) hyperexcitability was transient in the previous study (Devlin et al., 2015) and did not persist into symptomatic stages in animal models of ALS (Fuchs et al., 2013; Delestrée et al., 2014). However, it has recently been shown that MNs degenerate even in the absence of hyperexcitability and those that are hyperexcitable are typically spared in the disease (Leroy et al., 2014). Recent work supports this link between hyperexcitability and neuroprotection (Saxena et al., 2013), particularly when hyperexcitability is induced via activation of cholinergic C-bouton inputs to MNs (Miles et al., 2007; Zagoraiou et al., 2009) which are known to be enlarged presymptomatically in ALS model mice (Pullen and Athanasiou, 2009; Herron and Miles, 2012). In the present study, there was no evidence of hyperexcitability in control MNs during the early stages of co-culture with patient iPSC-derived astrocytes, however they still went on to become dysfunctional and lose the ability to produce functional output. Therefore, it is likely that the hyperexcitability seen at presymptomatic stages in ALS mouse

models and iPSC-derived MNs, and at symptom onset in ALS patients, is not the underlying cause of MN degeneration in ALS. It also shows that hyperexcitability is not required to cause the loss of functional output as previously described but rather a consequence of disrupted processes underlying ALS, with hyperexcitability acting as a compensatory mechanism.

In summary, the present study has provided important new insight into early ALS disease mechanisms by investigating pathophysiological changes in control iPSC-derived MNs when co-cultured with astrocytes from patients harbouring *TARDBP* or *C9ORF72* ALS mutations. It has been shown that MN output is severely compromised, due to the loss of voltage-activated currents, prior to any other overt signs of neurodegeneration when co-cultured with *C9ORF72* and *TARDBP* G298S astrocytes. These data suggest that non-cell autonomous disease mechanisms are a major contributor to the onset and progression of ALS, causing MNs to undergo a functional loss, rendering the motor system dysfunctional prior to neurodegeneration. Furthermore, these findings demonstrate the usefulness of sensitive physiological studies of human iPSC-derived astrocyte and MN co-cultures, where mutations are expressed at disease relevant levels, facilitating future work aiming to develop much needed therapeutics for this devastating disease.

# Chapter 4

# General discussion and conclusion

# 1 Summary

Neurodegenerative diseases, such as Parkinson's disease, Alzheimer's disease, multiple sclerosis and ALS, are characterized by an initial and progressive loss or dysfunction of a specific subset of neurons. These diseases are devastating, debilitating and largely incurable, affecting millions of people each year. Although ALS is largely a sporadic disorder, the clinical manifestations of familial and sporadic ALS are very similar; therefore determining the mechanisms underlying the progression of FALS may also provide insights into SALS. To date, studies into the the rare ALS- causing genetic mutations, discussed in the introduction, have led to several breakthroughs in our understanding of the neurobiology of this fatal paralytic disorder. These include, but are not limited to, the identification of pathogenic disease mechanisms such as mitochondrial dysfunction, oxidative stress, excitotoxicity, protein aggregate formation and non-cell autonomous processes. As alterations in electrophysiological properties have been revealed as the earliest changes to occur in mutant SOD1 mouse models of ALS (Pieri et al., 2003; Kuo et al., 2004; van Zundert et al., 2008; Quinlan et al., 2011), in this project, whole-cell patch-clamp recordings were obtained from ALS patient iPSC-derived MNs and compared to those derived from healthy controls iPSC-derived MNs. Given the evidence for the involvement of non-cell autonomous disease mechanisms in ALS (Boillée et al., 2006; Di Giorgio et al., 2007; Nagai et al., 2007; Ilieva et al., 2009), recordings were also obtained from control iPSC-derived MNs co-cultured with ALS patient iPSC-derived astrocytes. The findings from these studies are discussed below, along with future research directions.

For the first part of the study, described in Chapter 2, it is demonstrated that MNs derived from human iPSCs obtained from healthy individuals or patients harbouring

*TARDBP* or *C9ORF72* ALS mutations can develop appropriate physiological properties. However, despite the absence of overt changes in cell viability, patient iPSC-derived MNs display electrophysiological changes: an initial period of hyperexcitability, followed by a progressive loss of function. The loss of functional output appears to result from the progressive decrease in voltage-activated $Na^+$ and $K^+$ currents, likely due to a loss or dysfunction of ion channels. Further studies using RNA sequencing or immunocytochemistry would provide information on the levels of channel expression in these MN cultures, whilst pharmacologically isolating channels in voltage-clamp to reveal the functional properties of the channels would determine if the channels were dysfunctional.

The potential usefulness of human iPSC-derived neurons as a model for therapeutic drug screening, in combination with electrophysiological analysis, has also been demonstrated when iPSC-derived MNs harbouring *C9ORF72* mutations displayed improvement in their functional output after treatment with amiloride, which targets ion channels. Previous studies on mutant *SOD1* animal models have shown that hyperexcitability is often accompanied by increases in persistent $Na^+$ currents ($I_{NaP}$) (Kuo et al., 2005; Pieri et al., 2009; Quinlan et al., 2011). By modifying culture conditions using $Na^+$ channel blockers (Fritz et al., 2013) or $K^+$ channel activators (Wainger et al., 2014), hyperexcitability present pre-treatment was alleviated and MN death prevented. It remains unknown if the hyperexcitability phenotype seen in the present study or in previous work is required to initiate the degenerative pathways involved in ALS or if it is simply a consequence of the degenerative process and presents to act as a compensatory mechanism. Future studies in which the excitability of control iPSC-derived MNs is altered using pharmacological agents including $K^+$ channel blockers 4-aminopyridine (4-AP) or 3,4-diaminopyridine (3,4-DAP) may

uncover if MN degeneration occurs as a result of hyperexcitability.

The recent development of a new genetic techniques based on a bacterial Clustered Regularly Interspaced Short Palindromic Repeats (CRISPR)-associated protein-9 nuclease (Cas9) from *Streptococcus pyogenes* has provided an efficient and reliable way to make precise changes to the genome of living cells (Cong et al., 2013). Using this technique, iPSCs derived from patients with a *C9ORF72* mutation were genetically edited, removing the disease causing $G_4C_2$ hexanucleotide repeat expansion. The removal of the repeat expansion from Carrier-1, thus generating a gene edited, isogenic line, led to MNs retaining their functional output capability, behaving in a similar manner as MNs derived from healthy individuals. This further illustrates that the $G_4C_2$ hexanucleotide repeat expansion is responsible for the dysfunctional phenotype revealed in this project in the *C9ORF72* lines. It also provides hope for its potential use in gene therapies, providing remedies for genetic disorders. Among the unresolved technical challenges is figuring out the best way to deliver the treatment, based on this technology, to the target cells. Studies suggest that adeno-associated viruses or lipid nanoparticles are the most promising delivery methods so far (Cai and Yang, 2014; Feng et al., 2015).

In Chapter 3, the influence of astrocytes harbouring ALS mutations on healthy control MNs is investigated by performing whole-cell patch-clamp recordings of control human iPSC-derived MNs co-cultured with iPSC-derived astrocytes from healthy controls, ALS patients harbouring *TARDBP* and *C9ORF72* mutations and a gene edited C9 iPSC line. These analyses revealed a progressive loss of function of control MNs co-cultured with *C9ORF72* and *TARDBP* G298S iPSC-derived astrocytes, in parallel with decreases in $Na^+$ and $K^+$ currents, in the absence of overt changes in MN

viability. MNs co-cultured with the gene edited iPSC-derived astrocytes maintained their ability to produce functional output, providing further evidence that the presence of the $G_4C_2$ repeat expansion is deleterious to cells in which it is present as well as neighbouring cells.

From the data in Chapter 2, cell-autonomous disease mechanisms were associated with the loss or dysfunction of ion channels leading to the loss of functional output capabilities. However, the data in Chapter 3 strongly implicate non-cell autonomous disease mechanisms due to the severity of dysfunction demonstrated in control iPSC-derived MNs when co-cultured with ALS patient iPSC-derived astrocytes. This severe phenotype was not seen when MNs were cultured with the C9 gene edited iPSC-derived astrocytes. The MN enriched culture in Chapter 2 consisted of a population of 80% neurons, 50% of which were MNs, and 20% astrocytes. Therefore, it is likely that the astrocytes in the MN enriched culture contributed to the dysfunction seen in the mutation harbouring MNs, which were already vulnerable as they themselves contained the ALS mutation. Recently, a new protocol for MN generation from iPSCs was developed (Maury et al., 2015) which can consistently produce cultures of 95-98% neurons, 60% of which are MNs, with 2-5% glial cells. Therefore, using this new protocol to generate a purer neuronal culture, a clearer understanding of the mechanisms behind MN dysfunction could be found.

In chapter 2, hyperexcitability was demonstrated in patient iPSC-derived MNs and was followed by a progressive loss of function. However, as this was not seen in the data from chapter 3 in the control iPSC-derived MNs co-cultured with patient iPSC-derived astrocytes, it is unlikely that hyperexcitability is the cause of the later dysfunction uncovered in these studies. Future studies manipulating the excitability of

control MNs will help determine its true role.

iPSC-derived MNs and astrocytes harbouring *TARDBP* or *C9ORF72* mutations were used in this project. *TARDBP* encodes the RNA-binding protein TDP-43 which contributes to RNA stability and transport (Alami et al., 2014), mutations which are associated with deficits in RNA processing (Xu et al., 2011; Lagier-Tourenne et al., 2012). Although the exact function of *C9ORF72* remains unknown, its mutant form is associated with aberrant RNA processing and defects in membrane trafficking (DeJesus-Hernandez et al., 2011; Renton et al., 2011). Therefore, defects in RNA processing may contribute to loss of function in iPSC-derived MNs by affecting the protein synthesis and transport of ion channels, resulting in the loss of voltage activated currents seen in the patient iPSC-derived MNs and in the control iPSC-derived MNs after co-culturing with patient iPSC-derived astrocytes harbouring *C9ORF72* or *TARDBP G298S* mutations. As perturbations in ion channels and MN output have been demonstrated in other forms of ALS, including studies implicating cell autonomous and non-cell autonomous disease mechanisms, these may represent core disease mechanisms common to familial and sporadic ALS.

In conclusion, early diagnosis of ALS is difficult and is often delayed by the subtle onset of manifestations that mimic other conditions. The generally rapid progression of the disease makes conducting thorough clinical trials difficult, with patients dying before determining whether a treatment has any potential benefit or not. The development of human iPSC technology has provided an excellent model for the study of patient relevant cells, expressing mutations at disease relevant levels. In combination with the benefits they possess for relatively simple manipulation in culture and the ability to culture specific cells together and determine the interactions,

they can be used as a model for drug discovery, enabling high-throughput studies of many cell types and cell lines, especially in the current gene therapy drug discovery studies. As an increasing body of evidence suggests that non-cell autonomous processes play critical roles during the initiation and progression of ALS pathology, these findings describing early cell autonomous and early non-cell autonomous pathogenic mechanisms in a human iPSC-based model, provide a deeper understanding of the neurobiology of ALS and could aid the development of effective therapeutic approaches for preventing or reversing the progression of ALS.

Ackerley S, Grierson AJ, Brownlees J, Thornhill P, Anderton BH, Nigel Leigh P, Shaw CE, Miller CCJ (2000) Glutamate slows axonal transport of neurofilaments in transfected neurons. J Cell Biol 150:165–175.

Aggad D, Veriepe J, Tauffenberger a., Parker J a. (2014) TDP-43 Toxicity Proceeds via Calcium Dysregulation and Necrosis in Aging Caenorhabditis elegans Motor Neurons. J Neurosci 34:12093–12103.

Al-Chalabi A, Jones A, Troakes C, King A, Al-Sarraj S, den Berg LH (2012) The genetics and neuropathology of amyotrophic lateral sclerosis. Acta Neuropathol 124:339–352.

Alami NH, Smith RB, Carrasco M a, Williams L a, Winborn CS, Han SSW, Kiskinis E, Winborn B, Freibaum BD, Kanagaraj A, Clare AJ, Badders NM, Bilican B, Chaum E, Chandran S, Shaw CE, Eggan KC, Maniatis T, Taylor JP (2014) Axonal Transport of TDP-43 mRNA Granules Is Impaired by ALS-Causing Mutations. Neuron 81:536–543.

Alexander GM, Deitch JS, Seeburger JL, Del Valle L, Heiman-Patterson TD (2000) Elevated cortical extracellular fluid glutamate in transgenic mice expressing human mutant (G93A) Cu/Zn superoxide dismutase. J Neurochem 74:1666–1673.

Alexianu ME, Ho BK, Mohamed AH, La Bella V, Smith RG, Appel SH (1994) The role of calcium-binding proteins in selective motoneuron vulnerability in amyotrophic lateral sclerosis. Ann Neurol 36:846–858.

Almeida S, Gascon E, Tran H, Chou HJ, Gendron TF, Degroot S, Tapper AR, Sellier C, Charlet-Berguerand N, Karydas A, Seeley WW, Boxer AL, Petrucelli L, Miller BL, Gao F-B (2013) Modeling key pathological features of frontotemporal dementia with C9ORF72 repeat expansion in iPSC-derived human neurons. Acta Neuropathol 126:385–399.

Amoroso MW, Croft GF, Williams DJ, O'Keeffe S, Carrasco MA, Davis AR, Roybon L, Oakley DH, Maniatis T, Henderson CE, Wichterle H (2013) Accelerated high-yield generation of limb-innervating motor neurons from human stem cells. J Neurosci 33:574–586.

Arai T, Hasegawa M, Akiyama H, Ikeda K, Nonaka T, Mori H, Mann D, Tsuchiya K, Yoshida M, Hashizume Y, Oda T (2006) TDP-43 is a component of ubiquitin-positive tau-negative inclusions in frontotemporal lobar degeneration and amyotrophic lateral sclerosis. Biochem Biophys Res Commun 351:602–611.

Armstrong G a B, Drapeau P (2013) Calcium channel agonists protect against neuromuscular dysfunction in a genetic model of TDP-43 mutation in ALS. J Neurosci 33:1741–1752.

Arnold ES, Ling S-C, Huelga SC, Lagier-Tourenne C, Polymenidou M, Ditsworth D, Kordasiewicz HB, McAlonis-Downes M, Platoshyn O, Parone PA, Da Cruz S, Clutario KM, Swing D, Tessarollo L, Marsala M, Shaw CE, Yeo GW, Cleveland DW (2013) ALS-linked TDP-43 mutations produce aberrant RNA splicing and adult-onset motor neuron disease without aggregation or loss of nuclear TDP-43. Proc Natl Acad Sci U S A 110:E736–E745.

Ash PEA, Bieniek KF, Gendron TF, Caulfield T, Lin W-L, DeJesus-Hernandez M, van Blitterswijk MM, Jansen-West K, Paul III JW, Rademakers R, Boylan KB, Dickson DW, Petrucelli L (2013) Unconventional Translation of C9ORF72

GGGGCC Expansion Generates Insoluble Polypeptides Specific to c9FTD/ALS. Neuron 77:639–646.

Ash PEA, Zhang YJ, Roberts CM, Saldi T, Hutter H, Buratti E, Petrucelli L, Link CD (2010) Neurotoxic effects of TDP-43 overexpression in C. elegans. Hum Mol Genet 19:3206–3218.

Atkin JD, Farg M a, Turner BJ, Tomas D, Lysaght J a, Nunan J, Rembach A, Nagley P, Beart PM, Cheema SS, Horne MK (2006) Induction of the unfolded protein response in familial amyotrophic lateral sclerosis and association of protein-disulfide isomerase with superoxide dismutase 1. J Biol Chem 281:30152–30165.

Atkin JD, Farg M a, Walker AK, McLean C, Tomas D, Horne MK (2008) Endoplasmic reticulum stress and induction of the unfolded protein response in human sporadic amyotrophic lateral sclerosis. Neurobiol Dis 30:400–407.

Avossa D, Grandolfo M, Mazzarol F, Zatta M, Ballerini L (2006) Early signs of motoneuron vulnerability in a disease model system: Characterization of transverse slice cultures of spinal cord isolated from embryonic ALS mice. Neuroscience 138:1179–1194.

Ayala V, Granado-Serrano AB, Cacabelos D, Naudí A, Ilieva E V., Boada J, Caraballo-Miralles V, Lladó J, Ferrer I, Pamplona R, Portero-Otin M (2011) Cell stress induces TDP-43 pathological changes associated with ERK1/2 dysfunction: Implications in ALS. Acta Neuropathol 122:259–270.

Barber SC, Mead RJ, Shaw PJ (2006) Oxidative stress in ALS: A mechanism of neurodegeneration and a therapeutic target. Biochim Biophys Acta - Mol Basis Dis 1762:1051–1067.

Barber SC, Shaw PJ (2010) Oxidative stress in ALS: key role in motor neuron injury and therapeutic target. Free Radic Biol Med 48:629–641.

Barmada SJ, Serio A, Arjun A, Bilican B, Daub A, Ando DM, Tsvetkov A, Pleiss M, Li X, Peisach D, Shaw C, Chandran S, Finkbeiner S (2014) Autophagy induction enhances TDP43 turnover and survival in neuronal ALS models. Nat Chem Biol.

Beckman JS, Estévez a G, Crow JP, Barbeito L (2001) Superoxide dismutase and the death of motoneurons in ALS. Trends Neurosci 24:S15–S20.

Beers DR, Henkel JS, Xiao Q, Zhao W, Wang J, Yen A a, Siklos L, McKercher SR, Appel SH (2006) Wild-type microglia extend survival in PU.1 knockout mice with familial amyotrophic lateral sclerosis. Proc Natl Acad Sci U S A 103:16021–16026.

Bellingham MC (2011) A review of the neural mechanisms of action and clinical efficiency of riluzole in treating amyotrophic lateral sclerosis: what have we learned in the last decade? CNS Neurosci Ther 17:4–31.

Benatar M (2007) Lost in translation: Treatment trials in the SOD1 mouse and in human ALS. Neurobiol Dis 26:1–13.

Bendotti C, Calvaresi N, Chiveri L, Prelle A, Moggio M, Braga M, Silani V, De Biasi S (2001a) Early vacuolization and mitochondrial damage in motor neurons of FALS mice are not associated with apoptosis or with changes in cytochrome oxidase histochemical reactivity. J Neurol Sci 191:25–33.

Bendotti C, Tortarolo M, Suchak SK, Calvaresi N, Carvelli L, Bastone A, Rizzi M,

Rattray M, Mennini T (2001b) Transgenic SOD1 G93A mice develop reduced GLT-1 in spinal cord without alterations in cerebrospinal fluid glutamate levels. J Neurochem 79:737–746.

Benkler C, Ben-Zur T, Barhum Y, Offen D (2013) Altered astrocytic response to activation in SOD1G93A mice and its implications on amyotrophic lateral sclerosis pathogenesis. Glia 61:312–326.

Bensimon G, Lacomblez L, Meininger V (1994) A controlled trial of riluzole in amyotrophic lateral sclerosis. ALS/Riluzole Study Group. N Engl J Med 330:585–591.

Bento-Abreu A, Van Damme P, Van Den Bosch L, Robberecht W, Damme P Van, Bosch L Van Den, Robberecht W (2010) The neurobiology of amyotrophic lateral sclerosis. Eur J Neurosci 31:2247–2265.

Bergeron C (1995) Oxidative stress: its role in the pathogenesis of amyotrophic lateral sclerosis. J Neurol Sci 129 Suppl:81–84.

Bernard-Marissal N, Moumen A, Sunyach C, Pellegrino C, Dudley K, Henderson CE, Raoul C, Pettmann B (2012) Reduced calreticulin levels link endoplasmic reticulum stress and Fas-triggered cell death in motoneurons vulnerable to ALS. J Neurosci 32:4901–4912.

Bilican B, Serio A, Barmada SJ, Nishimura AL, Sullivan GJ, Carrasco M, Phatnani HP, Puddifoot CA, Story D, Fletcher J, Park I-H, Friedman BA, Daley GQ, Wyllie DJA, Hardingham GE, Wilmut I, Finkbeiner S, Maniatis T, Shaw CE, Chandran S (2012) Mutant induced pluripotent stem cell lines recapitulate aspects of TDP-43 proteinopathies and reveal cell-specific vulnerability. Proc Natl Acad Sci 109:5803–5808.

Bilsland LG, Nirmalananthan N, Yip J, Greensmith L, Duchen MR (2008) Expression of mutant SOD1 in astrocytes induces functional deficits in motoneuron mitochondria. J Neurochem 107:1271–1283.

Bilsland LG, Sahai E, Kelly G, Golding M, Greensmith L, Schiavo G (2010) Deficits in axonal transport precede ALS symptoms in vivo. Proc Natl Acad Sci U S A 107:20523–20528.

Blokhuis AM, Groen EJN, Koppers M, van den Berg LH, Pasterkamp RJ (2013) Protein aggregation in amyotrophic lateral sclerosis. Acta Neuropathol 125:777–794.

Boillée S, Vande Velde C, Cleveland DW (2006) ALS: A Disease of Motor Neurons and Their Nonneuronal Neighbors. Neuron 52:39–59.

Bories C, Amendola J, Lamotte d'Incamps B, Durand J (2007) Early electrophysiological abnormalities in lumbar motoneurons in a transgenic mouse model of amyotrophic lateral sclerosis. Eur J Neurosci 25:451–459.

Bosco DA, Morfini G, Karabacak NM, Song Y, Gros-Louis F, Pasinelli P, Goolsby H, Fontaine BA, Lemay N, McKenna-Yasek D, Frosch MP, Agar JN, Julien J-P, Brady ST, Brown RH (2010) Wild-type and mutant SOD1 share an aberrant conformation and a common pathogenic pathway in ALS. Nat Neurosci 13:1396–1403.

Bostock H, Sharief MK, Reid G, Murray NM (1995) Axonal ion channel dysfunction in amyotrophic lateral sclerosis. Brain 118 Pt 1:217–225.

Bowling AC, Schulz JB, Brown RH, Beal MF (1993) Superoxide dismutase activity, oxidative damage, and mitochondrial energy metabolism in familial and sporadic amyotrophic lateral sclerosis. J Neurochem 61:2322–2325.

Braun RJ, Sommer C, Carmona-Gutierrez D, Khoury CM, Ring J, Büttner S, Madeo F (2011) Neurotoxic 43-kDa TAR DNA-binding protein (TDP-43) triggers mitochondrion-dependent programmed cell death in yeast. J Biol Chem 286:19958–19972.

Brockington A, Ning K, Heath PR, Wood E, Kirby J, Fusi N, Lawrence N, Wharton SB, Ince PG, Shaw PJ (2013) Unravelling the enigma of selective vulnerability in neurodegeneration: Motor neurons resistant to degeneration in ALS show distinct gene expression characteristics and decreased susceptibility to excitotoxicity. Acta Neuropathol 125:95–109.

Bruijn LI, Becher MW, Lee MK, Anderson KL, Jenkins N a, Copeland NG, Sisodia SS, Rothstein JD, Borchelt DR, Price DL, Cleveland DW (1997) ALS-linked SOD1 mutant G85R mediates damage to astrocytes and promotes rapidly progressive disease with SOD1-containing inclusions. Neuron 18:327–338.

Bruijn LI, Miller TM, Cleveland DW (2004) Unraveling the mechanisms involved in motor neuron degeneration in ALS. Annu Rev Neurosci.

Brunet N, Tarabal O, Esquerda JE, Calderó J (2009) Excitotoxic motoneuron degeneration induced by glutamate receptor agonists and mitochondrial toxins in organotypic cultures of chick embryo spinal cord. J Comp Neurol 516:277–290.

Burkhardt MF, Martinez FJ, Wright S, Ramos C, Volfson D, Mason M, Garnes J, Dang V, Lievers J, Shoukat-Mumtaz U, Martinez R, Gai H, Blake R, Vaisberg E, Grskovic M, Johnson C, Irion S, Bright J, Cooper B, Nguyen L, Griswold-Prenner I, Javaherian A (2013) A cellular model for sporadic ALS using patient-derived induced pluripotent stem cells. Mol Cell Neurosci 56:355–364.

Butt SJB, Lebret JM, Kiehn O (2002) Organization of left-right coordination in the mammalian locomotor network. Brain Res Rev 40:107–117.

Byrne S, Elamin M, Bede P, Shatunov A, Walsh C, Corr B, Heverin M, Jordan N, Kenna K, Lynch C, McLaughlin RL, Iyer PM, O'Brien C, Phukan J, Wynne B, Bokde AL, Bradley DG, Pender N, Al-Chalabi A, Hardiman O (2012) Cognitive and clinical characteristics of patients with amyotrophic lateral sclerosis carrying a C9orf72 repeat expansion: a population-based cohort study. Lancet Neurol 11:232–240.

Cai M, Yang Y (2014) Targeted genome editing tools for disease modeling and gene therapy. Curr Gene Ther 14:2–9.

Caiazzo M, Giannelli S, Valente P, Lignani G, Carissimo A, Sessa A, Colasante G, Bartolomeo R, Massimino L, Ferroni S, Settembre C, Benfenati F, Broccoli V (2015) Direct Conversion of Fibroblasts into Functional Astrocytes by Defined Transcription Factors. Stem Cell Reports 4:25–36.

Carriedo SG, Sensi SL, Yin HZ, Weiss JH (2000) AMPA exposures induce mitochondrial Ca(2+) overload and ROS generation in spinal motor neurons in vitro. J Neurosci 20:240–250.

Cassina P, Cassina A, Pehar M, Castellanos R, Gandelman M, de León A, Robinson KM, Mason RP, Beckman JS, Barbeito L, Radi R (2008) Mitochondrial dysfunction in SOD1G93A-bearing astrocytes promotes motor neuron

degeneration: prevention by mitochondrial-targeted antioxidants. J Neurosci 28:4115–4122.

Cassina P, Pehar M, Vargas MR, Castellanos R, Barbeito AG, Estévez AG, Thompson J a, Beckman JS, Barbeito L (2005) Astrocyte activation by fibroblast growth factor-1 and motor neuron apoptosis: implications for amyotrophic lateral sclerosis. J Neurochem 93:38–46.

Catania M V, Aronica E, Yankaya B, Troost D (2001) Increased expression of neuronal nitric oxide synthase spliced variants in reactive astrocytes of amyotrophic lateral sclerosis human spinal cord. J Neurosci 21:RC148.

Cazalets JR, Borde M, Clarac F (1996) The synaptic drive from the spinal locomotor network to motoneurons in the newborn rat. J Neurosci 16:298–306.

Chang Q, Martin LJ (2009) Glycinergic innervation of motoneurons is deficient in amyotrophic lateral sclerosis mice: a quantitative confocal analysis. Am J Pathol 174:574–585.

Chen H, Qian K, Du Z, Cao J, Petersen A, Liu H, Blackbourn LW, Huang CL, Errigo A, Yin Y, Lu J, Ayala M, Zhang SC (2014) Modeling ALS with iPSCs reveals that mutant SOD1 misregulates neurofilament balance in motor neurons. Cell Stem Cell 14:796–809.

Chen K, Northington FJ, Martin LJ (2010) Inducible nitric oxide synthase is present in motor neuron mitochondria and Schwann cells and contributes to disease mechanisms in ALS mice. Brain Struct Funct 214:219–234.

Ciura S, Lattante S, Le Ber I, Latouche M, Tostivint H, Brice A, Kabashi E (2013) Loss of function of C9orf72 causes motor deficits in a zebrafish model of Amyotrophic Lateral Sclerosis. Ann Neurol:1–44.

Clement AM, Nguyen MD, Roberts EA, Garcia ML, Boillée S, Rule M, McMahon AP, Doucette W, Siwek D, Ferrante RJ, Brown RH, Julien J-P, Goldstein LSB, Cleveland DW (2003) Wild-type nonneuronal cells extend survival of SOD1 mutant motor neurons in ALS mice. Science 302:113–117.

Cleveland DW, Rothstein JD (2001) From Charcot to Lou Gehrig: deciphering selective motor neuron death in ALS. Nat Rev Neurosci 2:806–819.

Cluskey S, Ramsden DB (2001) Mechanisms of neurodegeneration in amyotrophic lateral sclerosis. Mol Pathol 54:386–392.

Collard JF, Côté F, Julien JP (1995) Defective axonal transport in a transgenic mouse model of amyotrophic lateral sclerosis. Nature 375:61–64.

Collingridge GL, Singer W (1990) Excitatory amino acid receptors and synaptic plasticity. Trends PharmacolSci 11:290–296.

Colombrita C, Zennaro E, Fallini C, Weber M, Sommacal A, Buratti E, Silani V, Ratti A (2009) TDP-43 is recruited to stress granules in conditions of oxidative insult. J Neurochem 111:1051–1061.

Comley L, Allodi I, Nichterwitz S, Nizzardo M, Simone C, Corti S, Hedlund E (2015) Motor neurons with differential vulnerability to degeneration show distinct protein signatures in health and ALS. Neuroscience 291:216–229.

Cong L, Ran FA, Cox D, Lin S, Barretto R, Habib N, Hsu PD, Wu X, Jiang W, Marraffini L a, Zhang F (2013) Multiplex genome engineering using CRISPR/Cas systems. Science 339:819–823.

Couratier P, Hugon J, Sindou P, Vallat JM, Dumas M (1993) Cell culture evidence for neuronal degeneration in amyotrophic lateral sclerosis being linked to glutamate AMPA/kainate receptors. Lancet 341:265–268.

Crill WE (1996) Persistent sodium current in mammalian central neurons. Annu Rev Physiol 58:349–362.

Cui Y, Masaki K, Yamasaki R, Imamura S, Suzuki SO, Hayashi S, Sato S, Nagara Y, Kawamura MF, Kira J (2014) Extensive dysregulations of oligodendrocytic and astrocytic connexins are associated with disease progression in an amyotrophic lateral sclerosis mouse model. J Neuroinflammation 11:42.

D'Amico E, Factor-Litvak P, Santella RM, Mitsumoto H (2013) Clinical perspective on oxidative stress in sporadic amyotrophic lateral sclerosis. Free Radic Biol Med 65:509–527.

Da Cruz S, Cleveland DW (2011) Understanding the role of TDP-43 and FUS/TLS in ALS and beyond. Curr Opin Neurobiol 21:904–919.

Davidson Y, Kelley T, Mackenzie IR a, Pickering-Brown S, Du Plessis D, Neary D, Snowden JS, Mann DM a (2007) Ubiquitinated pathological lesions in frontotemporal lobar degeneration contain the TAR DNA-binding protein, TDP-43. Acta Neuropathol 113:521–533.

Deitch JS, Alexander GM, Del Valle L, Heiman-Patterson TD (2002) GLT-1 glutamate transporter levels are unchanged in mice expressing G93A human mutant SOD1. J Neurol Sci 193:117–126.

DeJesus-Hernandez M, Mackenzie IR, Boeve BF, Boxer AL, Baker M, Rutherford NJ, Nicholson AM, Finch N a, Flynn H, Adamson J, Kouri N, Wojtas A, Sengdy P, Hsiung G-YR, Karydas A, Seeley WW, Josephs K a, Coppola G, Geschwind DH, Wszolek ZK, Feldman H, Knopman DS, Petersen RC, Miller BL, Dickson DW, Boylan KB, Graff-Radford NR, Rademakers R (2011) Expanded GGGGCC hexanucleotide repeat in noncoding region of C9ORF72 causes chromosome 9p-linked FTD and ALS. Neuron 72:245–256.

Delestrée N, Manuel M, Iglesias C, Elbasiouny SM, Heckman CJ, Zytnicki D (2014) Adult spinal motoneurones are not hyperexcitable in a mouse model of inherited amyotrophic lateral sclerosis. J Physiol 592:1687–1703.

Deng H, Shi Y, Furukawa Y, Zhai H, Fu R, Liu E, Gorrie GH, Khan MS, Hung W, Bigio EH, Lukas T, Dal Canto MC, O'Halloran T V, Siddique T (2006) Conversion to the amyotrophic lateral sclerosis phenotype is associated with intermolecular linked insoluble aggregates of SOD1 in mitochondria. Proc Natl Acad Sci U S A 103:7142–7147.

Deng H-X, Chen W, Hong S-T, Boycott KM, Gorrie GH, Siddique N, Yang Y, Fecto F, Shi Y, Zhai H, Jiang H, Hirano M, Rampersaud E, Jansen GH, Donkervoort S, Bigio EH, Brooks BR, Ajroud K, Sufit RL, Haines JL, Mugnaini E, Pericak-Vance M a, Siddique T (2011) Mutations in UBQLN2 cause dominant X-linked juvenile and adult-onset ALS and ALS/dementia. Nature 477:211–215.

Deng HX, Hentati A, Tainer JA, Iqbal Z, Cayabyab A, Hung WY, Getzoff ED, Hu P, Herzfeldt B, Roos RP (1993) Amyotrophic lateral sclerosis and structural defects in Cu,Zn superoxide dismutase. Science 261:1047–1051.

Devlin A, Burr K, Borooah S, Foster JD, Niven E, Shaw CE, Chandran S, Miles GB, Cleary EM, Geti I, Vallier L, Shaw CE, Chandran S, Miles GB, Niven E, Shaw

CE, Chandran S, Miles GB (2015) Human iPSC-derived motoneurons harbouring TARDBP or C9ORF72 ALS mutations are dysfunctional despite maintaining viability. Nat Commun 6:1–33.

Dewey CM, Cenik B, Sephton CF, Dries DR, Mayer P, Good SK, Johnson BA, Herz J, Yu G (2011) TDP-43 is directed to stress granules by sorbitol, a novel physiological osmotic and oxidative stressor. Mol Cell Biol 31:1098–1108.

Di Giorgio FP, Boulting GL, Bobrowicz S, Eggan KC (2008) Human embryonic stem cell-derived motor neurons are sensitive to the toxic effect of glial cells carrying an ALS-causing mutation. Cell Stem Cell 3:637–648.

Di Giorgio FP, Carrasco M a, Siao MC, Maniatis T, Eggan K (2007) Non-cell autonomous effect of glia on motor neurons in an embryonic stem cell-based ALS model. Nat Neurosci 10:608–614.

di Pellegrino G, Fadiga L, Fogassi L, Gallese V, Rizzolatti G (1992) Understanding motor events: a neurophysiological study. Exp Brain Res 91:176–180.

Diaper DC, Adachi Y, Sutcliffe B, Humphrey DM, Elliott CJH, Stepto A, Ludlow ZN, Vanden Broeck L, Callaerts P, Dermaut B, Al-Chalabi A, Shaw CE, Robinson IM, Hirth F (2013) Loss and gain of Drosophila TDP-43 impair synaptic efficacy and motor control leading to age-related neurodegeneration by loss-of-function phenotypes. Hum Mol Genet 22:1539–1557.

Diaz-Amarilla P, Olivera-Bravo S, Trias E, Cragnolini A, Martinez-Palma L, Cassina P, Beckman J, Barbeito L (2011) From the Cover: Phenotypically aberrant astrocytes that promote motoneuron damage in a model of inherited amyotrophic lateral sclerosis. Proc Natl Acad Sci 108:18126–18131.

Dimos JT, Rodolfa KT, Niakan KK, Weisenthal LM, Mitsumoto H, Chung W, Croft GF, Saphier G, Leibel R, Goland R, Wichterle H, Henderson CE, Eggan K (2008) Induced pluripotent stem cells generated from patients with ALS can be differentiated into motor neurons. Science 321:1218–1221.

Dong H, O'Brien RJ, Fung ET, Lanahan AA, Worley PF, Huganir RL (1997) GRIP: a synaptic PDZ domain-containing protein that interacts with AMPA receptors. Nature 386:279–284.

Dong H, Xu L, Wu L, Wang X, Duan W, Li H, Li C (2014) Curcumin abolishes mutant TDP-43 induced excitability in a motoneuron-like cellular model of ALS. Neuroscience 272:141–153.

Donnelly CJ, Zhang P-W, Pham JT, Heusler AR, Mistry NA, Vidensky S, Daley EL, Poth EM, Hoover B, Fines DM, Maragakis N, Tienari PJ, Petrucelli L, Traynor BJ, Wang J, Rigo F, Bennett CF, Blackshaw S, Sattler R, Rothstein JD (2013) RNA Toxicity from the ALS/FTD C9ORF72 Expansion Is Mitigated by Antisense Intervention. Neuron 80:415–428.

Dottori M, Hartley L, Galea M, Paxinos G, Polizzotto M, Kilpatrick T, Bartlett PF, Murphy M, Kontgen F, Boyd AW (1998) EphA4 (Sek1) receptor tyrosine kinase is required for the development of the corticospinal tract. Proc Natl Acad Sci U S A 95:13248–13253.

Drew T, Prentice S, Schepens B (2004) Cortical and brainstem control of locomotion. Prog Brain Res 143:251–261.

Duan W, Li X, Shi J, Guo Y, Li Z, Li C (2010) Mutant TAR DNA-binding protein-43

induces oxidative injury in motor neuron-like cell. Neuroscience 169:1621–1629.

Dupuis L, Gonzalez De Aguilar JL, Oudart H, De Tapia M, Barbeito L, Loeffler JP (2004) Mitochondria in amyotrophic lateral sclerosis: A trigger and a target. Neurodegener Dis 1:245–254.

Egawa N, Kitaoka S, Tsukita K, Naitoh M, Takahashi K, Yamamoto T, Adachi F, Kondo T, Okita K, Asaka I, Aoi T, Watanabe A, Yamada Y, Morizane A, Takahashi J, Ayaki T, Ito H, Yoshikawa K, Yamawaki S, Suzuki S, Watanabe D, Hioki H, Kaneko T, Makioka K, Okamoto K, Takuma H, Tamaoka A, Hasegawa K, Nonaka T, Hasegawa M, Kawata A, Yoshida M, Nakahata T, Takahashi R, Marchetto MCN, Gage FH, Yamanaka S, Inoue H (2012) Drug Screening for ALS Using Patient-Specific Induced Pluripotent Stem Cells. Sci Transl Med 4:145ra104–ra145ra104.

Ellis D, Rabe J, Sweadner K (2003) Global Loss of Na,K-ATPase and Its Nitric Oxide-Mediated Regulation in a Transgenic Mouse Model of Amyotrophic Lateral Sclerosis. J Neurosci 23:43–51.

Estes PS, Daniel SG, McCallum AP, Boehringer A V, Sukhina AS, Zwick R a, Zarnescu DC (2013) Motor neurons and glia exhibit specific individualized responses to TDP-43 expression in a Drosophila model of amyotrophic lateral sclerosis. Dis Model Mech 6:721–733.

Evans MJ, Kaufman MH (1981) Establishment in culture of pluripotential cells from mouse embryos. Nature 292:154–156.

Feiguin F, Godena VK, Romano G, D'Ambrogio A, Klima R, Baralle FE (2009) Depletion of TDP-43 affects Drosophila motoneurons terminal synapsis and locomotive behavior. FEBS Lett 583:1586–1592.

Feldmeyer D, Kask K, Brusa R, Kornau HC, Kolhekar R, Rozov A, Burnashev N, Jensen V, Hvalby O, Sprengel R, Seeburg PH (1999) Neurological dysfunctions in mice expressing different levels of the Q/R site-unedited AMPAR subunit GluR-B. Nat Neurosci 2:57–64.

Feng W, Dai Y, Mou L, Cooper D, Shi D, Cai Z (2015) The Potential of the Combination of CRISPR/Cas9 and Pluripotent Stem Cells to Provide Human Organs from Chimaeric Pigs. Int J Mol Sci 16:6545–6556.

Fernandes S a., Douglas AGL, Varela M a., Wood MJ a, Aoki Y (2013) Oligonucleotide-based therapy for FTD/ALS caused by the C9orf72 repeat expansion: A perspective. J Nucleic Acids 2013.

Ferraiuolo L, Kirby J, Grierson AJ, Sendtner M, Shaw PJ (2011) Molecular pathways of motor neuron injury in amyotrophic lateral sclerosis. Nat Rev Neurol 7:616–630.

Ferri A, Nencini M, Casciati A, Cozzolino M, Angelini DF, Longone P, Spalloni A, Rotilio G, Carrì MT (2004) Cell death in amyotrophic lateral sclerosis: interplay between neuronal and glial cells. FASEB J 18:1261–1263.

Finelli MJ, Liu KX, Wu Y, Oliver PL, Davies KE (2015) Oxr1 improves pathogenic cellular features of ALS-associated FUS and TDP-43 mutations. Hum Mol Genet:1–16.

Foran E, Trotti D (2009) Glutamate transporters and the excitotoxic path to motor neuron degeneration in amyotrophic lateral sclerosis. Antioxid Redox Signal

11:1587–1602.

Frakes AE, Ferraiuolo L, Haidet-Phillips AM, Schmelzer L, Braun L, Miranda CJ, Ladner KJ, Bevan AK, Foust KD, Godbout JP, Popovich PG, Guttridge DC, Kaspar BK (2014) Microglia induce motor neuron death via the classical NF-κB pathway in amyotrophic lateral sclerosis. Neuron 81:1009–1023.

Fray AE, Ince PG, Banner SJ, Milton ID, Usher PA, Cookson MR, Shaw PJ (1998) The expression of the glial glutamate transporter protein EAAT2 in motor neuron disease: an immunohistochemical study. Eur J Neurosci 10:2481–2489.

Frey D, Schneider C, Xu L, Borg J, Spooren W, Caroni P (2000) Early and selective loss of neuromuscular synapse subtypes with low sprouting competence in motoneuron diseases. J Neurosci 20:2534–2542.

Friese M a, Craner MJ, Etzensperger R, Vergo S, Wemmie J a, Welsh MJ, Vincent A, Fugger L (2007) Acid-sensing ion channel-1 contributes to axonal degeneration in autoimmune inflammation of the central nervous system. Nat Med 13:1483–1489.

Fritz E, Izaurieta P, Weiss A, Mir FR, Rojas P, Gonzalez D, Rojas F, Brown RH, Madrid R, van Zundert B (2013) Mutant SOD1-expressing astrocytes release toxic factors that trigger motoneuron death by inducing hyperexcitability. J Neurophysiol 109:2803–2814.

Fuchs A, Kutterer S, Mühling T, Duda J, Schütz B, Liss B, Keller BU, Roeper J (2013) Selective mitochondrial Ca2+ uptake deficit in disease endstage vulnerable motoneurons of the SOD1G93A mouse model of amyotrophic lateral sclerosis. J Physiol 591:2723–2745.

Gallardo G, Barowski J, Ravits J, Siddique T, Lingrel JB, Robertson J, Steen H, Bonni A (2014) An α2-Na/K ATPase/α-adducin complex in astrocytes triggers non–cell autonomous neurodegeneration. Nat Neurosci 17:1710–1719.

Gallart-Palau X, Tarabal O, Casanovas A, Sábado J, Correa FJ, Hereu M, Piedrafita L, Calderó J, Esquerda JE (2014) Neuregulin-1 is concentrated in the postsynaptic subsurface cistern of C-bouton inputs to α-motoneurons and altered during motoneuron diseases. FASEB J 28:3618–3632.

Geevasinga N, Menon P, Howells J, GA N, MC K, Vucic S (2015) AXonal ion channel dysfunction in c9orf72 familial amyotrophic lateral sclerosis. JAMA Neurol 72:49–57.

Gidalevitz T, Krupinski T, Garcia S, Morimoto RI (2009) Destabilizing protein polymorphisms in the genetic background direct phenotypic expression of mutant SOD1 toxicity. PLoS Genet 5.

Gijselinck I, Van Langenhove T, van der Zee J, Sleegers K, Philtjens S, Kleinberger G, Janssens J, Bettens K, Van Cauwenberghe C, Pereson S, Engelborghs S, Sieben A, De Jonghe P, Vandenberghe R, Santens P, De Bleecker J, Maes G, Bäumer V, Dillen L, Joris G, Cuijt I, Corsmit E, Elinck E, Van Dongen J, Vermeulen S, Van den Broeck M, Vaerenberg C, Mattheijssens M, Peeters K, Robberecht W, Cras P, Martin JJ, De Deyn PP, Cruts M, Van Broeckhoven C (2012) A C9orf72 promoter repeat expansion in a Flanders-Belgian cohort with disorders of the frontotemporal lobar degeneration-amyotrophic lateral sclerosis spectrum: A gene identification study. Lancet Neurol 11:54–65.

Giordana MT, Piccinini M, Grifoni S, De Marco G, Vercellino M, Magistrello M,

Pellerino A, Buccinnà B, Lupino E, Rinaudo MT (2010) TDP-43 redistribution is an early event in sporadic amyotrophic lateral sclerosis. Brain Pathol 20:351–360.

Goldshmit Y, Spanevello MD, Tajouri S, Li L, Rogers F, Pearse M, Galea M, Bartlett PF, Boyd AW, Turnley AM (2011) EphA4 blockers promote axonal regeneration and functional recovery following spinal cord injury in mice. PLoS One 6.

Gomez-Deza J, Lee Y, Troakes C, Nolan M, Al-Sarraj S, Gallo J-M, Shaw CE (2015) Dipeptide repeat protein inclusions are rare in the spinal cord and almost absent from motor neurons in C9ORF72 mutant amyotrophic lateral sclerosis and are unlikely to cause their degeneration. Acta Neuropathol Commun 3:38.

Greenway MJ, Andersen PM, Russ C, Ennis S, Cashman S, Donaghy C, Patterson V, Swingler R, Kieran D, Prehn J, Morrison KE, Green A, Acharya KR, Brown RH, Hardiman O (2006) ANG mutations segregate with familial and 'sporadic' amyotrophic lateral sclerosis. Nat Genet 38:411–413.

Grosskreutz J, Van Den Bosch L, Keller BU (2010) Calcium dysregulation in amyotrophic lateral sclerosis. Cell Calcium 47:165–174.

Guégan C, Vila M, Rosoklija G, Hays AP, Przedborski S (2001) Recruitment of the mitochondrial-dependent apoptotic pathway in amyotrophic lateral sclerosis. J Neurosci 21:6569–6576.

Guo H, Lai L, Butchbach E.R. MER, Stockinger MP, Shan X, Bishop G a., Lin CLG (2003) Increased expression of the glial glutamate transporter EAAT2 modulates excitotoxicity and delays the onset but not the outcome of ALS in mice. Hum Mol Genet 12:2519–2532.

Guo Y, Duan W, Li Z, Huang J, Yin Y, Zhang K, Wang Q, Zhang Z, Li C (2010) Decreased GLT-1 and increased SOD1 and HO-1 expression in astrocytes contribute to lumbar spinal cord vulnerability of SOD1-G93A transgenic mice. FEBS Lett 584:1615–1622.

Gurney ME, Pu H, Chiu AY, Dal Canto MC, Polchow CY, Alexander DD, Caliendo J, Hentati A, Kwon YW, Deng HX (1994) Motor neuron degeneration in mice that express a human Cu,Zn superoxide dismutase mutation. Science 264:1772–1775.

Hadano S, Otomo A, Kunita R, Suzuki-Utsunomiya K, Akatsuka A, Koike M, Aoki M, Uchiyama Y, Itoyama Y, Ikeda J-E (2010) Loss of ALS2/Alsin exacerbates motor dysfunction in a SOD1-expressing mouse ALS model by disturbing endolysosomal trafficking. PLoS One 5:e9805.

Haidet-Phillips AM, Gross SK, Williams T, Tuteja A, Sherman A, Ko M, Jeong YH, Wong PC, Maragakis NJ (2013) Altered astrocytic expression of TDP-43 does not influence motor neuron survival. Exp Neurol 250:250–259.

Haidet-Phillips AM, Hester ME, Miranda CJ, Meyer K, Braun L, Frakes A, Song S, Likhite S, Murtha MJ, Foust KD, Rao M, Eagle A, Kammesheidt A, Christensen A, Mendell JR, Burghes AHM, Kaspar BK (2011) Astrocytes from familial and sporadic ALS patients are toxic to motor neurons. Nat Biotechnol 29:824–828.

Hardiman O, van den Berg LH, Kiernan MC (2011) Clinical diagnosis and management of amyotrophic lateral sclerosis. Nat Rev Neurol 7:639–649.

Hayashi S, Amari M, Okamoto K (2013) Loss of calretinin- and parvalbumin-

immunoreactive axons in anterolateral columns beyond the corticospinal tracts of amyotrophic lateral sclerosis spinal cords. J Neurol Sci:6–11.

He SQ, Dum RP, Strick PL (1995) Topographic organization of corticospinal projections from the frontal-lobe- Motor areas on the medial surface of the hemisphere. J Neurosci 15:3284–3306.

Heath PR, Shaw PJ (2002) Update on the glutamatergic neurotransmitter system and the role of excitotoxicity in amyotrophic lateral sclerosis. Muscle and Nerve 26:438–458.

Hegedus J, Putman CT, Gordon T (2007) Time course of preferential motor unit loss in the SOD1 G93A mouse model of amyotrophic lateral sclerosis. Neurobiol Dis 28:154–164.

Herrero MT, Barcia C, Navarro JM (2002) Functional anatomy of thalamus and basal ganglia. Child's Nerv Syst 18:386–404.

Herron LR, Miles GB (2012) Gender-specific perturbations in modulatory inputs to motoneurons in a mouse model of amyotrophic lateral sclerosis. Neuroscience 226:313–323.

Higgins CMJ, Jung C, Xu Z (2003) ALS-associated mutant SOD1G93A causes mitochondrial vacuolation by expansion of the intermembrane space and by involvement of SOD1 aggregation and peroxisomes. BMC Neurosci 4:16.

Hirth F (2010) Drosophila melanogaster in the study of human neurodegeneration. CNS Neurol Disord Drug Targets 9:504–523.

Hodgkin AL, Huxley AF (1952) A quantitative description of membrane current and its applications to conduction and excitation in nerve. J Physiol 117:500–544.

Hollmann M, Hartley M, Heinemann S (1991) Ca2+ permeability of KA-AMPA--gated glutamate receptor channels depends on subunit composition. Science 252:851–853.

Howland DS, Liu J, She Y, Goad B, Maragakis NJ, Kim B, Erickson J, Kulik J, DeVito L, Psaltis G, DeGennaro LJ, Cleveland DW, Rothstein JD (2002) Focal loss of the glutamate transporter EAAT2 in a transgenic rat model of SOD1 mutant-mediated amyotrophic lateral sclerosis (ALS). Proc Natl Acad Sci U S A 99:1604–1609.

Hu BY, Zhang SC (2009) Differentiation of spinal motor neurons from pluripotent human stem cells. Nat Protoc 4:1295–1304.

Iguchi Y, Katsuno M, Niwa JI, Takagi S, Ishigaki S, Ikenaka K, Kawai K, Watanabe H, Yamanaka K, Takahashi R, Misawa H, Sasaki S, Tanaka F, Sobue G (2013) Loss of TDP-43 causes age-dependent progressive motor neuron degeneration. Brain 136:1371–1382.

Ikenaka K, Katsuno M, Kawai K, Ishigaki S, Tanaka F, Sobue G (2012) Disruption of axonal transport in motor neuron diseases. Int J Mol Sci 13:1225–1238.

Ilieva H, Polymenidou M, Cleveland DW (2009) Non-cell autonomous toxicity in neurodegenerative disorders: ALS and beyond. J Cell Biol 187:761–772.

Ilieva E V, Ayala V, Jové M, Dalfó E, Cacabelos D, Povedano M, Bellmunt MJ, Ferrer I, Pamplona R, Portero-Otín M (2007) Oxidative and endoplasmic reticulum stress interplay in sporadic amyotrophic lateral sclerosis. Brain 130:3111–3123.

Ince PG, Highley JR, Kirby J, Wharton SB, Takahashi H, Strong MJ, Shaw PJ (2011) Molecular pathology and genetic advances in amyotrophic lateral sclerosis: An emerging molecular pathway and the significance of glial pathology. Acta Neuropathol 122:657–671.

Ince PG, Lowe J, Shaw PJ (1998) Amyotrophic lateral sclerosis: Current issues in classification, pathogenesis and molecular pathology. Neuropathol Appl Neurobiol 24:104–117.

Ince PG, Slade J, Chinnery RM, McKenzie J, Royston C, Roberts GW, Shaw PJ (1995) Quantitative study of synaptophysin immunoreactivity of cerebral cortex and spinal cord in motor neuron disease. J Neuropathol Exp Neurol 54:673–679.

Ince PG, Stout N, Shaw PJ, Slade J, Hunziker W, Heizmann CW, Baimbridge KG (1993) Parvalbumin and calbindin D-28k in the human motor system and in motor neuron disease. Neuropathol Appl Neurobiol 19:291–299.

Israelson A, Arbel N, Da Cruz S, Ilieva H, Yamanaka K, Shoshan-Barmatz V, Cleveland DW (2010) Misfolded mutant SOD1 directly inhibits VDAC1 conductance in a mouse model of inherited ALS. Neuron 67:575–587.

Issa AN, Zhan WZ, Sieck GC, Mantilla CB (2010) Neuregulin-1 at synapses on phrenic motoneurons. J Comp Neurol 518:4213–4225.

Jaarsma D, Haasdijk ED, Grashorn J a, Hawkins R, van Duijn W, Verspaget HW, London J, Holstege JC (2000) Human Cu/Zn superoxide dismutase (SOD1) overexpression in mice causes mitochondrial vacuolization, axonal degeneration, and premature motoneuron death and accelerates motoneuron disease in mice expressing a familial amyotrophic lateral sclerosis mutant SO. Neurobiol Dis 7:623–643.

Jaarsma D, Rognoni F, van Duijn W, Verspaget HW, Haasdijk ED, Holstege JC (2001) CuZn superoxide dismutase (SOD1) accumulates in vacuolated mitochondria in transgenic mice expressing amyotrophic lateral sclerosis-linked SOD1 mutations. Acta Neuropathol 102:293–305.

Jaarsma D, Teuling E, Haasdijk ED, De Zeeuw CI, Hoogenraad CC (2008) Neuron-specific expression of mutant superoxide dismutase is sufficient to induce amyotrophic lateral sclerosis in transgenic mice. J Neurosci 28:2075–2088.

Jaiswal MK, Keller BU (2009) Cu/Zn superoxide dismutase typical for familial amyotrophic lateral sclerosis increases the vulnerability of mitochondria and perturbs Ca2+ homeostasis in SOD1G93A mice. Mol Pharmacol 75:478–489.

Jaiswal MK, Zech W-D, Goos M, Leutbecher C, Ferri A, Zippelius A, Carrì MT, Nau R, Keller BU (2009) Impairment of mitochondrial calcium handling in a mtSOD1 cell culture model of motoneuron disease. BMC Neurosci 10:64.

Janssens J, Van Broeckhoven C (2013) Pathological mechanisms underlying TDP-43 driven neurodegeneration in FTLD-ALS spectrum disorders. Hum Mol Genet 22:77–87.

Jessell TM (2000) Neuronal specification in the spinal cord: inductive signals and transcriptional codes. Nat Rev Genet 1:20–29.

Jiang M, Schuster JE, Fu R, Siddique T, Heckman CJ (2009) Progressive changes in synaptic inputs to motoneurons in adult sacral spinal cord of a mouse model of amyotrophic lateral sclerosis. J Neurosci 29:15031–15038.

Jiang Y-M, Yamamoto M, Kobayashi Y, Yoshihara T, Liang Y, Terao S, Takeuchi H, Ishigaki S, Katsuno M, Adachi H, Niwa J, Tanaka F, Doyu M, Yoshida M, Hashizume Y, Sobue G (2005) Gene expression profile of spinal motor neurons in sporadic amyotrophic lateral sclerosis. Ann Neurol 57:236–251.

Johnson JA, Johnson DA, Kraft AD, Calkins MJ, Jakel RJ, Vargas MR, Chen P-C (2009) The Nrf2-ARE Pathway: An Indicator and Modulator of Oxidative Stress in Neurodegeneration. Ann N Y Acad Sci 2:61–69.

Johnson JO, Mandrioli J, Benatar M, Abramzon Y, Van Deerlin VM, Trojanowski JQ, Gibbs JR, Brunetti M, Gronka S, Wuu J, Ding J, McCluskey L, Martinez-Lage M, Falcone D, Hernandez DG, Arepalli S, Chong S, Schymick JC, Rothstein J, Landi F, Wang YD, Calvo A, Mora G, Sabatelli M, Monsurrò MR, Battistini S, Salvi F, Spataro R, Sola P, Borghero G, Galassi G, Scholz SW, Taylor JP, Restagno G, Chiò A, Traynor BJ (2010) Exome Sequencing Reveals VCP Mutations as a Cause of Familial ALS. Neuron 68:857–864.

Joshi DC, Singh M, Krishnamurthy K, Joshi PG, Joshi NB (2011) AMPA induced Ca2+ influx in motor neurons occurs through voltage gated Ca2+ channel and Ca2+ permeable AMPA receptor. Neurochem Int 59:913–921.

Kabashi E, Lin L, Tradewell ML, Dion P a., Bercier V, Bourgouin P, Rochefort D, Bel Hadj S, Durham HD, Velde C Vande, Rouleau G a., Drapeau P (2009) Gain and loss of function of ALS-related mutations of TARDBP (TDP-43) cause motor deficits in vivo. Hum Mol Genet 19:671–683.

Kanai K, Kuwabara S, Misawa S, Tamura N, Ogawara K, Nakata M, Sawai S, Hattori T, Bostock H (2006) Altered axonal excitability properties in amyotrophic lateral sclerosis: impaired potassium channel function related to disease stage. Brain 129:953–962.

Kanai K, Shibuya K, Sato Y, Misawa S, Nasu S, Sekiguchi Y, Mitsuma S, Isose S, Fujimaki Y, Ohmori S, Koga S, Kuwabara S (2012) Motor axonal excitability properties are strong predictors for survival in amyotrophic lateral sclerosis. J Neurol Neurosurg Psychiatry 83:734–738.

Kang SH, Fukaya M, Yang JK, Rothstein JD, Bergles DE (2010) NG2+ CNS glial progenitors remain committed to the oligodendrocyte lineage in postnatal life and following neurodegeneration. Neuron 68:668–681.

Kang SH, Li Y, Fukaya M, Lorenzini I, Cleveland DW, Ostrow LW, Rothstein JD, Bergles DE (2013) Degeneration and impaired regeneration of gray matter oligodendrocytes in amyotrophic lateral sclerosis. Nat Neurosci 16:571–579.

Kang SJ, Sanchez I, Jing N, Yuan J (2003) Dissociation between neurodegeneration and caspase-11-mediated activation of caspase-1 and caspase-3 in a mouse model of amyotrophic lateral sclerosis. J Neurosci 23:5455–5460.

Kanning KC, Kaplan A, Henderson CE (2010) Motor neuron diversity in development and disease. Annu Rev Neurosci 33:409–440.

Karch CM, Borchelt DR (2008) A limited role for disulfide cross-linking in the aggregation of mutant SOD1 linked to familial amyotrophic lateral sclerosis. J Biol Chem 283:13528–13537.

Karumbayaram S, Kelly TK, Paucar A a., Roe AJT, Umbach J a., Charles A, Goldman S a., Kornblum HI, Wiedau-Pazos M (2009a) Human embryonic stem cell-derived motor neurons expressing SOD1 mutants exhibit typical signs of

motor neuron degeneration linked to ALS. Dis Model Mech 2:189–195.

Karumbayaram S, Novitch BG, Patterson M, Umbach J a, Richter L, Lindgren A, Conway AE, Clark AT, Goldman S a, Plath K, Wiedau-Pazos M, Kornblum HI, Lowry WE (2009b) Directed differentiation of human-induced pluripotent stem cells generates active motor neurons. Stem Cells 27:806–811.

Kawahara Y, Ito K, Sun H, Aizawa H, Kanazawa I, Kwak S (2004) Glutamate receptors: RNA editing and death of motor neurons. Nature 427:801.

Kawahara Y, Sun H, Ito K, Hideyama T, Aoki M, Sobue G, Tsuji S, Kwak S (2006) Underediting of GluR2 mRNA, a neuronal death inducing molecular change in sporadic ALS, does not occur in motor neurons in ALS1 or SBMA. Neurosci Res 54:11–14.

Kawamata H, Manfredi G (2010) Mitochondrial dysfunction and intracellular calcium dysregulation in ALS. Mech Ageing Dev 131:517–526.

Kawamata T, Akiyama H, Yamada T, McGeer PL (1992) Immunologic reactions in amyotrophic lateral sclerosis brain and spinal cord tissue. Am J Pathol 140:691–707.

Kernell D, Zwaagstra B (1989) Dendrites of cat's spinal motoneurones: relationship between stem diameter and predicted input conductance. J Physiol 413:255–269.

Kiernan MC (2009) Hyperexcitability, persistent Na+ conductances and neurodegeneration in amyotrophic lateral sclerosis. Exp Neurol 218:1–4.

Kim JM, Noh EM, Kwon KB, Kim JS, You YO, Hwang JK, Hwang BM, Kim MS, Lee SJ, Jung SH, Youn HJ, Chung EY, Lee YR (2013) Suppression of TPA-induced tumor cell invasion by sulfuretin via inhibition of NF-kappaB-dependent MMP-9 expression. Oncol Rep 29:1231–1237.

Kim K, Lee S-G, Kegelman TP, Su Z-Z, Das SK, Dash R, Dasgupta S, Barral PM, Hedvat M, Diaz P, Reed JC, Stebbins JL, Pellecchia M, Sarkar D, Fisher PB (2011) Role of excitatory amino acid transporter-2 (EAAT2) and glutamate in neurodegeneration: opportunities for developing novel therapeutics. J Cell Physiol 226:2484–2493.

Kiskinis E, Sandoe J, Williams LA, Boulting GL, Moccia R, Wainger BJ, Han S, Peng T, Thams S, Mikkilineni S, Mellin C, Merkle FT, Davis-Dusenbery BN, Ziller M, Oakley D, Ichida J, Di Costanzo S, Atwater N, Maeder ML, Goodwin MJ, Nemesh J, Handsaker RE, Paull D, Noggle S, McCarroll SA, Joung JK, Woolf CJ, Brown RH, Eggan K (2014) Pathways Disrupted in Human ALS Motor Neurons Identified through Genetic Correction of Mutant SOD1. Cell Stem Cell 14:781–795.

Koh S-H, Baek W, Kim SH (2011) Brief review of the role of glycogen synthase kinase-3β in amyotrophic lateral sclerosis. Neurol Res Int 2011:205761.

Kong J, Xu Z (1998) Massive mitochondrial degeneration in motor neurons triggers the onset of amyotrophic lateral sclerosis in mice expressing a mutant SOD1. J Neurosci 18:3241–3250.

Kraemer BC, Schuck T, Wheeler JM, Robinson LC, Trojanowski JQ, Lee VMY, Schellenberg GD (2010) Loss of Murine TDP-43 disrupts motor function and plays an essential role in embryogenesis. Acta Neuropathol 119:409–419.

Kruman II, Pedersen WA, Springer JE, Mattson MP (1999) ALS-linked Cu/Zn-SOD

mutation increases vulnerability of motor neurons to excitotoxicity by a mechanism involving increased oxidative stress and perturbed calcium homeostasis. Exp Neurol 160:28–39.

Kumar DR, Aslinia F, Yale SH, Mazza JJ (2011) Jean-martin charcot: The father of neurology. Clin Med Res 9:46–49.

Kuner R, Groom AJ, Bresink I, Kornau H-C, Stefovska V, Müller G, Hartmann B, Tschauner K, Waibel S, Ludolph AC, Ikonomidou C, Seeburg PH, Turski L (2005) Late-onset motoneuron disease caused by a functionally modified AMPA receptor subunit. Proc Natl Acad Sci U S A 102:5826–5831.

Kuo JJ, Lee RH, Zhang L, Heckman CJ (2006) Essential role of the persistent sodium current in spike initiation during slowly rising inputs in mouse spinal neurones. J Physiol 3:819–834.

Kuo JJ, Schonewille M, Siddique T, Schults AN a, Fu R, Bär PR, Anelli R, Heckman CJ, Kroese AB a (2004) Hyperexcitability of cultured spinal motoneurons from presymptomatic ALS mice. J Neurophysiol 91:571–575.

Kuo JJ, Siddique T, Fu R, Heckman CJ (2005) Increased persistent Na(+) current and its effect on excitability in motoneurones cultured from mutant SOD1 mice. J Physiol 563:843–854.

Kushner PD, Stephenson DT, Wright S (1991) Reactive astrogliosis is widespread in the subcortical white matter of amyotrophic lateral sclerosis brain. J Neuropathol Exp Neurol 50:263–277.

Kwak S, Hideyama T, Yamashita T, Aizawa H (2010) AMPA receptor-mediated neuronal death in sporadic ALS. In: Neuropathology, pp 182–188.

Kwiatkowski TJ, Bosco DA, Leclerc AL, Tamrazian E, Vanderburg CR, Russ C, Davis A, Gilchrist J, Kasarskis EJ, Munsat T, Valdmanis P, Rouleau GA, Hosler BA, Cortelli P, de Jong PJ, Yoshinaga Y, Haines JL, Pericak-Vance MA, Yan J, Ticozzi N, Siddique T, McKenna-Yasek D, Sapp PC, Horvitz HR, Landers JE, Brown RH (2009) Mutations in the FUS/TLS gene on chromosome 16 cause familial amyotrophic lateral sclerosis. Science 323:1205–1208.

Lagier-Tourenne C, Baughn M, Rigo F, Sun S, Liu P, Li H-R, Jiang J, Watt AT, Chun S, Katz M, Qiu J, Sun Y, Ling S-C, Zhu Q, Polymenidou M, Drenner K, Artates JW, McAlonis-Downes M, Markmiller S, Hutt KR, Pizzo DP, Cady J, Harms MB, Baloh RH, Vandenberg SR, Yeo GW, Fu X-D, Bennett CF, Cleveland DW, Ravits J (2013) Targeted degradation of sense and antisense C9orf72 RNA foci as therapy for ALS and frontotemporal degeneration. Proc Natl Acad Sci U S A.

Lagier-Tourenne C, Polymenidou M, Cleveland DW (2010) TDP-43 and FUS/TLS: Emerging roles in RNA processing and neurodegeneration. Hum Mol Genet 19:46–64.

Lagier-Tourenne C, Polymenidou M, Hutt KR, Vu AQ, Baughn M, Huelga SC, Clutario KM, Ling S-C, Liang TY, Mazur C, Wancewicz E, Kim AS, Watt A, Freier S, Hicks GG, Donohue JP, Shiue L, Bennett CF, Ravits J, Cleveland DW, Yeo GW (2012) Divergent roles of ALS-linked proteins FUS/TLS and TDP-43 intersect in processing long pre-mRNAs. Nat Neurosci 15:1488–1497.

Laird AS, van Hoecke A, De Muynck L, Timmers M, van den Bosch L, Van Damme P, Robberecht W (2010) Progranulin is neurotrophic in vivo and protects against a mutant TDP-43 induced axonopathy. PLoS One 5.

LaMonte BH, Wallace KE, Holloway B a, Shelly SS, Ascaño J, Tokito M, Van Winkle T, Howland DS, Holzbaur ELF (2002) Disruption of dynein/dynactin inhibits axonal transport in motor neurons causing late-onset progressive degeneration. Neuron 34:715–727.

Laplante M, Sabatini DM (2012) MTOR signaling in growth control and disease. Cell 149:274–293.

Lasiene J, Yamanaka K (2011) Glial cells in amyotrophic lateral sclerosis. Neurol Res Int 2011.

Laslo P, Lipski J, Nicholson LF, Miles GB, Funk GD (2001) GluR2 AMPA receptor subunit expression in motoneurons at low and high risk for degeneration in amyotrophic lateral sclerosis. Exp Neurol 169:461–471.

Lattante S, Rouleau GA, Kabashi E (2013) TARDBP and FUS Mutations Associated with Amyotrophic Lateral Sclerosis: Summary and Update. Hum Mutat 34:812–826.

Lee H, Shamy G Al, Elkabetz Y, Schofield CM, Harrsion NL, Panagiotakos G, Socci ND, Tabar V, Studer L (2007) Directed differentiation and transplantation of human embryonic stem cell-derived motoneurons. Stem Cells 25:1931–1939.

Lee JC, Seong J, Kim SH, Lee SJ, Cho YJ, An J, Nam DH, Joo KM, Cha CI (2012) Replacement of microglial cells using Clodronate liposome and bone marrow transplantation in the central nervous system of SOD1G93A transgenic mice as an in vivo model of amyotrophic lateral sclerosis. Biochem Biophys Res Commun 418:359–365.

Lee Y-B, Chen H-J, Peres JN, Gomez-Deza J, Attig J, Štalekar M, Troakes C, Nishimura AL, Scotter EL, Vance C, Adachi Y, Sardone V, Miller JW, Smith BN, Gallo J-M, Ule J, Hirth F, Rogelj B, Houart C, Shaw CE (2013) Hexanucleotide Repeats in ALS/FTD Form Length-Dependent RNA Foci, Sequester RNA Binding Proteins, and Are Neurotoxic. Cell Rep 5:1178–1186.

Lepore AC, O'Donnell J, Kim AS, Williams T, Tuteja A, Rao MS, Kelley LL, Campanelli JT, Maragakis NJ (2011) Human Glial-restricted progenitor transplantation into cervical spinal cord of the SOD1 G93A mouse model of ALS. PLoS One 6:1–17.

Lepore AC, Rauck B, Dejea C, Pardo AC, Rao MS, Rothstein JD, Maragakis NJ (2008) Focal transplantation-based astrocyte replacement is neuroprotective in a model of motor neuron disease. Nat Neurosci 11:1294–1301.

Leroy FF, Lamotte B, Imhoff-Manuel RD, Zytnicki D, Zytnicki D, Lamotte d'Incamps B, Imhoff-Manuel RD, Zytnicki D (2014) Early intrinsic hyperexcitability does not contribute to motoneuron degeneration in amyotrophic lateral sclerosis. Elife 3:1–24.

Levine TP, Daniels RD, Gatta AT, Wong LH, Hayes MJ (2013) The product of C9orf72, a gene strongly implicated in neurodegeneration, is structurally related to DENN Rab-GEFs. Bioinformatics 29:499–503.

Li M, Ona VO, Guégan C, Chen M, Jackson-Lewis V, Andrews LJ, Olszewski AJ, Stieg PE, Lee JP, Przedborski S, Friedlander RM (2000) Functional role of caspase-1 and caspase-3 in an ALS transgenic mouse model. Science 288:335–339.

Li X-J, Du Z-W, Zarnowska ED, Pankratz M, Hansen LO, Pearce R a, Zhang S-C (2005) Specification of motoneurons from human embryonic stem cells. Nat Biotechnol 23:215–221.

Li Y, Ray P, Rao EJ, Shi C, Guo W, Chen X, Woodruff EA, Fushimi K, Wu JY (2010) A Drosophila model for TDP-43 proteinopathy. Proc Natl Acad Sci U S A 107:3169–3174.

Lim MA, Selak MA, Xiang Z, Krainc D, Neve RL, Kraemer BC, Watts JL, Kalb RG (2012) Reduced Activity of AMP-Activated Protein Kinase Protects against Genetic Models of Motor Neuron Disease. J Neurosci 32:1123–1141.

Lin CLG, Bristol LA, Jin L, Dykes-Hoberg M, Crawford T, Clawson L, Rothstein JD (1998) Aberrant RNA processing in a neurodegenerative disease: The cause for absent EAAT2, a glutamate transporter, in amyotrophic lateral sclerosis. Neuron 20:589–602.

Ling S-C, Albuquerque CP, Han JS, Lagier-Tourenne C, Tokunaga S, Zhou H, Cleveland DW (2010) ALS-associated mutations in TDP-43 increase its stability and promote TDP-43 complexes with FUS/TLS. Proc Natl Acad Sci U S A 107:13318–13323.

Ling SC, Polymenidou M, Cleveland DW (2013) Converging mechanisms in als and FTD: Disrupted RNA and protein homeostasis. Neuron 79:416–438.

Lino MM, Schneider C, Caroni P (2002) Accumulation of SOD1 mutants in postnatal motoneurons does not cause motoneuron pathology or motoneuron disease. J Neurosci 22:4825–4832.

Linseman DA, Butts BD, Precht TA, Phelps RA, Le SS, Laessig TA, Bouchard RJ, Florez-McClure ML, Heidenreich KA (2004) Glycogen synthase kinase-3beta phosphorylates Bax and promotes its mitochondrial localization during neuronal apoptosis. J Neurosci 24:9993–10002.

Liu EY, Russ J, Wu K, Neal D, Suh E, McNally AG, Irwin DJ, Van Deerlin VM, Lee EB (2014) C9orf72 hypermethylation protects against repeat expansion-associated pathology in ALS/FTD. Acta Neuropathol:525–541.

Liu HN, Sanelli T, Horne P, Pioro EP, Strong MJ, Rogaeva E, Bilbao J, Zinman L, Robertson J (2009) Lack of evidence of monomer/misfolded superoxide dismutase-1 in sporadic amyotrophic lateral sclerosis. Ann Neurol 66:75–80.

Liu J, Lillo C, Jonsson PA, Velde C Vande, Ward CM, Miller TM, Subramaniam JR, Rothstein JD, Marklund S, Andersen PM, Brännström T, Gredal O, Wong PC, Williams DS, Cleveland DW (2004) Toxicity of familial ALS-linked SOD1 mutants from selective recruitment to spinal mitochondria. Neuron 43:5–17.

Liu KX, Edwards B, Lee S, Finelli MJ, Davies B, Davies KE, Oliver PL (2015) Neuron-specific antioxidant OXR1 extends survival of a mouse model of amyotrophic lateral sclerosis. Brain:1167–1181.

Lobsiger CS, Cleveland DW (2007) Glial cells as intrinsic components of non-cell-autonomous neurodegenerative disease. Nat Neurosci 10:1355–1360.

Lorenzo LE, Barbe A, Portalier P, Fritschy JM, Bras H (2006) Differential expression of GABAA and glycine receptors in ALS-resistant vs. ALS-vulnerable motoneurons: Possible implications for selective vulnerability of motoneurons. Eur J Neurosci 23:3161–3170.

Ludolph AC, Bendotti C, Blaugrund E, Chio A, Greensmith L, Loeffler J-P, Mead R, Niessen HG, Petri S, Pradat P-F, Robberecht W, Ruegg M, Schwalenstöcker B, Stiller D, van den Berg L, Vieira F, von Horsten S (2010) Guidelines for preclinical animal research in ALS/MND: A consensus meeting. In: Amyotrophic lateral sclerosis : official publication of the World Federation of Neurology Research Group on Motor Neuron Diseases, pp 38–45.

Mackenzie IRA, Bigio EH, Ince PG, Geser F, Neumann M, Cairns NJ, Kwong LK, Forman MS, Ravits J, Stewart H, Eisen A, McClusky L, Kretzschmar HA, Monoranu CM, Highley JR, Kirby J, Siddique T, Shaw PJ, Lee VMY, Trojanowski JQ (2007) Pathological TDP-43 distinguishes sporadic amyotrophic lateral sclerosis from amyotrophic lateral sclerosis with SOD1 mutations. Ann Neurol 61:427–434.

Mackenzie IRA, Rademakers R, Neumann M (2010) TDP-43 and FUS in amyotrophic lateral sclerosis and frontotemporal dementia. Lancet Neurol 9:995–1007.

Maekawa S, Al-Sarraj S, Kibble M, Landau S, Parnavelas J, Cotter D, Everall I, Leigh PN (2004) Cortical selective vulnerability in motor neuron disease: a morphometric study. Brain 127:1237–1251.

Magrané J, Cortez C, Gan WB, Manfredi G (2014) Abnormal mitochondrial transport and morphology are common pathological denominators in SOD1 and TDP43 ALS mouse models. Hum Mol Genet 23:1413–1424.

Magrané J, Manfredi G (2009) Mitochondrial function, morphology, and axonal transport in amyotrophic lateral sclerosis. Antioxid Redox Signal 11:1615–1626.

Mannen T, Iwata M, Toyokura Y, Nagashima K (1977) Preservation of a certain motoneurone group of the sacral cord in amyotrophic lateral sclerosis: its clinical significance. J Neurol Neurosurg Psychiatry 40:464–469.

Manto M, Bower JM, Conforto AB, Delgado-García JM, Da Guarda SNF, Gerwig M, Habas C, Hagura N, Ivry RB, Marien P, Molinari M, Naito E, Nowak DA, Ben Taib NO, Pelisson D, Tesche CD, Tilikete C, Timmann D (2012) Consensus paper: Roles of the cerebellum in motor control-the diversity of ideas on cerebellar involvement in movement. In: Cerebellum, pp 457–487.

Marat AL, Dokainish H, McPherson PS (2011) DENN domain proteins: regulators of Rab GTPases. J Biol Chem 286:13791–13800.

Marchetto MCN, Muotri AR, Mu Y, Smith AM, Cezar GG, Gage FH (2008) Non-cell-autonomous effect of human SOD1 G37R astrocytes on motor neurons derived from human embryonic stem cells. Cell Stem Cell 3:649–657.

Marinkovic P, Reuter MS, Brill MS, Godinho L, Kerschensteiner M, Misgeld T (2012) Axonal transport deficits and degeneration can evolve independently in mouse models of amyotrophic lateral sclerosis. Proc Natl Acad Sci U S A 109:4296–4301.

Martin E, Cazenave W, Cattaert D, Branchereau P (2013) Embryonic alteration of motoneuronal morphology induces hyperexcitability in the mouse model of amyotrophic lateral sclerosis. Neurobiol Dis 54:116–126.

Martin LJ (1999) Neuronal death in amyotrophic lateral sclerosis is apoptosis: possible contribution of a programmed cell death mechanism. J Neuropathol Exp Neurol 58:459–471.

Matsumoto S, Goto S, Kusaka H, Ito H, Imai T (1994) Synaptic pathology of spinal anterior horn cells in amyotrophic lateral sclerosis: An immunohistochemical study. J Neurol Sci 125:180–185.

Matus S, Valenzuela V, Medinas DB, Hetz C (2013) ER dysfunction and protein folding stress in ALS. Int J Cell Biol 2013.

Mauk MD, Medina JF, Nores WL, Ohyama T (2000) Cerebellar function: Coordination, learning or timing? Curr Biol 10.

Maury Y, Come J, Piskorowski RA, Salah-Mohellibi N, Chevaleyre V, Peschanski M, Martinat C, Nedelec S (2015) Combinatorial analysis of developmental cues efficiently converts human pluripotent stem cells into multiple neuronal subtypes. Nat Biotech 33:89–96.

McGoldrick P, Joyce PI, Fisher EMC, Greensmith L (2013) Rodent models of amyotrophic lateral sclerosis. Biochim Biophys Acta 1832:1421–1436.

McGown A, McDearmid JR, Panagiotaki N, Tong H, Al Mashhadi S, Redhead N, Lyon AN, Beattie CE, Shaw PJ, Ramesh TM (2013) Early interneuron dysfunction in ALS: insights from a mutant sod1 zebrafish model. Ann Neurol 73:246–258.

Menon P, Kiernan MC, Vucic S (2014) Cortical hyperexcitability precedes lower motor neuron dysfunction in ALS. Clin Neurophysiol.

Menzies FM, Cookson MR, Taylor RW, Turnbull DM, Chrzanowska-Lightowlers ZM a, Dong L, Figlewicz D a, Shaw PJ (2002) Mitochondrial dysfunction in a cell culture model of familial amyotrophic lateral sclerosis. Brain 125:1522–1533.

Meyer K, Ferraiuolo L, Miranda CJ, Likhite S, McElroy S, Renusch S, Ditsworth D, Lagier-Tourenne C, Smith R a, Ravits J, Burghes AH, Shaw PJ, Cleveland DW, Kolb SJ, Kaspar BK (2013) Direct conversion of patient fibroblasts demonstrates non-cell autonomous toxicity of astrocytes to motor neurons in familial and sporadic ALS. Proc Natl Acad Sci U S A 111:4–7.

Migheli A, Cavalla P, Marino S, Schiffer D (1994) A study of apoptosis in normal and pathologic nervous tissue after in situ end-labeling of DNA strand breaks. J Neuropathol Exp Neurol 53:606–616.

Miles GB, Hartley R, Todd AJ, Brownstone RM (2007) Spinal cholinergic interneurons regulate the excitability of motoneurons during locomotion. Proc Natl Acad Sci U S A 104:2448–2453.

Miles GB, Sillar KT (2011) Neuromodulation of Vertebrate Locomotor Control Networks. Physiology 26:393–411.

Miles GB, Yohn DC, Wichterle H, Jessell TM, Rafuse VF, Brownstone RM (2004) Functional properties of motoneurons derived from mouse embryonic stem cells. J Neurosci 24:7848–7858.

Millecamps S, Boillée S, Le Ber I, Seilhean D, Teyssou E, Giraudeau M, Moigneu C, Vandenberghe N, Danel-Brunaud V, Corcia P, Pradat P-F, Le Forestier N, Lacomblez L, Bruneteau G, Camu W, Brice A, Cazeneuve C, Leguern E, Meininger V, Salachas F (2012) Phenotype difference between ALS patients with expanded repeats in C9ORF72 and patients with mutations in other ALS-related genes. J Med Genet 49:258–263.

Millecamps S, Julien J-P (2013) Axonal transport deficits and neurodegenerative diseases. Nat Rev Neurosci 14:161–176.

Miquel E, Cassina A, Martínez-Palma L, Bolatto C, Trías E, Gandelman M, Radi R, Barbeito L, Cassina P (2012) Modulation of astrocytic mitochondrial function by dichloroacetate improves survival and motor performance in inherited amyotrophic lateral sclerosis. PLoS One 7:e34776.

Mitne-Neto M, Machado-Costa M, Marchetto MCN, Bengtson MH, Joazeiro CA, Tsuda H, Bellen HJ, Silva HCA, Oliveira ASB, Lazar M, Muotri AR, Zatz M (2011) Downregulation of VAPB expression in motor neurons derived from induced pluripotent stem cells of ALS8 patients. Hum Mol Genet 20:3642–3652.

Montgomery DL (1994) Astrocytes: form, functions, and roles in disease. Vet Pathol 31:145–167.

Mori F, Tanji K, Zhang HX, Nishihira Y, Tan CF, Takahashi H, Wakabayashi K (2008) Maturation process of TDP-43-positive neuronal cytoplasmic inclusions in amyotrophic lateral sclerosis with and without dementia. Acta Neuropathol 116:193–203.

Mori K, Weng S-M, Arzberger T, May S, Rentzsch K, Kremmer E, Schmid B, Kretzschmar HA, Cruts M, Van Broeckhoven C, Haass C, Edbauer D (2013) The C9orf72 GGGGCC Repeat Is Translated into Aggregating Dipeptide-Repeat Proteins in FTLD/ALS. Sci 339 :1335–1338.

Morrison BM, Janssen WGM, Gordon JW, Morrison JH (1998) Light and electron microscopic distribution of the AMPA receptor subunit, GluR2, in the spinal cord of control and G86R mutant superoxide dismutase transgenic mice. J Comp Neurol 395:523–534.

Mutihac R, Alegre-Abarrategui J, Gordon D, Farrimond L, Yamasaki-Mann M, Talbot K, Wade-Martins R (2015) TARDBP pathogenic mutations increase cytoplasmic translocation of TDP-43 and cause reduction of endoplasmic reticulum Ca2+ signaling in motor neurons. Neurobiol Dis 75:64–77.

Nachev P, Wydell H, O'Neill K, Husain M, Kennard C (2007) The role of the pre-supplementary motor area in the control of action. Neuroimage 36.

Nagai M, Aoki M, Miyoshi I, Kato M, Pasinelli P, Kasai N, Brown RH, Itoyama Y (2001) Rats expressing human cytosolic copper-zinc superoxide dismutase transgenes with amyotrophic lateral sclerosis: associated mutations develop motor neuron disease. J Neurosci 21:9246–9254.

Nagai M, Re DB, Nagata T, Wichterle H, Przedborski S, Chalazonitis A, Jessell TM, Wichterle H, Przedborski S (2007) Astrocytes expressing ALS-linked mutated SOD1 release factors selectively toxic to motor neurons. Nat Neurosci 10:615–622.

Nardo G, Pozzi S, Pignataro M, Lauranzano E, Spano G, Garbelli S, Mantovani S, Marinou K, Papetti L, Monteforte M, Torri V, Paris L, Bazzoni G, Lunetta C, Corbo M, Mora G, Bendotti C, Bonetto V (2011) Amyotrophic lateral sclerosis multiprotein biomarkers in peripheral blood mononuclear cells. PLoS One 6.

Neumann M, Sampathu DM, Kwong LK, Truax AC, Micsenyi MC, Chou TT, Bruce J, Schuck T, Grossman M, Clark CM, McCluskey LF, Miller BL, Masliah E, Mackenzie IR, Feldman H, Feiden W, Kretzschmar HA, Trojanowski JQ, Lee VM-Y (2006) Ubiquitinated TDP-43 in frontotemporal lobar degeneration and

amyotrophic lateral sclerosis. Science 314:130–133.

Nicoll RA, Malenka RC (1999) Expression mechanisms underlying NMDA receptor-dependent long-term potentiation. In: Annals of the New York Academy of Sciences, pp 515–525.

Nieto-Gonzalez JL, Moser J, Lauritzen M, Schmitt-John T, Jensen K (2011) Reduced GABAergic inhibition explains cortical hyperexcitability in the wobbler mouse model of ALS. Cereb Cortex 21:625–635.

Nishimura AL, Mitne-Neto M, Silva HCA, Richieri-Costa A, Middleton S, Cascio D, Kok F, Oliveira JRM, Gillingwater T, Webb J, Skehel P, Zatz M (2004) A mutation in the vesicle-trafficking protein VAPB causes late-onset spinal muscular atrophy and amyotrophic lateral sclerosis. Am J Hum Genet 75:822–831.

Nishiyama A, Komitova M, Suzuki R, Zhu X (2009) Polydendrocytes (NG2 cells): multifunctional cells with lineage plasticity. Nat Rev Neurosci 10:9–22.

Oliver PL, FinelliMatté MJ, Edwards B, Bitoun E, Butts DL, Becker EBE, Cheeseman MT, Davies B, Davies KE (2011) Oxr1 is essential for protection against oxidative stress-induced neurodegeneration. PLoS Genet 7.

Ozcan L, Tabas I, Manuscript A, Disorders O (2012) Role of Endoplasmic Reticulum Stress in Metabolic Disease and Other Disorders. Annu Rev Med 63:317–328.

Pambo-Pambo A, Durand J, Gueritaud J (2009) Early excitability changes in lumbar motoneurons of transgenic SOD1G85R and SOD1G(93A-Low) mice. J Neurophysiol 102:3627–3642.

Papadeas ST, Kraig SE, O'Banion C, Lepore AC, Maragakis NJ (2011) Astrocytes carrying the superoxide dismutase 1 (SOD1G93A) mutation induce wild-type motor neuron degeneration in vivo. Proc Natl Acad Sci U S A 108:17803–17808.

Pardo AC, Wong V, Benson LM, Dykes M, Tanaka K, Rothstein JD, Maragakis NJ (2006) Loss of the astrocyte glutamate transporter GLT1 modifies disease in SOD1G93A mice. Exp Neurol 201:120–130.

Park I, Zhao R, West JA, Yabuuchi A, Huo H, Ince TA, Lerou PH, Lensch MW, Daley GQ (2008) Reprogramming of human somatic cells to pluripotency with defined factors. Nature 451:141–146.

Parker SJ, Meyerowitz J, James JL, Liddell JR, Crouch PJ, Kanninen KM, White AR (2012) Endogenous TDP-43 localized to stress granules can subsequently form protein aggregates. Neurochem Int 60:415–424.

Pasinelli P, Houseweart MK, Brown RH, Cleveland DW (2000) Caspase-1 and -3 are sequentially activated in motor neuron death in Cu,Zn superoxide dismutase-mediated familial amyotrophic lateral sclerosis. Proc Natl Acad Sci U S A 97:13901–13906.

Pehar M, Beeson G, Beeson CC, Johnson J a., Vargas MR (2014) Mitochondria-targeted catalase reverts the neurotoxicity of hSOD1 G93A astrocytes without extending the survival of ALS-linked mutant hSOD1 mice. PLoS One 9:3–10.

Peljto M, Dasen JS, Mazzoni EO, Jessell TM, Wichterle H (2010) Functional diversity of ESC-derived motor neuron subtypes revealed through intraspinal transplantation. Cell Stem Cell 7:355–366.

Pellerin L, Bouzier-Sore AK, Aubert A, Serres S, Merle M, Costalat R, Magistretti PJ

(2007) Activity-dependent regulation of energy metabolism by astrocytes: An update. Glia 55:1251–1262.

Pellerin L, Magistretti PJ (1994) Glutamate uptake into astrocytes stimulates aerobic glycolysis: a mechanism coupling neuronal activity to glucose utilization. Proc Natl Acad Sci U S A 91:10625–10629.

Petri S, Körner S, Kiaei M (2012) Nrf2/ARE signaling pathway: Key mediator in oxidative stress and potential therapeutic target in ALS. Neurol Res Int 2012:1–7.

Phatnani HP, Guarnieri P, Friedman B a, Carrasco M a, Muratet M, O'Keeffe S, Nwakeze C, Pauli-Behn F, Newberry KM, Meadows SK, Tapia JC, Myers RM, Maniatis T (2013) Intricate interplay between astrocytes and motor neurons in ALS. Proc Natl Acad Sci U S A 110:E756–E765.

Philips T, Bento-Abreu A, Nonneman A, Haeck W, Staats K, Geelen V, Hersmus N, Küsters B, Van Den Bosch L, Van Damme P, Richardson WD, Robberecht W (2013) Oligodendrocyte dysfunction in the pathogenesis of amyotrophic lateral sclerosis. Brain 136:471–482.

Pieri M, Albo F, Gaetti C, Spalloni A, Bengtson CP, Longone P, Cavalcanti S, Zona C (2003) Altered excitability of motor neurons in a transgenic mouse model of familial amyotrophic lateral sclerosis. Neurosci Lett 351:153–156.

Pieri M, Carunchio I, Curcio L, Mercuri NB, Zona C (2009) Increased persistent sodium current determines cortical hyperexcitability in a genetic model of amyotrophic lateral sclerosis. Exp Neurol 215:368–379.

Polymenidou M, Lagier-Tourenne C, Hutt KR, Huelga SC, Moran J, Liang TY, Ling S-C, Sun E, Wancewicz E, Mazur C, Kordasiewicz H, Sedaghat Y, Donohue JP, Shiue L, Bennett CF, Yeo GW, Cleveland DW (2011) Long pre-mRNA depletion and RNA missplicing contribute to neuronal vulnerability from loss of TDP-43. Nat Neurosci 14:459–468.

Pramatarova A, Laganière J, Roussel J, Brisebois K, Rouleau GA (2001) Neuron-specific expression of mutant superoxide dismutase 1 in transgenic mice does not lead to motor impairment. J Neurosci 21:3369–3374.

Pullen AH, Athanasiou D (2009) Increase in presynaptic territory of C-terminals on lumbar motoneurons of G93A SOD1 mice during disease progression. Eur J Neurosci 29:551–561.

Pun S, Santos AF, Saxena S, Xu L, Caroni P (2006) Selective vulnerability and pruning of phasic motoneuron axons in motoneuron disease alleviated by CNTF. Nat Neurosci 9:408–419.

Quinlan KA, Schuster JE, Fu R, Siddique T, Heckman CJ (2011) Altered postnatal maturation of electrical properties in spinal motoneurons in a mouse model of amyotrophic lateral sclerosis. J Physiol 589:2245–2260.

Radunovíc a, Leigh PN (1996) Cu/Zn superoxide dismutase gene mutations in amyotrophic lateral sclerosis: correlation between genotype and clinical features. J Neurol Neurosurg Psychiatry 61:565–572.

Rakhit R, Cunningham P, Furtos-Matei A, Dahan S, Qi XF, Crow JP, Cashman NR, Kondejewski LH, Chakrabartty A (2002) Oxidation-induced misfolding and aggregation of superoxide dismutase and its implications for amyotrophic lateral

sclerosis. J Biol Chem 277:47551–47556.

Rao M V., Nixon RA (2003) Defective neurofilament transport in mouse models of amyotrophic lateral sclerosis: A review. Neurochem Res 28:1041–1047.

Re DB, Le Verche V, Yu C, Amoroso MW, Politi K a., Phani S, Ikiz B, Hoffmann L, Koolen M, Nagata T, Papadimitriou D, Nagy P, Mitsumoto H, Kariya S, Wichterle H, Henderson CE, Przedborski S (2014) Necroptosis drives motor neuron death in models of both sporadic and familial ALS. Neuron 81:1001–1008.

Reaume AG, Elliott JL, Hoffman EK, Kowall NW, Ferrante RJ, Siwek DF, Wilcox HM, Flood DG, Beal MF, Brown RH, Scott RW, Snider WD (1996) Motor neurons in Cu/Zn superoxide dismutase-deficient mice develop normally but exhibit enhanced cell death after axonal injury. Nat Genet 13:43–47.

Rekling JC, Funk GD, Bayliss D a, Dong XW, Feldman JL (2000) Synaptic control of motoneuronal excitability. Physiol Rev 80:767–852.

Renton AE, Chiò A, Traynor BJ (2014) State of play in amyotrophic lateral sclerosis genetics. Nat Neurosci 17:17–23.

Renton AE, Majounie E, Waite A, Simón-Sánchez J, Rollinson S, Gibbs JR, Schymick JC, Laaksovirta H, van Swieten JC, Myllykangas L, Kalimo H, Paetau A, Abramzon Y, Remes AM, Kaganovich A, Scholz SW, Duckworth J, Ding J, Harmer DW, Hernandez DG, Johnson JO, Mok K, Ryten M, Trabzuni D, Guerreiro RJ, Orrell RW, Neal J, Murray A, Pearson J, Jansen IE, Sondervan D, Seelaar H, Blake D, Young K, Halliwell N, Callister JB, Toulson G, Richardson A, Gerhard A, Snowden J, Mann D, Neary D, Nalls M a, Peuralinna T, Jansson L, Isoviita V-M, Kaivorinne A-L, Hölttä-Vuori M, Ikonen E, Sulkava R, Benatar M, Wuu J, Chiò A, Restagno G, Borghero G, Sabatelli M, Heckerman D, Rogaeva E, Zinman L, Rothstein JD, Sendtner M, Drepper C, Eichler EE, Alkan C, Abdullaev Z, Pack SD, Dutra A, Pak E, Hardy J, Singleton A, Williams NM, Heutink P, Pickering-Brown S, Morris HR, Tienari PJ, Traynor BJ (2011) A hexanucleotide repeat expansion in C9ORF72 is the cause of chromosome 9p21-linked ALS-FTD. Neuron 72:257–268.

Reyes NA, Fisher JK, Austgen K, VandenBerg S, Huang EJ, Oakes SA (2010) Blocking the mitochondrial apoptotic pathway preserves motor neuron viability and function in a mouse model of amyotrophic lateral sclerosis. J Clin Invest 120:3673–3679.

Robberecht W, Philips T (2013) The changing scene of amyotrophic lateral sclerosis. Nat Rev Neurosci 14:248–264.

Rojas F, Cortes N, Abarzua S, Dyrda A, van Zundert B (2014) Astrocytes expressing mutant SOD1 and TDP43 trigger motoneuron death that is mediated via sodium channels and nitroxidative stress. Front Cell Neurosci 8:24.

Rosen DR, Siddique T, Patterson D, Figlewicz DA, Sapp P, Hentati A, Donaldson D, Goto J, O'Regan JP, Deng HX, et a. l. (1993) Mutations in Cu/Zn superoxide dismutase gene are associated with familial amyotrophic lateral sclerosis [published erratum appears in Nature 1993 Jul 22;364(6435):362] [see comments]. Nature 362:59–62.

Rothstein JD, Dykes-Hoberg M, Pardo CA, Bristol LA, Jin L, Kuncl RW, Kanai Y, Hediger MA, Wang Y, Schielke JP, Welty DF (1996) Knockout of glutamate

transporters reveals a major role for astroglial transport in excitotoxicity and clearance of glutamate. Neuron 16:675–686.

Rothstein JD, Martin LJ, Kuncl RW (1992) Decreased glutamate transport by the brain and spinal cord in amyotrophic lateral sclerosis. N Engl J Med 326:1464–1468.

Rothstein JD, Tsai G, Kuncl RW, Clawson L, Cornblath DR, Drachman DB, Pestronk A, Stauch BL, Coyle JT (1990) Abnormal excitatory amino acid metabolism in amyotrophic lateral sclerosis. Ann Neurol 28:18–25.

Rothstein JD, Van Kammen M, Levey AI, Martin LJ, Kuncl RW (1995) Selective loss of glial glutamate transporter GLT-1 in amyotrophic lateral sclerosis. Ann Neurol 38:73–84.

Rotunno MS, Bosco D a (2013) An emerging role for misfolded wild-type SOD1 in sporadic ALS pathogenesis. Front Cell Neurosci 7:253.

Roybon L, Lamas N, Garcia-Diaz A, Yang E, Sattler R, Jackson-Lewis V, Kim Y, Kachel CA, Rothstein J, Przedborski S, Wichterle H, Henderson C (2013) Human stem cell-derived spinal cord astrocytes with defined mature or reactive phenotypes. Cell Rep 4:1035–1048.

Rutherford NJ, Zhang Y-J, Baker M, Gass JM, Finch NA, Xu Y-F, Stewart H, Kelley BJ, Kuntz K, Crook RJP, Sreedharan J, Vance C, Sorenson E, Lippa C, Bigio EH, Geschwind DH, Knopman DS, Mitsumoto H, Petersen RC, Cashman NR, Hutton M, Shaw CE, Boylan KB, Boeve B, Graff-Radford NR, Wszolek ZK, Caselli RJ, Dickson DW, Mackenzie IR, Petrucelli L, Rademakers R (2008) Novel Mutations in <italic>TARDBP</italic> (TDP-43) in Patients with Familial Amyotrophic Lateral Sclerosis. PLoS Genet 4:e1000193.

Sakowski SA, Lunn JS, Busta AS, Oh SS, Zamora-Berridi G, Palmer M, Rosenberg AA, Philip SG, Dowling JJ, Feldman EL (2012) Neuromuscular effects of G93A-SOD1 expression in zebrafish. Mol Neurodegener 7:44.

Sanes JN, Donoghue JP (2000) Plasticity and primary motor cortex. Annu Rev Neurosci 23:393–415.

Sareen D, O'Rourke JG, Meera P, Muhammad AKMG, Grant S, Simpkinson M, Bell S, Carmona S, Ornelas L, Sahabian A, Gendron T, Petrucelli L, Baughn M, Ravits J, Harms MB, Rigo F, Bennett CF, Otis TS, Svendsen CN, Baloh RH (2013) Targeting RNA foci in iPSC-derived motor neurons from ALS patients with a C9ORF72 repeat expansion. Sci Transl Med 5:208ra149.

Sasaki S (2011) Autophagy in spinal cord motor neurons in sporadic amyotrophic lateral sclerosis. J Neuropathol Exp Neurol 70:349–359.

Sasaki S, Iwata M (1996a) Ultrastructural study of synapses in the anterior horn neurons of patients with amyotrophic lateral sclerosis. Neurosci Lett 204:53–56.

Sasaki S, Iwata M (1996b) Impairment of fast axonal transport in the proximal axons of anterior horn neurons in amyotrophic lateral sclerosis. Neurology 47:535–540.

Sasaki S, Maruyama S (1994) Synapse loss in anterior horn neurons in amyotrophic lateral sclerosis. Acta Neuropathol 88:222–227.

Sasaki S, Takeda T, Shibata N, Kobayashi M (2010) Alterations in subcellular localization of TDP-43 immunoreactivity in the anterior horns in sporadic amyotrophic lateral sclerosis. Neurosci Lett 478:72–76.

Sathasivam S, Shaw PJ (2005) Apoptosis in amyotrophic lateral sclerosis--what is the evidence? Lancet Neurol 4:500–509.

Satoh J, Asahina N, Kitano S, Kino Y (2015) A Comprehensive Profile of ChIP-Seq-Based Olig2 Target Genes in Motor Neuron Progenitor Cells Suggests the Possible Involvement of Olig2 in the Pathogenesis of Amyotrophic Lateral Sclerosis. :1–14.

Saxena S, Cabuy E, Caroni P (2009) A role for motoneuron subtype-selective ER stress in disease manifestations of FALS mice. Nat Neurosci 12:627–636.

Saxena S, Roselli F, Singh K, Leptien K, Julien J-P, Gros-Louis F, Caroni P (2013) Neuroprotection through excitability and mTOR required in ALS motoneurons to delay disease and extend survival. Neuron 80:80–96.

Schiffer D, Cordera S, Cavalla P, Migheli A (1996) Reactive astrogliosis of the spinal cord in amyotrophic lateral sclerosis. In: Journal of the Neurological Sciences, pp 27–33.

Schiffer D, Cordera S, Giordana MT, Attanasio A, Pezzulo T (1995) Synaptic vesicle proteins, synaptophysin and chromogranin A in amyotrophic lateral sclerosis. In: Journal of the Neurological Sciences, pp 68–74.

Schiffer D, Fiano V (2004) Astrogliosis in ALS: possible interpretations according to pathogenetic hypotheses. Amyotroph Lateral Scler Other Motor Neuron Disord 5:22–25.

Schutz B (2005) Imbalanced excitatory to inhibitory synaptic input precedes motor neuron degeneration in an animal model of amyotrophic lateral sclerosis. Neurobiol Dis 20:131–140.

Seeburg PH (1993) The TINS/TiPS lecture: The molecular biology of mammalian glutamate receptor channels. In: Trends in Neurosciences, pp 359–365.

Sen I, Nalini A, Joshi NB, Joshi PG (2005) Cerebrospinal fluid from amyotrophic lateral sclerosis patients preferentially elevates intracellular calcium and toxicity in motor neurons via AMPA/kainate receptor. J Neurol Sci 235:45–54.

Sephton CF, Good SK, Atkin S, Dewey CM, Mayer P, Herz J, Yu G (2010) TDP-43 is a developmentally regulated protein essential for early embryonic development. J Biol Chem 285:6826–6834.

Serio A, Bilican B, Barmada SJ, Ando DM, Zhao C, Siller R, Burr K, Haghi G, Story D, Nishimura AL, Carrasco M a, Phatnani HP, Shum C, Wilmut I, Maniatis T, Shaw CE, Finkbeiner S, Chandran S (2013) Astrocyte pathology and the absence of non-cell autonomy in an induced pluripotent stem cell model of TDP-43 proteinopathy. Proc Natl Acad Sci U S A 110:4697–4702.

Shan X, Chiang P, Price DL, Wong PC (2010) Altered distributions of Gemini of coiled bodies and mitochondria in motor neurons of TDP-43 transgenic mice. Proc Natl Acad Sci U S A 107:16325–16330.

Shaw PJ, Chinnery RM, Ince PG (1994) Non-NMDA receptors in motor neuron disease (MND): a quantitative autoradiographic study in spinal cord and motor cortex using [3H]CNQX and [3H]kainate. Brain Res 655:186–194.

Shaw PJ, Eggett CJ (2000) Molecular factors underlying selective vulnerability of motor neurons to neurodegeneration in amyotrophic lateral sclerosis. J Neurol 247 Suppl :I17–I27.

Shaw PJ, Forrest V, Ince PG, Richardson JP, Wastell HJ (1995a) CSF and plasma amino acid levels in motor neuron disease: elevation of CSF glutamate in a subset of patients. Neurodegeneration 4:209–216.

Shaw PJ, Ince PG (1997) Glutamate, excitotoxicity and amyotrophic lateral sclerosis. J Neurol 244 Suppl :S3–S14.

Shaw PJ, Ince PG, Falkous G, Mantle D (1995b) Oxidative damage to protein in sporadic motor neuron disease spinal cord. Ann Neurol 38:691–695.

Shaw PJ, Williams TL, Slade JY, Eggett CJ, Ince PG (1999) Low expression of GluR2 AMPA receptor subunit protein by human motor neurons. Neuroreport 10:261–265.

Sherman MY, Goldberg AL (2001) Cellular defenses against unfolded proteins: A cell biologist thinks about neurodegenerative diseases. Neuron 29:15–32.

Shibata N, Hirano A, Kobayashi M, Sasaki S, Kato T, Matsumoto S, Shiozawa Z, Komori T, Ikemoto A, Umahara T (1994) Cu/Zn superoxide dismutase-like immunoreactivity in Lewy body-like inclusions of sporadic amyotrophic lateral sclerosis.

Shibuya K, Misawa S, Arai K, Nakata M, Kanai K, Yoshiyama Y, Ito K, Isose S, Noto Y, Nasu S, Sekiguchi Y, Fujimaki Y, Ohmori S, Kitamura H, Sato Y, Kuwabara S (2011) Markedly reduced axonal potassium channel expression in human sporadic amyotrophic lateral sclerosis: an immunohistochemical study. Exp Neurol 232:149–153.

Shin S, Dalton S, Stice SL (2005) Human motor neuron differentiation from human embryonic stem cells. Stem Cells Dev 14:266–269.

Shneider NA, Brown MN, Smith CA, Pickel J, Alvarez FJ (2009) Gamma motor neurons express distinct genetic markers at birth and require muscle spindle-derived GDNF for postnatal survival. Neural Dev 4:42.

Singh N, Nakano T, Xuing L, Kang J (2005) Enhancer-specified GFP-based FACS purification of human spinal motor neurons from embryonic stem cells. 196:224–234.

Sommer B, Köhler M, Sprengel R, Seeburg PH (1991) RNA editing in brain controls a determinant of ion flow in glutamate-gated channels. Cell 67:11–19.

Soo KY, Farg M, Atkin JD (2011) Molecular motor proteins and amyotrophic lateral sclerosis. Int J Mol Sci 12:9057–9082.

Sreedharan J, Blair IP, Tripathi VB, Hu X, Vance C, Rogelj B, Ackerley S, Durnall JC, Williams KL, Buratti E, Baralle F, de Belleroche J, Mitchell JD, Leigh PN, Al-Chalabi A, Miller CC, Nicholson G, Shaw CE (2008) TDP-43 mutations in familial and sporadic amyotrophic lateral sclerosis. Science 319:1668–1672.

Stafstrom CE (2007) Persistent Sodium Current and Its Role in Epilepsy. Epilepsy Curr 7:15–22.

Stephens B, Guiloff RJ, Navarrete R, Newman P, Nikhar N, Lewis P (2006) Widespread loss of neuronal populations in the spinal ventral horn in sporadic motor neuron disease. A morphometric study. J Neurol Sci 244:41–58.

Stepto A, Gallo JM, Shaw CE, Hirth F (2014) Modelling C9ORF72 hexanucleotide repeat expansion in amyotrophic lateral sclerosis and frontotemporal dementia. Acta Neuropathol 127:377–389.

Stewart H, Rutherford NJ, Briemberg H, Krieger C, Cashman N, Fabros M, Baker M, Fok A, DeJesus-Hernandez M, Eisen A, Rademakers R, Mackenzie IRA (2012) Clinical and pathological features of amyotrophic lateral sclerosis caused by mutation in the C9ORF72 gene on chromosome 9p. Acta Neuropathol 123:409–417.

Stieber A, Gonatas JO, Gonatas NK (2000) Aggregates of mutant protein appear progressively in dendrites, in periaxonal processes of oligodendrocytes, and in neuronal and astrocytic perikarya of mice expressing the SOD1(G93A) mutation of familial amyotrophic lateral sclerosis. J Neurol Sci 177:114–123.

Strong MJ, Kesavapany S, Pant HC (2005) The pathobiology of amyotrophic lateral sclerosis: a proteinopathy? J Neuropathol Exp Neurol 64:649–664.

Swarup V, Phaneuf D, Bareil C, Robertson J, Rouleau G a, Kriz J, Julien J-P (2011) Pathological hallmarks of amyotrophic lateral sclerosis/frontotemporal lobar degeneration in transgenic mice produced with TDP-43 genomic fragments. Brain 134:2610–2626.

Takahashi K, Tanabe K, Ohnuki M, Narita M, Ichisaka T, Tomoda K, Yamanaka S (2007) Induction of Pluripotent Stem Cells from Adult Human Fibroblasts by Defined Factors. Cell 131:861–872.

Takahashi K, Yamanaka S (2006) Induction of pluripotent stem cells from mouse embryonic and adult fibroblast cultures by defined factors. Cell 126:663–676.

Takakusaki K, Saitoh K, Harada H, Kashiwayanagi M (2004) Role of basal ganglia-brainstem pathways in the control of motor behaviors. Neurosci Res 50:137–151.

Takuma H, Kwak S, Yoshizawa T, Kanazawa I (1999) Reduction of GluR2 RNA editing, a molecular change that increases calcium influx through AMPA receptors, selective in the spinal ventral gray of patients with amyotrophic lateral sclerosis. Ann Neurol 46:806–815.

Tamura N, Kuwabara S, Misawa S, Kanai K, Nakata M, Sawai S, Hattori T (2006) Increased nodal persistent Na+ currents in human neuropathy and motor neuron disease estimated by latent addition. Clin Neurophysiol 117:2451–2458.

Tanji J, Shima K (1994) Role for supplementary motor area cells in planning several movements ahead. Nature 371:413–416.

Tashiro Y, Urushitani M, Inoue H, Koike M, Uchiyama Y, Komatsu M, Tanaka K, Yamazaki M, Abe M, Misawa H, Sakimura K, Ito H, Takahashia R (2012) Motor neuron-specific disruption of proteasomes, but not autophagy, replicates amyotrophic lateral sclerosis. J Biol Chem 287:42984–42994.

Thielsen KD, Moser JM, Schmitt-John T, Jensen MS, Jensen K, Holm MM (2013) The Wobbler Mouse Model of Amyotrophic Lateral Sclerosis (ALS) Displays Hippocampal Hyperexcitability, and Reduced Number of Interneurons, but No Presynaptic Vesicle Release Impairments. PLoS One 8:e82767.

Thomson JA (1998) Embryonic Stem Cell Lines Derived from Human Blastocysts. Science (80- ) 282:1145–1147.

Tolle TR, Berthele A, Zieglgansberger W, Seeburg PH, Wisden W (1993) The differential expression of 16 NMDA and non-NMDA receptor subunits in the rat spinal cord and in periaqueductal gray. J Neurosci 13:5009–5028.

Tollervey JR, Curk T, Rogelj B, Briese M, Cereda M, Kayikci M, König J,

Hortobágyi T, Nishimura AL, Zupunski V, Patani R, Chandran S, Rot G, Zupan B, Shaw CE, Ule J (2011) Characterizing the RNA targets and position-dependent splicing regulation by TDP-43. Nat Neurosci 14:452–458.

Tong J, Huang C, Bi F, Wu Q, Huang B, Liu X, Li F, Zhou H, Xia X (2013) Expression of ALS-linked TDP-43 mutant in astrocytes causes non-cell-autonomous motor neuron death in rats. EMBO J 32:1917–1926.

Tradewell ML, Cooper LA, Minotti S, Durham HD (2011) Calcium dysregulation, mitochondrial pathology and protein aggregation in a culture model of amyotrophic lateral sclerosis: Mechanistic relationship and differential sensitivity to intervention. Neurobiol Dis 42:265–275.

Troost D, Aten J, Morsink F, de Jong JM (1995) Apoptosis in amyotrophic lateral sclerosis is not restricted to motor neurons. Bcl-2 expression is increased in unaffected post-central gyrus. Neuropathol Appl Neurobiol 21:498–504.

Tu PH, Raju P, Robinson KA, Gurney ME, Trojanowski JQ, Lee VM (1996) Transgenic mice carrying a human mutant superoxide dismutase transgene develop neuronal cytoskeletal pathology resembling human amyotrophic lateral sclerosis lesions. Proc Natl Acad Sci U S A 93:3155–3160.

Turner BJ, Talbot K (2008) Transgenics, toxicity and therapeutics in rodent models of mutant SOD1-mediated familial ALS. Prog Neurobiol 85:94–134.

Turner MR, Osei-Lah AD, Hammers A, Al-Chalabi A, Shaw CE, Andersen PM, Brooks DJ, Leigh PN, Mills KR (2005) Abnormal cortical excitability in sporadic but not homozygous D90A SOD1 ALS. J Neurol Neurosurg Psychiatry 76:1279–1285.

Urbani A, Belluzzi O (2000) Riluzole inhibits the persistent sodium current in mammalian CNS neurons. Eur J Neurosci 12:3567–3574.

Urushitani M, Kurisu J, Tsukita K, Takahashi R (2002) Proteasomal inhibition by misfolded mutant superoxide dismutase 1 induces selective motor neuron death in familial amyotrophic lateral sclerosis. J Neurochem 83:1030–1042.

Urushitani M, Tomoki, Nakamizo, Inoue R, Sawada H, Kihara T, Honda K, Akaike A, Shimohama S (2001) N-methyl-D-aspartate receptor-mediated mitochondrial Ca2+ overload in acute excitotoxic motor neuron death: A mechanism distinct from chronic neurotoxicity after Ca2+ influx. J Neurosci Res 63:377–387.

Van Damme P, Bogaert E, Dewil M, Hersmus N, Kiraly D, Scheveneels W, Bockx I, Braeken D, Verpoorten N, Verhoeven K, Timmerman V, Herijgers P, Callewaert G, Carmeliet P, Van Den Bosch L, Robberecht W (2007) Astrocytes regulate GluR2 expression in motor neurons and their vulnerability to excitotoxicity. Proc Natl Acad Sci U S A 104:14825–14830.

Van Damme P, Braeken D, Callewaert G, Robberecht W, Van Den Bosch L (2005a) GluR2 deficiency accelerates motor neuron degeneration in a mouse model of amyotrophic lateral sclerosis. J Neuropathol Exp Neurol 64:605–612.

Van Damme P, Dewil M, Robberecht W, Van Den Bosch L (2005b) Excitotoxicity and amyotrophic lateral sclerosis. Neurodegener Dis 2:147–159.

Van Damme P, Van Den Bosch L, Van Houtte E, Callewaert G, Robberecht W (2002) GluR2-dependent properties of AMPA receptors determine the selective vulnerability of motor neurons to excitotoxicity. J Neurophysiol 88:1279–1287.

Van Den Bosch L, Van Damme P, Bogaert E, Robberecht W (2006) The role of excitotoxicity in the pathogenesis of amyotrophic lateral sclerosis. Biochim Biophys Acta - Mol Basis Dis 1762:1068–1082.

Van Hoecke A, Schoonaert L, Lemmens R, Timmers M, Staats KA, Laird AS, Peeters E, Philips T, Goris A, Dubois B, Andersen PM, Al-Chalabi A, Thijs V, Turnley AM, van Vught PW, Veldink JH, Hardiman O, Van Den Bosch L, Gonzalez-Perez P, Van Damme P, Brown RH, van den Berg LH, Robberecht W (2012) EPHA4 is a disease modifier of amyotrophic lateral sclerosis in animal models and in humans. Nat Med 18:1418–1422.

van Zundert B, Peuscher MH, Hynynen M, Chen A, Neve RL, Jr RHB, Constantine-paton M, Bellingham MC (2008) Disturbance in a Mouse Model of the Adult-Onset Neurodegenerative Disease Amyotrophic Lateral Sclerosis. J Neurosci 28:10864–10874.

Vance C, Rogelj B, Hortobágyi T, De Vos KJ, Nishimura AL, Sreedharan J, Hu X, Smith B, Ruddy D, Wright P, Ganesalingam J, Williams KL, Tripathi V, Al-Saraj S, Al-Chalabi A, Leigh PN, Blair IP, Nicholson G, de Belleroche J, Gallo J-M, Miller CC, Shaw CE (2009) Mutations in FUS, an RNA processing protein, cause familial amyotrophic lateral sclerosis type 6. Science 323:1208–1211.

Vandenberghe W, Robberecht W, Brorson JR (2000) AMPA receptor calcium permeability, GluR2 expression, and selective motoneuron vulnerability. J Neurosci 20:123–132.

Vargas MR, Johnson D a, Sirkis DW, Messing A, Johnson J a (2008) Nrf2 activation in astrocytes protects against neurodegeneration in mouse models of familial amyotrophic lateral sclerosis. J Neurosci 28:13574–13581.

Vehviläinen P, Koistinaho J, Gundars G (2014) Mechanisms of mutant SOD1 induced mitochondrial toxicity in amyotrophic lateral sclerosis. Front Cell Neurosci 8:126.

von Lewinski F, Fuchs J, Vanselow BK, Keller BU (2008) Low Ca2+ buffering in hypoglossal motoneurons of mutant SOD1 (G93A) mice. Neurosci Lett 445:224–228.

Vucic S, Cheah BC, Kiernan MC (2009) Defining the mechanisms that underlie cortical hyperexcitability in amyotrophic lateral sclerosis. Exp Neurol 220:177–182.

Vucic S, Kiernan MC (2006) Axonal excitability properties in amyotrophic lateral sclerosis. Clin Neurophysiol 117:1458–1466.

Vucic S, Kiernan MC (2007) Abnormalities in cortical and peripheral excitability in flail arm variant amyotrophic lateral sclerosis. J Neurol Neurosurg Psychiatry 78:849–852.

Vucic S, Kiernan MC (2010) Upregulation of persistent sodium conductances in familial ALS. J Neurol Neurosurg Psychiatry 81:222–227.

Vucic S, Nicholson GA, Kiernan MC (2008) Cortical hyperexcitability may precede the onset of familial amyotrophic lateral sclerosis. Brain 131:1540–1550.

Wada T, Honda M, Minami I, Tooi N, Amagai Y, Nakatsuji N, Aiba K (2009) Highly efficient differentiation and enrichment of spinal motor neurons derived from human and monkey embryonic stem cells. PLoS One 4.

Wainger BJ, Kiskinis E, Mellin C, Wiskow O, Han SSW, Sandoe J, Perez NP, Williams L a., Lee S, Boulting G, Berry JD, Brown RH, Cudkowicz ME, Bean BP, Eggan K, Woolf CJ (2014) Intrinsic membrane hyperexcitability of amyotrophic lateral sclerosis patient-derived motor neurons. Cell Rep 7:1–11.

Walker AK, Soo KY, Sundaramoorthy V, Parakh S, Ma Y, Farg MA, Wallace RH, Crouch PJ, Turner BJ, Horne MK, Atkin JD (2013) ALS-associated TDP-43 induces endoplasmic reticulum stress, which drives cytoplasmic TDP-43 accumulation and stress granule formation. PLoS One 8.

Walter P, Ron D (2011) The Unfolded Protein Response: From Stress Pathway to Homeostatic Regulation. Science (80- ) 334:1081–1086.

Wang L, Sharma K, Deng H-X, Siddique T, Grisotti G, Liu E, Roos RP (2008) Restricted expression of mutant SOD1 in spinal motor neurons and interneurons induces motor neuron pathology. Neurobiol Dis 29:400–408.

Wang W, Li L, Lin WL, Dickson DW, Petrucelli L, Zhang T, Wang X (2013) The ALS disease-associated mutant TDP-43 impairs mitochondrial dynamics and function in motor neurons. Hum Mol Genet 22:4706–4719.

Watanabe M, Dykes-Hoberg M, Culotta VC, Price DL, Wong PC, Rothstein JD (2001) Histological evidence of protein aggregation in mutant SOD1 transgenic mice and in amyotrophic lateral sclerosis neural tissues. Neurobiol Dis 8:933–941.

Watkins JC, Evans RH (1981) Excitatory amino acid transmitters. Annu Rev Pharmacol Toxicol 21:165–204.

Watson MR, Lagow RD, Xu K, Zhang B, Bonini NM (2008) A drosophila model for amyotrophic lateral sclerosis reveals motor neuron damage by human SOD1. J Biol Chem 283:24972–24981.

Wegorzewska I, Baloh RH (2011) TDP-43-based animal models of neurodegeneration: New insights into ALS pathology and pathophysiology. Neurodegener Dis 8:262–274.

Wegorzewska I, Bell S, Cairns NJ, Miller TM, Baloh RH (2009) TDP-43 mutant transgenic mice develop features of ALS and frontotemporal lobar degeneration. Proc Natl Acad Sci U S A 106:18809–18814.

Wichterle H, Lieberam I, Porter J a, Jessell TM (2002) Directed differentiation of embryonic stem cells into motor neurons. Cell 110:385–397.

Williams TL, Day NC, Ince PG, Kamboj RK, Shaw PJ (1997) Calcium-permeable alpha-amino-3-hydroxy-5-methyl-4-isoxazole propionic acid receptors: a molecular determinant of selective vulnerability in amyotrophic lateral sclerosis. Ann Neurol 42:200–207.

Williamson TL, Cleveland DW (1999) Slowing of axonal transport is a very early event in the toxicity of ALS-linked SOD1 mutants to motor neurons. Nat Neurosci 2:50–56.

Wils H, Kleinberger G, Janssens J, Pereson S, Joris G, Cuijt I, Smits V, Ceuterick-de Groote C, Van Broeckhoven C, Kumar-Singh S (2010) TDP-43 transgenic mice develop spastic paralysis and neuronal inclusions characteristic of ALS and frontotemporal lobar degeneration. Proc Natl Acad Sci U S A 107:3858–3863.

Wong PC, Pardo C a, Borchelt DR, Lee MK, Copeland NG, Jenkins N a, Sisodia SS,

Cleveland DW, Price DL (1995) An adverse property of a familial ALS-linked SOD1 mutation causes motor neuron disease characterized by vacuolar degeneration of mitochondria. Neuron 14:1105–1116.

Wright A, Vissel B (2012) The essential role of AMPA receptor GluR2 subunit RNA editing in the normal and diseased brain. Front Mol Neurosci 5:1–13.

Wu L-S, Cheng W-C, Hou S-C, Yan Y-T, Jiang S-T, Shen C-KJ (2010) TDP-43, a neuro-pathosignature factor, is essential for early mouse embryogenesis. Genesis 48:56–62.

Wu LS, Cheng WC, Shen CKJ (2012) Targeted depletion of TDP-43 expression in the spinal cord motor neurons leads to the development of amyotrophic lateral sclerosis-like phenotypes in mice. J Biol Chem 287:27335–27344.

Xu Y-F, Gendron TF, Zhang Y-J, Lin W-L, D'Alton S, Sheng H, Casey MC, Tong J, Knight J, Yu X, Rademakers R, Boylan K, Hutton M, McGowan E, Dickson DW, Lewis J, Petrucelli L (2010) Wild-type human TDP-43 expression causes TDP-43 phosphorylation, mitochondrial aggregation, motor deficits, and early mortality in transgenic mice. J Neurosci 30:10851–10859.

Xu Y-F, Zhang Y-J, Lin W-L, Cao X, Stetler C, Dickson DW, Lewis J, Petrucelli L (2011) Expression of mutant TDP-43 induces neuronal dysfunction in transgenic mice. Mol Neurodegener 6:73.

Yamanaka K, Chun SJ, Boillee S, Fujimori-Tonou N, Yamashita H, Gutmann DH, Takahashi R, Misawa H, Cleveland DW (2008) Astrocytes as determinants of disease progression in inherited amyotrophic lateral sclerosis. Nat Neurosci 11:251–253.

Yang C, Wang H, Qiao T, Yang B, Aliaga L, Qiu L, Tan W, Salameh J, McKenna-Yasek DM, Smith T, Peng L, Moore MJ, Brown RH, Cai H, Xu Z (2014) Partial loss of TDP-43 function causes phenotypes of amyotrophic lateral sclerosis. Proc Natl Acad Sci U S A 111:E1121–E1129.

Yang YM, Gupta SK, Kim KJ, Powers BE, Cerqueira A, Wainger BJ, Ngo HD, Rosowski K a, Schein P a, Ackeifi C a, Arvanites AC, Davidow LS, Woolf CJ, Rubin LL (2013) A small molecule screen in stem-cell-derived motor neurons identifies a kinase inhibitor as a candidate therapeutic for ALS. Cell Stem Cell 12:713–726.

Ying Q-L, Wray J, Nichols J, Batlle-Morera L, Doble B, Woodgett J, Cohen P, Smith A (2008) The ground state of embryonic stem cell self-renewal. Nature 453:519–523.

Yu J, Vodyanik M a, Smuga-Otto K, Antosiewicz-Bourget J, Frane JL, Tian S, Nie J, Jonsdottir G a, Ruotti V, Stewart R, Slukvin II, Thomson J a (2007) Induced pluripotent stem cell lines derived from human somatic cells. Science 318:1917–1920.

Yusa K, Rashid ST, Strick-Marchand H, Varela I, Liu P, Paschon DE, Miranda E, Ordóñez A, Hannan NRF, Rouhani FJ, Darche S, Alexander G, Marciniak SJ, Fusaki N, Hasegawa M, Holmes MC, Di Santo JP, Lomas DA, Bradley A, Vallier L (2011) Targeted gene correction of α1-antitrypsin deficiency in induced pluripotent stem cells. Nature 478:391–394.

Zagoraiou L, Akay T, Martin JF, Brownstone RM, Jessell TM, Miles GB (2009) A Cluster of Cholinergic Premotor Interneurons Modulates Mouse Locomotor

Activity. Neuron 64:645–662.

Zanette G, Tamburin S, Manganotti P, Refatti N, Forgione A, Rizzuto N (2002) Different mechanisms contribute to motor cortex hyperexcitability in amyotrophic lateral sclerosis. Clin Neurophysiol 113:1688–1697.

Zhan L, Hanson KA, Kim SH, Tare A, Tibbetts RS (2013) Identification of Genetic Modifiers of TDP-43 Neurotoxicity in Drosophila. PLoS One 8:e57214.

Zhan L, Xie Q, Tibbetts RS (2014) Opposing roles of p38 and JNK in a Drosophila model of TDP-43 proteinopathy reveal oxidative stress and innate immunity as pathogenic components of neurodegeneration. Hum Mol Genet 24:757–772.

Zhang D, Iyer LM, He F, Aravind L (2012) Discovery of Novel DENN Proteins: Implications for the Evolution of Eukaryotic Intracellular Membrane Structures and Human Disease. Front Genet 3:283.

Zhang F, Wang W, Siedlak SL, Liu Y, Liu J, Jiang K, Perry G, Zhu X, Wang X (2015) Miro1 deficiency in amyotrophic lateral sclerosis. Front Aging Neurosci 7:1–8.

Zhang Y-J, Jansen-West K, Xu Y-F, Gendron TF, Bieniek KF, Lin W-L, Sasaguri H, Caulfield T, Hubbard J, Daughrity L, Chew J, Belzil V V, Prudencio M, Stankowski JN, Castanedes-Casey M, Whitelaw E, Ash PE a, DeTure M, Rademakers R, Boylan KB, Dickson DW, Petrucelli L (2014) Aggregation-prone c9FTD/ALS poly(GA) RAN-translated proteins cause neurotoxicity by inducing ER stress. Acta Neuropathol.

Zhang Z, Almeida S, Lu Y, Nishimura AL, Peng L, Sun D, Wu B, Karydas AM, Tartaglia MC, Fong JC, Miller BL, Farese R V, Moore MJ, Shaw CE, Gao F-B (2013) Downregulation of microRNA-9 in iPSC-derived neurons of FTD/ALS patients with TDP-43 mutations. PLoS One 8:e76055.

Zhao P, Ignacio S, Beattie EC, Abood ME (2008) Altered presymptomatic AMPA and cannabinoid receptor trafficking in motor neurons of ALS model mice: Implications for excitotoxicity. Eur J Neurosci 27:572–579.

Zhou H, Huang C, Chen H, Wang D, Landel CP, Xia PY, Bowser R, Liu YJ, Xia XG (2010) Transgenic rat model of neurodegeneration caused by mutation in the TDP gene. PLoS Genet 6.

Zhu YB, Sheng ZH (2011) Increased axonal mitochondrial mobility does not slow amyotrophic lateral sclerosis (ALS)-like disease in mutant SOD1 mice. J Biol Chem 286:23432–23440.

Ziemann U, Winter M, Reimers CD, Reimers K, Tergau F, Paulus W (1997) Impaired motor cortex inhibition in patients with amyotrophic lateral sclerosis. Evidence from paired transcranial magnetic stimulation. Neurology 49:1292–1298.

Zona C, Pieri M, Carunchio I (2006) Voltage-dependent sodium channels in spinal cord motor neurons display rapid recovery from fast inactivation in a mouse model of amyotrophic lateral sclerosis. J Neurophysiol 96:3314–3322.